Oxygen dynamics in the bottom waters of lakes:
Understanding the past to predict the future

Abigail S. L. Lewis

Dissertation submitted to the faculty of the Virginia Polytechnic Institute and State
University in partial fulfillment of the requirements for the degree of

Doctor of Philosophy

In

Biological Sciences

Cayelan C. Carey, Chair

J. E. Barrett
Paul C. Hanson
Madeline E. Schreiber
R. Quinn Thomas

3 May 2024

Blacksburg, Virginia

Keywords: Air temperature, anoxia, carbon cycling, climate change, dissolved oxygen,
ecological forecasting, ecological memory, hypolimnion, iron,
iron-bound organic carbon, lake, reservoir, water temperature

Oxygen dynamics in the bottom waters of lakes:
Understanding the past to predict the future

Abigail S. L. Lewis

ABSTRACT

Dissolved oxygen concentrations are declining in the bottom waters of many lakes around the world, posing critical water quality concerns. Throughout my dissertation, I assessed how bottom-water dissolved oxygen may mediate the effects of climate and land use change on water quality in lakes. First, I characterized causes of variation in summer bottom-water temperature and dissolved oxygen. I demonstrated that spring air temperatures may play a greater role than summer air temperatures in shaping summer bottom-water dynamics. I then characterized the effects of declining bottom-water oxygen concentrations across diverse scales of analysis (i.e., using microcosm incubations, whole-ecosystem oxygenation experiments, and data analysis of >600 widespread lakes). I found that low dissolved oxygen concentrations contributed to release of nutrients and organic carbon from lake sediments, potentially altering the role of lakes in global biogeochemical cycles. Importantly, I also found support for a previously-hypothesized Anoxia Begets Anoxia feedback, whereby bottom-water anoxia (i.e., no dissolved oxygen) in a given year promotes increasingly severe occurrences of anoxia in following summers. This finding demonstrates the need for forecasts of future oxygen dynamics in lakes, as management actions to preempt the first occurrence of anoxia will be more effective than actions to restore ecological function after oxygen

concentrations have already declined. To build the capacity for such forecasts, I led a systematic review of ecological forecasting literature that characterized the state of the field, emerging best practices, and relative predictability of four ecological variables. Combined, my dissertation provides a mechanistic examination of the effects of climate change on water quality in lakes worldwide, ultimately helping to anticipate, mitigate, and preempt future water quality declines.

Oxygen dynamics in the bottom waters of lakes:
Understanding the past to predict the future

Abigail S. L. Lewis

GENERAL AUDIENCE ABSTRACT

Changes in climate and land use have caused dissolved oxygen concentrations to decline in many lakes around the world. These declines are concerning because low oxygen concentrations can cause substantial water quality problems. If we could better predict future water quality, we may be able to develop more effective lake management programs. To help meet this need, I analyzed how dissolved oxygen has mediated historical changes in water quality, and how dissolved oxygen may affect water quality in the future. I focused on bottom-water (rather than surface-water) dissolved oxygen, because bottom waters are more likely to experience very low oxygen concentrations that can lead to water quality problems. I started by assessing the drivers of summer bottom-water dissolved oxygen in 615 lakes. Across these lakes, spring air temperatures played a greater role than summer air temperatures in shaping summer bottom-water temperature and dissolved oxygen. I then characterized the effects of declining bottom-water oxygen concentrations using small-scale incubations in the lab, manipulations of oxygen concentrations in a whole reservoir, and data analysis across 656 lakes. I found that low dissolved oxygen conditions led to the release of nutrients and organic carbon from lake sediments, which may worsen water quality. Importantly, I also found support for a feedback effect, whereby low bottom-water dissolved oxygen in one summer perpetuates

oxygen declines in following summers. This finding motivates the need for forecasts of future dissolved oxygen concentrations, as management actions to stop the first occurrence of low oxygen concentrations will be more effective than actions to restore water quality after oxygen concentrations have already started to decline. To build capacity for lake oxygen forecasts, I synthesized many published papers that have predicted future ecological states, and I documented proposed best practices in this emerging field. Ultimately, by advancing our understanding of how climate and land use change affect water quality in lakes worldwide, my dissertation research will help to anticipate, mitigate, and preempt future water quality declines.

ACKNOWLEDGEMENTS

All of the best parts of my Ph.D. are rooted in connections with collaborators, mentors, friends, and family members. *Thank you* for giving this work its joy, motivation, and significance. In particular, I am deeply grateful for support from each of the following people.

First and foremost, thank you to my advisor, Cayelan Carey. Cayelan, your mentorship over the past five years has been inspiring and empowering. Thank you for countless manuscript reviews, for helpful 1:1 meetings, for support in developing a new graduate seminar, and for being a consistent advocate for my work. Your enthusiasm for freshwater science is contagious, and I am continually inspired by your leadership in building supportive, collaborative research teams. I feel incredibly fortunate to have had the opportunity to learn from you throughout my Ph.D. Thank you!

Next, thank you to my graduate committee—Madeline Schreiber, Jeb Barrett, Paul Hanson, and Quinn Thomas. Maddy, your support has been invaluable, both to my research and to me, personally. Thank you for sharing your biogeochemical expertise and for being a kind, encouraging mentor over the past five years. Jeb, it has been such a joy to talk about ecosystem science with you over the years. Thank you for offering me access to your lab and equipment and for helping broaden my perspective to think about biogeochemical cycling across the aquatic-terrestrial interface. Paul, thank you for generously sharing your time to talk through lake ecosystem models. Your patience, thoughtfulness, and expertise have been important at pivotal points in my Ph.D. Finally, Quinn, thank you for contributing your expertise in ecological forecasting and ecosystem modeling. Your teaching materials are fantastic, and I have learned a lot about forecasting and ecosystem science from talking with you over the past five years.

My graduate work has been supported in many ways by help and feedback from Bobbie Niederlehner and the Virginia Tech Reservoir Group. Many thanks to Bobbie, whose help with protocol development and troubleshooting fundamentally enabled my iron-bound organic carbon chapter. Likewise, many members of the Virginia Tech Reservoir Research Group have all played an important role in my Ph.D., through data collection, feedback, and friendship. Thanks in particular to Heather Wander, who has been the best lab twin, collaborator, roommate, and friend I could have asked for. Thanks also to Whitney Woelmer, Dexter Howard, Mary Lofton, and Freya Olsson, who have all gone above and beyond to provide thoughtful and critical feedback on drafts and code over the past several years. More broadly, all of the graduate students and postdocs in Reservoir Group (past and present) have served as strong role models for how to do rigorous, socially-motivated freshwater research, and I am grateful to have had the opportunity to learn from you all. My research has been supported in multiple ways by the reservoir monitoring program at Falling Creek and Beaverdam Reservoirs, and I am deeply grateful to the Western Virginia Water Authority for enabling this research. Thanks also to Adrienne Breef-Pilz for helping to manage field logistics, the oxygenation system, and data processing. Lastly, thanks to many dedicated Reservoir Group undergraduate students, especially Arpita Das, who worked with me throughout the four years of her undergraduate degree. Arpita’s careful attention to detail underlies multiple chapters of my graduate research. I am grateful for her help in weighing hundreds of sediment samples, synthesizing numerous published papers, and carefully considering the human implications of my ecosystem research.

One of the joys of my Ph.D. has been the opportunity to interact closely with a broad array of researchers at Virginia Tech and around the world. Thank you to the Virginia Tech Stream Team and the Interfaces of Global Change graduate training program for conversations that have broadened my understanding of freshwater biogeochemistry in a changing world. Likewise, many thanks to the Center for Communicating Science at Virginia Tech, especially Carolyn Kroehler and Patty Raun, who have been kind role models and mentors, and have enabled much of the science outreach work I have done during my Ph.D. Beyond Virginia Tech, two chapters of my dissertation were enabled by collaborations within the Global Lake Ecological Observatory Network (GLEON). I am incredibly grateful for the fun, exciting, and collaborative academic home that GLEON has provided throughout my Ph.D. Thanks also to the Ecological Forecasting Initiative (EFI), particularly the Theory Working Group, Education Working Group, and EFI Student Association, for conversations throughout my Ph.D. that have fundamentally shaped the way I approach scientific research.

I am involved in research today largely because of the exceptional mentors I have had throughout my academic career. Thanks in particular to David Richardson and Kathleen Weathers who supervised my first freshwater research internship in 2017. It would be hard to overstate the impact that Dave and Kathie’s mentorship has had on me over the past seven years. Thanks also to many inspirational teachers and mentors from Pomona College, especially Marty Meyer, whose support for multiple independent research projects during my undergraduate degree dramatically strengthened my skills in writing, experimental design, and critical thinking.

So many friends have been a part of my Ph.D. journey, both in Blacksburg and beyond. Thanks in particular to Heather Wander, Dexter Howard, Whitney Woelmer, Grace O'Malley, Cameron Braswell, Cameron Lockett, and Carla López Lloreda from the Virginia Tech Stream Team. Thanks also to Ashley and Josh Dugan for many long conversations that have helped keep me sane and grounded over the past five years. Outside of Blacksburg, I am especially grateful for the long-term friendship of Wentao Guo, Paige Pepitone, Alex Krauska, Addie Radandt, and Shannon Blair.

My love for the environment and for education are gifts passed down from my family. Thank you especially to my parents, Susan Lewis and Eric "Nature Eric" Larson for so many forms of love and support that have helped me become the person I am today. In particular, thanks for hosting me for three pandemic months in the first year of my Ph.D. I so enjoyed that stolen golden time together. Thanks also to my brother, Bjorn Larson. Bjorn has a remarkable ability to find, create, and appreciate the coolness of the world. Thanks for sharing this with me as a life-long friend and adventure buddy.

Lastly, to Wentao Guo. Wentao, your love, support, feedback, and ideas have shaped this dissertation in uncountable ways. You continually inspire me to be a better researcher and a better person. I am profoundly grateful for the time we have spent together.

Throughout my Ph.D., I have received financial support from diverse sources. In particular, my graduate research was funded by the U.S. National Science Foundation (NSF) Graduate Research Fellowship Program (GRFP; DGE-1840995), NSF DEB-

1753639, and the Institute for Critical Technology and Applied Science (ICTAS) Doctoral Scholars program at Virginia Tech. I am grateful for further support from the College of Science Roundtable, the Graduate and Professional Student Senate (GPSS), the Biological Sciences department, the Schaeffer family, the American Geophysical Union, and the Ecological Society of America. Many thanks to each of these organizations for enabling my research and professional development.

TABLE OF CONTENTS

Chapter I: Introduction

Anthropogenic climate and land use change have profoundly altered ecosystems around the world, with critical social and cultural consequences (Adger et al., 2013; IPCC, 2023b; Bellard et al., 2012; O'Reilly et al., 2015). Predicting future ecological impacts of anthropogenic change may be necessary to prepare for and preempt socially relevant loss of ecosystem function (Clark et al., 2001; Dietze et al., 2018). However, **developing these predictions will require fundamental understanding of ecosystem dynamics, in addition to conceptual and practical frameworks for predicting future ecosystem states.**

Freshwater lakes and reservoirs (hereafter: "lakes") have been classified among the ecosystems that are most threatened by anthropogenic climate and land use change (IPCC, 2023b; MA, 2005; Zhi et al., 2023). On average, surface-water temperatures increased faster in lakes than in other aquatic ecosystems from ca. 1980–present (Dokulil et al., 2021; O'Reilly et al., 2015; Zhi et al., 2023). Furthermore, due to concurrent changes in ice dynamics, cloud cover, water clarity, and other factors, lake surface-water temperatures have often increased even faster than overlying air temperatures (Austin & Colman, 2007; Dokulil et al., 2021; Huang et al., 2023; O'Reilly et al., 2015; Schmid & Köster, 2016; Woolway & Merchant, 2017). These changes in waterbody physics, in combination with other anthropogenic impacts, can then propagate to affect the chemistry and biology of lake ecosystems (e.g., Comte et al., 2013; Ho et al., 2019; Jane et al., 2021). For example, dissolved oxygen concentrations are decreasing in many aquatic ecosystems as a result of both climate and land use change, and the rate of oxygen decline in lakes has exceeded that of both rivers and oceans from ca. 1950–present (Jane et al., 2021; Zhi et al., 2023). As lakes have experienced particularly rapid anthropogenic changes relative to other ecosystems, they have been conceptualized as sentinels of global change (Adrian et al., 2009; Williamson et al. 2008; Williamson et al., 2009). Consequently, understanding changes in lake ecosystem function may help to characterize and anticipate broader environmental changes worldwide.

Lakes play a critical role in supporting both local ecosystem services and global biogeochemical cycling, and both of these functions have the potential to be disrupted by changes in climate and land use. Locally, many lakes help to support drinking water provision, recreation, and biodiversity preservation, with critical importance to local human populations (Finlayson et al., 2018; Lynch et al., 2023; Reid et al., 2019; Reynaud & Lanzanova, 2017). However, the ability of lakes to support these services is often dependent on adequate water quality (Reynaud & Lanzanova, 2017). On a global scale, lakes are increasingly recognized as important players in global biogeochemical cycling (Bastviken et al., 2011; Battin et al., 2009; Maranger et al. 2018; Raymond et al., 2013; Tranvik et al., 2018). In particular, lakes receive substantial organic carbon inputs from their surrounding terrestrial watersheds and serve as active sites for both carbon burial (Dean & Gorham, 1998; Knoll et al., 2013; Mendonça et al., 2017; Pacheco et al., 2014; USGCRP, 2018) and greenhouse gas emission (Deemer et al., 2016; DelSontro et al., 2018). Climate and land use change have the potential to alter the balance between carbon burial and emission in lakes worldwide, creating a potential feedback to the global carbon cycling processes that regulate Earth's climate (Carey et al., 2018, 2022b; Peter et al., 2017; Sobek et al., 2009). As freshwater lakes represent critical ecosystems for both local ecosystem services and global biogeochemical cycling, effects of climate change on water quality in lakes may have far-reaching importance.

Summer bottom-water dynamics mediate ecological function year-round

While lake surface water characteristics have been broadly used to characterize water quality across many lakes because of their ease of sampling (Crosby, 1884; Mason et al., 2010; Votruba & Corman, 2020; Yang et al., 2022), summer bottom-water conditions may play an equal or greater role in determining whole-ecosystem function. In particular, summer bottom-water dissolved oxygen concentrations can regulate habitat suitability for aquatic organisms (e.g., Pilla & Williamson, 2023; Schindler, 2017), carbon cycling pathways (e.g., Encinas Fernández et al., 2014; Hounshell et al., 2021; Vachon et al., 2017), and internal nutrient loading (e.g., Carey et al., 2022b; Hupfer & Lewandowski, 2008 and references therein), with whole-ecosystem implications. Consequently, characterizing summer bottom-water dissolved oxygen dynamics may be critical to understanding current water quality conditions and anticipating future changes in water quality across lakes worldwide.

During the summer, thermal stratification inhibits mixing of surface and bottom waters in many temperate lakes, isolating bottom waters from atmospheric gas exchange (Wetzel, 2001). As a result, biological and chemical oxygen consumption in bottom waters typically cause bottom-water dissolved oxygen concentrations to decrease throughout the stratified period (Wetzel, 2001). Depending on the rate of oxygen decline and the duration of thermal stratification, dissolved oxygen concentrations may reach critically low thresholds of hypoxia (2 mg/L) or anoxia (~0 mg/L), which are associated with negative water quality impacts during the summer stratified period (e.g., Carey et al., 2022b; Hupfer & Lewandowski, 2008; Jane et al., 2023; Schindler, 2017). Later, at the end of summer, cooling surface-water temperatures may allow the lake to mix, and solutes that accumulated in bottom waters during the summer stratified period (e.g., nutrients and greenhouse gases) can exchange throughout the water column (Bastviken et al., 2004b; Encinas Fernández et al., 2014; Nürnberg & Peters, 1984; Vachon et al., 2017; Zimmermann et al., 2021). Thus, summer-bottom water conditions may lead to visible surface water quality changes in subsequent seasons and years.

Causes of bottom-water oxygen decline: Climate and land use change

Across many temperate lakes, changes in climate and land use have led oxygen concentrations to reach progressively lower concentrations in summer, potentially driving increased duration and severity of hypoxia and anoxia (Bartosiewicz et al., 2019; Jane et al., 2023; Jenny et al., 2016a). Historical (i.e., ca. 1700–1950) changes in land use resulted in increased nutrient inputs to lakes (Jenny et al., 2016a, 2016b). These nutrient inputs appear to have played an important role in driving deoxygenation by increasing phytoplankton biomass, which consequently fuels increased bottom-water oxygen demand during the summer stratified period (Jenny et al., 2016a, 2016b; Ladwig et al., 2021; Müller et al., 2019; Pace & Prairie, 2005; Schindler, 1974). Furthermore, increased air temperature appears to have intensified deoxygenation in recent decades (ca. 1950–

2020; Jane et al., 2023) by driving a longer duration and greater magnitude of thermal stratification in many lakes (Foley et al., 2012; North et al., 2013; Oleksy & Richardson, 2021; Woolway et al., 2021). Increased duration of stratification provides more time for bottom-water dissolved oxygen depletion to occur, thereby resulting in lower late-summer dissolved oxygen concentrations (Jane et al., 2023). Consequently, both climate and land use change likely contribute to dissolved oxygen declines, with the relative importance of these two mechanisms varying both among lakes and within lakes over time.

In addition to regulating stratification strength and duration, increases in air temperature may also contribute to changes in bottom-water temperature, further regulating dissolved oxygen concentrations (Oleksy & Richardson, 2021; Pace & Prairie, 2005; Yvon-Durocher et al., 2012). Warming bottom-water temperature contributes to decreased oxygen solubility and increased rates of oxygen demand, ultimately decreasing late-summer oxygen concentrations in the bottom waters of stratified lakes (Pace & Prairie, 2005; Yvon-Durocher et al., 2012). However, while surface-water temperatures are generally increasing in response to increased air temperature, summer bottom-water temperature trends are highly variable among lakes from ca. 1970–2010 (i.e., increasing in some lakes and decreasing in others) and show little to no correlation with summer or mean-annual air temperature trends (Kraemer et al., 2015; Pilla et al., 2020; Richardson et al., 2017; Winslow et al., 2017; Zhou et al., 2019). As summer bottom-water temperature is a critical determinant of bottom-water oxygen dynamics, a better understanding of the factors that drive increases or decreases in summer bottom-water temperature may improve our ability to predict future changes in dissolved oxygen concentrations across lakes worldwide.

Consequences of bottom-water oxygen decline: Internal nutrient loading and altered carbon cycling processes

Bottom-water oxygen declines have the potential to substantially alter biogeochemical cycling in lakes, with important implications for lake ecosystem services (Jansen et al., 2022; LaRowe & Van Cappellen, 2011; Mortimer, 1941; Nürnberg, 1984; Orihel et al., 2017). In particular, iron (Fe) and other redox-sensitive elements are often central to these oxygen-mediated interactions. Under oxic conditions, Fe(III) can form complexes with phosphorus and/or organic carbon, which may precipitate into sediment and help to promote burial of both nutrients and carbon (Mortimer, 1941; Nierop et al., 2002; Nürnberg, 1984; Orihel et al., 2017; Riedel et al., 2013). Conversely, under low-oxygen conditions, Fe(III) reduction and dissolution may release phosphorus and organic carbon to the water column (e.g., Mortimer, 1941; Nürnberg, 1984; Orihel et al., 2017; Pan et al., 2016; Patzner et al., 2020; Skoog & Arias-Esquivel, 2009), either as a direct result of hypoxia or through resultant increases in pH (Kirk, 2004; Thompson et al., 2006).

Existing ecological theory suggests that increases in phosphorus release from sediment under low-oxygen conditions may contribute to a positive feedback, whereby anoxia during a given year drives increasingly frequent and severe occurrences of anoxia in subsequent years. In this hypothesized “anoxia begets anoxia” (ABA) feedback, anoxic conditions promote phosphorus release from sediment, thereby stimulating phytoplankton growth (e.g., Mortimer, 1941; Nürnberg, 1984; Orihel et al., 2017). Subsequent phytoplankton decomposition in turn fuels increased heterotrophic respiration and further accelerates bottom-water dissolved oxygen declines over time (e.g., Jenny et al., 2016a, 2016b). However, while the individual relationships in the hypothesized ABA feedback cycle are well-established, these relationships occur over multiple timescales and amidst numerous other interacting factors that could prevent the detection of the overall feedback. For example, while anoxia enhances internal loading of phosphorus, sediment characteristics (e.g., abundance of redox-sensitive metals), microbial processing, and catchment inputs may also play important roles in phosphorus dynamics (e.g., Hupfer & Lewandowski, 2008; Orihel et al., 2017). Likewise, while phosphorus concentrations stimulate phytoplankton growth in many lakes, many other important factors, including nitrogen concentrations, climate, and light intensity, also contribute to regulating phytoplankton growth (e.g., Paerl & Huisman, 2008; Reinl et al., 2023). Given the inherent complexity to each of these relationships, all operating on different timescales, data analyses of many diverse lakes are needed to characterize the extent to which the full positive feedback plays a role in controlling dissolved oxygen dynamics within lakes around the world.

In comparison with many of the relationships in the ABA feedback, effects of dissolved oxygen on Fe-mediated organic carbon cycling have received less attention. However, observational studies provide support for a strong association between Fe and organic carbon dynamics in lakes. In particular, dissolved organic carbon concentrations are strongly correlated with concentrations of Fe across many freshwater ecosystems (Björnerås et al., 2017; von Wachenfeldt et al., 2008; Weyhenmeyer et al., 2014), and high aqueous Fe concentrations are associated with increased sediment organic carbon accumulation in boreal lakes (Einola et al., 2011). Moreover, it is well-documented that dissolved organic carbon can be released from aquatic sediments under low-oxygen conditions, which is often attributed to reductive dissolution of Fe(III) (Kim & Kim, 2020; Peter et al., 2017; Yang et al., 2014). In soils and marine sediments, associations between iron and organic carbon appear to play a critical role in carbon sequestration over decades to millennia (e.g., Barber et al., 2017; Hemingway et al., 2019; Kramer & Chadwick, 2018; Lalonde et al., 2012). However, few studies have examined whether reactions involving iron-bound organic carbon (Fe-OC) complexes are responsible for observed correlations between dissolved Fe and organic carbon in freshwater environments. Given the conflicting patterns that Fe-OC complexes can be preserved in soils and sediments over decades to millennia and yet may be unstable under the reducing conditions which commonly occur on day to month timescales in freshwater lake sediments, it ultimately remains unclear how changing oxygen dynamics will affect coupled organic carbon and Fe cycling in freshwater lakes.

Predicting the effects of dynamic oxygen conditions on sediment organic carbon is further complicated by altered rates of respiration under low-oxygen conditions. While reactions involving Fe-OC are expected to decrease carbon sequestration in sediment under low-oxygen conditions (i.e., through reductive dissolution of Fe(III) in Fe-OC complexes), respiration rates are also expected to be slower under anoxic conditions due to enzymatic limitations and because alternative electron acceptors result in a lower microbial energy yield than oxygen (Bastviken et al., 2003, 2004a). In the absence of changes in Fe-OC, decreased respiration rates could therefore lead to increased burial of organic carbon under low-oxygen conditions (Bastviken et al., 2003, 2004a; Carey et al., 2018, 2022b; Sobek et al., 2009, 2011, 2017). However, it is unknown whether decreases in organic carbon respiration rates outweigh increases in iron-mediated organic carbon release from sediment to determine the net effect of low oxygen conditions on organic carbon sequestration in lake sediment.

In summary, numerous questions remain with respect to the consequences of anoxia in lakes worldwide. Effects of anoxia on internal nutrient loading have been well-established by decades of studies on microcosm to local or regional scales (e.g., Mortimer, 1941; Nürnberg, 1984; Orihel et al., 2017). However, it is unknown whether these changes extend to create a detectable positive feedback that promotes subsequent anoxia across widespread lakes. Furthermore, the strength of the ABA feedback is likely to differ across lakes as a result of variation in lake characteristics including size and residence time (e.g., Jagtman et al., 1992; Zhao et al., 2023), though these mediating interactions had not been assessed at a broad spatial scale prior to this work. For carbon cycling, anoxia is expected to disrupt Fe-OC compounds in sediment, decreasing carbon burial. However, levels of Fe-OC are poorly characterized in freshwater sediment, and it is unknown whether changes in iron-mediated organic carbon release outweigh decreased respiration rates under anoxic conditions to shape the net effects of anoxia on sediment organic carbon burial. Ultimately, as oxygen concentrations continue to decline in many lakes around the world (e.g., Jane et al., 2021; Jenny et al., 2016a), resolving these uncertainties will help predict future changes in lake ecosystem functioning at both local and global scales.

Antecedent conditions mediate summer bottom-water dissolved oxygen dynamics

Both the causes and consequences of changes in bottom-water dissolved oxygen across lakes may be mediated, in part, by conditions occurring months to years before the time of analysis. Here, we use the term “ecological memory” to describe the role of antecedent conditions in shaping the present state of the ecosystem (following, e.g., Dugan, 2021; Hanson et al. 2023; Johnstone et al. 2016; Ogle et al., 2015; Pilla et al., 2023). Accounting for ecological memory may be important to predicting future change in bottom-water biogeochemistry. For example, through the ABA feedback described above, anoxic bottom-water conditions in previous years are expected to play an important role in perpetuating anoxia, even in the absence of continued climate or land use change. Similarly, the stability of Fe-OC compounds in sediment is likely dependent in part upon antecedent environmental conditions, as bonds between Fe and organic matter form over time through the rearrangement of organic molecules (Kaiser et al., 2007).

Current efforts to predict future anoxia are limited by the fact that bottom-water temperature trends are highly variable across lakes and show little to no correlation with summer air temperature trends (Pilla et al., 2020; Winslow et al., 2017; Zhou et al., 2023), and we anticipate that ecological memory may play a role in this disconnect.

While summer thermal stratification limits the correlation between summer air temperature and summer bottom water temperature or dissolved oxygen dynamics (Wetzel 2001), heat can exchange throughout the entire water column during the mixing period prior to the onset of stratification. Increased water temperature during the spring mixing period could then decrease oxygen solubility and increase the rate of oxygen demand throughout the subsequent stratified period (Oleksy & Richardson, 2021; Pilla et al., 2023; Yvon-Durocher et al., 2012). This thermal exchange prior to stratification, in combination with effects of spring air temperature on the phenology of ice thaw and/or stratification onset (e.g., Dugan, 2021; Jane et al., 2023; Ladwig et al., 2021), may then cause summer bottom-water conditions to be more correlated with spring, compared to summer, air temperatures. However, while there are plausible reasons to expect ecological memory effects on temperature and dissolved oxygen dynamics in the bottom waters of temperate lakes, this mechanism has not been characterized across widespread lakes. Ultimately, as climate change is associated with differential changes in air temperature among seasons (IPCC, 2023a), characterizing the existence and strength of ecological memory across lakes worldwide will help anticipate future effects of climate change on summer bottom-water oxygen dynamics.

Ecological forecasts: Specific, quantitative predictions to advance climate resilience

Predicting *future* changes in lake biogeochemistry will require not only fundamental ecological understanding, but also rigorous frameworks for the prediction of future ecosystem states (Clark et al., 2001; Dietze et al., 2018; Luo et al., 2011). Over the past several decades, advances in data availability, computational power, and statistical methodologies have enabled a substantial increase in the development and application of ecological forecasts across many ecosystems (Hampton et al., 2013; LaDeau et al., 2017; Luo et al., 2011; Petrovskii & Petrovskaya, 2012). These forecasts have been developed for a wide range of horizons (the amount of time into the future for which predictions are made), enabling improved ecological management days to centuries in the future. In particular, near-term (daily to decadal) ecological forecasts have been especially helpful for guiding ecological management decisions, which are frequently made over these shorter-term timescales (Carey et al., 2022a; Dietze et al., 2018).

As forecast production has increased, there have been numerous calls for the adoption of standardized best practices in near-term ecological forecasting (Carey et al., 2022a; Clark et al., 2001; Dietze et al., 2018, 2023; Harris et al., 2018; Hobday et al., 2019; Pielke & Conant, 2003; White et al., 2019). Developing and adhering to best practices advances the contributions of forecasting to both basic and applied research, as it allows for comparisons of forecast accuracy and increases the reliability of forecast products as decision support tools (Armstrong, 2001; Dietze et al., 2023). However, there has been no systematic analysis of best practices in ecological forecasting prior to this dissertation, making it difficult to synthesize diverse research efforts and prioritize future developments for this emerging field.

Notably, while ecological forecasts are often developed with the goal of advancing ecological management, ecological forecasts also have the potential to contribute to the development of ecological theory (Dietze, 2017; Dietze et al., 2018;

Lewis et al., 2023). In particular, as the number of published near-term ecological forecasts has increased over the past several decades (Dietze et al., 2018; Luo et al., 2011), we now have the opportunity to compare across studies and analyze the relative predictability of environmental variables at varying forecast horizons. Previous theoretical and modeling-based analyses suggest that seemingly distinct ecological phenomena (e.g., dissolved oxygen, epidemics, invasive species) may show congruent patterns of predictability (Lewis et al., 2023; Petchey et al., 2015; Ward et al., 2014). Analyzing the patterns of predictability across ecological variables may thus provide transferable insight for addressing new ecological questions. In doing so, we can harness research findings across sub-disciplines of ecology to advance a broader understanding of ecological function across scales and variables. Similarly, analysis of predictability across ecological variables may be useful as a means of identifying areas (i.e., variables, locations, and forecast horizons) where we would expect forecasts to perform well, helping to target forecast development for management and ecological insight (see Bolam et al., 2019; Pennekamp et al., 2019; Şen et al., 2023). Ultimately, ecological forecasting is a particularly powerful test of predictability, as forecasting requires predicting novel conditions beyond the range of observed data (Dietze et al., 2018; Lewis et al., 2023) and synthesis of ecological forecasts is needed to empirically characterize the drivers of forecast performance across scales and variables.

Scope of dissertation chapters

Throughout my dissertation, I aimed to build a predictive understanding of how bottom-water dissolved oxygen may mediate changes in water quality across widespread temperate lakes (Figure 1). To do so, I analyzed both the causes (Chapters II and III) and consequences (Chapters III and IV) of bottom-water oxygen decline over multiple spatiotemporal scales (Figure 1), and I synthesized research to advance the development of near-term ecological forecasting (Chapter V). Specifically, I first aimed to characterize the role of climate change in driving bottom-water dissolved oxygen declines by assessing the relative influence of spring vs. summer air temperature on bottom-water dynamics in >600 widespread lakes (Chapter II; Lewis et al. *in review*). I then analyzed whether data from these widespread lakes support the existence of an ABA feedback, through which low-oxygen conditions promote eutrophication and perpetuate anoxia in future years (Chapter III; Lewis et al. 2024). Third, I used experiments on both microcosm and whole-ecosystem scales to assess how low oxygen conditions affect coupled organic carbon and Fe cycling over both short-term (2–4 weeks) and multi-annual timescales (Chapter IV; Lewis et al. 2023). Ultimately, forecasts of future biogeochemical dynamics will be central to making these insights actionable for lake management. In Chapter V (Lewis et al. 2022), I conducted a systematic literature review to characterize emerging best practices in near-term ecological forecasting, contributing to the development of this new field (Figure 1). As a whole, my dissertation provides a temporally-explicit examination of biogeochemical processes occurring in the bottom-waters of temperate lakes, using historical dynamics to help understand and predict the effects of anthropogenic change on lake ecosystems worldwide.

Chapter I References

Adger, W. N., Barnett, J., Brown, K., Marshall, N., & O'Brien, K. (2013). Cultural dimensions of climate change impacts and adaptation. *Nature Climate Change, 3*(2), 112–117. https://doi.org/10.1038/nclimate1666

Adrian, R., O'Reilly, C. M., Zagarese, H., Baines, S. B., Hessen, D. O., Keller, W., Livingstone, D. M., Sommaruga, R., Straile, D., Van Donk, E., Weyhenmeyer, G. A., & Winder, M. (2009). Lakes as sentinels of climate change. *Limnology and Oceanography*, *54*(6part2), 2283–2297. https://doi.org/10.4319/lo.2009.54.6_part_2.2283

Armstrong, J. S. (2001). Standards and Practices for Forecasting. In J. S. Armstrong (Ed.), *Principles of Forecasting: A Handbook for Researchers and Practitioners* (pp. 679–732). Boston, MA: Springer US. https://doi.org/10.1007/978-0-306-47630-3_31

Austin, J. A., & Colman, S. M. (2007). Lake Superior summer water temperatures are increasing more rapidly than regional air temperatures: A positive ice-albedo feedback. *Geophysical Research Letters*, *34*(6). https://doi.org/10.1029/2006GL029021

Barber, A., Brandes, J., Leri, A., Lalonde, K., Balind, K., Wirick, S., Wang, J., & Gélinas, Y. (2017). Preservation of organic matter in marine sediments by inner-sphere interactions with reactive iron. *Scientific Reports*, *7*(1), 366. https://doi.org/10.1038/s41598-017-00494-0

Bartosiewicz, M., Przytulska, A., Lapierre, J.-F., Laurion, I., Lehmann, M. F., & Maranger, R. (2019). Hot tops, cold bottoms: Synergistic climate warming and shielding effects increase carbon burial in lakes. *Limnology and Oceanography Letters*, *4*(5), 132–144. https://doi.org/10.1002/lol2.10117

Bastviken, D., Olsson, M., & Tranvik, L. (2003). Simultaneous measurements of organic carbon mineralization and bacterial production in oxic and anoxic lake sediments. *Microbial Ecology*, *46*(1), 73–82. https://doi.org/10.1007/s00248-002-1061-9

Bastviken, D., Persson, L., Odham, G., & Tranvik, L. (2004a). Degradation of dissolved organic matter in oxic and anoxic lake water. *Limnology and Oceanography*, *49*(1), 109–116. https://doi.org/10.4319/lo.2004.49.1.0109

Bastviken, D., Cole, J., Pace, M., & Tranvik, L. (2004b). Methane emissions from lakes: Dependence of lake characteristics, two regional assessments, and a global estimate. *Global Biogeochemical Cycles*, *18*(4). https://doi.org/10.1029/2004GB002238

Bastviken, D., Tranvik, L. J., Downing, J. A., Crill, P. M., & Enrich-Prast, A. (2011). Freshwater methane emissions offset the continental carbon sink. *Science*, *331*(6013), 50–50. https://doi.org/10.1126/science.1196808

Battin, T. J., Luyssaert, S., Kaplan, L. A., Aufdenkampe, A. K., Richter, A., & Tranvik, L. J. (2009). The boundless carbon cycle. *Nature Geoscience*, *2*(9), 598–600. https://doi.org/10.1038/ngeo618

Bellard, C., Bertelsmeier, C., Leadley, P., Thuiller, W., & Courchamp, F. (2012). Impacts of climate change on the future of biodiversity. *Ecology Letters*, *15*(4), 365–377. https://doi.org/10.1111/j.1461-0248.2011.01736.x

Björnerås, C., Weyhenmeyer, G. A., Evans, C. D., Gessner, M. O., Grossart, H.-P., Kangur, K., Kokorite, I., Kortelainen, P., Laudon, H., Lehtoranta, J., Lottig, N., Monteith, D. T., Nõges, P., Nõges, T., Oulehle, F., Riise, G., Rusak, J. A., Räike, A., Sire, J., Sterling, S., & Kritzberg, E. S. (2017). Widespread increases in iron concentration in European and North American freshwaters. *Global Biogeochemical Cycles*, *31*(10), 1488–1500. https://doi.org/10.1002/2017GB005749

Bolam, F. C., Grainger, M. J., Mengersen, K. L., Stewart, G. B., Sutherland, W. J., Runge, M. C., & McGowan, P. J. K. (2019). Using the Value of Information to improve conservation decision making. *Biological Reviews*, *94*(2), 629–647. https://doi.org/10.1111/brv.12471

Carey, C. C., Doubek, J. P., McClure, R. P., & Hanson, P. C. (2018). Oxygen dynamics control the burial of organic carbon in a eutrophic reservoir. *Limnology and Oceanography Letters*, *3*(3), 293–301. https://doi.org/10.1002/lol2.10057

Carey, C. C., Woelmer, W. M., Lofton, M. E., Figueiredo, R. J., Bookout, B. J., Corrigan, R. S., Daneshmand, V., Hounshell, A. G., Howard, D. W., Lewis, A. S. L., McClure, R. P., Wander, H. L., Ward, N. K., & Thomas, R. Q. (2022a). Advancing lake and reservoir water quality management with near-term, iterative ecological forecasting. *Inland Waters*, *12*(1), 107–120. https://doi.org/10.1080/20442041.2020.1816421

Carey, C. C., Hanson, P. C., Thomas, R. Q., Gerling, A. B., Hounshell, A. G., Lewis, A. S. L., Lofton, M. E., McClure, R. P., Wander, H. L., Woelmer, W. M., Niederlehner, B. R., & Schreiber, M. E. (2022b). Anoxia decreases the magnitude of the carbon, nitrogen, and phosphorus sink in freshwaters. *Global Change Biology*, *28*(16), 4861–4881. https://doi.org/10.1111/gcb.16228

Clark, J. S., Carpenter, S. R., Barber, M., Collins, S., Dobson, A., Foley, J. A., Lodge, D. M., Pascual, M., Pielke, R., Pizer, W., Pringle, C., Reid, W. V., Rose, K. A., Sala, O., Schlesinger, W. H., Wall, D. H., & Wear, D. (2001). Ecological Forecasts: An Emerging Imperative. *Science*, *293*(5530), 657–660. https://doi.org/10.1126/science.293.5530.657

Comte, L., Buisson, L., Daufresne, M., & Grenouillet, G. (2013). Climate-induced changes in the distribution of freshwater fish: observed and predicted trends. *Freshwater Biology*, *58*(4), 625–639. https://doi.org/10.1111/fwb.12081

Crosby, W. O. (1884). The Colors of Natural Waters. *Science*, *ns-3*(62), 445–446. https://doi.org/10.1126/science.ns-3.62.445

Dean, W. E., & Gorham, E. (1998). Magnitude and significance of carbon burial in lakes, reservoirs, and peatlands, 4.

Deemer, B. R., Harrison, J. A., Li, S., Beaulieu, J. J., DelSontro, T., Barros, N., Bezerra-Neto, J. F., Powers, S. M., dos Santos, M. A., & Vonk, J. A. (2016). Greenhouse gas emissions from reservoir water surfaces: A new global synthesis. *BioScience*, *66*(11), 949–964. https://doi.org/10.1093/biosci/biw117

DelSontro, T., Beaulieu, J. J., & Downing, J. A. (2018). Greenhouse gas emissions from lakes and impoundments: Upscaling in the face of global change. *Limnology and Oceanography Letters*, *3*(3), 64–75. https://doi.org/10.1002/lol2.10073

Dietze, M. C. (2017). Scientific Workflows and the Informatics of Model-Data Fusion. In *Ecological Forecasting* (pp. 44–52). Princeton University Press. https://doi.org/10.2307/j.ctvc7796h.8

Dietze, M. C., Fox, A., Beck-Johnson, L. M., Betancourt, J. L., Hooten, M. B., Jarnevich, C. S., Keitt, T. H., Kenney, M. A., Laney, C. M., Larsen, L. G., Loescher, H. W., Lunch, C. K., Pijanowski, B. C., Randerson, J. T., Read, E. K., Tredennick, A. T., Vargas, R., Weathers, K. C., & White, E. P. (2018). Iterative near-term ecological forecasting: Needs, opportunities, and challenges. *Proceedings of the National Academy of Sciences*, *115*(7), 1424–1432. https://doi.org/10.1073/pnas.1710231115

Dietze, M. C., Thomas, R. Q., Peters, J., Boettiger, C., Koren, G., Shiklomanov, A. N., & Ashander, J. (2023). A community convention for ecological forecasting: Output files and metadata version 1.0. *Ecosphere*, *14*(11), e4686. https://doi.org/10.1002/ecs2.4686

Dokulil, M. T., de Eyto, E., Maberly, S. C., May, L., Weyhenmeyer, G. A., & Woolway, R. I. (2021). Increasing maximum lake surface temperature under climate change. *Climatic Change*, *165*(3), 56. https://doi.org/10.1007/s10584-021-03085-1

Dugan, H. A. (2021). A Comparison of Ecological Memory of Lake Ice-Off in Eight North-Temperate Lakes. *Journal of Geophysical Research: Biogeosciences*, *126*(6), e2020JG006232. https://doi.org/10.1029/2020JG006232

Einola, E., Rantakari, M., Kankaala, P., Kortelainen, P., Ojala, A., Pajunen, H., Mäkelä, S., & Arvola, L. (2011). Carbon pools and fluxes in a chain of five boreal lakes: A dry and wet year comparison. *Journal of Geophysical Research: Biogeosciences*, *116*(G3). https://doi.org/10.1029/2010JG001636

Encinas Fernández, J., Peeters, F., & Hofmann, H. (2014). Importance of the Autumn Overturn and Anoxic Conditions in the Hypolimnion for the Annual Methane Emissions from a Temperate Lake. *Environmental Science & Technology*, *48*(13), 7297–7304. https://doi.org/10.1021/es4056164

Finlayson, C. M., de Groot, R. S., Hughes, F. M. R., & Sullivan, C. A. (2018). Freshwater Ecosystem Services and Functions. In J. Hughes (Ed.), *Freshwater Ecology and Conservation: Approaches and Techniques* (p. 0). Oxford University Press. https://doi.org/10.1093/oso/9780198766384.003.0015

Foley, B., Jones, I. D., Maberly, S. C., & Rippey, B. (2012). Long-term changes in oxygen depletion in a small temperate lake: effects of climate change and eutrophication. *Freshwater Biology*, *57*(2), 278–289. https://doi.org/10.1111/j.1365-2427.2011.02662.x

Hampton, S. E., Strasser, C. A., Tewksbury, J. J., Gram, W. K., Budden, A. E., Batcheller, A. L., Duke, C. S., & Porter, J. H. (2013). Big data and the future of ecology. *Frontiers in Ecology and the Environment*, *11*(3), 156–162. https://doi.org/10.1890/120103

Hanson, P. C., Ladwig, R., Buelo, C., Albright, E. A., Delany, A. D., & Carey, C. C. (2023). Legacy Phosphorus and Ecosystem Memory Control Future Water Quality in a Eutrophic Lake. *Journal of Geophysical Research: Biogeosciences*, *128*(12), e2023JG007620. https://doi.org/10.1029/2023JG007620

Harris, D. J., Taylor, S. D., & White, E. P. (2018). Forecasting biodiversity in breeding birds using best practices. *PeerJ*, *6*, e4278. https://doi.org/10.7717/peerj.4278

Hemingway, J. D., Rothman, D. H., Grant, K. E., Rosengard, S. Z., Eglinton, T. I., Derry, L. A., & Galy, V. V. (2019). Mineral protection regulates long-term global preservation of natural organic carbon. *Nature*, *570*(7760), 228–231. https://doi.org/10.1038/s41586-019-1280-6

Ho, J. C., Michalak, A. M., & Pahlevan, N. (2019). Widespread global increase in intense lake phytoplankton blooms since the 1980s. *Nature*, *574*(7780), 667–670. https://doi.org/10.1038/s41586-019-1648-7

Hobday, A. J., Hartog, J. R., Manderson, J. P., Mills, K. E., Oliver, M. J., Pershing, A. J., & Siedlecki, S. (2019). Ethical considerations and unanticipated consequences associated with ecological forecasting for marine resources. *ICES Journal of Marine Science*, *76*(5), 1244–1256. https://doi.org/10.1093/icesjms/fsy210

Hounshell, A. G., McClure, R. P., Lofton, M. E., & Carey, C. C. (2021). Whole-ecosystem oxygenation experiments reveal substantially greater hypolimnetic methane concentrations in reservoirs during anoxia. *Limnology and Oceanography Letters*, *6*(1), 33–42. https://doi.org/10.1002/lol2.10173

Huang, L., Wang, X., Yan, Y., Jin, L., Yang, K., Chen, A., Zheng, R., Ottlé, C., Wang, C., Cui, Y., & Piao, S. (2023). Attribution of Lake Surface Water Temperature Change in Large Lakes Across China Over Past Four Decades. *Journal of Geophysical Research: Atmospheres*, *128*(21), e2022JD038465. https://doi.org/10.1029/2022JD038465

Hupfer, M., & Lewandowski, J. (2008). Oxygen Controls the Phosphorus Release from Lake Sediments – a Long-Lasting Paradigm in Limnology. *International Review of Hydrobiology*, *93*(4–5), 415–432. https://doi.org/10.1002/iroh.200711054

IPCC. (2023a). Climate Change 2021 – The Physical Science Basis: Working Group I Contribution to the Sixth Assessment Report of the Intergovernmental Panel on Climate Change (1st ed.). Cambridge University Press. https://doi.org/10.1017/9781009157896

IPCC. (2023b). Climate Change 2023: Synthesis Report. Contribution of Working Groups I, II and III to the Sixth Assessment Report of the Intergovernmental Panel on Climate Change. (H. Core Writing Team, H. Lee, & J. Romero, Eds.). Genva, Switzerland. Retrieved from 10.59327/IPCC/AR6-9789291691647

Jagtman, E., Van der Molen, D. T., & Vermij, S. (1992). The influence of flushing on nutrient dynamics, composition and densities of algae and transparency in Veluwemeer, The Netherlands. *Hydrobiologia*, *233*(1), 187–196. https://doi.org/10.1007/BF00016107

Jane, S. F., Hansen, G., Kraemer, B., Leavitt, P., Mincer, J., North, R., Pilla, R., Stetler, J., Williamson, C., Woolway, R., Arvola, L., Chandra, S., DeGasperi, C., Diemer, L., Dunalska, J., Erina, O., Flaim, G., Grossart, H.-P., Hambright, K., & Rose, K. (2021). Widespread deoxygenation of temperate lakes. *Nature*, *594*. https://doi.org/10.1038/s41586-021-03550-y

Jane, S. F., Mincer, J. L., Lau, M. P., Lewis, A. S. L., Stetler, J. T., & Rose, K. C. (2023). Longer duration of seasonal stratification contributes to widespread increases in lake hypoxia and anoxia. *Global Change Biology*, *29*(4), 1009–1023. https://doi.org/10.1111/gcb.16525

Jansen, J., Woolway, R. I., Kraemer, B. M., Albergel, C., Bastviken, D., Weyhenmeyer, G. A., Marcé, R., Sharma, S., Sobek, S., Tranvik, L. J., Perroud, M., Golub, M., Moore, T. N., Råman Vinnå, L., La Fuente, S., Grant, L., Pierson, D. C., Thiery, W., & Jennings, E. (2022). Global increase in methane production under future warming of lake bottom waters. *Global Change Biology*, *28*(18), 5427–5440. https://doi.org/10.1111/gcb.16298

Jenny, J.-P., Francus, P., Normandeau, A., Lapointe, F., Perga, M.-E., Ojala, A., Schimmelmann, A., & Zolitschka, B. (2016a). Global spread of hypoxia in freshwater ecosystems during the last three centuries is caused by rising local human pressure. *Global Change Biology*, *22*(4), 1481–1489. https://doi.org/10.1111/gcb.13193

Jenny, J.-P., Normandeau, A., Francus, P., Taranu, Z. E., Gregory-Eaves, I., Lapointe, F., Jautzy, J., Ojala, A. E. K., Dorioz, J.-M., Schimmelmann, A., & Zolitschka, B.

(2016b). Urban point sources of nutrients were the leading cause for the historical spread of hypoxia across European lakes. *Proceedings of the National Academy of Sciences*, *113*(45), 12655–12660. https://doi.org/10.1073/pnas.1605480113

Johnstone, J. F., Allen, C. D., Franklin, J. F., Frelich, L. E., Harvey, B. J., Higuera, P. E., Mack, M. C., Meentemeyer, R. K., Metz, M. R., Perry, G. L., Schoennagel, T., & Turner, M. G. (2016). Changing disturbance regimes, ecological memory, and forest resilience. *Frontiers in Ecology and the Environment*, *14*(7), 369–378. https://doi.org/10.1002/fee.1311

Kaiser, K., Mikutta, R., & Guggenberger, G. (2007). Increased stability of organic matter sorbed to ferrihydrite and goethite on aging. *Soil Science Society of America Journal*, *71*(3), 711–719. https://doi.org/10.2136/sssaj2006.0189

Kim, J., & Kim, T.-H. (2020). Distribution of Humic Fluorescent Dissolved Organic Matter in Lake Shihwa: the Role of the Redox Condition. *Estuaries and Coasts*, *43*(3), 578–588. https://doi.org/10.1007/s12237-018-00491-0

Kirk, G. (2004). Reduction and Oxidation. In G. Kirk (Ed.), *The Biogeochemistry of Submerged Soils* (pp. 93–134). John Wiley & Sons, Ltd. https://doi.org/10.1002/047086303X.ch4

Knoll, L. B., Vanni, M. J., Renwick, W. H., Dittman, E. K., & Gephart, J. A. (2013). Temperate reservoirs are large carbon sinks and small CO2 sources: Results from high-resolution carbon budgets. *Global Biogeochemical Cycles*, *27*(1), 52–64. https://doi.org/10.1002/gbc.20020

Kraemer, B. M., Anneville, O., Chandra, S., Dix, M., Kuusisto, E., Livingstone, D. M., Rimmer, A., Schladow, S. G., Silow, E., Sitoki, L. M., Tamatamah, R., Vadeboncoeur, Y., & McIntyre, P. B. (2015). Morphometry and average temperature affect lake stratification responses to climate change. *Geophysical Research Letters*, *42*(12), 4981–4988. https://doi.org/10.1002/2015GL064097

Kramer, M. G., & Chadwick, O. A. (2018). Climate-driven thresholds in reactive mineral retention of soil carbon at the global scale. *Nature Climate Change*, *8*(12), 1104–1108. https://doi.org/10.1038/s41558-018-0341-4

LaDeau, S. L., Han, B. A., Rosi-Marshall, E. J., & Weathers, K. C. (2017). The Next Decade of Big Data in Ecosystem Science. *Ecosystems*, *20*(2), 274–283. https://doi.org/10.1007/s10021-016-0075-y

Ladwig, R., Hanson, P. C., Dugan, H. A., Carey, C. C., Zhang, Y., Shu, L., Duffy, C. J., & Cobourn, K. M. (2021). Lake thermal structure drives interannual variability in summer anoxia dynamics in a eutrophic lake over 37 years. *Hydrology and Earth System Sciences*, *25*(2), 1009–1032. https://doi.org/10.5194/hess-25-1009-2021

Lalonde, K., Mucci, A., Ouellet, A., & Gélinas, Y. (2012). Preservation of organic matter in sediments promoted by iron. *Nature*, *483*(7388), 198–200. https://doi.org/10.1038/nature10855

LaRowe, D. E., & Van Cappellen, P. (2011). Degradation of natural organic matter: A thermodynamic analysis. *Geochimica et Cosmochimica Acta*, *75*(8), 2030–2042. https://doi.org/10.1016/j.gca.2011.01.020

Lewis, A. S. L., Rollinson, C. R., Allyn, A. J., Ashander, J., Brodie, S., Brookson, C. B., Collins, E., Dietze, M. C., Gallinat, A. S., Juvigny-Khenafou, N., Koren, G., McGlinn, D. J., Moustahfid, H., Peters, J. A., Record, N. R., Robbins, C. J., Tonkin, J., & Wardle, G. M. (2023). The power of forecasts to advance ecological theory. *Methods in Ecology and Evolution*, *14*(3), 746–756. https://doi.org/10.1111/2041-210X.13955

Luo, Y., Ogle, K., Tucker, C., Fei, S., Gao, C., LaDeau, S., Clark, J. S., & Schimel, D. S. (2011). Ecological forecasting and data assimilation in a data-rich era. *Ecological Applications*, *21*(5), 1429–1442. https://doi.org/10.1890/09-1275.1

Lynch, A. J., Cooke, S. J., Arthington, A. H., Baigun, C., Bossenbroek, L., Dickens, C., Harrison, I., Kimirei, I., Langhans, S. D., Murchie, K. J., Olden, J. D., Ormerod, S. J., Owuor, M., Raghavan, R., Samways, M. J., Schinegger, R., Sharma, S., Tachamo-Shah, R.-D., Tickner, D., Tweddle, D., Young, N., & Jähnig, S. C. (2023). People need freshwater biodiversity. *WIREs Water*, 10(3), e1633. https://doi.org/10.1002/wat2.1633

Millennium Ecosystem Assessment (MA). (2005). Ecosystems and human well-being: wetlands and water synthesis. Island Press, Washington DC.

Maranger, R., Jones, S. E., & Cotner, J. B. (2018). Stoichiometry of carbon, nitrogen, and phosphorus through the freshwater pipe. *Limnology and Oceanography Letters*, *3*(3), 89-101. https://doi.org/10.1002/lol2.10080

Mason, P. J., Zillman, J. W., Simmons, A., Lindstrom, E. J., Harrison, D. E., Dolman, H., Bojinski, S., Fischer, A., Latham, J., Rasmussen, J., Arkin, P., Armstrong, R., Braathen, G., Brouchkov, A., DeWayne Cecil, L., Digiacomo, P. M., Drinkwater, M. R., Goldammer, J. G., Goldberg, M. D., Goodison, B., Haeberli, W., Hilsenrath, E., Jones, P., Kajfez-Bogataj, L., Kent, E. C., Kundzewicz, Z. W., Lafeuille, J., Levelt, P. F., Looser, U., Ogallo, L. A., Ondras, M., Peterson, T. C., Pinty, B., Quegan, S., Saunders, R., Schmetz, J., Song, L., Stammer, D., Steffen, K., Tanner, M., Tansey, K., Trenberth, K. E., Verstraete, M. M., Visbeck, M., Vuglinsky, V., Westermeyer, W., & Wooster, M. (2010, August). Implementation Plan for the Global Observing System for Climate in Support of the UNFCCC (2010 Update) [Monograph]. Retrieved February 5, 2024, from https://eprints.soton.ac.uk/162953/

Mendonça, R., Müller, R. A., Clow, D., Verpoorter, C., Raymond, P., Tranvik, L. J., & Sobek, S. (2017). Organic carbon burial in global lakes and reservoirs. *Nature Communications*, *8*(1), 1694. https://doi.org/10.1038/s41467-017-01789-6

Mortimer, C. H. (1941). The Exchange of Dissolved Substances Between Mud and Water in Lakes. *Journal of Ecology*, *29*(2), 280–329. https://doi.org/10.2307/2256395

Müller, B., Steinsberger, T., Schwefel, R., Gächter, R., Sturm, M., & Wüest, A. (2019). Oxygen consumption in seasonally stratified lakes decreases only below a marginal phosphorus threshold. *Scientific Reports*, *9*(1), 18054. https://doi.org/10.1038/s41598-019-54486-3

Nierop, K. G. J., Jansen, B., & Verstraten, J. M. (2002). Dissolved organic matter, aluminium and iron interactions: precipitation induced by metal/carbon ratio, pH and competition. *The Science of the Total Environment*, *300*(1–3), 201–211. https://doi.org/10.1016/s0048-9697(02)00254-1

North, R. L., Barton, D., Crowe, A. S., Dillon, P. J., Dolson, R. M. L., Evans, D. O., Ginn, B. K., Håkanson, L., Hawryshyn, J., Jarjanazi, H., King, J. W., La Rose, J. K. L., León, L., Lewis, C. F. M., Liddle, G. E., Lin, Z. H., Longstaffe, F. J., Macdonald, R. A., Molot, L., Ozersky, T., Palmer, M. E., Quinlan, R., Rennie, M. D., Robillard, M. M., Rodé, D., Rühland, K. M., Schwalb, A., Smol, J. P., Stainsby, E., Trumpickas, J. J., Winter, J. G., & Young, J. D. (2013). The state of Lake Simcoe (Ontario, Canada): the effects of multiple stressors on phosphorus and oxygen dynamics. *Inland Waters*, *3*(1), 51–74. https://doi.org/10.5268/IW-3.1.529

Nürnberg, G., & Peters, R. H. (1984). The importance of internal phosphorus load to the eutrophication of lakes with anoxic hypolimnia. *SIL Proceedings, 1922-2010*, *22*(1), 190–194. https://doi.org/10.1080/03680770.1983.11897287

Nürnberg, G. K. (1984). The prediction of internal phosphorus load in lakes with anoxic hypolimnia1. *Limnology and Oceanography*, *29*(1), 111–124. https://doi.org/10.4319/lo.1984.29.1.0111

Ogle, K., Barber, J. J., Barron-Gafford, G. A., Bentley, L. P., Young, J. M., Huxman, T. E., Loik, M. E., & Tissue, D. T. (2015). Quantifying ecological memory in plant and ecosystem processes. *Ecology Letters*, *18*(3), 221–235. https://doi.org/10.1111/ele.12399

Oleksy, I. A., & Richardson, D. C. (2021). Climate change and teleconnections amplify lake stratification with differential local controls of surface water warming and deep water cooling. *Geophysical Research Letters*, *48*(5), e2020GL090959. https://doi.org/10.1029/2020GL090959

O'Reilly, C. M., Sharma, S., Gray, D. K., Hampton, S. E., Read, J. S., Rowley, R. J., Schneider, P., Lenters, J. D., McIntyre, P. B., Kraemer, B. M., Weyhenmeyer, G. A., Straile, D., Dong, B., Adrian, R., Allan, M. G., Anneville, O., Arvola, L., Austin, J., Bailey, J. L., Baron, J. S., Brookes, J. D., Eyto, E. de, Dokulil, M. T., Hamilton, D. P., Havens, K., Hetherington, A. L., Higgins, S. N., Hook, S., Izmest'eva, L. R., Joehnk, K. D., Kangur, K., Kasprzak, P., Kumagai, M., Kuusisto, E., Leshkevich, G., Livingstone, D. M., MacIntyre, S., May, L., Melack, J. M., Mueller-Navarra, D. C., Naumenko, M., Noges, P., Noges, T., North, R. P., Plisnier, P.-D., Rigosi, A., Rimmer, A., Rogora, M., Rudstam, L. G., Rusak, J. A., Salmaso, N., Samal, N. R., Schindler, D. E., Schladow, S. G., Schmid, M., Schmidt, S. R., Silow, E., Soylu, M. E., Teubner, K., Verburg, P., Voutilainen, A., Watkinson, A., Williamson, C. E., & Zhang, G. (2015). Rapid and highly variable warming of lake surface waters around the globe. *Geophysical Research Letters*, *42*(24), 10,773-10,781. https://doi.org/10.1002/2015GL066235

Orihel, D. M., Baulch, H. M., Casson, N. J., North, R. L., Parsons, C. T., Seckar, D. C. M., & Venkiteswaran, J. J. (2017). Internal phosphorus loading in Canadian fresh waters: a critical review and data analysis. *Canadian Journal of Fisheries and Aquatic Sciences*, *74*(12), 2005–2029. https://doi.org/10.1139/cjfas-2016-0500

Pace, M. L., & Prairie, Y. T. (2005). Respiration in lakes. In P. del Giorgio & P. Williams (Eds.), *Respiration in Aquatic Ecosystems* (pp. 103–121). Oxford University Press. https://doi.org/10.1093/acprof:oso/9780198527084.003.0007

Pacheco, F. S., Roland, F., & Downing, J. A. (2014). Eutrophication reverses whole-lake carbon budgets. *Inland Waters*, *4*(1), 41–48. https://doi.org/10.5268/IW-4.1.614

Paerl, H. W., & Huisman, J. (2008). Blooms Like It Hot. *Science*, *320*(5872), 57–58. https://doi.org/10.1126/science.1155398

Pan, W., Kan, J., Inamdar, S., Chen, C., & Sparks, D. (2016). Dissimilatory microbial iron reduction release DOC (dissolved organic carbon) from carbon-ferrihydrite association. *Soil Biology and Biochemistry*, *103*, 232–240. https://doi.org/10.1016/j.soilbio.2016.08.026

Patzner, M. S., Mueller, C. W., Malusova, M., Baur, M., Nikeleit, V., Scholten, T., Hoeschen, C., Byrne, J. M., Borch, T., Kappler, A., & Bryce, C. (2020). Iron mineral dissolution releases iron and associated organic carbon during permafrost thaw. *Nature Communications*, *11*(1), 6329. https://doi.org/10.1038/s41467-020-20102-6

Pennekamp, F., Iles, A. C., Garland, J., Brennan, G., Brose, U., Gaedke, U., Jacob, U., Kratina, P., Matthews, B., Munch, S., Novak, M., Palamara, G. M., Rall, B. C., Rosenbaum, B., Tabi, A., Ward, C., Williams, R., Ye, H., & Petchey, O. L. (2019). The intrinsic predictability of ecological time series and its potential to guide forecasting. *Ecological Monographs*, *89*(2), e01359. https://doi.org/10.1002/ecm.1359

Petchey, O. L., Pontarp, M., Massie, T. M., Kéfi, S., Ozgul, A., Weilenmann, M., Palamara, G. M., Altermatt, F., Matthews, B., Levine, J. M., Childs, D. Z., McGill, B. J., Schaepman, M. E., Schmid, B., Spaak, P., Beckerman, A. P., Pennekamp, F., & Pearse, I. S. (2015). The ecological forecast horizon, and examples of its uses and determinants. *Ecology Letters*, *18*(7), 597–611. https://doi.org/10.1111/ele.12443

Peter, S., Agstam, O., & Sobek, S. (2017). Widespread release of dissolved organic carbon from anoxic boreal lake sediments. *Inland Waters*, *7*(2), 151–163. https://doi.org/10.1080/20442041.2017.1300226

Petrovskii, S., & Petrovskaya, N. (2012). Computational ecology as an emerging science. *Interface Focus*, *2*(2), 241–254. https://doi.org/10.1098/rsfs.2011.0083

Pielke, R. A., & Conant, R. T. (2003). Best Practices in Prediction for Decision-Making: Lessons from the Atmospheric and Earth Sciences. *Ecology*, *84*(6), 1351–1358. https://doi.org/10.1890/0012-9658(2003)084[1351:BPIPFD]2.0.CO;2

Pilla, R. M., & Williamson, C. E. (2023). Multidecadal trends in ultraviolet radiation, temperature, and dissolved oxygen have altered vertical habitat availability for Daphnia in temperate Lake Giles, USA. *Freshwater Biology*, *68*(3), 523–533. https://doi.org/10.1111/fwb.14044

Pilla, R. M., Williamson, C. E., Adamovich, B. V., Adrian, R., Anneville, O., Chandra, S., Colom-Montero, W., Devlin, S. P., Dix, M. A., Dokulil, M. T., Gaiser, E. E., Girdner, S. F., Hambright, K. D., Hamilton, D. P., Havens, K., Hessen, D. O., Higgins, S. N., Huttula, T. H., Huuskonen, H., Isles, P. D. F., Joehnk, K. D., Jones, I. D., Keller, W. B., Knoll, L. B., Korhonen, J., Kraemer, B. M., Leavitt, P. R., Lepori, F., Luger, M. S., Maberly, S. C., Melack, J. M., Melles, S. J., Müller-Navarra, D. C., Pierson, D. C., Pislegina, H. V., Plisnier, P.-D., Richardson, D. C., Rimmer, A., Rogora, M., Rusak, J. A., Sadro, S., Salmaso, N., Saros, J. E., Saulnier-Talbot, É., Schindler, D. E., Schmid, M., Shimaraeva, S. V., Silow, E. A., Sitoki, L. M., Sommaruga, R., Straile, D., Strock, K. E., Thiery, W., Timofeyev, M. A., Verburg, P., Vinebrooke, R. D., Weyhenmeyer, G. A., & Zadereev, E. (2020). Deeper waters are changing less consistently than surface waters in a global analysis of 102 lakes. *Scientific Reports*, *10*(1), 20514. https://doi.org/10.1038/s41598-020-76873-x

Pilla, R. M., Williamson, C. E., Overholt, E. P., Rose, K. C., Berger, S. A., Couture, R.-M., De Wit, H. A., Granados, I., Grossart, H.-P. F., Kirillin, G. B., Laas, A., Nejstgaard, J. C., Rusak, J. A., Swinton, M. W., Toro, M., & Yao, H. (2023). Deepwater dissolved oxygen shows little ecological memory between lake phenological seasons. *Inland Waters*, 1–12. https://doi.org/10.1080/20442041.2023.2265802

Raymond, P. A., Hartmann, J., Lauerwald, R., Sobek, S., McDonald, C., Hoover, M., Butman, D., Striegl, R., Mayorga, E., Humborg, C., Kortelainen, P., Dürr, H., Meybeck, M., Ciais, P., & Guth, P. (2013). Global carbon dioxide emissions from inland waters. *Nature*, *503*(7476), 355–359. https://doi.org/10.1038/nature12760

Reid, A. J., Carlson, A. K., Creed, I. F., Eliason, E. J., Gell, P. A., Johnson, P. T. J., Kidd, K. A., MacCormack, T. J., Olden, J. D., Ormerod, S. J., Smol, J. P., Taylor, W.

W., Tockner, K., Vermaire, J. C., Dudgeon, D., & Cooke, S. J. (2019). Emerging threats and persistent conservation challenges for freshwater biodiversity. *Biological Reviews*, *94*(3), 849–873. https://doi.org/10.1111/brv.12480

Reinl, K. L., Harris, T. D., North, R. L., Almela, P., Berger, S. A., Bizic, M., Burnet, S. H., Grossart, H.-P., Ibelings, B. W., Jakobsson, E., Knoll, L. B., Lafrancois, B. M., McElarney, Y., Morales-Williams, A. M., Obertegger, U., Ogashawara, I., Paule-Mercado, M. C., Peierls, B. L., Rusak, J. A., Sarkar, S., Sharma, S., Trout-Haney, J. V., Urrutia-Cordero, P., Venkiteswaran, J. J., Wain, D. J., Warner, K., Weyhenmeyer, G. A., & Yokota, K. (2023). Blooms also like it cold. *Limnology and Oceanography Letters*, *8*(4), 546–564. https://doi.org/10.1002/lol2.10316

Reynaud, A., & Lanzanova, D. (2017). A Global Meta-Analysis of the Value of Ecosystem Services Provided by Lakes. *Ecological Economics*, *137*, 184–194. https://doi.org/10.1016/j.ecolecon.2017.03.001

Richardson, D. C., Melles, S. J., Pilla, R. M., Hetherington, A. L., Knoll, L. B., Williamson, C. E., Kraemer, B. M., Jackson, J. R., Long, E. C., Moore, K., Rudstam, L. G., Rusak, J. A., Saros, J. E., Sharma, S., Strock, K. E., Weathers, K. C., & Wigdahl-Perry, C. R. (2017). Transparency, Geomorphology and Mixing Regime Explain Variability in Trends in Lake Temperature and Stratification across Northeastern North America (1975–2014). *Water*, *9*(6), 442. https://doi.org/10.3390/w9060442

Riedel, T., Zak, D., Biester, H., & Dittmar, T. (2013). Iron traps terrestrially derived dissolved organic matter at redox interfaces. *Proceedings of the National*

Academy of Sciences, *110*(25), 10101–10105. https://doi.org/10.1073/pnas.1221487110

Schindler, D. E. (2017). Warmer climate squeezes aquatic predators out of their preferred habitat. *Proceedings of the National Academy of Sciences*, *114*(37), 9764–9765. https://doi.org/10.1073/pnas.1712818114

Schindler, D. W. (1974). Eutrophication and Recovery in Experimental Lakes: Implications for Lake Management. *Science*, *184*(4139), 897–899.

Schmid, M., & Köster, O. (2016). Excess warming of a Central European lake driven by solar brightening. *Water Resources Research*, *52*(10), 8103–8116. https://doi.org/10.1002/2016WR018651

Şen, B., Che-Castaldo, C., Krumhardt, K. M., Landrum, L., Holland, M. M., LaRue, M. A., Long, M. C., Jenouvrier, S., & Lynch, H. J. (2023). Spatio-temporal transferability of environmentally-dependent population models: Insights from the intrinsic predictabilities of Adélie penguin abundance time series. *Ecological Indicators*, *150*, 110239. https://doi.org/10.1016/j.ecolind.2023.110239

Skoog, A. C., & Arias-Esquivel, V. A. (2009). The effect of induced anoxia and reoxygenation on benthic fluxes of organic carbon, phosphate, iron, and manganese. *Science of The Total Environment*, *407*(23), 6085–6092. https://doi.org/10.1016/j.scitotenv.2009.08.030

Sobek, S., Durisch-Kaiser, E., Zurbrügg, R., Wongfun, N., Wessels, M., Pasche, N., & Wehrli, B. (2009). Organic carbon burial efficiency in lake sediments controlled by oxygen exposure time and sediment source. *Limnology and Oceanography*, *54*(6), 2243–2254. https://doi.org/10.4319/lo.2009.54.6.2243

Sobek, S., Zurbrügg, R., & Ostrovsky, I. (2011). The burial efficiency of organic carbon in the sediments of Lake Kinneret. *Aquatic Sciences*, *73*(3), 355–364. https://doi.org/10.1007/s00027-011-0183-x

Sobek, S., Gudasz, C., Koehler, B., Tranvik, L. J., Bastviken, D., & Morales-Pineda, M. (2017). Temperature Dependence of Apparent Respiratory Quotients and Oxygen Penetration Depth in Contrasting Lake Sediments. *Journal of Geophysical Research: Biogeosciences*, *122*(11), 3076–3087. https://doi.org/10.1002/2017JG003833

Thompson, A., Chadwick, O. A., Rancourt, D. G., & Chorover, J. (2006). Iron-oxide crystallinity increases during soil redox oscillations. *Geochimica et Cosmochimica Acta*, *70*(7), 1710–1727. https://doi.org/10.1016/j.gca.2005.12.005

Tranvik, L. J., Cole, J. J., & Prairie, Y. T. (2018). The study of carbon in inland waters—from isolated ecosystems to players in the global carbon cycle. *Limnology and Oceanography Letters*, *3*(3), 41–48. https://doi.org/10.1002/lol2.10068

USGCRP. (2018). *Second State of the Carbon Cycle Report* (pp. 1–470). U.S. Global Change Research Program, Washington, DC. Retrieved from https://carbon2018.globalchange.gov/chapter/1

Vachon, D., Solomon, C. T., & del Giorgio, P. A. (2017). Reconstructing the seasonal dynamics and relative contribution of the major processes sustaining CO2 emissions in northern lakes. *Limnology and Oceanography*, *62*(2), 706–722. https://doi.org/10.1002/lno.10454

Votruba, A. M., & Corman, J. R. (2020). Definitions of Water Quality: A Survey of Lake-Users of Water Quality-Compromised Lakes. *Water*, *12*(8), 2114. https://doi.org/10.3390/w12082114

von Wachenfeldt, E., Sobek, S., Bastviken, D., & Tranvik, L. J. (2008). Linking allochthonous dissolved organic matter and boreal lake sediment carbon sequestration: The role of light-mediated flocculation. *Limnology and Oceanography*, *53*(6), 2416–2426. https://doi.org/10.4319/lo.2008.53.6.2416

Ward, E. J., Holmes, E. E., Thorson, J. T., & Collen, B. (2014). Complexity is costly: a meta-analysis of parametric and non-parametric methods for short-term population forecasting. *Oikos*, *123*(6), 652–661. https://doi.org/10.1111/j.1600-0706.2014.00916.x

Wetzel, R. G. (2001). 6 - FATE OF HEAT. In R. G. Wetzel (Ed.), *Limnology (Third Edition)* (pp. 71–92). San Diego: Academic Press. https://doi.org/10.1016/B978-0-08-057439-4.50010-1

Weyhenmeyer, G. A., Prairie, Y. T., & Tranvik, L. J. (2014). Browning of boreal freshwaters coupled to carbon-iron interactions along the aquatic continuum. *PloS One*, *9*(2), e88104. https://doi.org/10.1371/journal.pone.0088104

White, E. P., Yenni, G. M., Taylor, S. D., Christensen, E. M., Bledsoe, E. K., Simonis, J. L., & Ernest, S. K. M. (2019). Developing an automated iterative near-term forecasting system for an ecological study. *Methods in Ecology and Evolution*, *10*(3), 332–344. https://doi.org/10.1111/2041-210X.13104

Williamson, C. E., Dodds, W., Kratz, T. K., & Palmer, M. A. (2008). Lakes and streams as sentinels of environmental change in terrestrial and atmospheric processes. Frontiers in Ecology and the Environment, 6(5), 247–254. https://doi.org/10.1890/070140

Williamson, C. E., Saros, J. E., Vincent, W. F., & Smol, J. P. (2009). Lakes and reservoirs as sentinels, integrators, and regulators of climate change. *Limnology and Oceanography*, *54*(6part2), 2273–2282. https://doi.org/10.4319/lo.2009.54.6_part_2.2273

Winslow, L. A., Read, J. S., Hansen, G. J. A., Rose, K. C., & Robertson, D. M. (2017). Seasonality of change: Summer warming rates do not fully represent effects of climate change on lake temperatures. *Limnology and Oceanography*, *62*(5), 2168–2178. https://doi.org/10.1002/lno.10557

Woolway, R. I., & Merchant, C. J. (2017). Amplified surface temperature response of cold, deep lakes to inter-annual air temperature variability. *Scientific Reports*, *7*(1), 4130. https://doi.org/10.1038/s41598-017-04058-0

Woolway, R. I., Sharma, S., Weyhenmeyer, G. A., Debolskiy, A., Golub, M., Mercado-Bettín, D., Perroud, M., Stepanenko, V., Tan, Z., Grant, L., Ladwig, R., Mesman, J., Moore, T. N., Shatwell, T., Vanderkelen, I., Austin, J. A., DeGasperi, C. L., Dokulil, M., La Fuente, S., Mackay, E. B., Schladow, S. G., Watanabe, S., Marcé, R., Pierson, D. C., Thiery, W., & Jennings, E. (2021). Phenological shifts in lake stratification under climate change. *Nature Communications*, *12*(1), 2318. https://doi.org/10.1038/s41467-021-22657-4

Yang, L., Choi, J. H., & Hur, J. (2014). Benthic flux of dissolved organic matter from lake sediment at different redox conditions and the possible effects of biogeochemical processes. *Water Research*, *61*, 97–107. https://doi.org/10.1016/j.watres.2014.05.009

Yang, X., O'Reilly, C. M., Gardner, J. R., Ross, M. R. V., Topp, S. N., Wang, J., & Pavelsky, T. M. (2022). The Color of Earth's Lakes. *Geophysical Research Letters*, *49*(18), e2022GL098925. https://doi.org/10.1029/2022GL098925

Yvon-Durocher, G., Caffrey, J. M., Cescatti, A., Dossena, M., Giorgio, P. del, Gasol, J. M., Montoya, J. M., Pumpanen, J., Staehr, P. A., Trimmer, M., Woodward, G., & Allen, A. P. (2012). Reconciling the temperature dependence of respiration across timescales and ecosystem types. *Nature*, *487*(7408), 472–476. https://doi.org/10.1038/nature11205

Zhao, L., Zhu, R., Zhou, Q., Jeppesen, E., & Yang, K. (2023). Trophic status and lake depth play important roles in determining the nutrient-chlorophyll a relationship: Evidence from thousands of lakes globally. *Water Research*, 120182. https://doi.org/10.1016/j.watres.2023.120182

Zhi, W., Klingler, C., Liu, J., & Li, L. (2023). Widespread deoxygenation in warming rivers. *Nature Climate Change*, *13*(10), 1105–1113. https://doi.org/10.1038/s41558-023-01793-3

Zhou, J., Leavitt, P. R., Rose, K. C., Wang, X., Zhang, Y., Shi, K., & Qin, B. (2023). Controls of thermal response of temperate lakes to atmospheric warming. *Nature Communications*, *14*(1), 6503. https://doi.org/10.1038/s41467-023-42262-x

Zhou, Z., Huang, T., Gong, W., Li, Y., Liu, Y., Zhou, S., & Cao, M. (2019). Water Quality Responses during the Continuous Mixing Process and Informed Management of a Stratified Drinking Water Reservoir. *Sustainability*, *11*(24), 7106. https://doi.org/10.3390/su11247106

Zimmermann, M., Mayr, M. J., Bürgmann, H., Eugster, W., Steinsberger, T., Wehrli, B., Brand, A., & Bouffard, D. (2021). Microbial methane oxidation efficiency and robustness during lake overturn. *Limnology and Oceanography Letters*, *6*(6), 320–328. https://doi.org/10.1002/lol2.10209

Chapter I Figures

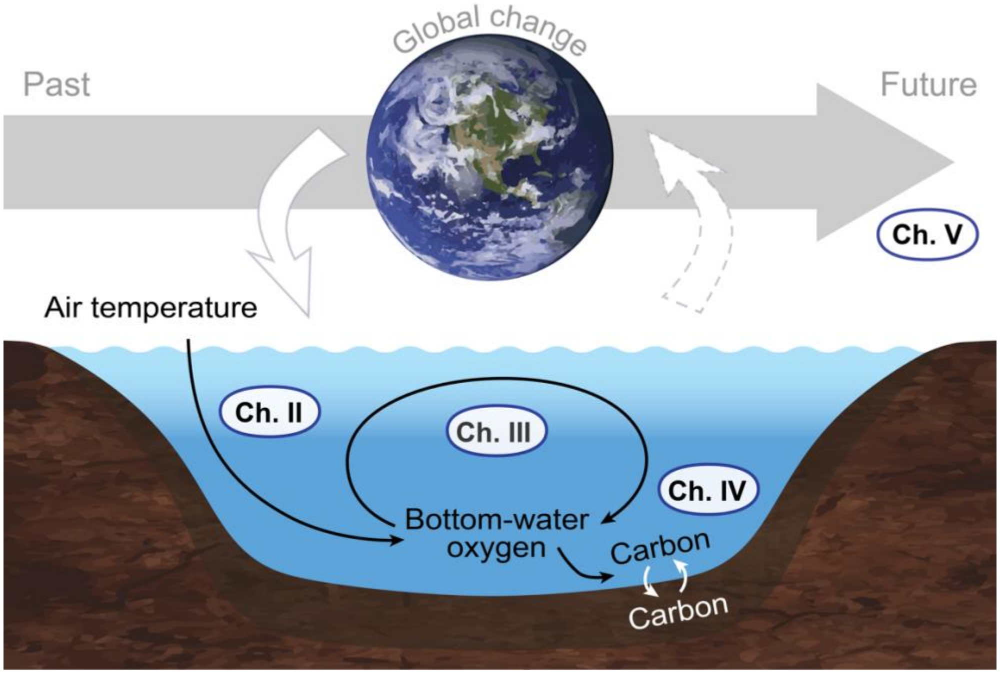

Figure 1: Through my dissertation, I aimed to develop a predictive understanding of oxygen dynamics in the bottom-waters of widespread lakes. Here, black arrows indicate hypothesized causes and consequences of changes in bottom-water dissolved oxygen, including effects of air temperature on bottom-water dissolved oxygen (Ch. 2), a positive feedback to low-oxygen conditions (Ch. 3), and interactions between bottom-water oxygen and bottom-water carbon cycling processes (Ch. 4). A gray arrow from past to future highlights the use of historical dynamics to generate anticipatory predictions, with Ch. 5 explicitly focusing on the emerging field of near-term ecological forecasting. White arrows between the Earth and lake reference the effects of global change on lake ecosystems (left; solid outline) and the potential implications of changes in bottom-water dissolved oxygen for lake ecosystem services on a global scale (right; dashed outline).

Chapter II: Spring air temperature drives summer water quality dynamics in temperate lakes

Abigail S. L. Lewis[1*], Cayelan C. Carey[1]

[1] Department of Biological Sciences, Virginia Tech, Blacksburg, VA USA

In review at *Limnology and Oceanography Letters*.

Abstract

In many temperate lakes, summer bottom-water temperature and dissolved oxygen regulate both habitat viability and biogeochemical cycling, affecting ecological functioning year-round. To characterize drivers of variation in summer bottom-water dynamics, we analyzed data from 615 temperate lakes. We found that summer bottom-water temperature and dissolved oxygen tended to be more associated with spring air temperature than summer air temperature. Conversely, summer surface-water temperature was more associated with summer air temperature. Across lakes, the relative correlation between bottom-water dynamics and spring vs. summer air temperature was mediated by the strength of thermal stratification and lake size, with the timing of thermal stratification regulating which window of air temperature was most influential. Our results help explain why trends in summer bottom-water temperature diverge from trends in summer air temperature and suggest that predicting future water quality may require accounting for differential changes in climate among seasons.

1. Introduction

Summer water temperature and dissolved oxygen (DO) dynamics are changing across lakes worldwide, often causing detrimental effects on water quality (e.g., O'Reilly et al. 2015; Jane et al. 2021). While surface-water temperatures are generally increasing, summer bottom-water temperature trends are highly variable among lakes and show little to no correlation with summer or mean-annual air temperature trends (e.g., Richardson et al. 2017; Pilla et al. 2020; Jane et al. 2021; Zhou et al. 2023). As summer bottom-water conditions play a critical role in regulating internal nutrient loading, habitat availability, and greenhouse gas dynamics (e.g., Hounshell et al. 2021; Carey et al. 2022; Jane et al. 2024; Lewis et al. 2024), characterizing drivers of summer bottom-water temperature and DO is necessary to anticipate future lake ecosystem function.

Counterintuitively, spring air temperatures have the potential to exert a *stronger* influence on summer bottom-water dynamics in temperate lakes than summer air temperatures (Figure 2a; Del Giudice et al. 2018; Dugan 2021; Oleksy and Richardson 2021; Piccolroaz et al. 2021), though this effect has not yet been characterized across widespread lakes. Summer thermal stratification inhibits mixing between surface and bottom waters in many temperate lakes, limiting the association between summer air temperature and summer bottom-water temperature or DO dynamics (MacIntyre and Hamilton 2024). Conversely, heat can exchange throughout the entire water column during the mixing period prior to the onset of stratification, which decreases oxygen solubility and may increase the rate of oxygen demand throughout the stratified period (Yvon-Durocher et al. 2012; MacIntyre and Hamilton 2024). Thus, thermal exchange prior to stratification, in combination with effects of spring air temperature on the phenology of ice thaw and/or stratification onset (Dugan 2021; Ladwig et al. 2021; Jane et al. 2023), may lead bottom-water conditions to be more correlated with spring, compared to summer, air temperatures (Figure 2a).

Characterizing the role of antecedent spring air temperatures in driving bottom-water dynamics across widespread lakes is needed to improve predictions of future water quality. Notably, the specific spring dates that are most influential in driving bottom-water dynamics may vary across lakes as a result of differences in spring air temperature phenology, stratification dynamics, and other factors (Dugan 2021; Oleksy and Richardson 2021; Stetler et al. 2021). Likewise, the relative influence of spring vs. summer air temperature may vary across lakes with differences in stratification, lake size, mixing dynamics, and transparency, among other factors (Rose et al. 2016; Toffolon et al. 2020; Dugan 2021). These relationships remain largely untested because they can only be identified through analysis of long-term monitoring data across many widespread lakes. As climate change is associated with differential changes in air temperature among seasons (IPCC 2023), characterizing the relative influence of spring vs. summer air temperature will help more accurately anticipate future effects of climate change on water quality.

In this study, we analyzed the influence of seasonal air temperature dynamics on bottom-water temperature and DO across n=615 diverse stratified lakes (Figure 1). Our analysis addressed two primary research questions: Q1) Which season of air temperature exerts the strongest influence over summer bottom-water temperature and DO dynamics (both interannual variability and long-term trends)? and Q2) What lake characteristics control the relative influence of summer vs. spring air temperatures on bottom-water temperature and DO? While our study was focused on empirical data analysis across hundreds of temperate lakes, we sought additional mechanistic validation of our results by examining modeled water temperatures in a subset of lakes (n = 42). Through these analyses, we provide a robust assessment of how seasonal air temperature dynamics affect water quality amidst a changing climate.

2. Methods

2.1 Dataset and data processing

To explore associations between seasonal air temperatures and bottom-water dynamics, we analyzed a database of temperature and DO profiles from 615 widespread lakes, all of which exhibit stable summer thermal stratification (Lewis et al. 2023, 2024). This database includes a median of 30 years of data from lakes across 18 countries and 5 continents (Figure 1). Lakes in the database have a median depth of 14 m (Z_{max}; range: 6–370 m) and median surface area of 100 ha (range: 1–126,909 ha). Detailed data descriptions are provided by Lewis et al. (2023, 2024). All data analyses were performed in R, version 4.3.2 (R Core Team, 2023), and analysis code is archived on Zenodo (Lewis 2024).

2.1.1 Summer in-lake metrics

We calculated mean summer water temperature and DO in surface and bottom waters for each lake-year following Lewis et al. (2024). Briefly, we interpolated summer temperature and DO profiles to a 1-m depth resolution, then averaged all depth-interpolated data from the epilimnion and hypolimnion to generate surface- and bottom-water means for each summer, respectively (Winslow et al. 2019). Summer was operationally defined as July and August in the northern hemisphere and January and February in the southern hemisphere, and changing the summer duration did not qualitatively affect results (Figure S1).

We calculated the rate of DO depletion in bottom waters as volume-weighted hypolimnetic oxygen demand (VHOD; hereafter oxygen demand) during the entire summer stratified period of each lake-year (see Lewis et al. 2024). Modeled and measured bathymetric contours for this analysis were provided by Lewis et al. (2023).

We used maximum buoyancy frequency at the thermocline to assess the strength of thermal stratification. For each profile, we calculated maximum buoyancy frequency using *rLakeAnalyzer*, and then averaged values from all profiles collected throughout the summer separately for each lake-year (Winslow et al. 2019).

To assess whether correlations between spring air temperature and summer bottom-water dynamics corresponded with summer stratification onset, we calculated the median date of thermal stratification onset across all lake-years. For each lake-year, we identified the latest non-stratified thermal profile before July (northern hemisphere) or January (southern hemisphere). If a subsequent stratified profile was recorded within one week, we approximated the onset of thermal stratification as the midpoint between these two profiles. Stratification was defined by a minimum density difference of 0.1 kg/m^3 (Wilson et al. 2020).

2.1.2 Climate data

We collated daily 2-m air temperature for 1980–2022 from the ERA5 climate reanalysis (Hersbach et al. 2019). ERA5 is a commonly used climate reanalysis product and provides meteorological data on a 0.25-degree global grid (Hersbach et al. 2019).

2.2 Interannual variability

To assess which sub-annual periods of air temperature are most strongly correlated with interannual variability in summer water temperature and DO dynamics in each lake, we calculated the correlations between 30-day rolling mean air temperatures in January–August and four summer focal variables: surface-water temperature, bottom-water temperature, bottom-water oxygen demand, and bottom-water DO. For this analysis, we used partial Spearman's correlation accounting for measurement year to isolate the role of interannual variability, as opposed to long-term trends (see *Section 2.3* and Figure S2). We included all lakes with at least 10 years of paired data for air temperature and any of the four focal variables from 1980–2022. For DO, we only included lakes that had at least one year with DO >1 mg/L, as lakes that were consistently anoxic did not exhibit sufficient variability to assess effects of air temperature. Changing the duration of the rolling mean window did not substantially alter results (Figure S3).

2.2.1 Seasonal Air Temperature Effect (SATE)

We quantified the relative influence of summer vs. spring air temperatures on each summer focal variable (surface-water temperature, bottom-water temperature, bottom-water oxygen demand, and bottom-water DO concentration). First, we calculated the correlations between our summer focal variables and all possible 30-day rolling windows of spring air temperature during March–May (Rho_{spring}) to identify which days yielded the maximum absolute correlation. We then repeated this analysis using all possible 30-day rolling windows in July–August (Rho_{summer}). We compared the maximum summer correlation to the maximum spring correlation for each focal variable to calculate a Seasonal Air Temperature Effect (*SATE*) value following EQ1.

EQ1: $Seasonal\ Air\ Temperature\ Effect\ (SATE) = |Rho_{summer}| - |Rho_{spring}|$

Consequently, positive values of *SATE* indicate a stronger correlation with summer air temperature and negative values indicate a stronger correlation with spring air temperature (Figure S4). Using the maximum correlation from spring and summer rather than, e.g., the mean correlation throughout these periods, allowed us to isolate the specific windows of air temperature that were most important in driving variation in each summer focal variable, as seasonal phenology (e.g., timing of spring thaw and stratification onset) varies with lake size, geographic location, wind dynamics, and other factors (Magee and Wu 2017; Woolway et al. 2021).

We assessed how *SATE* may vary across lakes using multiple linear regression. For this analysis, we selected candidate explanatory variables that describe lake size (surface area and maximum depth) and stratification strength (median buoyancy frequency at the thermocline across all years), both of which were expected to mediate the influence of spring air temperatures on summer water quality. All explanatory variables were z-transformed prior to analysis. We selected the optimal model based on second-order corrected Akaike Information Criterion (AICc), using the R package *MuMIn* (Bartoń 2023).

2.3 Multiannual trends

To assess the correspondence between water temperature and spring/summer air temperature trends, we calculated non-parametric trends in spring air temperature, summer air temperature, summer bottom-water temperature and summer bottom-water DO across all lakes. We accounted for variation in seasonal phenology across lakes by using the air temperature dates that were maximally correlated with bottom-water temperature and DO during the spring and summer periods respectively, as identified in section 2.2.1. Consistently anoxic lakes (maximum summer DO <1 mg/L) were excluded from the DO trend analysis. We used Sen's slope as a non-parametric trend statistic and performed these calculations using the *trend* R package (Pohlert 2023).

2.4 ISIMIP-lakes model-based verification

We examined the robustness of our across-lake results by analyzing within-lake patterns over multiple decades with hydrodynamic modeling. We compiled daily water temperature estimates for 42 lakes in our dataset that were modeled as part of the Inter-Sectoral Impact Model Intercomparison Project lakes sector (ISIMIP global lakes v3a). For this analysis, we used output from the widely-used General Ocean Turbulence Model (GOTM), which was also driven by ERA5 climate data (Golub et al. 2022). We limited our analysis to years ≥1980 to correspond with our empirical analyses above.

Using the ISIMIP-modeled daily water temperatures of these 42 lakes, we re-ran the analyses described in sections 2.1 and 2.2. Modeled daily water temperature output allowed us to precisely quantify the timing of summer stratification onset in each lake-year. Consequently, we assessed whether the timing of stratification onset was related to the timing of peak correlation between spring air temperature and summer bottom-water temperature across lakes, and whether earlier stratification onset date was associated with increased summer bottom-water temperature.

3. Results

Across the lakes in this analysis, summer surface-water temperature tended to be more strongly correlated with summer air temperature than spring air temperature (Figures 1, S5, S6). Conversely, all of the summer bottom-water variables we examined in this study (i.e., bottom-water temperature, DO demand, DO concentrations, and DO saturation) were more closely correlated with spring air temperature than summer air temperature (Figures 1, S5, S6, S7).

The relative influence of antecedent spring air temperatures (i.e., *SATE*) was mediated by stratification strength and lake size (Table S1). For both summer bottom-water temperatures and DO concentrations, *SATE* was significantly related to buoyancy frequency and surface area, whereby bottom-water conditions in large, stably-stratified lakes were much more strongly correlated with spring air temperature vs. summer air temperature (Figure 3, Table S1). *SATE* for summer bottom-water oxygen demand was not significantly mediated by any lake characteristics included in the analysis (Table S1).

The spring period just prior to the onset of summer thermal stratification tended to be the most influential in setting summer bottom-water temperature, oxygen demand, and

DO concentrations. Specifically, absolute correlations with air temperature increased for rolling windows of air temperature from the start of the year to late April (northern hemisphere) for all bottom-water variables, then declined rapidly at the transition from spring to summer (Figure 4). The peak correlation in all three bottom-water variables closely coincided with the median onset of stratification across lakes (Figure 4). Analyzing ISIMIP-modeled daily water temperatures, we found an approximately 1:1 correlation between stratification onset date and the window of spring air temperature that was most correlated with summer bottom-water temperature (Figure S8). Furthermore, years with early onset of summer stratification tended to have increased summer bottom-water temperature within the time series of ISIMIP-modeled water temperature (1980–2022) at each lake (Figure S9).

Decadal trends in summer bottom-water dynamics were significantly associated with trends in spring, but not summer, air temperature (Figure 5). Specifically, a 1 ºC increase in spring air temperature was associated with a 0.60 ºC increase in bottom-water temperature and a 0.56 mg/L decrease in bottom-water DO. Notably, across the lakes in this dataset, spring air temperature trends were less positive and more variable than summer air temperature trends (mean±SD = 0.07± 0.27 ºC/decade in spring vs. 0.27±0.13 ºC/decade in summer from 1980–2022; Figure 5).

4. Discussion

Through our analysis of 615 widespread lakes, we found that spring air temperatures played a more important role in regulating bottom-water temperature and

DO dynamics than summer air temperatures (Figures 2, 5, S5). Our results help explain why previous studies have found little to no association between summer air temperature and summer bottom-water dynamics (Winslow et al. 2017; Pilla et al. 2020; Zhou et al. 2023), and highlight the important, yet cryptic, role that climate change plays in driving changes in bottom-water temperature and DO.

The mechanisms underlying an influence of spring air temperature on bottom-water dynamics in temperate lakes are well-supported by decades of research (e.g., Dugan 2021; Oleksy and Richardson 2021) and by our integrated empirical and modeling approach. Prior to the onset of summer thermal stratification, heat and oxygen can exchange between air and water, then mix throughout the water column (Figure 2a). Atmospheric fluxes of heat and oxygen are subsequently limited throughout stratification. Consequently, the starting conditions at the onset of thermal stratification play an important role in shaping summer bottom-water dynamics, and bottom-water conditions may be more associated with spring, rather than summer, air temperature.

We find that increased spring air temperature could contribute to bottom-water oxygen declines via at least three mechanisms. By increasing bottom-water temperature at the onset of thermal stratification, increased spring air temperature may (1) directly decrease the solubility of dissolved oxygen and (2) increase summer bottom-water oxygen demand (Figure 2). These effects are compounded by (3) earlier onset of thermal stratification during years with warm spring air temperature (Dugan 2021; Ladwig et al. 2021; Jane et al. 2023; Figure S9). Consequently, both the solubility of dissolved oxygen and the percent saturation of dissolved oxygen tended to be lower in lake-years with warm spring air temperature (Figures 2, S7).

Ultimately, variation in spring air temperature is likely associated with simultaneous changes in ice dynamics, mixing period duration, and stratification onset date, and the relative importance of these factors in shaping summer bottom-water dynamics varies across lakes (e.g., Toffolon et al. 2020; Dugan 2021; Powers et al. 2022). Limited spring data availability prevented us from empirically examining these mechanisms, and more broadly, it is unlikely that long-term spring data exist across many widespread lakes due to the logistical challenges of sampling during intermittently ice-covered periods. In the absence of spring observations, our analysis of ISIMIP-modeled daily water temperatures provided a complementary approach for determining the relationship between stratification onset and air temperature lags, yielding robust support for our empirical analysis. As stratification and ice dynamics continue to change across lakes worldwide, mechanistic characterization of the broad-scale patterns identified in this study will be helpful for predicting future changes in lake ecosystem function.

Changes in spring air temperature, as described in our study, likely operate in addition to, and in interaction with, numerous other controls over bottom-water temperature and DO dynamics. Notably, our analysis was focused on temperate stratified lakes, and our conclusions may therefore not apply to tropical, boreal, or polymictic systems. Because the relative influence of spring vs. summer air temperatures was strongly mediated by the timing and strength of summer stratification, we expect that this effect would be substantially weaker in polymictic lakes. Wind patterns, which are changing over time across many lakes, also exert a strong influence over stratification, ice, and mixing dynamics (Woolway et al. 2019; Janatian et al. 2020; Stetler et al. 2021). However, substantial uncertainty in locally downscaled wind data across lakes (e.g., Wu et al. 2024) limited our ability to include wind in our analysis. Confounding effects of wind, in addition to other chemical, biological, and hydrological drivers within and among lakes, may have contributed to slightly greater *SATE* estimates for modeled vs. observed water temperature (Figures 2b, S5). Ultimately, accounting for these additional impacts and characterizing seasonal air temperature effects across a broader latitudinal gradient will aid in predicting the effects of changing seasonal air temperatures across widespread lakes.

Among the lakes examined in this analysis, increases in spring air temperature have been substantially slower and more variable than increases in summer air temperature (Figure 5). This seasonal difference in climate warming may explain why bottom-water temperatures are not warming as fast as surface-water temperatures in many lakes (Kraemer et al. 2015; O'Reilly et al. 2015; Richardson et al. 2017; Pilla et al. 2020), though changes in bottom-water temperature are further regulated by changes in transparency, among other factors (e.g., Rose et al. 2016; Bartosiewicz et al. 2019). Because of these differences in warming, we would overestimate predicted lake bottom-water warming and deoxygenation by a factor of four if we expected bottom-water dynamics to be driven by summer air temperature rather than spring. Over time, slower rates of bottom-water warming compared to surface-water warming may contribute to strengthened thermal stability (Kraemer et al. 2015; Crossman et al. 2016; Richardson et al. 2017), which could potentially increase the relative importance of spring vs. summer air temperature across lakes (Figure 3).

Our analysis indicates that for every 1 ºC increase in spring air temperature, we may expect approximately 0.60 ºC increase in summer bottom-water temperature and 0.56 mg/L decrease in summer bottom-water DO (Figure 5), which will have important consequences for lake water quality. Increased bottom-water temperature and decreased bottom-water DO could lead to greater bottom-water methane accumulation (Juutinen et al. 2009; Hounshell et al. 2021; Soued and Prairie 2022), greater internal nutrient loading (Mortimer 1941; Nürnberg 1984; Orihel et al. 2017), and decreased habitat availability for aerobic organisms (e.g., Schindler 2017; Pilla and Williamson 2023), in addition to other effects on water quality. Ultimately, as climate change continues to alter ecosystem functioning in lakes around the world, our results emphasize that it may be necessary to consider both concurrent and antecedent conditions when predicting future water quality dynamics.

Acknowledgements

Many thanks to the Inter-Sectoral Impact Model Intercomparison Project (ISIMIP) lakes sector and GOTM team for providing modeled lake temperature for this analysis, and Daniel Mercado-Bettín for collating and processing these data. Thanks also to the Virginia Tech Reservoir Group for helpful feedback on the figures and analyses in this paper, especially Dexter Howard for discussions in the early phases of this analysis and Freya Olsson for a constructive review. This analysis would not be possible without long-term data collection across widespread lakes. Many thanks to the myriad of researchers, managers, and community members who have collected and compiled these data over several decades. In particular, we thank members of the Global Lake Ecological Observatory Network for data contributions and helpful discussions throughout the process of writing this paper. This project was financially supported by the U.S. National Science Foundation (NSF; DEB-1753639), an NSF graduate research fellowship to ASL (DGE-1840995), and funding from the Virginia Tech College of Science Roundtable. CCC was supported by DEB-2327030 and EF-2318661.

Author Contribution Statement

ASL and CCC conceptualized this project. ASL performed data analysis, developed visualizations, and wrote the manuscript with substantial input from CCC.

Data Availability Statement

The in-lake data used in this study are published in the Environmental Data Initiative repository (EDI; Lewis et al., 2023). We additionally used openly-available data from ISIMIP (Golub et al. 2022) and the ERA5 climate reanalysis (Hersbach et al., 2019). Analysis code to reproduce the results in this manuscript is available in a Zenodo repository (Lewis 2024).

Chapter II References

Bartoń, K. 2023. [R package] MuMIn: Multi-Model Inference (Version 1.47.5).

Bartosiewicz, M., A. Przytulska, J.-F. Lapierre, I. Laurion, M. F. Lehmann, and R. Maranger. 2019. Hot tops, cold bottoms: Synergistic climate warming and shielding effects increase carbon burial in lakes. Limnology and Oceanography Letters **4**: 132–144. doi:10.1002/lol2.10117

Carey, C. C., P. C. Hanson, R. Q. Thomas, and others. 2022. Anoxia decreases the magnitude of the carbon, nitrogen, and phosphorus sink in freshwaters. Global Change Biology **28**: 4861–4881. doi:10.1111/gcb.16228

Del Giudice, D., Y. Zhou, E. Sinha, and A. M. Michalak. 2018. Long-Term Phosphorus Loading and Springtime Temperatures Explain Interannual Variability of Hypoxia in a Large Temperate Lake. Environ. Sci. Technol. **52**: 2046–2054. doi:10.1021/acs.est.7b04730

Dugan, H. A. 2021. A Comparison of Ecological Memory of Lake Ice-Off in Eight North-Temperate Lakes. Journal of Geophysical Research: Biogeosciences **126**: e2020JG006232. doi:10.1029/2020JG006232

Golub, M., W. Thiery, R. Marcé, and others. 2022. A framework for ensemble modelling of climate change impacts on lakes worldwide: the ISIMIP Lake Sector. Geoscientific Model Development **15**: 4597–4623. doi:10.5194/gmd-15-4597-2022

Hersbach, H., B. Bell, P. Berrisford, and others. 2019. ERA5 monthly averaged data on single levels from 1979 to present. Copernicus Climate Change Service (C3S) Climate Data Store (CDS). doi:10.24381/CDS.F17050D7

Hounshell, A. G., R. P. McClure, M. E. Lofton, and C. C. Carey. 2021. Whole-ecosystem oxygenation experiments reveal substantially greater hypolimnetic methane concentrations in reservoirs during anoxia. Limnology and Oceanography Letters **6**: 33–42. doi:10.1002/lol2.10173

IPCC, 2023. Climate Change 2021 – The Physical Science Basis: Working Group I Contribution to the Sixth Assessment Report of the Intergovernmental Panel on Climate Change. Cambridge University Press.

Janatian, N., K. Olli, F. Cremona, A. Laas, and P. Nõges. 2020. Atmospheric stilling offsets the benefits from reduced nutrient loading in a large shallow lake. Limnology and Oceanography **65**: 717–731. doi:10.1002/lno.11342

Jane, S. F., T. M. Detmer, S. L. Larrick, K. C. Rose, E. A. Randall, K. J. Jirka, and P. B. McIntyre. 2024. Concurrent warming and browning eliminate cold-water fish habitat in many temperate lakes. Proceedings of the National Academy of Sciences **121**: e2306906120. doi:10.1073/pnas.2306906120

Jane, S. F., G. Hansen, B. Kraemer, and others. 2021. Widespread deoxygenation of temperate lakes. Nature **594**. doi:10.1038/s41586-021-03550-y

Jane, S. F., J. L. Mincer, M. P. Lau, A. S. L. Lewis, J. T. Stetler, and K. C. Rose. 2023. Longer duration of seasonal stratification contributes to widespread increases in lake hypoxia and anoxia. Global Change Biology **29**: 1009–1023. doi:10.1111/gcb.16525

Juutinen, S., M. Rantakari, P. Kortelainen, J. T. Huttunen, T. Larmola, J. Alm, J. Silvola, and P. J. Martikainen. 2009. Methane dynamics in different boreal lake types. Biogeosciences **6**: 209–223. doi:10.5194/bg-6-209-2009

Kraemer, B. M., O. Anneville, S. Chandra, and others. 2015. Morphometry and average temperature affect lake stratification responses to climate change. Geophysical Research Letters **42**: 4981–4988. doi:10.1002/2015GL064097

Ladwig, R., P. C. Hanson, H. A. Dugan, C. C. Carey, Y. Zhang, L. Shu, C. J. Duffy, and K. M. Cobourn. 2021. Lake thermal structure drives interannual variability in summer anoxia dynamics in a eutrophic lake over 37 years. Hydrol. Earth Syst. Sci. **25**: 1009–1032. doi:10.5194/hess-25-1009-2021

Lewis, A. S. L., M. P. Lau, S. F. Jane, and others. 2023. Dissolved oxygen, temperature, chlorophyll-a, total phosphorus, total nitrogen, and dissolved organic carbon at multiple depths in 822 lakes from 1921-2022 [dataset] *ver 1*. Environmental Data Initiative. doi:10.6073/pasta/2cd6628a942de2a8b12d2b19962712a0

Lewis, A. S. L., M. P. Lau, S. F. Jane, and others. 2024. Anoxia begets anoxia: A positive feedback to the deoxygenation of temperate lakes. Global Change Biology **30**: e17046. doi:10.1111/gcb.17046

Lewis, A. S. L. 2024. abbylewis/Spring_memory: Data analysis of bottom-water temperature and oxygen dynamics in 615 lakes (v1.0.0). Zenodo. doi:10.5281/zenodo.10714287.

MacIntyre, S., and D. P. Hamilton. 2024. Chapter 7 - Fate of Heat, p. 95–153. *In* I.D. Jones and J.P. Smol [eds.], Wetzel's Limnology (Fourth Edition). Academic Press.

Magee, M. R., and C. H. Wu. 2017. Effects of changing climate on ice cover in three morphometrically different lakes. Hydrological Processes **31**: 308–323. doi:10.1002/hyp.10996

Mortimer, C. H. 1941. The Exchange of Dissolved Substances Between Mud and Water in Lakes. Journal of Ecology **29**: 280–329. doi:10.2307/2256395

Nürnberg, G. K. 1984. The prediction of internal phosphorus load in lakes with anoxic hypolimnia1. Limnology and Oceanography **29**: 111–124. doi:10.4319/lo.1984.29.1.0111

Oleksy, I. A., and D. C. Richardson. 2021. Climate change and teleconnections amplify lake stratification with differential local controls of surface water warming and deep water cooling. Geophysical Research Letters **48**: e2020GL090959. doi:10.1029/2020GL090959

O'Reilly, C. M., S. Sharma, D. K. Gray, and others. 2015. Rapid and highly variable warming of lake surface waters around the globe. Geophysical Research Letters **42**: 10773–10781. doi:10.1002/2015GL066235

Orihel, D. M., H. M. Baulch, N. J. Casson, R. L. North, C. T. Parsons, D. C. M. Seckar, and J. J. Venkiteswaran. 2017. Internal phosphorus loading in Canadian fresh waters: a critical review and data analysis. Can. J. Fish. Aquat. Sci. **74**: 2005–2029. doi:10.1139/cjfas-2016-0500

Piccolroaz, S., S. Zhu, M. Ptak, M. Sojka, and X. Du. 2021. Warming of lowland Polish lakes under future climate change scenarios and consequences for ice cover and mixing dynamics. Journal of Hydrology: Regional Studies **34**: 100780. doi:10.1016/j.ejrh.2021.100780

Pilla, R. M., and C. E. Williamson. 2023. Multidecadal trends in ultraviolet radiation, temperature, and dissolved oxygen have altered vertical habitat availability for Daphnia in temperate Lake Giles, USA. Freshwater Biology **68**: 523–533. doi:10.1111/fwb.14044

Pilla, R. M., C. E. Williamson, B. V. Adamovich, and others. 2020. Deeper waters are changing less consistently than surface waters in a global analysis of 102 lakes. Scientific Reports **10**: 20514. doi:10.1038/s41598-020-76873-x

Pohlert, T. 2023. [R package] trend: Non-Parametric Trend Tests and Change-Point Detection (Version 1.1.6).

Powers, S., S. Fradkin, W. Baccus, and others. 2022. Summer ecosystem structure in mountain lakes linked to interannual variability of lake ice, snowpack, and landscape attributes. Limnology and Oceanography **67**. doi:10.1002/lno.12188

Richardson, D. C., S. J. Melles, R. M. Pilla, and others. 2017. Transparency, Geomorphology and Mixing Regime Explain Variability in Trends in Lake Temperature and Stratification across Northeastern North America (1975–2014). Water **9**: 442. doi:10.3390/w9060442

Rose, K. C., L. A. Winslow, J. S. Read, and G. J. A. Hansen. 2016. Climate-induced warming of lakes can be either amplified or suppressed by trends in water clarity. Limnology and Oceanography Letters **1**: 44–53. doi:10.1002/lol2.10027

Schindler, D. E. 2017. Warmer climate squeezes aquatic predators out of their preferred habitat. Proceedings of the National Academy of Sciences **114**: 9764–9765. doi:10.1073/pnas.1712818114

Soued, C., and Y. T. Prairie. 2022. Patterns and Regulation of Hypolimnetic CO2 and CH4 in a Tropical Reservoir Using a Process-Based Modeling Approach. Journal of Geophysical Research: Biogeosciences **127**: e2022JG006897. doi:10.1029/2022JG006897

Stetler, J. T., S. Girdner, J. Mack, L. A. Winslow, T. H. Leach, and K. C. Rose. 2021. Atmospheric stilling and warming air temperatures drive long-term changes in lake stratification in a large oligotrophic lake. Limnology and Oceanography **66**: 954–964. doi:10.1002/lno.11654

Toffolon, M., S. Piccolroaz, and E. Calamita. 2020. On the use of averaged indicators to assess lakes' thermal response to changes in climatic conditions. Environ. Res. Lett. **15**: 034060. doi:10.1088/1748-9326/ab763e

Wilson, H. L., A. I. Ayala, I. D. Jones, and others. 2020. Variability in epilimnion depth estimations in lakes. Hydrology and Earth System Sciences **24**: 5559–5577. doi:10.5194/hess-24-5559-2020

Winslow, L. A., J. S. Read, G. J. A. Hansen, K. C. Rose, and D. M. Robertson. 2017. Seasonality of change: Summer warming rates do not fully represent effects of climate change on lake temperatures. Limnology and Oceanography **62**: 2168–2178. doi:10.1002/lno.10557

Winslow, L., J. Read, R. Woolway, J. Brentrup, T. Leach, J. Zwart, S. Albers, and D. Collinge. 2019. [R package] rLakeAnalyzer: Lake Physics Tools (version 1.11.4.1).

Woolway, R. I., C. J. Merchant, J. Van Den Hoek, C. Azorin-Molina, P. Nõges, A. Laas, E. B. Mackay, and I. D. Jones. 2019. Northern Hemisphere Atmospheric Stilling Accelerates Lake Thermal Responses to a Warming World. Geophysical Research Letters **46**: 11983–11992. doi:10.1029/2019GL082752

Woolway, R. I., S. Sharma, G. A. Weyhenmeyer, and others. 2021. Phenological shifts in lake stratification under climate change. Nat Commun **12**: 2318. doi:10.1038/s41467-021-22657-4

Wu, L., H. Su, X. Zeng, D. J. Posselt, S. Wong, S. Chen, and A. Stoffelen. 2024. Uncertainty of Atmospheric Winds in Three Widely Used Global Reanalysis Datasets. Journal of Applied Meteorology and Climatology **63**: 165–180. doi:10.1175/JAMC-D-22-0198.1

Yvon-Durocher, G., J. M. Caffrey, A. Cescatti, and others. 2012. Reconciling the temperature dependence of respiration across timescales and ecosystem types. Nature **487**: 472–476. doi:10.1038/nature11205

Zhou, J., P. R. Leavitt, K. C. Rose, X. Wang, Y. Zhang, K. Shi, and B. Qin. 2023. Controls of thermal response of temperate lakes to atmospheric warming. Nat Commun **14**: 6503. doi:10.1038/s41467-023-42262-x

Chapter II Figures

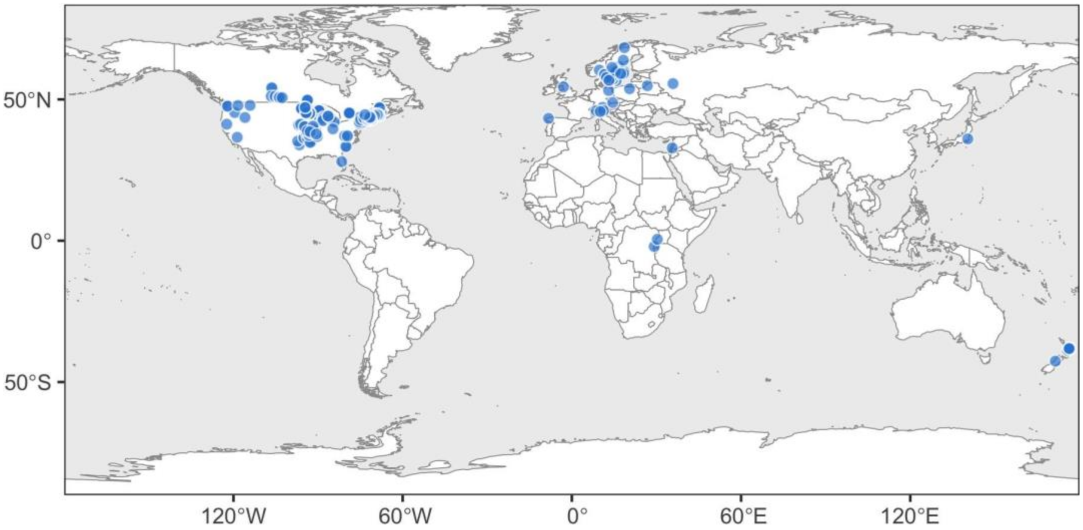

Figure 1: Map of all lakes included in this analysis (*n* = 615 stratified lakes).

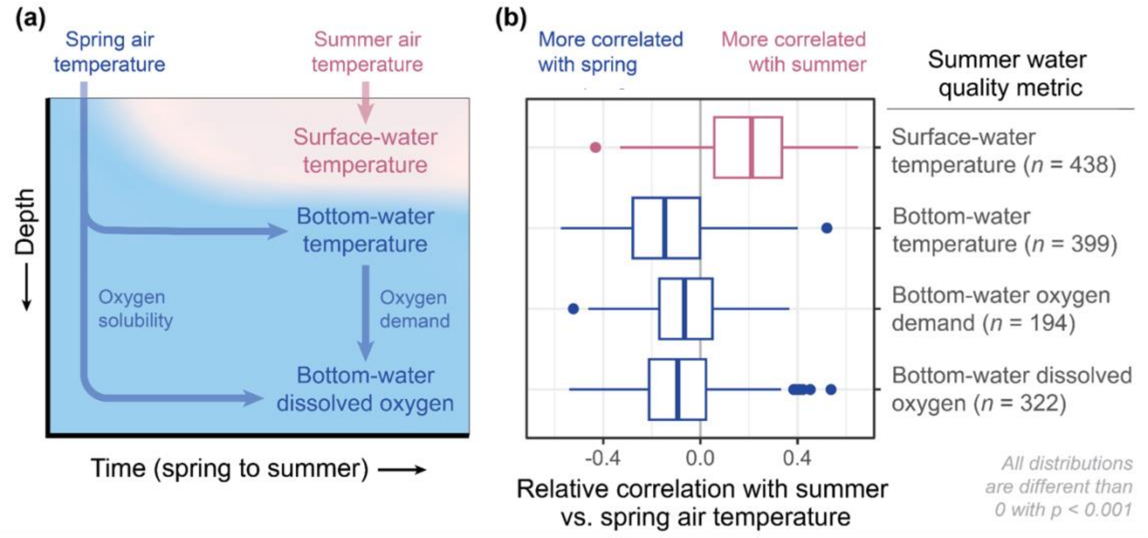

Figure 2: Hypothesized (a) and observed (b) associations between seasonal air temperatures and summer water quality variables. (a) Background color indicates the thermal gradient in the lake, with pink indicating warm surface water during the period of thermal stratification. (b) Relative correlation between summer water quality variables and summer vs. spring air temperatures. Here, each data point represents one lake. Data availability differs among variables within our dataset, and the total number of lakes for each variable is indicated in the y-axis text.

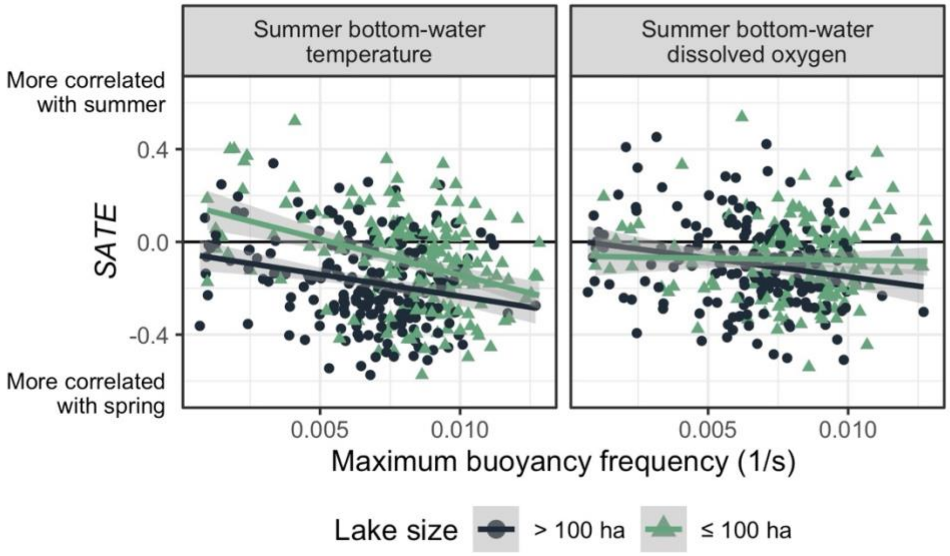

Figure 3: For both summer bottom-water temperature (left) and summer bottom-water dissolved oxygen (right), the relative correlation with summer vs. spring air temperature (i.e., *SATE*) was mediated by thermal stratification and lake surface area. Thermal stratification was quantified as buoyancy frequency at the thermocline (multiannual median). Here, each data point represents one lake.

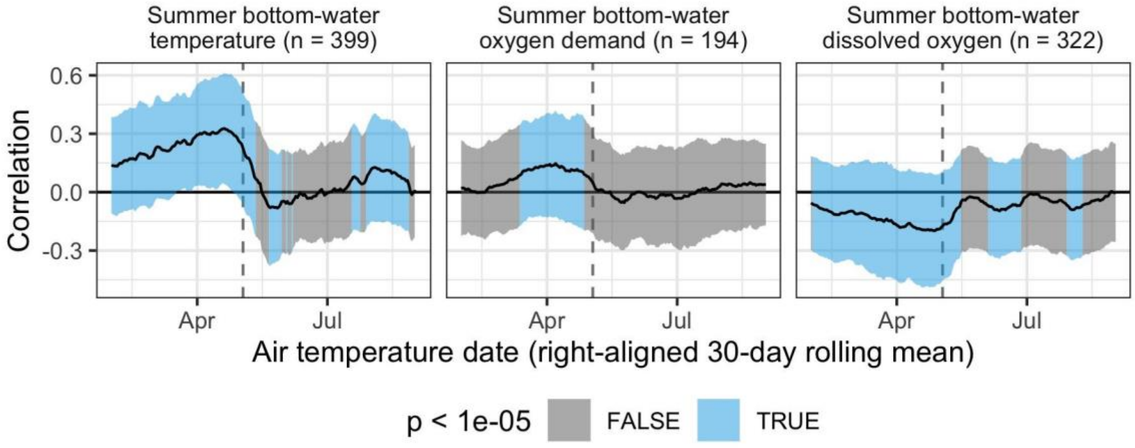

Figure 4: Across all lakes, summer bottom-water temperatures (left), oxygen demand (center), and dissolved oxygen (right) tended to be most strongly correlated with spring air temperatures. Here, each data point is the partial Spearman's correlation between 30-day rolling mean air temperature and the specified variable, while accounting for measurement year. Correlations are calculated on an annual time step over the entire time series at a given lake (number of lakes given in panel title) and are summarized to mean (black line) and standard deviation (shaded ribbon). Ribbon color indicates whether the distribution of correlations across all lakes was symmetric about 0 (blue indicates a Wilcox test with $p < 0.00001$, whereas gray periods denote non-significant relationships). X-axis text indicates the right-aligned 30-day rolling window of air temperature, standardized to the northern hemisphere. Vertical dashed lines indicate the median onset of stratification across $n = 27$ lakes where stratification onset could be identified within one week from observations.

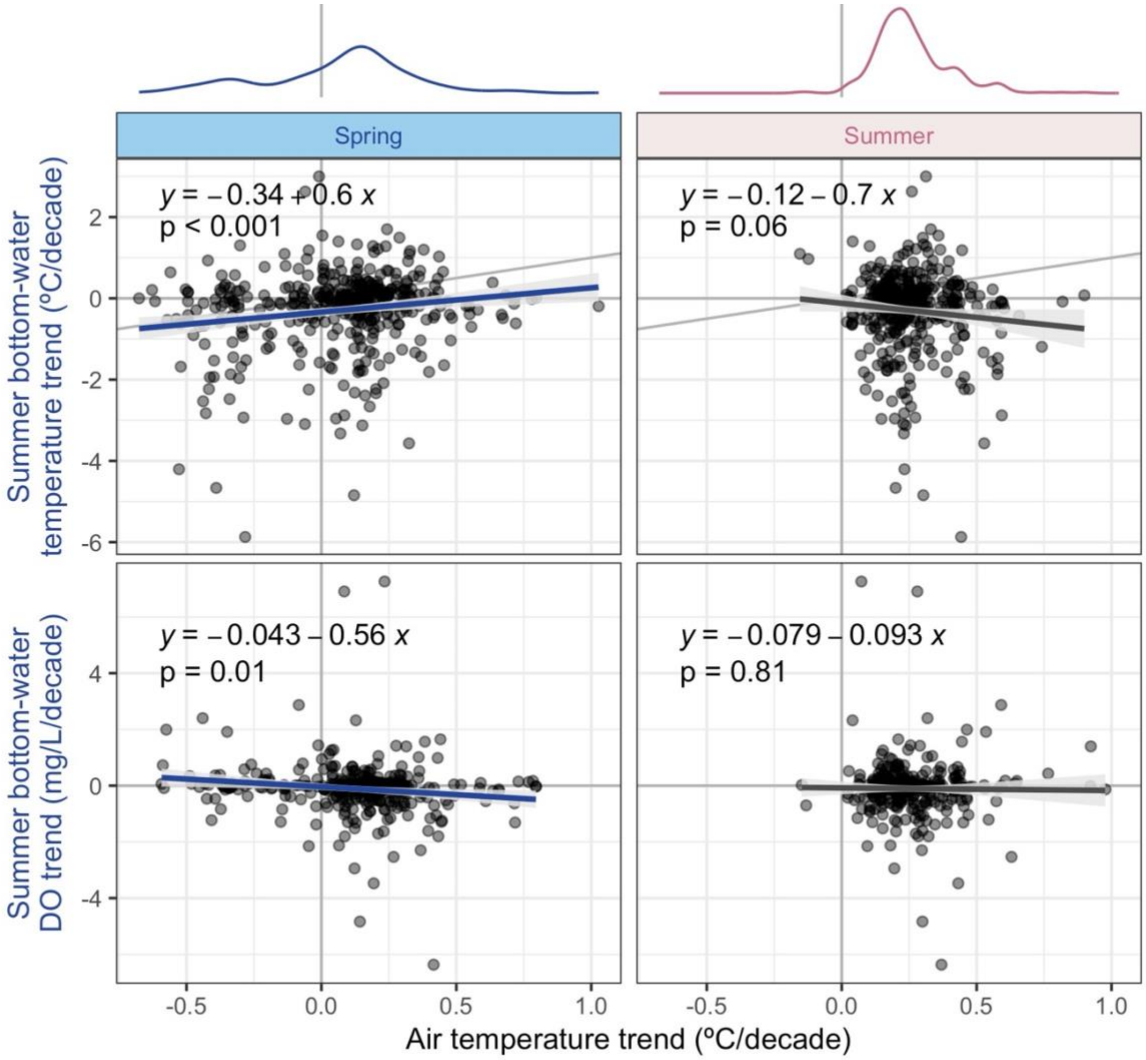

Figure 5: Across all lakes, spring (left), but not summer (right), air temperature trends were significantly associated with summer bottom-water dynamics. Here each point represents one lake. Blue and pink distributions at the top of each panel summarize the distribution of spring and summer air temperature trends, respectively, with the vertical gray lines denoting a 0 ^{o}C/decade air temperature trend. Lines in each panel indicate a linear regression between air and water temperature trends, with the regression equation

and significance presented at the top of the panel. A 1:1 relationship between air and water temperature trends is indicated by a light gray solid line in the top two panels.

Supporting Information for Chapter II

Contents

- Figures S1 to S9
- Table S1

Introduction

This supporting information document provides 9 supplemental figures and one supplemental table that are referenced throughout Chapter II.

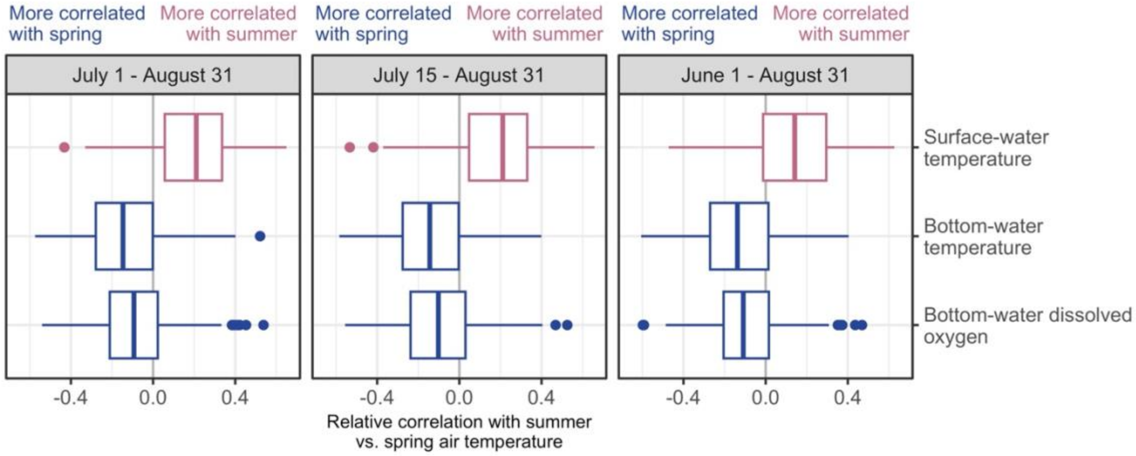

Figure S1: To test the sensitivity of our results to the specific time period used to calculate summer surface- and bottom-water means, we re-ran our analysis using two alternative definitions of summer (standardized to northern hemisphere months). In the analysis presented in the main text, we use means from July and August (panel a). In panel b, we shortened this window to July 15–August 31, following Jane et al. (2021). In panel c, we extended this window to June 1–August 31 (i.e., “JJA”; following IPCC 2023). Ultimately all three temporal windows support that spring air temperature has a stronger effect on summer bottom-water temperature and dissolved oxygen than summer air temperature. Here, we exclude VHOD, which inherently had to be calculated during the entire summer stratified period (Lewis et al. 2024).

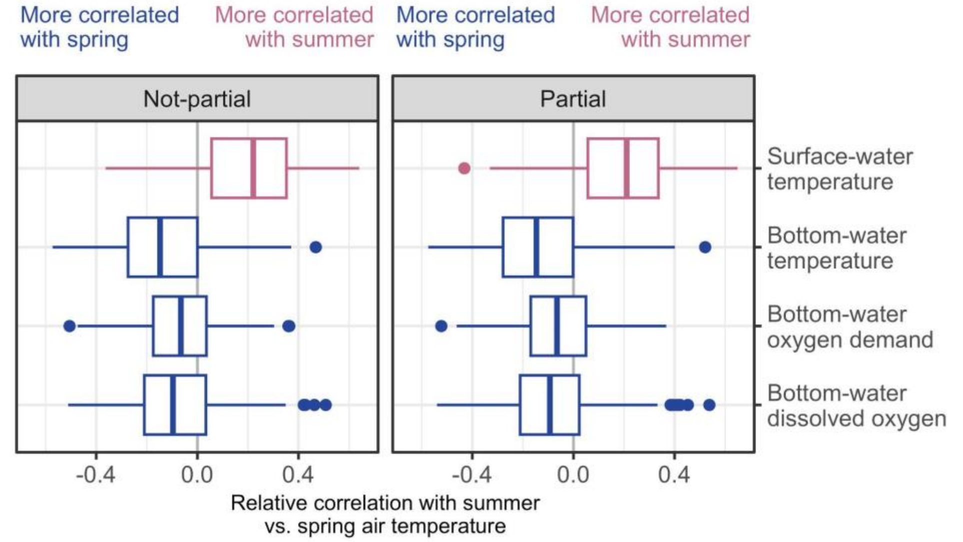

Figure S2: We tested the sensitivity of our results to the use of Spearman's correlation (without accounting for measurement year, left panel) vs. partial Spearman's correlation (accounting for measurement year, right panel). Ultimately both analyses support that spring weather has a stronger effect on summer bottom-water temperature and dissolved oxygen than summer weather.

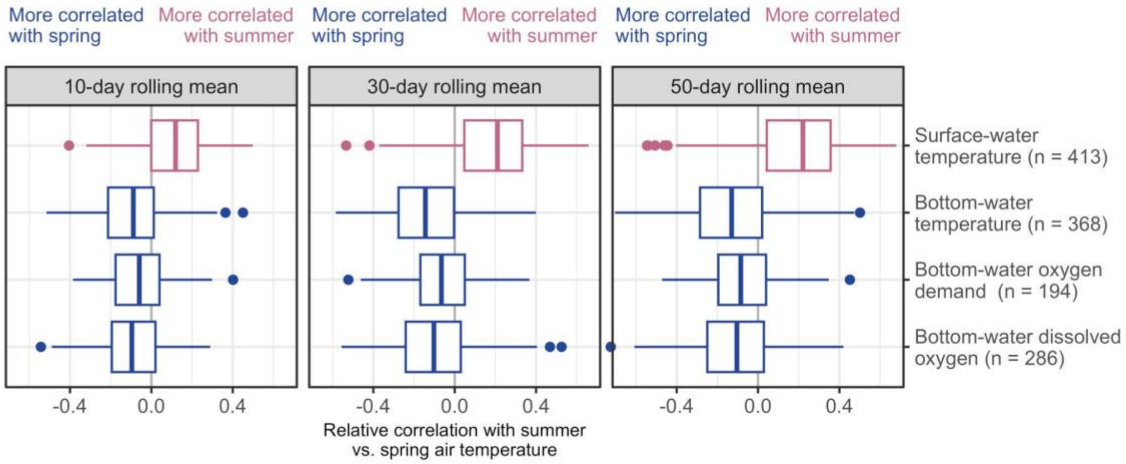

Figure S3: To test the sensitivity of our results to the duration of rolling-mean air temperature we used, we re-ran our analysis using 10-day, 30-day (the window presented in the main text), and 50-day rolling means. Ultimately, the results from analyses using all three durations support that spring weather has a stronger effect on summer bottom-water temperature and dissolved oxygen than summer weather.

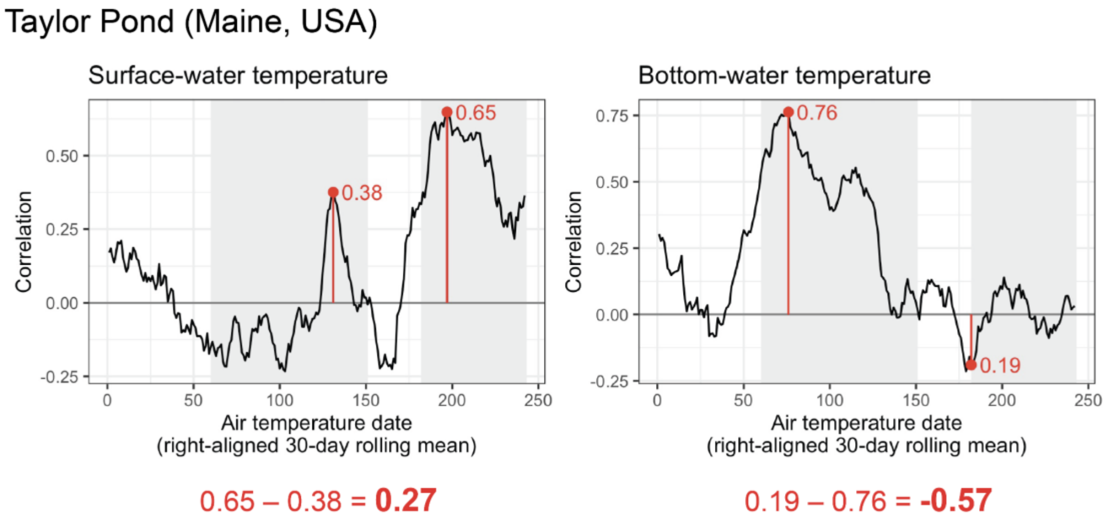

Figure S4: Examples of the Seasonal Air Temperature Effect (*SATE*) calculation for summer surface-water (left) and bottom-water (right) temperature at Taylor Pond (Maine, USA). We calculated the correlation between 30-day windows of air temperature and each of our summer focal variables, then identified the maximum absolute correlation in spring and summer respectively (shaded in grey). We then subtracted the maximum spring correlation from the maximum summer correlation to get our final *SATE* value (bold red number). The positive number in the left panel indicates surface-water temperature was more closely associated with summer air temperature, and the negative number in the right panel indicates that bottom-water temperature was more closely associated with spring air temperature.

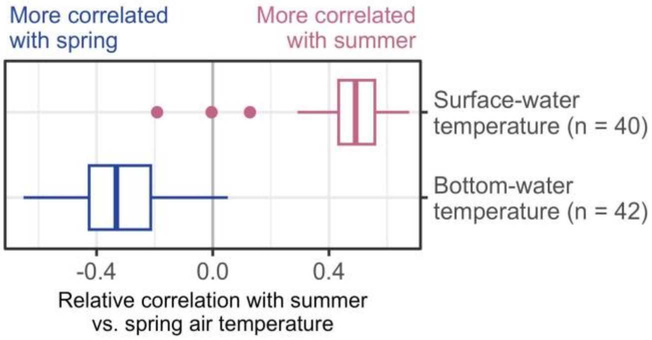

Figure S5: We assessed whether the correlation between spring air temperature and summer bottom-water temperature in our 615-lake dataset was also supported by daily modeled water temperature from 42 lakes. Specifically, we analyzed daily modeled water temperature from the widely-used General Ocean Turbulence Model (GOTM) lake thermodynamic model. The data were accessed from the Inter-Sectoral Impact Model Intercomparison Project (ISIMIP) lakes simulation (global lakes, v3a). Ultimately, our results with modeled water temperature provide further support for the conclusion that spring weather has a stronger effect on summer bottom-water temperature than summer weather.

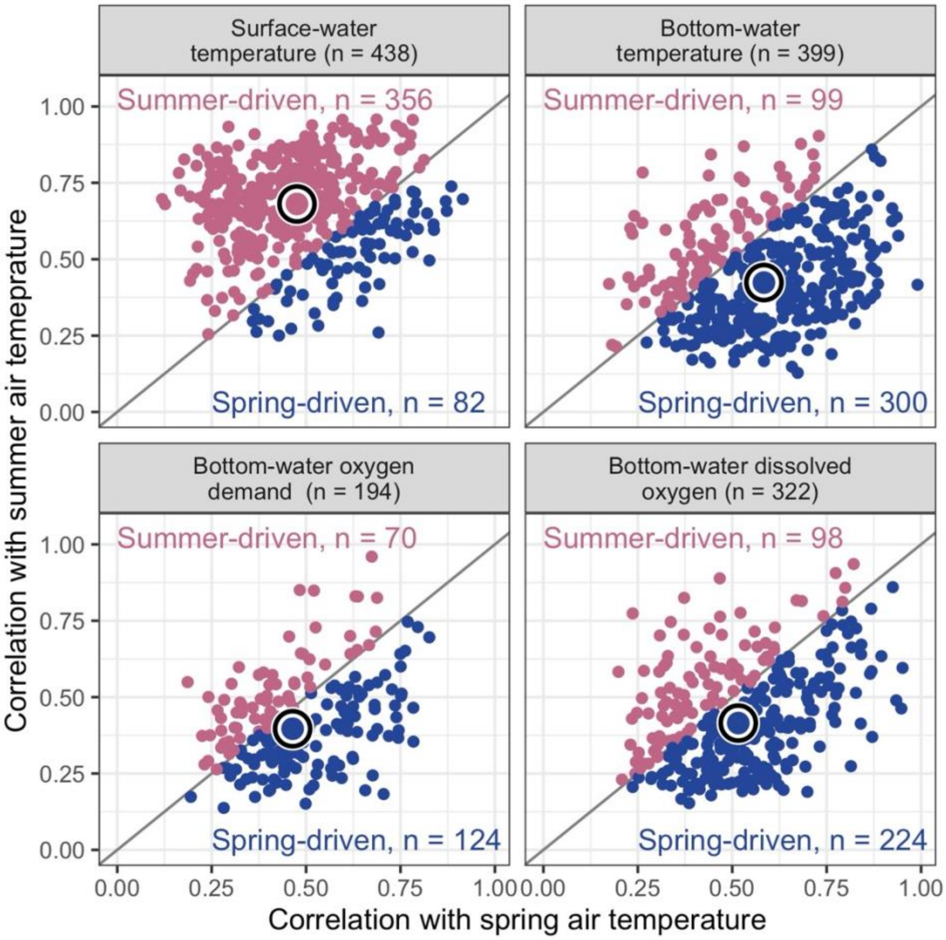

Figure S6: Correlations of the four summer focal lake variables with spring air temperature (x-axis) and with summer air temperature (y-axis); each point represents one lake. Pink points indicate a stronger effect of summer air temperatures on the variable, whereas blue points indicate a stronger effect of spring air temperatures on the variable. The number of lakes on each side of the 1:1 line (grey) is indicated in the bottom-right and top left corners of each panel. Within each panel, the black circle represents the median correlation with spring and summer air temperature across all lakes for each variable.

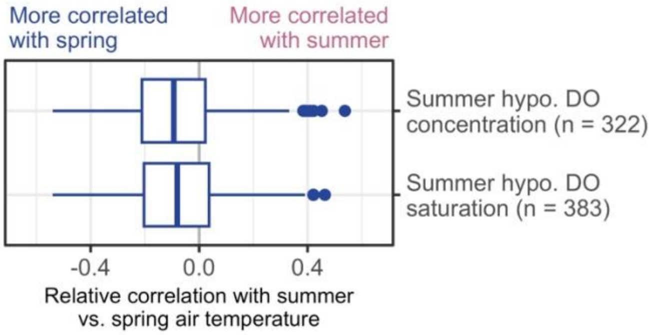

Figure S7: Hypolimnetic dissolved oxygen (hypo. DO) concentration and saturation both tended to be more correlated with spring air temperature than summer air temperature. For lakes where DO saturation was not provided in the original data publication, it was calculated based on DO concentration, water temperature, and elevation using the *rMR* package in R (Moulton 2018).

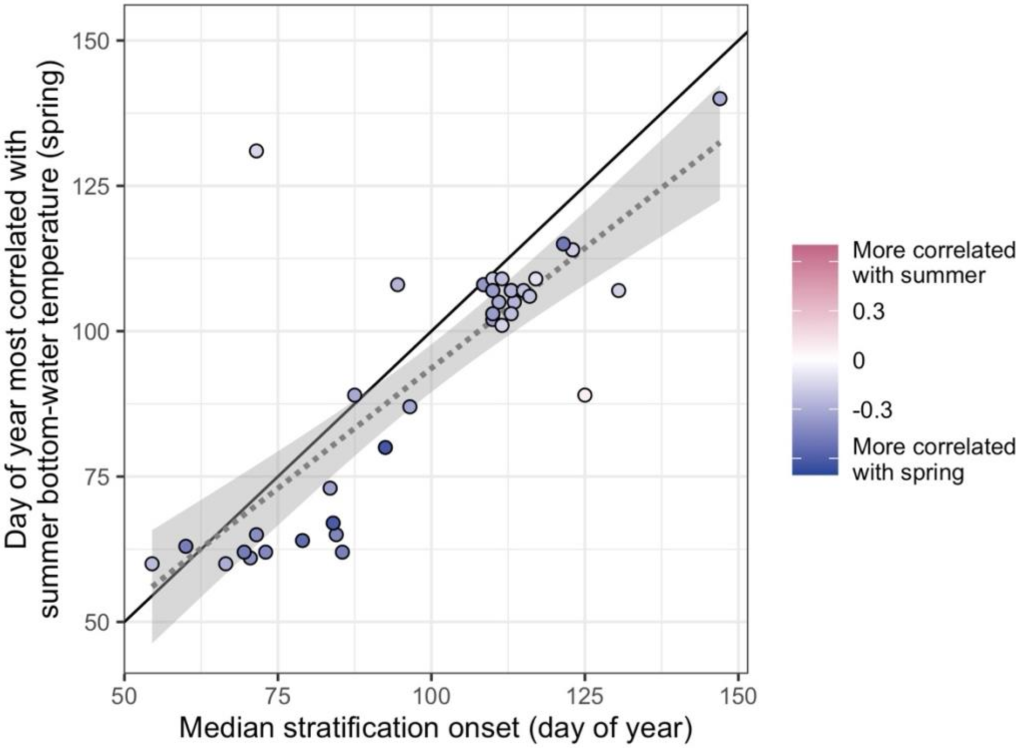

Figure S8: Using modeled water temperature of *n*=42 lakes from the ISIMIP dataset, we calculated the median onset of thermal stratification at each lake and compared this date with the spring date of greatest absolute correlation with bottom-water temperature. Color indicates the Seasonal Air Temperature Effect (*SATE*), in which most lakes' summer bottom-water temperatures were more correlated with spring (blue), compared to summer (red), air temperature.

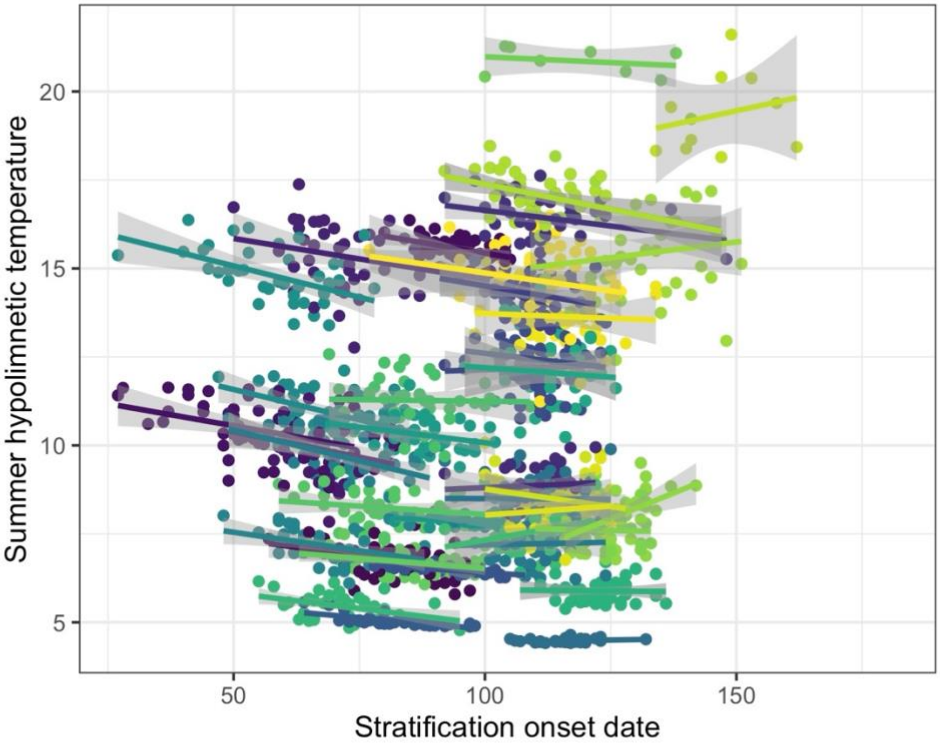

Figure S9: Within the ISIMIP-modeled lake time series, earlier stratification onset dates in a given year tended to be correlated with increased late-summer hypolimnetic temperature. This negative correlation was observed at 32 out of the 40 ISIMIP-modeled lakes represented in our dataset. Here, colors delineate different lakes, and points represent lake-years of modeled data. Linear regressions with standard error were calculated for each lake individually and are plotted as lines on the figure.

Table S1: The magnitude of Seasonal Air Temperature Effect (*SATE*) was mediated by three lake characteristics we were able to examine with our *n*=615 lake dataset: buoyancy frequency at the thermocline (a metric of stratification strength), maximum depth, and surface area. Here, we present the top linear models within two units of AICc for each of our four summer focal variables (surface-water temperature, bottom-water temperature, bottom-water dissolved oxygen, and bottom-water oxygen demand). For each model, we provide model coefficients, degrees of freedom (df), log-likelihood, and AICc. We note that maximum depth and surface area were log-transformed, and all explanatory variables were z-standardized prior to analysis. For each variable, the model with the lowest AICc is in bold.

	Intercept	Buoyancy freq.	Surface area	Max. depth	df	Log-likelihood	AICc
Surface-water temperature	**0.188**				**2**	**82.5**	**-161**
	0.188	0.01			3	83	-160
	0.188		-0.003		3	82.6	-159
	0.188			0.002	3	82.6	-159
Bottom-water temperature	**-0.133**	**-0.069**	**-0.056**		**4**	**106.1**	**-204**
	-0.133	-0.071	-0.049	-0.013	5	106.7	-203
Bottom-water dissolved oxygen	**-0.087**	**-0.030**	**-0.023**		**4**	**98.1**	**-188**
	-0.087	**-0.029**		**-0.023**	**4**	**98.1**	**-188**
	-0.087	-0.032	-0.015	-0.015	5	98.7	-187
Bottom-water oxygen demand	**-0.058**				**2**	**74.5**	**-145**
	-0.058	-0.013			3	75.1	-144
	-0.058			-0.007	3	74.7	-143

References

IPCC. 2023. Climate Change 2021 – The Physical Science Basis: Working Group I Contribution to the Sixth Assessment Report of the Intergovernmental Panel on Climate Change, 1st ed. Cambridge University Press.

Jane, S. F., G. Hansen, B. Kraemer, and others. 2021. Widespread deoxygenation of temperate lakes. Nature **594**. doi:10.1038/s41586-021-03550-y

Lewis, A. S. L., M. P. Lau, S. F. Jane, and others. 2024. Anoxia begets anoxia: A positive feedback to the deoxygenation of temperate lakes. Global Change Biology **30**: e17046. doi:10.1111/gcb.17046

Moulton, T. L. (2018). rMR: Importing Data from Loligo Systems Software, Calculating Metabolic Rates and Critical Tensions (Version 1.1.0). https://cran.r-project.org/web/packages/rMR/index.html

Chapter III: Anoxia Begets Anoxia: A positive feedback to the deoxygenation of temperate lakes

Abigail S. L. Lewis[1], Maximilian P. Lau[2], Stephen F. Jane[3], Kevin C. Rose[4], Yaron Be'eri-Shlevin[5], Sarah H. Burnet[6], François Clayer[7], Heidrun Feuchtmayr[8], Hans-Peter Grossart[9, 10], Dexter W. Howard[1], Heather Mariash[11], Jordi Delgado Martin[12], Rebecca L. North[13], Isabella Oleksy[14], Rachel M. Pilla[15], Amy P. Smagula[16], Ruben Sommaruga[17], Sara E. Steiner[16], Piet Verburg[18], Danielle Wain[19], Gesa A. Weyhenmeyer[20], and Cayelan C. Carey[1]

[1] Department of Biological Sciences, Virginia Tech, Blacksburg, VA, USA

[2] Interdisciplinary Environmental Research Centre, Technical University of Mining and Resources Freiberg, 09599 Freiberg, Germany

[3] Cornell Atkinson Center for Sustainability, Department of Natural Resources and the Environment, Cornell University, Ithaca, NY 14853, USA

[4] Department of Biological Sciences, Rensselaer Polytechnic Institute, Troy, NY 12180 USA

[5] The Kinneret Limnological Laboratory, Israel Oceanographic and Limnological Research, Migdal 14950, Israel

[6] Department of Fish and Wildlife Sciences, University of Idaho, Moscow, ID 83844, USA

[7] Norwegian Institute of Water Research, Oslo, Norway

[8] Lake Ecosystems Group, UK Centre for Ecology & Hydrology, Lancaster, UK

[9] Department of Plankton and Microbial Ecology, Leibniz Institute of Freshwater Ecology and Inland Fisheries (IGB), 16775 Stechlin Germany

[10] Department of Biochemistry and Biology, Potsdam University, 14469 Potsdam, Germany

[11] Prince Albert National Park, Parks Canada, SK, Canada

[12] Department of Civil Engineering, Universidade da Coruña, A Coruña, Spain

[13] School of Natural Resources, University of Missouri-Columbia, Columbia, Missouri, USA

[14] Institute of Arctic and Alpine Research, University of Colorado, Boulder, Colorado, USA

[15] Environmental Sciences Division, Oak Ridge National Laboratory, Oak Ridge, TN, USA

[16] New Hampshire Department of Environmental Services, Concord, NH, USA

[17] Department of Ecology, Universität Innsbruck, 6020 Innsbruck, Austria

[18] National Institute of Water and Atmospheric Research, Wellington, New Zealand.

Published in *Global Change Biology* with the citation:

Lewis, A. S. L., Lau, M. P., Jane, S. F., Rose, K. C., Be'eri-Shlevin, Y., Burnet, S. H., Clayer, F., Feuchtmayr, H., Grossart, H.-P., Howard, D. W., Mariash, H., Delgado Martin, J., North, R. L., Oleksy, I., Pilla, R. M., Smagula, A. P., Sommaruga, R., Steiner, S. E., Verburg, P., Wain, D., Weyhenmeyer, G. A., and Carey, C. C. (2024). Anoxia begets anoxia: A positive feedback to the deoxygenation of temperate lakes. *Global Change Biology*, 30, e17046. https://doi.org/10.1111/gcb.17046

Abstract

Declining oxygen concentrations in the deep waters of lakes worldwide pose a pressing environmental and societal challenge. Existing theory suggests that low deep-water dissolved oxygen (DO) concentrations could trigger a positive feedback through which anoxia (i.e., very low DO) during a given summer begets increasingly severe occurrences of anoxia in following summers. Specifically, anoxic conditions can promote nutrient release from sediments, thereby stimulating phytoplankton growth, and subsequent phytoplankton decomposition can fuel heterotrophic respiration, resulting in increased spatial extent and duration of anoxia. However, while the individual relationships in this feedback are well established, to our knowledge there has not been a systematic analysis within or across lakes that simultaneously demonstrates all of the mechanisms necessary to produce a positive feedback that reinforces anoxia. Here, we compiled data from 656 widespread temperate lakes and reservoirs to analyze the proposed Anoxia Begets Anoxia (ABA) feedback. Lakes in the dataset span a broad range of surface area (1–126,909 ha), maximum depth (6–370 m), and morphometry, with a median time series duration of 30 years at each lake. Using linear mixed models, we found support for each of the positive feedback relationships between anoxia, phosphorus concentrations, chlorophyll-*a* concentrations, and oxygen demand across the 656-lake dataset. Likewise, we found further support for these relationships by analyzing time series data from individual lakes. Our results indicate that the strength of these feedback relationships may vary with lake-specific characteristics: for example, we found that surface phosphorus concentrations were more positively associated with chlorophyll-*a* in high-phosphorus lakes, and oxygen demand had a stronger influence on the extent of anoxia in deep lakes. Taken together, these results support the

existence of a positive feedback that could magnify the effects of climate change and other anthropogenic pressures driving the development of anoxia in lakes around the world.

1. Introduction

Dissolved oxygen (DO) concentrations are declining in the bottom-waters of many aquatic ecosystems around the world (Jenny et al. 2016a; Schmidtko et al. 2017; Breitburg et al. 2018; Jane et al. 2021; Zhi et al. 2023). These declines pose a significant threat to both marine and freshwater ecosystems, as low DO conditions can decrease habitat suitability for numerous aquatic organisms (e.g., Rosenberg et al. 1991; Vaquer-Sunyer and Duarte 2008; Schindler 2017; Pilla and Williamson 2023), and decrease redox potential, promoting methane production (e.g., Encinas Fernández et al. 2014; Vachon et al. 2017; Hounshell et al. 2021), and altering aquatic nutrient cycling (e.g., Hupfer and Lewandowski 2008; Middelburg and Levin 2009; Carey et al. 2022a). In freshwater lakes, the trend of decreasing DO concentrations may be particularly severe, with rates of decline up to 10 times higher than those observed in marine ecosystems (Jane et al. 2021). As freshwaters are critical ecosystems for drinking water, recreation, irrigation, and biodiversity (Reynaud and Lanzanova 2017; Finlayson et al. 2018; Reid et al. 2019; Lynch et al. 2023), understanding and addressing changes in freshwater DO is essential to ensuring water security and ecosystem functioning in the face of global change.

Declines in bottom-water DO concentrations are often attributed to climate change and/or increased nutrient inputs (Jenny et al. 2016a; Bartosiewicz et al. 2019; Jane et al. 2023). Increased air temperatures have been shown to drive increased duration of thermal stratification (Foley et al. 2012; North et al. 2013; Oleksy and Richardson 2021; Woolway et al. 2021), which reduces or inhibits mixing of oxygen to the bottom waters (hypolimnion). Consequently, increases in stratification duration may provide more time for hypolimnetic DO depletion to occur, resulting in lower late-summer DO concentrations and increased duration of anoxia. Changes in stratification duration appear to be a particularly important driver of DO declines in recent decades (ca. 1950-2020; Jane et al. 2023). However, historical nutrient inputs have likely also played a role in deoxygenation by increasing phytoplankton biomass and consequently oxygen demand (Jenny et al. 2016a; b). The relative importance of these two pathways to deoxygenation (i.e., greater stratification duration due to climate change and greater oxygen demand due to eutrophication) likely varies both among lakes and within lakes over time. Consequently, understanding interannual DO dynamics across many lakes may be critical to disentangling the independent effects of stratification duration and eutrophication amidst ongoing changes in global climate and land use (e.g., Moss 2011; Parmesan et al. 2022).

Here, we analyze a positive feedback, derived from decades of aquatic research, by which anoxia (i.e., DO at or near 0 mg/L) during a given year begets increasingly frequent and severe occurrences of anoxia in subsequent years. In this "anoxia begets anoxia" (ABA) feedback, anoxic conditions promote internal phosphorus release, thereby stimulating phytoplankton growth and subsequent decomposition, which in turn fuels increased heterotrophic respiration and further accelerates hypolimnetic DO declines over time (Figure 1). As long-term limnological data have become increasingly accessible (e.g., Pilla et al. 2020; Jane et al. 2021), we now have the opportunity to test the strength and ubiquity of this feedback on a multi-continental scale.

While the individual relationships in the ABA feedback cycle (Figure 1) are well-established, these relationships occur over multiple timescales and amidst numerous other interacting factors (e.g., climate variation) that could prevent the detection of the overall feedback. Hypolimnetic anoxia has been shown to enhance internal loading of phosphorus from sediments (e.g., Mortimer 1941; Nürnberg 1984; Orihel et al. 2017; Figure 1a). However, while redox-controlled phosphorus release fluxes have received significant attention, sediment characteristics, microbial processing, and catchment inputs may also play important roles in phosphorus dynamics (e.g., Hupfer and Lewandowski 2008; Orihel et al. 2017). Increases in hypolimnetic phosphorus are expected to increase surface water (epilimnetic) phosphorus concentrations within a summer stratified period through both biological and physical processes (e.g., organism-mediated transport, diffusion, and internal seiche dynamics; Carpenter et al. 1992; Kamarainen et al. 2009; Haupt et al. 2010; Cottingham et al. 2015) or during autumn mixis when epilimnetic and hypolimnetic waters homogenize (e.g., Nürnberg and Peters 1984, Wetzel 2001; Figure 1b). Higher epilimnetic phosphorus concentrations in turn can stimulate phytoplankton growth in many lakes, thereby increasing chlorophyll-*a* (chl-a, Figure 1c; Schindler 1974), though many other important factors, including nitrogen concentrations, climate, and light availability, also contribute to phytoplankton growth (e.g., Paerl and Huisman 2008; Reinl et al. 2023). Increased phytoplankton biomass and subsequent decomposition may fuel increased biological oxygen demand (Figure 1d; Pace and Prairie 2005; Müller et al. 2019; Ladwig et al. 2021) and result in earlier onset of anoxia (Figure 1e), although climate can also play an important role in driving DO dynamics in many lakes, as discussed above. Given the substantial complexity to each of these relationships, all operating on different time scales, it remains unclear the extent to which the full positive feedback plays a role in controlling DO dynamics within lakes around the world.

Lake characteristics including size and residence time could potentially mediate the strength of the ABA feedback across lakes, though these relationships remain largely untested because they can only be characterized with long-term monitoring data across many diverse lakes. Lakes with longer residence time or larger sediment area:volume ratios may have greater sediment-water interactions, increasing the influence of oxygen demand on hypolimnetic DO, as well as the influence of hypolimnetic DO on hypolimnetic TP (e.g., Jagtman et al. 1992). Likewise, lake size may control the importance of mixing dynamics between the epilimnion and hypolimnion, and residence time may affect the extent to which chl-a and hypolimnetic TP influence biogeochemical dynamics the following year (Wetzel 2001). While many of these expected relationships have not been assessed across lakes, an empirical analysis of data from 2849 lakes suggests that the impact of phosphorus concentrations on chlorophyll-a may be stronger in shallow lakes relative to deep lakes, potentially due to differences in light availability and macrophyte cover (Zhao et al. 2023). Characterizing the effect of lake characteristics on the ABA feedback relationships is needed to identify which lakes are most susceptible to the feedback, enabling managers to prioritize conservation efforts across lakes.

In this study, we analyzed data from 656 widespread temperate lakes to study the drivers and consequences of interannual changes in hypolimnetic DO. Our research had three primary goals: first, we assessed the extent of support for each of the hypothesized relationships between anoxia, hypolimnetic phosphorus concentrations, epilimnetic phosphorus concentrations, epilimnetic chl-a, and oxygen demand across and within lakes (Figure 1). Second, we analyzed records of air temperature at each lake to assess how the ABA feedback may interact with changes in climate (Figure 1). We focused on climate as an external driver of the ABA feedback in lieu of accessible nutrient loading records for the study lakes. Third, we analyzed whether the strength of ABA relationships may vary with lake characteristics including lake depth and residence time. While our multi-lake approach precluded detailed consideration of external nutrient inputs and use of causal inference methods within a lake over time, analyzing data from many lakes was essential to testing the proposed relationships in this study and disentangling lake-specific effects amidst substantial heterogeneity.

2. Methods

2.1 Overview of data compilation and analysis

Analyzing the ABA feedback required time series data for hypolimnetic DO, hypolimnetic total phosphorus (TP), epilimnetic TP, epilimnetic chlorophyll-*a* (chl-a), hypolimnetic oxygen demand, and climate records across numerous lakes (Figure 1). We compiled in-lake data from 656 geographically widespread stratified lakes to enable these analyses (*2.2 Dataset compilation*). We used linear mixed models, including relevant lags and climatic data when appropriate (*2.3.2 Mixed effects modeling*) to assess support for the ABA feedback relationships across all lakes. We then ran the same linear models within individual lakes when sufficient data were available to assess whether the strength of ABA relationships may vary with lake characteristics (*2.3.3 Within-lake regressions*). All data compilation and analyses are described in detail below.

2.2 Dataset compilation

2.2.1 In-lake data

We synthesized data from a total of 656 temperate, seasonally-stratified lakes (Figure 2; Appendix S1: Text S1.1). Data were collated from Jane et al. (2021; *n* = 316 unique lakes not also available in the other datasets described here), the U.S. Wisconsin Department of Natural Resources (DNR; *n* = 163), the U.S. New Hampshire Volunteer Lake Assessment Program

(VLAP; *n* = 93), the U.S. Lake Stewards of Maine (LSM) Volunteer Lake Monitoring Program (*n* = 48), the U.S. Adirondack lakes database (Winslow et al. 2018; Leach et al. 2018; *n* = 17), and members of the Global Lake Ecological Observatory Network (GLEON; *n* = 29). Chlorophyll-*a* data from Filazzola et al. (2020) were added for *n* = 15 lakes for which we did not have any other chl-a data.

Data availability and collection methods differed substantially among sites (documented in Lewis et al. 2023). For each site, we collated available data for DO, water temperature, TP, and chl-a, as well as lake metadata including geographic coordinates, depth (mean and maximum), surface area, and elevation (Lewis et al. 2023). Total nitrogen (TN) and dissolved organic carbon (DOC) were also compiled but were more limited in availability (*n* = 111 lakes for DOC and *n* = 119 lakes for TN), motivating us to primarily focus on TP in our analyses below. To harmonize multiple datasets, quality control was performed on all data, as described in the data publication (Lewis et al. 2023).

In sum, the complete dataset consisted of 108,736 distinct water temperature and DO profiles across 656 lakes during 1938-2022 (Appendix S2: Figure S2.1). The median data duration was 30 years at each lake (range: 3–81 years). Lakes in the dataset had a median depth of 14 m (Z_{max}; range: 6–370 m), median surface area of 100 ha (range: 1–126,909 ha), and median elevation of 264 m (range: -215–2804 m). The lakes were located in 18 countries across 5 continents, with latitudes ranging from -42.6 to 68.3 (Lewis et al. 2023).

2.2.1.1 HydroLAKES

We collated additional metadata for each lake using HydroLAKES, a global database of 1.4 million lakes (with surface area ≥10 ha; Messager et al. 2016). For lakes with missing mean or maximum depth (i.e., the depths were not reported with the data; $n = 43$), we used HydroLAKES data to fill in these values (Lewis et al. 2023). We also compiled residence time estimates from HydroLAKES to assess whether the strength of ABA feedback relationships may vary with differences in residence time across lakes.

2.2.2 Epilimnetic and hypolimnetic concentrations

2.2.2.1 Profile interpolation

We interpolated all temperature and DO profiles to a 1-m resolution following Jane et al. (2021). Briefly, we selected all profiles with at least three depths, then used the *pchip()* function of the *pracma* R package (Borchers 2022) to interpolate measurements from the surface to the deepest sampled depth.

To account for variation and error in sampling procedures, we implemented a standardized screening protocol to remove temperature and DO profiles that were substantially shallower or deeper than the reported maximum depth of the lake (Appendix S3).

2.2.2.2 Mean concentrations

We averaged data for all focal variables to an annual timestep using data from the entire stratified period and, separately, the late-summer period at each lake (Appendix S1: Text S1.2). The late summer (i.e., mid-July through August in the northern hemisphere, following Jane et al. 2021) is when DO concentrations are likely to approach their lowest value (Wetzel 2001), and may consequently be a critical time period for some processes in the ABA feedback. Conversely, other processes occurring throughout the entire summer stratified period (e.g., oxygen demand, hypolimnetic temperature) can also be critical to the ABA feedback, motivating the study of both periods within a year.

For each profile during either the entire summer stratified period or the late-summer period, we calculated the depths of the top and bottom of the metalimnion (the middle thermal layer of the lake) using the *rLakeAnalyzer* R package (Winslow et al. 2019). We used mean metalimnion depths to estimate the bottom of the epilimnion and top of the hypolimnion for each lake-year. We then averaged all hypolimnetic and epilimnetic water quality measurements throughout the time-period of analysis, using interpolated profiles for temperature and DO and all measurements for TP, chl-a, TN, and DOC. To estimate the strength of stratification at the thermocline, we calculated maximum buoyancy frequency using *rLakeAnalyzer* (Read et al., 2011; Winslow et al. 2019) for each temperature profile. Maximum buoyancy frequency was averaged throughout the stratified period for each lake-year (Table 1).

2.2.3 Volume-weighted hypolimnetic oxygen demand

We calculated volume-weighted hypolimnetic oxygen demand (VHOD; hereafter oxygen demand) within each lake-year, following Wetzel and Likens (2000). Briefly, we used measured or modeled bathymetric contours and interpolated DO profiles to calculate the volume-weighted hypolimnetic DO concentration for each sampling date, then used linear regression models to calculate the rate of decline in volume-weighted hypolimnetic DO concentrations within the summer stratified period. We calculated an oxygen demand rate based on the raw data, as well as a temperature-corrected oxygen demand rate following Pace & Prairie (2005). Detailed methods for both calculations are provided in Appendix S4.

2.2.4 Anoxic Factor

Anoxic factor (AF) describes the spatial and temporal extent of anoxia within a lake, and is therefore a useful metric of deoxygenation in lakes that experience hypolimnetic anoxia (Nürnberg 1995; Nürnberg 2019). AF is expected to increase with increased oxygen demand and can predict internal TP loading in lakes that experience hypolimnetic anoxia (Nürnberg 1995; Nürnberg 2019; Figure 1). Here, we calculated AF within each lake-year following Nürnberg (1988) and Nürnberg (2019), modified to address limited data availability across and within lakes (Appendix S5). Briefly, we estimated the duration of anoxia using oxygen profiles, oxygen demand, and modeled turnover dates, and we used modeled or measured bathymetry to quantify the spatial extent of anoxia within each lake-year. The DO threshold for anoxia was defined operationally, as described below (*2.3.3 Operational definition of anoxia*), with detailed methods provided in Appendix S5.

2.2.5 Climate data

To disentangle the roles of changing climate and in-lake processes on DO dynamics in stratified lakes, we collated monthly air temperature and precipitation data for every lake in our dataset from the ERA5 climate reanalysis. ERA5 is a fifth-generation product from the European Centre for Medium-Range Weather Forecasts (ECMWF) and provides meteorological data from 1959–2022 on a 0.25-degree global grid (Hersbach et al. 2019). For our analysis, we used the monthly 2-m air temperature and total precipitation ERA5 data products and found the closest gridded values for every lake in our dataset. We summarized "seasonal" air temperature and precipitation values by averaging across multiple months for each lake-year, with southern hemisphere data offset by six months. Spring values were calculated as the average of March and

April air temperature or precipitation (following, e.g., Williamson et al. 2015). While stratification onset varies across latitudes and lakes, these spring months are the most likely to correspond to ice melt and spring mixing across the temperate lakes in this study (Woolway et al. 2021; Appendix S1: Figure S1.2). Summer values were calculated as the average of July and August air temperature or precipitation, as these summer months most closely correspond with our late-summer in-lake data and were the warmest two months on average across the dataset (Appendix S2: Figure S2.4). Winter temperature and precipitation were calculated as the average of January and February air temperature and precipitation. These winter months were, on average, the coldest months in our dataset (Appendix S2: Figure S2.4), and likely constituted a significant portion of the ice-covered period in lakes that experience seasonal ice cover (Magnuson et al. 2000).

2.3 Data analysis

To analyze the proposed ABA relationships, we used lag analysis (*Section 2.3.1*), mixed effects modeling (*Section 2.3.2*), and within-lake regressions (*Section 2.3.3*). All data analyses were performed in R, version 4.2.1 (R Core Team, 2021). Analysis code is archived as a Zenodo repository for reproducibility (Lewis and Lau, 2023).

2.3.1 Lag analysis

Several of the relationships in the proposed ABA feedback may operate across years, rather than within one year. To assess the appropriate lag for each step, we calculated the Spearman correlation between each variable of analysis and the preceding variable in the feedback cycle (e.g., between oxygen demand and chl-a; Figure 1) with 0, 1, and 2-year lags.

These correlations were calculated separately for each lake with at least 10 years of paired data for the target parameters. Across all lakes, we calculated whether the mean of the resulting distribution of correlations was significantly different than zero using Wilcox tests with $\alpha = 0.05$.

2.3.2 Mixed effects modeling

To assess the proposed mechanisms by which anoxia could create a positive feedback that promotes subsequent anoxia (Figure 1), we used linear mixed models to estimate the magnitude and direction of effect for drivers of AF, epilimnetic and hypolimnetic TP, epilimnetic chl-a, and oxygen demand among lake-years. To assess the relationship between oxygen demand and hypolimnetic DO concentrations in lakes that did not experience anoxia (i.e., AF = 0 days throughout the entire time series), we conducted an additional regression analysis for oxygen demand and late-summer hypolimnetic DO concentrations, rather than AF (Appendix S6). Lake ID was included as a random effect on the intercept in all models. Mixed effect models were run using the package *lme4* in R (Bates et al. 2023).

For each response variable, we filtered all data to only include lake-years with complete data for all proposed explanatory variables (Table 1). We log-transformed chl-a and TP concentrations due to the substantial positive skew of these data, and we Z-standardized all explanatory variables. We fit linear mixed models for all possible combinations of explanatory variables and identified the best model using corrected Akaike Information Criterion (AICc). We report all selected models within two AICc units of the best model (Burnham & Anderson 2002). We assessed the multicollinearity of all models using the variance inflation factor, which we calculated using the *vif()* function from the package *car* in R (Fox et al. 2022).

We plotted the coefficient estimate for all fixed effects in the selected models to visually compare the magnitude of effect for each explanatory variable. For these visualizations, we calculated 95% confidence intervals of the fixed effects using the *confint.merMod()* function from *lme4* (Bates et al. 2023).

2.3.3 Operational definition of anoxia

We used an operational DO threshold to define hypolimnetic anoxia, following other studies on anoxia in lakes (e.g., Elshout et al. 2013; Nürnberg et al. 2019; LaBrie et al. 2023). To identify this threshold, we performed a breakpoint analysis and piecewise regression for hypolimnetic DO and TP using the package *segmented* in R (Muggeo, 2023; Appendix S6: Text S6.1). We then added slope-difference (U) and change-point (G0) parameters for the breakpoint relationship, and used the resulting breakpoint as a threshold value for our calculation of AF (Appendix S5).

2.3.4 Within-lake regressions

To assess whether the across-lake trends identified using mixed models were observable within individual lakes, we performed linear regressions separately at each lake. For each of our focal response variables (see Table 1), we used the same model formulations from the across-lakes analysis (i.e., the explanatory variables from Table 1 that were selected via AICc) to perform regressions within a lake. We saved the resulting coefficient estimates for each explanatory variable used to predict this focal response. We then plotted the distribution of coefficient estimates for all explanatory variables across all lakes, and we compared the median of these distributions to the mixed effect model coefficient estimates. For each response variable, we only included lakes that had at least 10 years of paired data for the response variable and all selected explanatory variables. We removed *n* = 81 lakes that never experienced anoxia (i.e., AF = 0 throughout the timeseries) from the within-lake analysis of the drivers of AF.

2.3.4.1 Driver analysis

The coefficient estimates for explanatory variables included in the ABA feedback (e.g., the coefficient of epilimnetic TP for predicting epilimnetic chl-a) indicates the magnitude of the response, while accounting for other drivers (Table 1). As an exploratory analysis to assess which lakes are most susceptible to the ABA feedback, we analyzed whether there were significant differences in these coefficients based on differences in lake characteristics. For this analysis, we developed linear models predicting the coefficient estimate for each focal variable in the ABA feedback (Table 1) based upon (individually) maximum depth, surface area, mean depth, residence time, dynamic ratio (square root of lake area divided by mean depth; Håkanson 1982), and mean concentrations of focal (ABA) variables (i.e., hypolimnetic DO, epilimnetic and hypolimnetic TP, epilimnetic chl-a, and oxygen demand). We then used AICc to select the model(s) with the greatest explanatory power. We did not assess more complicated model structures (e.g., multiple drivers and interaction effects) due to the relatively small sample size for some of these analyses (e.g., *n* = 35 lakes for oxygen demand).

2.3.5 Climate effects

To summarize the effects of climatic variation on oxygen dynamics, we analyzed monthly and annual air temperature data. First, we calculated correlations between monthly air temperatures and, separately, hypolimnetic temperature, oxygen demand, AF, and late-summer

DO concentrations (Appendix S8). Then, we summarized the effects of high and low annual air temperature anomalies on AF and late-summer oxygen concentrations (Appendix S8).

3. Results

3.1 Operational definition of hypolimnetic anoxia

We identified a breakpoint relationship whereby hypolimnetic TP increased substantially after DO decreased below a threshold of 1.8 mg/L (56 µmol/L), averaged throughout the hypolimnion (Figure 3). Subsequently, we used 1.8 mg/L as our DO threshold for anoxia in all analyses. Of the 356 lakes with at least 10 years of hypolimnetic DO data, 146 lakes (34%) crossed the threshold of 1.8 mg/L during their time series (i.e., had at least one year with hypolimnion-averaged DO <1.8 mg/L and at least one year with DO ≥1.8 mg/L). Lakes that crossed this threshold (n = 146) were more common than lakes that had consistently anoxic (n = 120) or consistently oxic (n = 90) hypolimnia. Furthermore, lakes that crossed the threshold of 1.8 mg/L had lower DO concentrations in the year following the first year of anoxia than in the year prior to the first year of anoxia (Appendix S9; Figure S9.1).

3.2 Regression analyses support expected relationships within and across lakes

Our analyses across 656 lakes provided support for the ABA feedback. Of the explanatory variables used in our model selection process (Table 1), all variables that were predicted to promote the ABA feedback were found to be statistically significant drivers of their predicted responses (Figure 4), with expected temporal lags as applicable (0–1 years; Appendix S7). High AF was associated with high hypolimnetic TP (Figure 4a), and high hypolimnetic TP was associated with high epilimnetic TP, both within and between years (i.e., both Hypo TP and

Hypo TP_{t-1} had positive coefficients; Figure 4b). High epilimnetic TP was in turn associated with high chl-a within a year (Figure 4c), and high chl-a was associated with high oxygen demand (both VHOD and $VHOD_{std\ 10°C}$) the following year (Figure 4d; Appendix S10). Lastly, high oxygen demand was associated with greater AF in the lakes that experienced hypolimnetic anoxia (Figure 4e). For the lakes that did not exhibit anoxia during their time series, high oxygen demand was associated with low late-summer DO concentrations (Appendix S6).

All of the ABA relationships observed to be significant across hundreds of lakes (n = 111–386; Figure 4) were also supported by regression analyses conducted within individual lake time series (with n = 35–157 lakes for each analysis; Figure 5). The direction of each of the ABA relationships was identical within and across lakes (Figure 5). The magnitude of the median coefficient estimates for ABA explanatory variables within lakes (e.g., the coefficient for chl-a in the multiple linear regression with oxygen demand as a response variable) tended to be slightly smaller than the mixed model coefficient estimate (Figure 5) for each relationship, except for oxygen demand as a predictor of AF (Figure 5e).

While the hypothesized ABA feedback was supported by regression analyses, variability in the focal response variables (i.e., AF, TP, chl-a, and oxygen demand; Table 1) was also modulated by additional driving factors, as expected (Figure 1; Appendix S8). Specifically, climatic variables were selected as part of the optimal model for nearly all focal variables: spring air temperatures were important drivers of AF and chl-a, spring and summer precipitation were significant drivers of epilimnetic TP, and winter precipitation was a significant driver of hypolimnetic TP (Figure 4; Figure 5). Water temperature also played a role in explaining variation in several focal responses: hypolimnetic temperatures were a significant predictor of both AF and oxygen demand (Figure 4; Figure 5). For all responses, we found substantial variability in the random intercept of the mixed-model regressions among lakes (Table 2) and variability in within-lake regression coefficients (Figure 5), indicating external lake-specific factors that influence the state of each response variable at a given lake. Random effects were largest for AF, and residual standard deviation from mixed-model analyses was highest for oxygen demand and epilimnetic chl-a (Table 2).

Across lakes, our analyses indicate that the relative strength of ABA relationships varied with lake characteristics. Specifically, the coefficient for the effect of epilimnetic TP on chl-a was larger for lakes with high mean epilimnetic TP values; the coefficient for the effect of oxygen demand on AF was larger for lakes with deep mean depth; and the coefficient for the effect of chl-a on oxygen demand was larger for lakes with long residence time (Figure 6). The other ABA feedback relationships were not significantly mediated by any one of our candidate predictors (*Section 2.3.4.1*).

4. Discussion

In analyzing ABA relationships both across and within 656 lakes, we found support for all linkages in the hypothesized ABA feedback (Figure 4; Figure 5). These results provide empirical support for the existence of a positive feedback mechanism that could intensify the development of anoxia in lakes around the world. Furthermore, our results indicate that the strength of these relationships likely varies with lake characteristics, including mean depth, TP concentrations, and residence time. To our knowledge, our work is the first to quantitatively document all of the relationships that enable anoxia to beget increasingly frequent or more intense anoxia in future years across a large, multi-continental dataset of lakes.

4.1 Decades of research facilitate identification of ABA feedback

Individual relationships in the ABA feedback have been the subject of substantial research inquiry over the past century or longer (e.g., Sachs 1874; Thienemann 1928; Schindler 1974). While these previous studies primarily focused on examining biogeochemical dynamics within one lake, they provided support for the individual relationships in the ABA feedback (Figure 1). Modeling studies provided a means of simultaneously considering all ABA relationships and have shown mechanistic support for the existence of an ABA feedback in seasonally-stratified lakes (Carpenter 2003; Carpenter and Lathrop 2008). However, model simulations have indicated that the susceptibility of individual lakes to a trophic regime shift, as a result of the ABA feedback, depends on multiple lake-specific parameters (i.e., macrophyte presence, temperature, mean depth; Genkai-Kato & Carpenter, 2005), highlighting the need for a multi-lake empirical approach.

By synthesizing data across many lakes, our mixed model approach allowed us to identify biogeochemical dynamics that likely would have been difficult to detect in individual lakes. The strength of this approach is reflected in the fact that coefficient estimates from our mixed model regressions, which integrate data from many lakes, were typically slightly larger in magnitude than the median coefficient estimates of regressions run within individual lakes (Figure 5), although both approaches showed support for the existence of the ABA feedback. Across-lake regressions included a larger range of variation for predictor variables than is typically observed within individual lakes, which likely facilitated the detection of more substantial predictor-response effects. Through study of the hypothesized ABA feedback, we found support for several individual limnological relationships, some of which had not been previously analyzed on a widespread scale. Below we discuss our findings for each ABA relationship and their implications in the context of previous work (*Sections 4.1.1–4.1.5*).

4.1.1 Effect of anoxia on hypolimnetic TP (Figure 1a)

In this study, we observed a strong positive relationship between hypolimnetic anoxia and TP concentrations both within and across lakes. Across lakes, our breakpoint analysis detected a threshold relationship whereby hypolimnetic DO had a stronger effect on TP when DO concentrations decreased to levels approaching anoxia (<1.8 mg/L; Figure 3). Our results reinforce previous research affirming that AF (the duration and spatial extent of anoxia) may be strongly positively correlated with hypolimnetic TP concentrations (Figure 4; Figure 5; e.g., North et al. 2014; Nürnberg et al. 2019). A threshold relationship between DO and TP is well-supported by previous research across sediment core incubations, *in situ* sediment chamber measurements, and mass-balance whole ecosystem analyses (e.g., Einsele 1936; Mortimer 1942; Orihel et al. 2017; Anderson et al. 2021). Here, our threshold value of 1.8 mg/L DO, averaged throughout the entire hypolimnion, likely reflects DO conditions of ~0 mg/L near the sediment-water interface (which inherently is challenging to quantify empirically), resulting in enhanced TP loading (Nürnberg 2019). We note that our identified breakpoint of 1.8 mg/L is also remarkably similar to those identified in previous sediment incubation work (Matisoff et al. 2016; Doig et al. 2017; Orihel et al. 2017). Overall, this analysis indicates that the ABA mechanism may require hypolimnetic DO concentrations to decrease to low levels (i.e., <1.8 mg/L) before a feedback effect will occur.

In our dataset, it was common for lakes to cross the threshold of 1.8 mg/L (34% of *n* = 356 lakes). Lakes where oxygen concentrations declined below 1.8 mg/L had lower DO concentrations in the year following the onset of anoxia than in the year prior to the onset of anoxia (Appendix S9; Figure S9.1). While our dataset was not a random or fully representative sample of global lakes, the large number of lakes which crossed the 1.8 mg/L threshold in this study suggests that the ABA feedback may be prevalent.

4.1.2 Effect of hypolimnetic TP on epilimnetic TP (Figure 1b)

We found moderately strong support for an effect of hypolimnetic TP on epilimnetic TP both within one year and between years (i.e., hypolimnetic TP influences epilimnetic TP the following year). While the directionality of this relationship can be difficult to identify in the absence of detailed nutrient input data (i.e., epilimnetic TP can affect hypolimnetic TP, vice versa, or a third driver may simultaneously influence both), existing research provides strong support for this effect. Elevated hypolimnetic TP concentrations can increase epilimnetic TP concentrations within a summer stratified period through organism-mediated transport, diffusion, and internal seiche dynamics (e.g., Carpenter et al. 1992; Soranno et al. 1997; Kamarainen et al. 2009; Nürnberg 2009; Haupt et al. 2010; Cottingham et al. 2015). At the onset of autumn mixing, the concentration of TP in the hypolimnion fundamentally determines the amount of potential TP input to the epilimnion, which can have legacy effects throughout the subsequent autumn, winter, and spring (e.g., Nürnberg and Peters 1984; Wang et al. 2019).

4.1.3 Effect of epilimnetic nutrients on epilimnetic chl-a (Figure 1c)

We found a strong positive association between surface water TP concentrations and surface water chl-a, both within and across lakes, likely reflecting the fact that interannual variability in phosphorus concentrations can play an important role in regulating phytoplankton growth in lakes (Figure 4; Figure 5). Our study follows many decades of data that illustrate the positive effect of TP on phytoplankton biomass (Schindler 1974; Smith 1982; MacKeigan et al. 2023). In this study, we were unable to identify an effect of epilimnetic TN concentrations on chl-a, suggesting that in these lakes, TP may play a more important role in regulating phytoplankton growth. However, we note that data availability was substantially greater for TP (n = 387 lakes) than for TN (n = 86 lakes), and complexities of nitrogen forms (not considered here) may hinder the detection of a nitrogen effect. Previous research has documented the importance of nitrogen for limiting or co-limiting phytoplankton growth in some lakes, over multiple timescales (Elser et al. 2007; Lewis Jr. and Wurtsbaugh 2008; Paerl et al. 2016; Scott et al. 2019; Lewis et al. 2020). Consequently, our study highlights the need for long-term, speciated nitrogen data to disentangle the role of nitrogen in the ABA feedback.

4.1.4 Effect of epilimnetic chl-a on oxygen demand (Figure 1d)

Support for the relationship between epilimnetic chl-a and oxygen demand was relatively weaker than for the other ABA relationships, although still consistent within and across lakes. We expected that this relationship would be more challenging to detect than the other ABA relationships due to high levels of spatio-temporal heterogeneity in chl-a and uncertainty associated with oxygen demand calculations (e.g., modeled bathymetry and the assumption of a closed system). Interestingly, the effect of chl-a appeared to occur at least as strongly between years as within a year. Legacy effects of chl-a on oxygen demand are intuitive and expected, as decomposition of sediment organic matter (including settled phytoplankton biomass) may constitute the majority of the total hypolimnetic oxygen demand in many lakes (Steinsberger et al. 2020). Likewise, limited sampling of early-season bloom events could have partially obscured the role of within-year chl-a on oxygen demand. Regardless, our analyses provide support for both within-year and between-year effects of phytoplankton blooms in perpetuating anoxia.

4.1.5 Effect of oxygen demand on hypolimnetic anoxia (Figure 1e)

The positive relationship between oxygen demand and AF is well-supported by this study and is also intuitive: as biological and chemical demand for oxygen increases, the onset of anoxia is likely to occur earlier in the stratified period, increasing the total duration of anoxia (Figure 4; Figure 5). Furthermore, in lakes that did not experience anoxia throughout the time series of data used in this study, oxygen demand was negatively associated with late-summer DO concentrations (Appendix S6: Text S6.2), supporting that oxygen demand and DO concentrations are closely coupled in both oxic and anoxic lakes. Across the dataset, the effect of oxygen demand on hypolimnetic oxygen conditions occurred simultaneously with an additional positive effect of spring air temperatures (Figure 4; Figure 5, Appendix S6: Text S6.2), and in anoxic lakes AF was further regulated by autumn air temperatures (Figure 4; Figure 5). Positive associations between anoxia and spring and autumn air temperatures may highlight the important role that stratification duration (i.e., both onset in spring and end in autumn) can play in driving the spatial and temporal extent of anoxia (e.g., Nürnberg, 1995; Jane et al. 2023). Previous work has identified that the duration of summer stratification is increasing across many lakes (Woolway et al. 2021), driving decreased late-summer oxygen concentrations (Jane et al. 2023).

However, the factors that control oxygen demand are changing less consistently: temporal trends in hypolimnetic temperature are highly variable across lakes (Pilla et al. 2020; Richardson et al. 2017), as are trends in chl-a from 1980–present (Kraemer et al. 2022). Consequently, it is not surprising that trends in oxygen demand appear to be inconsistent across lakes (Jane et al. 2023). In this study, our focus on annual and sub-annual timescales allowed us to more precisely investigate the mechanisms at play within and across 386 lakes (Figure 4E), identifying that variability in oxygen demand has the potential to drive a feedback effect in some lakes that experience hypolimnetic anoxia.

4.2 Lake characteristics can increase susceptibility to the ABA feedback

Through our cross-lake analyses, we identified that the ABA feedback may be stronger in some lakes than others. In particular, mean epilimnetic TP concentrations, mean depth, and residence time each modulated ABA feedback relationships (Figure 6).

First, the effect of TP on chl-a was strongest in lakes with high mean epilimnetic TP concentrations, especially for lakes with TP concentrations greater than ~10 µg/L (Figure 6a). These mesotrophic to eutrophic/hypertrophic lakes also tended to experience substantial variability in epilimnetic TP concentrations, which likely made the effect of changing TP concentrations more detectable in our standardized linear regression analyses (Appendix S11: Figure S11.1). Ultimately, our finding that TP and chl-a are more closely correlated at high TP concentrations may provide some resistance to the initiation of the ABA feedback in oligotrophic lakes, while further accelerating the ABA feedback as eutrophication proceeds due to external or internal nutrient loading.

Second, the effect of the previous year’s chl-a on oxygen demand was strongest in lakes with long residence times (Figure 6b). In these lakes, decomposing chl-a and autochthonous organic carbon may have more time to settle and accumulate on the hypolimnetic sediments, fueling oxygen demand the following year. Conversely, the effect of the previous year’s chl-a on oxygen demand was negligible in lakes with residence time less than ~100 days (Figure 6b), as chl-a may be quickly flushed and exported downstream from these lakes. Consequently, lakes with longer residence time may be more susceptible to the ABA feedback.

Third, the magnitude of the effect of oxygen demand on AF generally increased with increasing mean depth of the lake (Figure 6c). Mechanistically, deeper lakes often have relatively lower oxygen demand due to low sediment area to hypolimnetic volume ratios (Livingstone and Imboden 1996; Müller et al. 2012; Steinsberger et al. 2020). Consequently, variation in oxygen demand can substantially affect the amount of time it takes to reach anoxia in these deep lakes. Conversely, in shallow lakes, hypolimnetic DO concentrations may be more strongly impacted by factors other than oxygen demand, including hypolimnetic primary production, stratification phenology, and mixing events (Wetzel 2001). Ultimately, deep lakes (i.e., mean depth > 5 m; Figure 6) appear to have a particularly strong coupling between oxygen demand and AF, strengthening the ABA feedback in these lakes.

Combined, these results suggest that deep mesotrophic or eutrophic lakes with long residence times are particularly likely to be susceptible to the ABA feedback, though more data are needed to test these hypotheses. Importantly, our identification of factors that may affect the strength of the ABA feedback across lakes would not have been possible without the use of a multi-lake dataset like the one analyzed in this study.

4.3 Climate change has the potential to trigger the ABA feedback

Our analysis of 656 widespread lakes suggests a strong relationship between climate variation and deoxygenation. Importantly, this climate variability may have the potential to push hypolimnetic DO below the ~1.8 mg/L threshold that is associated with increased hypolimnetic TP release from sediment, thereby initiating the ABA feedback.

4.2.1 High spring air temperatures are associated with anoxia

Our results suggest that increased spring air temperatures can contribute to DO declines not only by prolonging summer stratification, as demonstrated previously (Woolway et al. 2021; Jane et al. 2023), but also by increasing chl-a, hypolimnetic temperature, and oxygen demand (Figure 4c; Appendix S8). While we saw a clear effect of spring air temperatures on hypolimnetic DO dynamics, we did not observe a similar effect for summer temperatures (Appendix S8: Figure S8.1). Spring may be a particularly influential time period for the DO and temperature dynamics of warm monomictic and dimictic lakes, as this period sets the beginning of stratification and the initial heat and oxygen content of the hypolimnion (Shatwell et al. 2019; Woolway et al. 2021; Jane et al. 2023). While mean air temperatures are increasing around the world as a result of anthropogenic climate change, these impacts are not consistent across seasons or locations (Masson-Delmotte et al. 2021). Specifically, the time period during which temperatures fall in the historical range of spring temperatures is shortening across Northern Hemisphere mid-latitudes, which are representative of most of the lakes in this study (Wang et al. 2021). Conversely, the time period during which temperatures fall in the historical range of summer temperatures is lengthening (Wang et al. 2021; Woolway 2023). Our work highlights the importance of accounting for these differential changes in seasonal air temperatures, not just annual means, when anticipating how changes in climate may affect hypolimnetic DO dynamics. Furthermore, as spring air temperatures continue to increase across many lakes, our work suggests that these climatic changes may play a role in causing hypolimnetic oxygen concentrations to decline, potentially initiating the ABA feedback.

4.4 Strengths and limitations of this analysis

Using regression models within and across lakes, we were able to simultaneously analyze the extent of support for each of the relationships in the hypothesized ABA feedback. Lakes analyzed in this study span five orders of magnitude in surface area and two orders of magnitude in maximum depth (Z_{max}; Lewis et al. 2023). Amidst these substantial differences, we found consistent support for the ABA feedback relationships within and across lakes.

While the dataset analyzed here is larger than those used in previous studies, data limitations continued to constrain our analysis. Specifically, we were unable to analyze the effects of external nutrient loads, or DOC concentrations on the ABA feedback due to lack of data, and we were unable to use causal inference methods to study ABA dynamics within individual lakes over time. Moreover, the majority (82%) of lakes analyzed here are temperate lakes located in the U.S.; consequently, results may not be fully generalizable to global lakes, and more research is needed to characterize DO dynamics in a broader, representative range of ecosystems, especially in tropical and southern hemisphere lakes. Our calculated AF values have substantial uncertainty, particularly with respect to stratification end dates, though we have done our best to minimize these uncertainties through detailed methodological testing (Appendix S5). To standardize across a wide range of lakes and sampling regimes, our analysis considered the entire hypolimnion as one homogenized layer, averaging over potentially meaningful variation in

DO dynamics across a depth gradient in the hypolimnion (e.g., LaBrie et al. 2023). Given the promising results we observed here, further exploration of depth-resolved DO declines across lakes likely has substantial potential to further our understanding of biogeochemical processing in lakes.

4.5 Conclusions and global change implications

We found widespread empirical support for the ABA feedback in analyzing time series data across 656 diverse lakes. Relationships were particularly strong between oxygen demand and AF; AF and hypolimnetic TP; and epilimnetic TP and chl-a. Conversely, the effect of epilimnetic chl-a on oxygen demand was comparatively less strong, though still detectable both within and across lakes. As oxygen concentrations are decreasing in many lakes around the world, accounting for the ABA feedback may help effectively prioritize restoration and conservation efforts. Notably, our work suggests that catchment-scale nutrient management may be particularly critical for preventing deterioration of water quality in lakes with late-summer hypolimnetic DO concentrations just above 1.8 mg/L that have not yet crossed this threshold. These lakes are less likely to currently experience feedback effects of anoxia, but may cross this threshold in the future, thereby initiating an ABA feedback that, once triggered, will make water quality management more challenging. As climate and land use continue to change on a global scale, understanding and accounting for the ABA feedback may enable more effective conservation of culturally, economically, and ecologically important lake ecosystems.

Acknowledgements

Many thanks to the Global Lake Ecological Observatory Network (GLEON) Metabolism Working Group for catalyzing this analysis. Specifically, Ted Harris, Paul Hanson, Jim Rusak, Oxana Erina, Jim Watkins, and April James contributed to the development of this manuscript. Thanks to Arpita Das for helping to match the lakes in this study with lake IDs from HydroLAKES and Filazzola et al. (2020), to Young Ho Yun for aiding in statistical analyses, and to the Virginia Tech Reservoir Group for feedback throughout the manuscript development process. We are grateful to Gertrud Nürnberg for providing constructive comments that substantially improved this manuscript.

This analysis would not have been possible without long-term data collection across many institutions. We thank the many researchers and community members who have collected, analyzed, and compiled the data used in this study. In particular, we would like to acknowledge Catherine Hein and Jacob Dickmann from the Wisconsin Department of Natural Resources who facilitated use of data from many Wisconsin lakes.

Data collection and manuscript development for this project have been supported by numerous grants. Abigail S. L. Lewis is supported by the U.S. National Science Foundation (NSF) graduate research fellowship program (DGE-1840995), NSF grant 1753639, the Institute for Critical Technology and Applied Science (ICTAS), and the College of Science Roundtable at Virginia Tech. Cayelan C. Carey receives support from NSF grants 1753639, 1933016, and 1737424. Stephen F. Jane is supported by the Cornell Atkinson Center for Sustainability. Rebecca L. North acknowledges support from the Missouri Department of Natural Resources, which funds the Missouri Statewide Lake Assessment Program (SLAP) coordinated by the University of Missouri (MU) Limnology Laboratory. Hans-Peter Grossart receives support from the Leibniz Institute of Freshwater Biology and Inland Fisheries (IGB) and teams of scientists and technicians who run the Stechlin and Müggelsee long-term monitoring, as well as the German Research Foundation (DFG), which funds Project Pycnotrap (GR1540/37-1). Rachel M. Pilla notes that this research was supported by the U.S. Department of Energy (DOE), Office of Energy Efficiency and Renewable Energy, Water Power Technologies Office, and Environmental Sciences Division at Oak Ridge National Laboratory (ORNL). ORNL is managed by UT-Battelle, LLC, for the U.S. DOE under contract DE-AC05-00OR22725. Kevin C. Rose acknowledges support from NSF grants 1754265 and 2048031. Ruben Sommaruga acknowledges support from the LTSER platform Tyrolean Alps (LTER-Austria). Gesa A. Weyhenmeyer received financial support for this study from the Swedish Research Council (VR; Grant No. 2020-03222) and the Swedish Research Council for Environment, Agricultural Sciences and Spatial Planning (FORMAS; Grant No. 2020-01091). Piet Verburg acknowledges support from MBIE under grant number C01X2205. Jordi Delgado Martin acknowledges support from the EMALCSA Chair. Isabella Oleksy receives support from the NSF under grant EPS-2019528. Heidrun Feuchtmayr acknowledges support from the Natural Environmental Research Council award number NE/R016429/1 as part of the UK-SCaPE programme delivering National Capability. Many thanks to all of the funding sources that enabled this international lake analysis.

Author Contributions

ASLL and MPL led the early conceptualization of this project, with significant contributions from SFJ, KCR, HPG, DWH, RS, and GAW. ASLL and MPL collated all data, which was contributed by ASLL, SFJ, KCR, YBS, SHB, FC, HF, HM, JDM, RLN, IAO, RMP, RS, PV, DW, GAW, SES, APS, and CCC. Supplemental methods text was written and contributed by ASLL, SFJ, YBS, SHB, FC, HF, HM, JDM, RLN, IAO, RMP, RS, PV, DW, GAW, SES, APS, and CCC. ASLL led data analysis, developed figures, and wrote the manuscript with substantial contributions from MPL and CCC. DWH and SHB reviewed the data publication and analysis code. Additionally, SFJ, KCR, YBS, HF, HPG, DWH, HM, RLN, IAO, RMP, RS, DW, GAW, and CCC made significant intellectual contributions to the development of methods and interpretation of results in this analysis.

Data Availability

The in-lake data used in this study are published in the Environmental Data Initiative repository (EDI; Lewis et al. 2023; https://doi.org/10.6073/pasta/2cd6628a942de2a8b12d2b19962712a0), and include compiled data from multiple separately-published datasets (Maberly et al. 2017; Leach et al. 2018; Lentz et al. 2023; Winslow et al. 2018; Jones et al. 2020; Feuchtmayr et al. 2021; Stetler et al. 2021; Carey et al. 2022b, c, d, e; Williamson 2022; Solomon et al. 2022), in addition to other, previously-unpublished data. Additional data and metadata were drawn from openly accessible data sources, namely HydroLAKES (Messager et al. 2016; http://www.hydrosheds.org), Filazzola et al. (2020; https://doi.org/10.5063/F1JH3JKZ), and the ERA5 climate reanalysis (Hersbach and others 2019; https://cds.climate.copernicus.eu). Analysis code to reproduce the results in this manuscript is available in a Zenodo repository (Lewis & Lau, 2023; https://doi.org/10.5281/zenodo.10086950).

Chapter III References

Anderson, H. S., T. H. Johengen, R. Miller, and C. M. Godwin. 2021. Accelerated sediment phosphorus release in Lake Erie's central basin during seasonal anoxia. Limnology and Oceanography **66**: 3582–3595. doi:10.1002/lno.11900

Bartosiewicz, M., A. Przytulska, J.-F. Lapierre, I. Laurion, M. F. Lehmann, and R. Maranger. 2019. Hot tops, cold bottoms: Synergistic climate warming and shielding effects increase carbon burial in lakes. Limnology and Oceanography Letters **4**: 132–144. doi:10.1002/lol2.10117

Bates, D., M. Maechler, B. Bolker, and others. 2023. lme4: Linear Mixed-Effects Models using "Eigen" and S4.

Borchers, H. W. 2022. pracma: Practical Numerical Math Functions.

Breitburg, D., L. A. Levin, A. Oschlies, and others. 2018. Declining oxygen in the global ocean and coastal waters. Science **359**: eaam7240. doi:10.1126/science.aam7240

Burns, N. M. (1995). Using hypolimnetic dissolved oxygen depletion rates for monitoring lakes. New Zealand Journal of Marine and Freshwater Research, 29(1), 1–11. doi:10.1080/00288330.1995.9516634

Carey, C. C., P. C. Hanson, R. Q. Thomas, and others. 2022. Anoxia decreases the magnitude of the carbon, nitrogen, and phosphorus sink in freshwaters. Global Change Biology **28**: 4861–4881. doi:10.1111/gcb.16228

Carey, C. C., A. S. L. Lewis, D. W. Howard, W. M. Woelmer, P. A. Gantzer, K. A. Bierlein, J. C. Little, and WVWA. 2022b. Bathymetry and watershed area for Falling Creek Reservoir, Beaverdam Reservoir, and Carvins Cove Reservoir. doi:10.6073/PASTA/352735344150F7E77D2BC18B69A22412

Carey, C. C., A. S. L. Lewis, R. P. McClure, A. B. Gerling, A. Breef-Pilz, and A. Das. 2022c. Time series of high-frequency profiles of depth, temperature, dissolved oxygen, conductivity, specific conductance, chlorophyll a, turbidity, pH, oxidation-reduction potential, photosynthetic active radiation, and descent rate for Beaverdam Reservoir, Carvins Cove Reservoir, Falling Creek Reservoir, Gatewood Reservoir, and Spring Hollow Reservoir in Southwestern Virginia, USA 2013-2021. doi:10.6073/PASTA/C4C45B5B10B4CB4CD4B5E613C3EFFBD0

Carey, C. C., H. L. Wander, D. W. Howard, B. R. Niederlehner, W. M. Woelmer, M. E. Lofton, A. B. Gerling, and A. Breef-Pilz. 2022d. Water chemistry time series for Beaverdam Reservoir, Carvins Cove Reservoir, Falling Creek Reservoir, Gatewood Reservoir, and Spring Hollow Reservoir in southwestern Virginia, USA 2013-2021. doi:10.6073/PASTA/7BD797155CDBB5F1ACDF0547C6BA9023

Carey, C. C., J. H. Wynne, M. E. Lofton, and others. 2022e. Filtered chlorophyll a time series for Beaverdam Reservoir, Carvins Cove Reservoir, Claytor Lake, Falling Creek Reservoir, Gatewood Reservoir, Smith Mountain Lake, Spring Hollow Reservoir in southwestern Virginia and Lake Sunapee in Sunapee, New Hampshire, USA during 2014-2021. doi:10.6073/PASTA/6BA5BEED2869A05C854C34251144A76E

Carpenter, S. R. 2003. Regime Shifts in Lake Ecosystems: Pattern and Variation: 15, International Ecology Institute.

Carpenter, S. R., K. L. Cottingham, and D. E. Schindler. 1992. Biotic feedbacks in Lake phosphorus cycles. Trends in Ecology & Evolution **7**: 332–336. doi:10.1016/0169-5347(92)90125-U

Carpenter, S. R., and R. C. Lathrop. 2008. Probabilistic Estimate of a Threshold for Eutrophication. Ecosystems **11**: 601–613.

Cottingham, K. L., H. A. Ewing, M. L. Greer, C. C. Carey, and K. C. Weathers. 2015. Cyanobacteria as biological drivers of lake nitrogen and phosphorus cycling. Ecosphere **6**: art1. doi:10.1890/ES14-00174.1

Doig, L. E., R. L. North, J. J. Hudson, C. Hewlett, K.-E. Lindenschmidt, and K. Liber. 2017. Phosphorus release from sediments in a river-valley reservoir in the northern Great Plains of North America. Hydrobiologia **787**: 323–339. doi:10.1007/s10750-016-2977-2

Downing, J. A., and E. McCauley. 1992. The nitrogen : phosphorus relationship in lakes. Limnology and Oceanography **37**: 936–945. doi:10.4319/lo.1992.37.5.0936

Einsele, W. 1936. Über die Beziehungen des Eisenkreislaufs zum Phosphatkreislauf im eutrophen See. Archiv für Hydrobiologie **29**: 664–686.

Elser, J. J., M. E. S. Bracken, E. E. Cleland, and others. 2007. Global analysis of nitrogen and phosphorus limitation of primary producers in freshwater, marine and terrestrial ecosystems. Ecology Letters **10**: 1135–1142. doi:10.1111/j.1461-0248.2007.01113.x

Elshout, P. M. F., Dionisio Pires, L. M., Leuven, R. S. E. W., Wendelaar Bonga, S. E., & Hendriks, A. J. (2013). Low oxygen tolerance of different life stages of temperate freshwater fish species. *Journal of Fish Biology*, *83*(1), 190–206. https://doi.org/10.1111/jfb.12167

Encinas Fernández, J., F. Peeters, and H. Hofmann. 2014. Importance of the Autumn Overturn and Anoxic Conditions in the Hypolimnion for the Annual Methane Emissions from a Temperate Lake. Environ. Sci. Technol. **48**: 7297–7304. doi:10.1021/es4056164

Feuchtmayr, H., M. A. Clarke, M. M. De Ville, B. A. Dodd, J. Fletcher, H. Guyatt, A. G. Hunt, J. B. James, E. B. Mackay, G. Rhodes, S. J. Thackeray, S. C. Maberly. 2021. Surface temperature, surface oxygen, water clarity, water chemistry and phytoplankton chlorophyll a data from Blelham Tarn, 2014 to 2018. NERC Environmental Information Data Centre. doi: 10.5285/ae8c850d-211e-4560-8b37-437b6e0e2a16

Filazzola, A., O. Mahdiyan, A. Shuvo, and others. 2020. A global database of chlorophyll and water chemistry in freshwater lakes. doi:10.5063/F1JH3JKZ

Finlayson, C. M., R. S. de Groot, F. M. R. Hughes, and C. A. Sullivan. 2018. Freshwater Ecosystem Services and Functions. *In* J. Hughes [ed.], Freshwater Ecology and Conservation: Approaches and Techniques. Oxford University Press.

Foley, B., I. D. Jones, S. C. Maberly, and B. Rippey. 2012. Long-term changes in oxygen depletion in a small temperate lake: effects of climate change and eutrophication. Freshwater Biology **57**: 278–289. doi:10.1111/j.1365-2427.2011.02662.x

Forsythe, G. E., Malcolm, M. A., & Moler, C. B. (1977). Computer Methods for Mathematical Computations. Prentice Hall Professional Technical Reference.

Fox, J., S. Weisberg, B. Price, and others. 2022. car: Companion to Applied Regression.

Håkanson, L. (2005). The Importance of Lake Morphometry for the Structure and Function of Lakes. International Review of Hydrobiology, 90(4), 433–461. https://doi.org/10.1002/iroh.200410775

Haupt, F., M. Stockenreiter, E. S. Reichwaldt, M. Baumgartner, W. Lampert, M. Boersma, and H. Stibor. 2010. Upward phosphorus transport by Daphnia diel vertical migration. Limnology and Oceanography **55**: 529–534. doi:10.4319/lo.2010.55.2.0529

Hersbach, H., B. Bell, P. Berrisford, and others. 2019. ERA5 monthly averaged data on single levels from 1979 to present. doi:10.24381/CDS.F17050D7

Hounshell, A. G., R. P. McClure, M. E. Lofton, and C. C. Carey. 2021. Whole-ecosystem oxygenation experiments reveal substantially greater hypolimnetic methane concentrations in reservoirs during anoxia. Limnology and Oceanography Letters **6**: 33–42.

Hupfer, M., and J. Lewandowski. 2008. Oxygen Controls the Phosphorus Release from Lake Sediments – a Long-Lasting Paradigm in Limnology. International Review of Hydrobiology **93**: 415–432. doi:10.1002/iroh.200711054

Jagtman, E., D. T. Van der Molen, and S. Vermij. 1992. The influence of flushing on nutrient dynamics, composition and densities of algae and transparency in Veluwemeer, The Netherlands. Hydrobiologia **233**: 187–196. doi:10.1007/BF00016107

Jane, S. F., G. Hansen, B. Kraemer, and others. 2021. Widespread deoxygenation of temperate lakes. Nature **594**. doi:10.1038/s41586-021-03550-y

Jane, S. F., J. L. Mincer, M. P. Lau, A. S. L. Lewis, J. T. Stetler, and K. C. Rose. 2023. Longer duration of seasonal stratification contributes to widespread increases in lake hypoxia and anoxia. Global Change Biology **29**: 1009–1023. doi:10.1111/gcb.16525

Jenny, J.-P., P. Francus, A. Normandeau, F. Lapointe, M.-E. Perga, A. Ojala, A. Schimmelmann, and B. Zolitschka. 2016a. Global spread of hypoxia in freshwater ecosystems during the last three centuries is caused by rising local human pressure. Global Change Biology **22**: 1481–1489. doi:10.1111/gcb.13193

Jenny, J.-P., A. Normandeau, P. Francus, and others. 2016b. Urban point sources of nutrients were the leading cause for the historical spread of hypoxia across European lakes.

Proceedings of the National Academy of Sciences **113**: 12655–12660. doi:10.1073/pnas.1605480113

Jones, J. R., A. Argerich, D. V. Obrecht, A. P. Thorpe, and R. L. North. 2020. Missouri Lakes and Reservoirs Long-term Limnological Dataset. doi:10.6073/PASTA/86D8D176E91410566B4DE51DF44C2624

Kamarainen, A. M., H. Yuan, C. H. Wu, and S. R. Carpenter. 2009. Estimates of phosphorus entrainment in Lake Mendota: a comparison of one-dimensional and three-dimensional approaches. Limnology and Oceanography: Methods **7**: 553–567. doi:10.4319/lom.2009.7.553

Kraemer, B. M., K. Kakouei, C. Munteanu, M. W. Thayne, and R. Adrian. 2022. Worldwide moderate-resolution mapping of lake surface chl-a reveals variable responses to global change (1997–2020). PLOS Water **1**: e0000051. doi:10.1371/journal.pwat.0000051

LaBrie, R., M. Hupfer, and M. P. Lau. 2023. Anaerobic duration predicts biogeochemical consequences of oxygen depletion in lakes. Limnology and Oceanography Letters **8**: 666–674. doi:10.1002/lol2.10324

Ladwig, R., P. C. Hanson, H. A. Dugan, C. C. Carey, Y. Zhang, L. Shu, C. J. Duffy, and K. M. Cobourn. 2021. Lake thermal structure drives interannual variability in summer anoxia dynamics in a eutrophic lake over 37 years. Hydrol. Earth Syst. Sci. **25**: 1009–1032. doi:10.5194/hess-25-1009-2021

Leach, T. H., L. A. Winslow, F. W. Acker, and others. 2018. Long-term dataset on aquatic responses to concurrent climate change and recovery from acidification. Sci Data **5**: 180059. doi:10.1038/sdata.2018.59

Lentz, M., S. Schmidt, J. Woodhouse, P. Kasprzak, S. Wollrab, S. A. Berger, U. Beyer, M. Bodenlos, M. Degebrodt, R. Degebrodt, T. Gonsiorczyk, E. Huth, M. Uta, M. Elke, J. C. Nejstgaard, M. Papke, S. Pinnow, R. Roßberg, M. Sachtleben, A. Scheffler, W. Scheffler, L. Krienitz, P. Casper, M. O Gessner, H-P. Grossart, R. Koschel. 2023. Lake Stechlin vertical profiles of multiparameter probe data 1970-2020. IGB Leibniz-Institute of Freshwater Ecology and Inland Fisheries. Dataset. doi:10.18728/igb-fred-823.1

Lewis, A. S. L., and M. P. Lau. 2023. abbylewis/Anoxia-Begets-Anoxia: Data analysis of biogeochemical dynamics in 656 lakes: v1.1.1. Zenodo. doi:10.5281/zenodo.10086950.

Lewis, A. S. L., B. S. Kim, H. L. Edwards, and others. 2020. Prevalence of phytoplankton limitation by both nitrogen and phosphorus related to nutrient stoichiometry, land use, and primary producer biomass across the northeastern United States. Inland Waters 1–9. doi:10.1080/20442041.2019.1664233

Lewis, A. S. L., M. P. Lau, S. F. Jane, Y. Beeri-Shlevin, S. H. Burnet, F. Clayer, H. Feuchtmayr, H. Grossart, D. W. Howard, H. Mariash, J. Delgado-Martin, R. L. North, I. Oleksy, R. M. Pilla, K. C. Rose, A. P. Smagula, R. Sommaruga, S. E. Steiner, P. Verburg, D. Wain, G. A. Weyhenmeyer, and C. C. Carey. 2023. Dissolved oxygen, temperature, chlorophyll-a, total phosphorus, total nitrogen, and dissolved organic carbon at multiple depths in 822 lakes from 1921-2022 ver 9. Environmental Data Initiative. https://doi.org/10.6073/pasta/2cd6628a942de2a8b12d2b19962712a0

Lewis Jr., W. M., and W. A. Wurtsbaugh. 2008. Control of Lacustrine Phytoplankton by Nutrients: Erosion of the Phosphorus Paradigm. International Review of Hydrobiology **93**: 446–465. doi:10.1002/iroh.200811065

Livingstone, D. M., & Imboden, D. M. 1996. The prediction of hypolimnetic oxygen profiles: A plea for a deductive approach. Canadian Journal of Fisheries and Aquatic Sciences **53**: 924–932. https://doi.org/10.1139/f95-230

Lynch, A. J., Cooke, S. J., Arthington, A. H., Baigun, C., Bossenbroek, L., Dickens, C., Harrison, I., Kimirei, I., Langhans, S. D., Murchie, K. J., Olden, J. D., Ormerod, S. J., Owuor, M., Raghavan, R., Samways, M. J., Schinegger, R., Sharma, S., Tachamo-Shah, R.-D., Tickner, D., Tweddle, D., Young, N., & Jähnig, S. C. (2023). People need freshwater biodiversity. WIREs Water, 10(3), e1633. https://doi.org/10.1002/wat2.1633

Maberly, S.C.; B. Brierley, H. T. Carter, M. A. Clarke, M. M. De Ville, J. M. Fletcher, J. B. James, P. Keenan, J. L. Kelly, E. B. Mackay, J. E. Parker, M. Patel, M. G. Pereira, G. Rhodes, B. Tanna, S. J. Thackeray, C. Vincent, H. Feuchtmayr. 2017. Surface temperature, surface oxygen, water clarity, water chemistry and phytoplankton chlorophyll a data from Blelham Tarn, 1945 to 2013. NERC Environmental Information Data Centre. doi: 10.5285/393a5946-8a22-4350-80f3-a60d753beb00

MacKeigan, P. W., Z. E. Taranu, F. R. Pick, B. E. Beisner, and I. Gregory-Eaves. 2023. Both biotic and abiotic predictors explain significant variation in cyanobacteria biomass across lakes from temperate to subarctic zones. Limnology and Oceanography **68**: 1360–1375. doi:10.1002/lno.12352

Magnuson, J. J., D. M. Robertson, B. J. Benson, and others. 2000. Historical Trends in Lake and River Ice Cover in the Northern Hemisphere. Science **289**: 1743–1746. doi:10.1126/science.289.5485.1743

Matisoff, G., E. M. Kaltenberg, R. L. Steely, and others. 2016. Internal loading of phosphorus in western Lake Erie. Journal of Great Lakes Research **42**: 775–788. doi:10.1016/j.jglr.2016.04.004

Masson-Delmotte, V., Zhai, P., Pirani, A., Connors, S. L., Péan, C., Berger, S., Caud, N., Chen, Y., Goldfarb, L., Gomis, M. I., Huang, M., Leitzell, K., Lonnoy, E., Matthews, J. B. R., Maycock, T. K., Waterfield, T., Yelekçi, Ö., Yu, R., & Zhou, B. (Eds.). 2021. Climate Change 2021: The Physical Science Basis. Contribution of Working Group I to the Sixth Assessment Report of the Intergovernmental Panel on Climate Change. Cambridge University Press. doi:10.1017/9781009157896

Messager, M. L., B. Lehner, G. Grill, I. Nedeva, and O. Schmitt. 2016. Estimating the volume and age of water stored in global lakes using a geo-statistical approach. Nat Commun **7**: 13603. doi:10.1038/ncomms13603

Middelburg, J. J., and L. A. Levin. 2009. Coastal hypoxia and sediment biogeochemistry. Biogeosciences **6**: 1273–1293. doi:10.5194/bg-6-1273-2009

Mortimer, C. H. 1941. The Exchange of Dissolved Substances Between Mud and Water in Lakes. Journal of Ecology **29**: 280–329. doi:10.2307/2256395

Mortimer, C. H. 1942. The Exchange of Dissolved Substances between Mud and Water in Lakes. Journal of Ecology **30**: 147–201. doi:10.2307/2256691

Moss, B. 2011. Allied attack: climate change and eutrophication. Inland Waters **1**: 101–105. doi:10.5268/IW-1.2.359

Muggeo, V. M. R. 2023. segmented: Regression Models with Break-Points / Change-Points (with Possibly Random Effects) Estimation (1.6-3). https://CRAN.R-project.org/package=segmented

Müller, B., Bryant, L. D., Matzinger, A., & Wüest, A. 2012. Hypolimnetic Oxygen Depletion in Eutrophic Lakes. Environmental Science & Technology, **46** 9964–9971. https://doi.org/10.1021/es301422r

Müller, B., T. Steinsberger, R. Schwefel, R. Gächter, M. Sturm, and A. Wüest. 2019. Oxygen consumption in seasonally stratified lakes decreases only below a marginal phosphorus threshold. Sci Rep **9**: 18054. doi:10.1038/s41598-019-54486-3

North, R. L., D. Barton, A. S. Crowe, and others. 2013. The state of Lake Simcoe (Ontario, Canada): the effects of multiple stressors on phosphorus and oxygen dynamics. Inland Waters **3**: 51–74. doi:10.5268/IW-3.1.529

North, R. P., North, R. L., Livingstone, D. M., Köster, O., & Kipfer, R. 2014. Long-term changes in hypoxia and soluble reactive phosphorus in the hypolimnion of a large temperate lake: Consequences of a climate regime shift. Global Change Biology **20:** 811–823. https://doi.org/10.1111/gcb.12371

Nürnberg, G. K. 1984. The prediction of internal phosphorus load in lakes with anoxic hypolimnia. Limnology and Oceanography **29**: 111–124. doi:10.4319/lo.1984.29.1.0111

Nürnberg, G., & Peters, R. H. 1984. The importance of internal phosphorus load to the eutrophication of lakes with anoxic hypolimnia. SIL Proceedings, 1922-2010 **22**: 190–194. doi:10.1080/03680770.1983.11897287

Nürnberg, G. K. 1988. A simple model for predicting the date of fall turnover in thermally stratified lakes. Limnology and Oceanography **33:** 1190–1195. doi: 10.4319/lo.1988.33.5.1190

Nürnberg, G. K. 1995. Quantifying anoxia in lakes. Limnology and Oceanography **40:** 1100–1111. https://doi.org/10.4319/lo.1995.40.6.1100

Nürnberg, G. K. 2009. Assessing internal phosphorus load – Problems to be solved. Lake and Reservoir Management **25**: 419–432. doi:10.1080/00357520903458848

Nürnberg, G. K. 2019. Quantification of Anoxia and Hypoxia in Water Bodies. In *Encyclopedia of Water* (pp. 1–9). John Wiley & Sons, Ltd. https://doi.org/10.1002/9781119300762.wsts0081

Nürnberg, G. K., Howell, T., & Palmer, M. 2019. Long-term impact of Central Basin hypoxia and internal phosphorus loading on north shore water quality in Lake Erie. Inland Waters **9**: 362–373. https://doi.org/10.1080/20442041.2019.1568072

Oleksy, I. A., and D. C. Richardson. 2021. Climate Change and Teleconnections Amplify Lake Stratification With Differential Local Controls of Surface Water Warming and Deep Water Cooling. Geophysical Research Letters **48**: e2020GL090959. doi:10.1029/2020GL090959

Orihel, D. M., H. M. Baulch, N. J. Casson, R. L. North, C. T. Parsons, D. C. M. Seckar, and J. J. Venkiteswaran. 2017. Internal phosphorus loading in Canadian fresh waters: a critical review and data analysis. Can. J. Fish. Aquat. Sci. **74**: 2005–2029. doi:10.1139/cjfas-2016-0500

Pace, M. L., and Y. T. Prairie. 2005. Respiration in lakes, p. 103–121. *In* P. Del Giorgio and P. Williams [eds.], Respiration in Aquatic Ecosystems. Oxford University Press.

Paerl, H. W., and J. Huisman. 2008. Blooms Like It Hot. Science **320**: 57–58. doi:10.1126/science.1155398

Paerl, H. W., J. T. Scott, M. J. McCarthy, and others. 2016. It Takes Two to Tango: When and Where Dual Nutrient (N & P) Reductions Are Needed to Protect Lakes and Downstream Ecosystems. Environ. Sci. Technol. **50**: 10805–10813. doi:10.1021/acs.est.6b02575

Parmesan, C., M. D. Morecroft, Y. Trisurat, and others. 2022. Terrestrial and Freshwater Ecosystems and Their Services H.O. Pörtner, D.C. Roberts, M. Tignor, et al. [eds.]. Climate Change 2022: Impacts, Adaptation and Vulnerability. Contribution of Working Group II to the Sixth Assessment Report of the Intergovernmental Panel on Climate Change 197–378. doi:10.1017/9781009325844.004.198

Pilla, R. M., and C. E. Williamson. 2023. Multidecadal trends in ultraviolet radiation, temperature, and dissolved oxygen have altered vertical habitat availability for Daphnia in temperate Lake Giles, USA. Freshwater Biology **68**: 523–533. doi:10.1111/fwb.14044

Pilla, R. M., C. E. Williamson, B. V. Adamovich, and others. 2020. Deeper waters are changing less consistently than surface waters in a global analysis of 102 lakes. Scientific Reports **10**: 20514. doi:10.1038/s41598-020-76873-x

Quinlan, R., Paterson, A. M., Smol, J. P., Douglas, M. S. V., & Clark, B. J. (2005). Comparing different methods of calculating volume-weighted hypolimnetic oxygen (VWHO) in lakes. Aquatic Sciences, 67(1), 97–103. https://doi.org/10.1007/s00027-004-0717-6

Reid, A. J., A. K. Carlson, I. F. Creed, and others. 2019. Emerging threats and persistent conservation challenges for freshwater biodiversity. Biological Reviews **94**: 849–873. doi:10.1111/brv.12480

Reinl, K. L., T. D. Harris, R. L. North, and others. 2023. Blooms also like it cold. Limnology and Oceanography Letters **8**: 546–564. doi:10.1002/lol2.10316

Reynaud, A., and D. Lanzanova. 2017. A Global Meta-Analysis of the Value of Ecosystem Services Provided by Lakes. Ecological Economics **137**: 184–194. doi:10.1016/j.ecolecon.2017.03.001

Richardson, D. C., Melles, S. J., Pilla, R. M., Hetherington, A. L., Knoll, L. B., Williamson, C. E., Kraemer, B. M., Jackson, J. R., Long, E. C., Moore, K., Rudstam, L. G., Rusak, J. A., Saros, J. E., Sharma, S., Strock, K. E., Weathers, K. C., & Wigdahl-Perry, C. R. 2017. Transparency, Geomorphology and Mixing Regime Explain Variability in Trends in Lake Temperature and Stratification across Northeastern North America (1975–2014). Water **9**: 442. doi:10.3390/w9060442

Rosenberg, R., B. Hellman, and B. Johansson. 1991. Hypoxic tolerance of marine benthic fauna. Mar. Ecol. Prog. Ser. **79**: 127–131. doi:10.3354/meps079127

Sachs, J. 1874. Lehrbuch der botanik, Engelmann.

Schindler, D. E. 2017. Warmer climate squeezes aquatic predators out of their preferred habitat. Proceedings of the National Academy of Sciences **114**: 9764–9765. doi:10.1073/pnas.1712818114

Schindler, D. W. 1974. Eutrophication and Recovery in Experimental Lakes: Implications for Lake Management. Science **184**: 897–899.

Schmidtko, S., L. Stramma, and M. Visbeck. 2017. Decline in global oceanic oxygen content during the past five decades. Nature **542**: 335–339. doi:10.1038/nature21399

Scott, J. T., M. J. McCarthy, and H. W. Paerl. 2019. Nitrogen transformations differentially affect nutrient-limited primary production in lakes of varying trophic state. Limnology and Oceanography Letters **4**: 96–104. doi:10.1002/lol2.10109

Shatwell, T., W. Thiery, and G. Kirillin. 2019. Future projections of temperature and mixing regime of European temperate lakes. Hydrology and Earth System Sciences **23**: 1533–1551. doi:10.5194/hess-23-1533-2019

Smith, V. H. 1982. The nitrogen and phosphorus dependence of algal biomass in lakes: An empirical and theoretical analysis1. Limnology and Oceanography **27**: 1101–1111. doi:10.4319/lo.1982.27.6.1101

Solomon, C., S. Jones, B. C. Weidel, and others. 2022. MFE database: Data from ecosystem ecology research by Jones, Solomon, and collaborators on the ecology and biogeochemistry of lakes and lake organisms in the Upper Midwest, USA. doi:10.25390/caryinstitute.7438598.v6

Soranno, P. A., S. R. Carpenter, and R. C. Lathrop. 1997. Internal phosphorus loading in Lake Mendota: response to external loads and weather. Can. J. Fish. Aquat. Sci. **54**: 1883–1893. doi:10.1139/f97-095

Steinsberger, T., R. Schwefel, A. Wüest, and B. Müller. 2020. Hypolimnetic oxygen depletion rates in deep lakes: Effects of trophic state and organic matter accumulation. Limnology and Oceanography **65**: 3128–3138. doi:10.1002/lno.11578

Stetler, J. T., S. F. Jane, J. L. Mincer, M. N. Sanders, and K. C. Rose. 2021. Long-term lake dissolved oxygen and temperature data, 1941-2018. doi:10.6073/PASTA/C45EFE4826B5F615023B857DC59856F3

Thienemann, A. 1928. Der Sauerstoff im eutrophen und obligotrophen See.

Vachon, D., C. T. Solomon, and P. A. del Giorgio. 2017. Reconstructing the seasonal dynamics and relative contribution of the major processes sustaining CO2 emissions in northern lakes. Limnol. Oceanogr. **62**: 706–722. doi:10.1002/lno.10454

Vaquer-Sunyer, R., and C. M. Duarte. 2008. Thresholds of hypoxia for marine biodiversity. PNAS **105**: 15452–15457. doi:10.1073/pnas.0803833105

Wang, J., Y. Guan, L. Wu, X. Guan, W. Cai, J. Huang, W. Dong, and B. Zhang. 2021. Changing Lengths of the Four Seasons by Global Warming. Geophysical Research Letters **48**: e2020GL091753. doi:10.1029/2020GL091753

Wang, M., X. Xu, Z. Wu, and others. 2019. Seasonal Pattern of Nutrient Limitation in a Eutrophic Lake and Quantitative Analysis of the Impacts from Internal Nutrient Cycling. Environ. Sci. Technol. **53**: 13675–13686. doi:10.1021/acs.est.9b04266

Wetzel, R. G. 2001. 13 - THE PHOSPHORUS CYCLE, p. 239–288. *In* R.G. Wetzel [ed.], Limnology (Third Edition). Academic Press.

Wetzel, R. G., and G. E. Likens. 2000. Estimates of Whole Lake Metabolism: Hypolimnetic Oxygen Deficits and Carbon Dioxide Accumulation, p. 373–382. *In* R.G. Wetzel and G.E. Likens [eds.], Limnological Analyses. Springer.

Williamson, C. E., E. P. Overholt, R. M. Pilla, T. H. Leach, J. A. Brentrup, L. B. Knoll, E. M. Mette, and R. E. Moeller. 2015. Ecological consequences of long-term browning in lakes. Sci Rep **5**: 1–10. doi:10.1038/srep18666

Williamson, C. E. 2022. Three decades of limnological data from lakes in the Pocono Mountains region, Pennsylvania USA, 1988-2021. doi:10.6073/PASTA/0D764453DD98D7FA978D517E6787538F

Wilson, H. L., Ayala, A. I., Jones, I. D., Rolston, A., Pierson, D., de Eyto, E., Grossart, H.-P., Perga, M.-E., Woolway, R. I., & Jennings, E. (2020). Variability in epilimnion depth estimations in lakes. Hydrology and Earth System Sciences **24**: 5559–5577. Doi:10.5194/hess-24-5559-2020

Winslow, L., T. Leach, and T. Hahn. 2018. adklakedata: Adirondack Long-Term Lake Data.

Winslow, L., J. Read, R. Woolway, J. Brentrup, T. Leach, J. Zwart, S. Albers, and D. Collinge. 2019. rLakeAnalyzer: Lake Physics Tools.

Woolway, R. I. 2023. The pace of shifting seasons in lakes. Nat Commun **14**: 2101. doi:10.1038/s41467-023-37810-4

Woolway, R. I., S. Sharma, G. A. Weyhenmeyer, and others. 2021. Phenological shifts in lake stratification under climate change. Nat Commun **12**: 2318. doi:10.1038/s41467-021-22657-4

Zhao, L., R. Zhu, Q. Zhou, E. Jeppesen, and K. Yang. 2023. Trophic status and lake depth play important roles in determining the nutrient-chlorophyll a relationship: Evidence from thousands of lakes globally. Water Research 120182. doi:10.1016/j.watres.2023.120182

Zhi, W., Klingler, C., Liu, J., & Li, L. (2023). Widespread deoxygenation in warming rivers. Nature Climate Change, 13(10). doi: 10.1038/s41558-023-01793-3

Chapter III Tables

Table 1: Explanatory variables used for mixed model regression. We tested several possible explanatory variables for each response variable using a mixed model approach. The time period over which mean values were calculated for each lake-year is provided for all water column variables. For information on lags used, see Appendix S7: Figure S1–S5. Epilimnion and hypolimnion are abbreviated as epi. and hypo. throughout.

Response variable	Proposed explanatory variables	Time period	Motivation for inclusion
Anoxic factor	Oxygen demand	Stratified	ABA feedback
	Spring average air temp.		Stratification onset
	Autumn average air temp.		Stratification end
	Winter average air temp.		Ice dynamics
	Hypo. temperature	Late summer	Solubility, stratification end
Late-summer hypo. TP	Anoxic factor	Late summer	ABA feedback
	Epi. TP	Stratified	Diffusion/sinking
	Maximum buoyancy frequency	Stratified	Diffusion
	Hypo. temp	Late summer	Temperature dependence of sediment flux
	Spring precipitation		Catchment inputs/flushing
	Summer precipitation		Catchment inputs/flushing
	Winter precipitation		Catchment inputs/flushing
	Mean TP measurement date	Late summer	Seasonal change
Stratified epi. TP	Hypo. TP	Late summer	ABA feedback
	Hypo. TP (t-1)	Late summer	Autumn mixing
	Epi. TP (t-1)	Late summer	Legacy effect
	Spring precipitation		Catchment inputs/flushing
	Summer precipitation		Catchment inputs/flushing
	Winter precipitation		Catchment inputs/flushing
	Maximum buoyancy frequency	Stratified	Diffusion
	Mean TP measurement date	Stratified	Seasonal change
Stratified epi. chl-a	Epi. TP	Stratified	ABA feedback
	Epi. TN	Stratified	Potential limiting nutrient
	Spring average air temp. Summer average air temp.		Temperature-dependence of phytoplankton growth
	Mean chl-a measurement date	Stratified	Seasonal change

Oxygen demand	Epi. chl-a	Stratified	ABA feedback
	Epi. chl-a (t-1)	Stratified	ABA feedback
	Hypolimnetic temp.	Stratified	Temperature-dependence of respiration
	Hypo. surface area to volume ratio	Stratified	Sediment oxygen demand
	Maximum buoyancy frequency	Stratified	Diffusion

Table 2: Random and residual variation from linear mixed models. Model structure and fixed effects are summarized in Figure 4.

Response variable	Random effect standard deviation (intercept)	Residual standard deviation
Anoxic factor (AF)	0.982	0.337
Hypolimnetic TP	0.665	0.286
Epilimnetic TP	0.248	0.340
Epilimnetic chl-a	0.635	0.415
Oxygen demand	0.630	0.597

Chapter III Figures

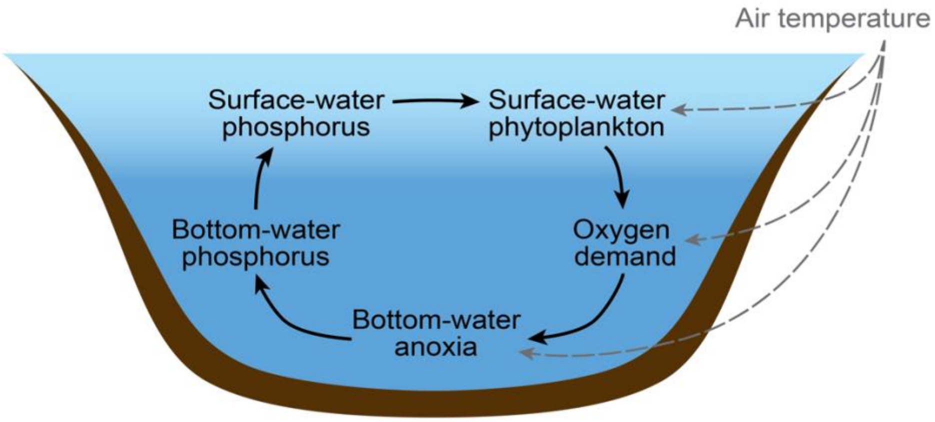

Figure 1: The proposed positive feedback through which "anoxia begets anoxia" (ABA). Hypolimnetic anoxia results in internal hypolimnetic phosphorus (TP) loading (a), which in turn increases epilimnetic TP (b) and stimulates phytoplankton growth, resulting in increased chlorophyll-*a* (chl-a; c). Phytoplankton decomposition fuels increased oxygen demand rates (d), which further drive hypolimnetic oxygen declines (e). This feedback can be externally influenced by increased air temperatures (gray dashed lines), among other factors.

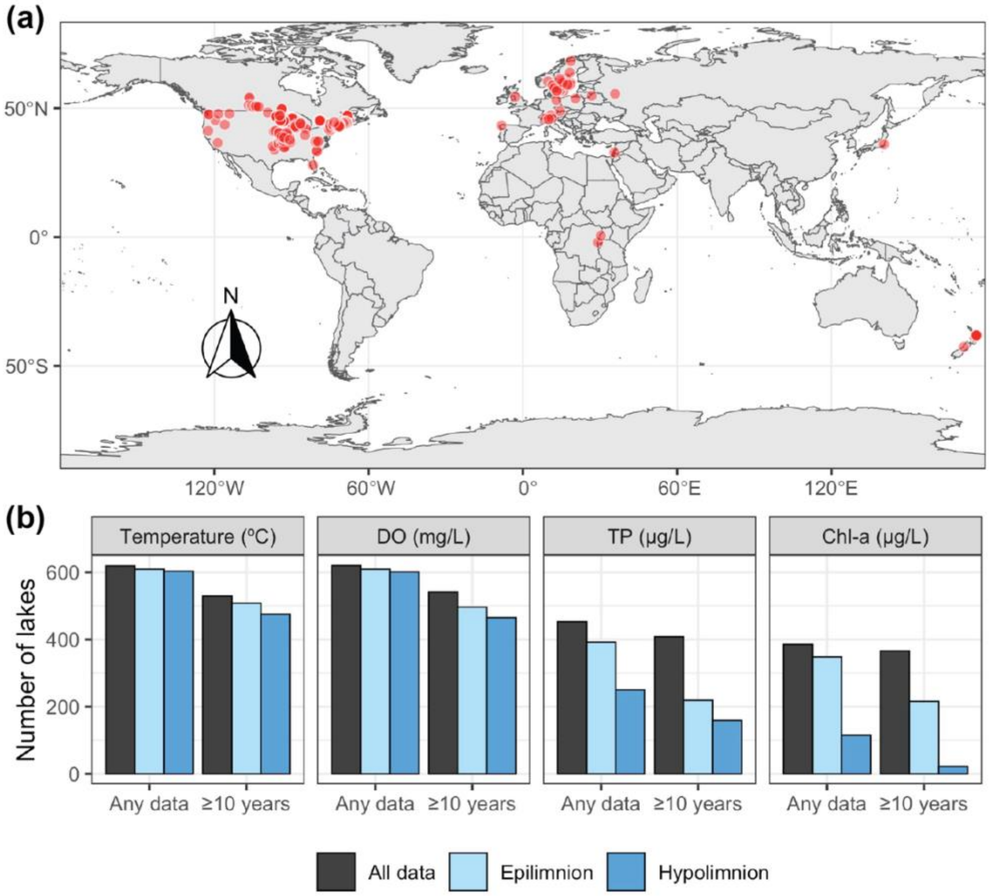

Figure 2: Data were compiled from a total of 656 widespread temperate lakes, with data availability differing across sites. (a): map of all sites included in this dataset. Note that due to overlapping data points, many sites are not visible. More detailed maps of the United States and Europe are provided in Appendix S2: Figure S2 and S3. Map lines delineate study areas and do not necessarily depict accepted national boundaries. (b): Summary of data availability for water temperature, dissolved oxygen (DO), total phosphorus (TP), and chlorophyll-*a* (chl-a) in the epilimnion (epi.) and hypolimnion (hypo.) of lakes in this study.

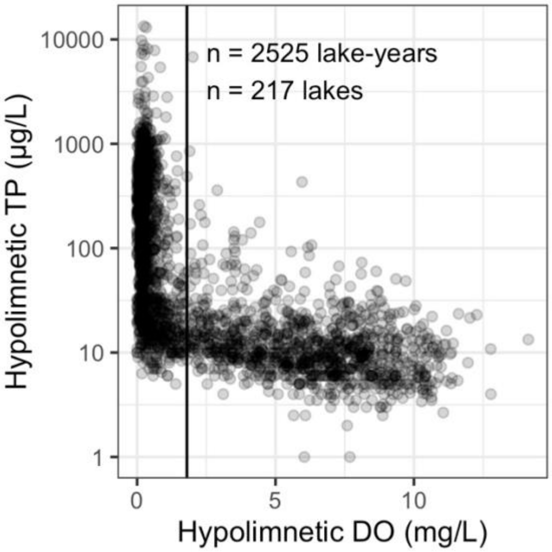

Figure 3: Piecewise mixed model regression identified a breakpoint in the relationship between hypolimnetic DO and TP at 1.8 mg/L DO. Here, points represent individual lake-years.

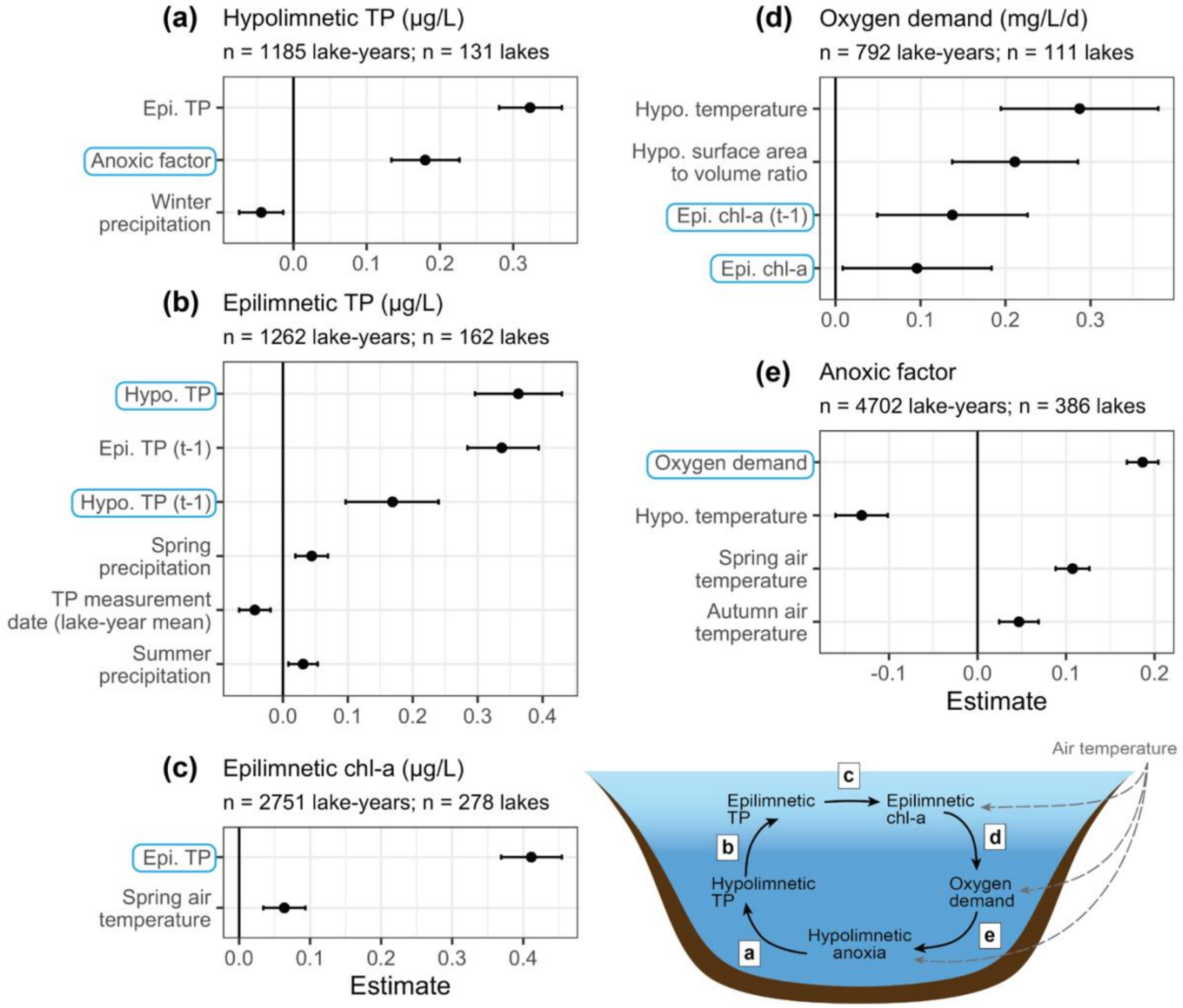

Figure 4: The proposed "anoxia begets anoxia" (ABA) feedback (bottom right) was supported by linear mixed model results across all variables (see Table 1). Here, panel titles indicate the response variable for each panel and y-axis labels indicate explanatory variables. X-axes indicate the magnitude and 95% confidence interval of the parameter estimate for each explanatory variable presented on the y-axis. The black vertical lines in panels a-e denote a parameter estimate of zero. Blue rectangles highlight drivers in the hypothesized ABA feedback (bottom right). Explanatory variables are ordered by the magnitude of the parameter estimate within each panel.

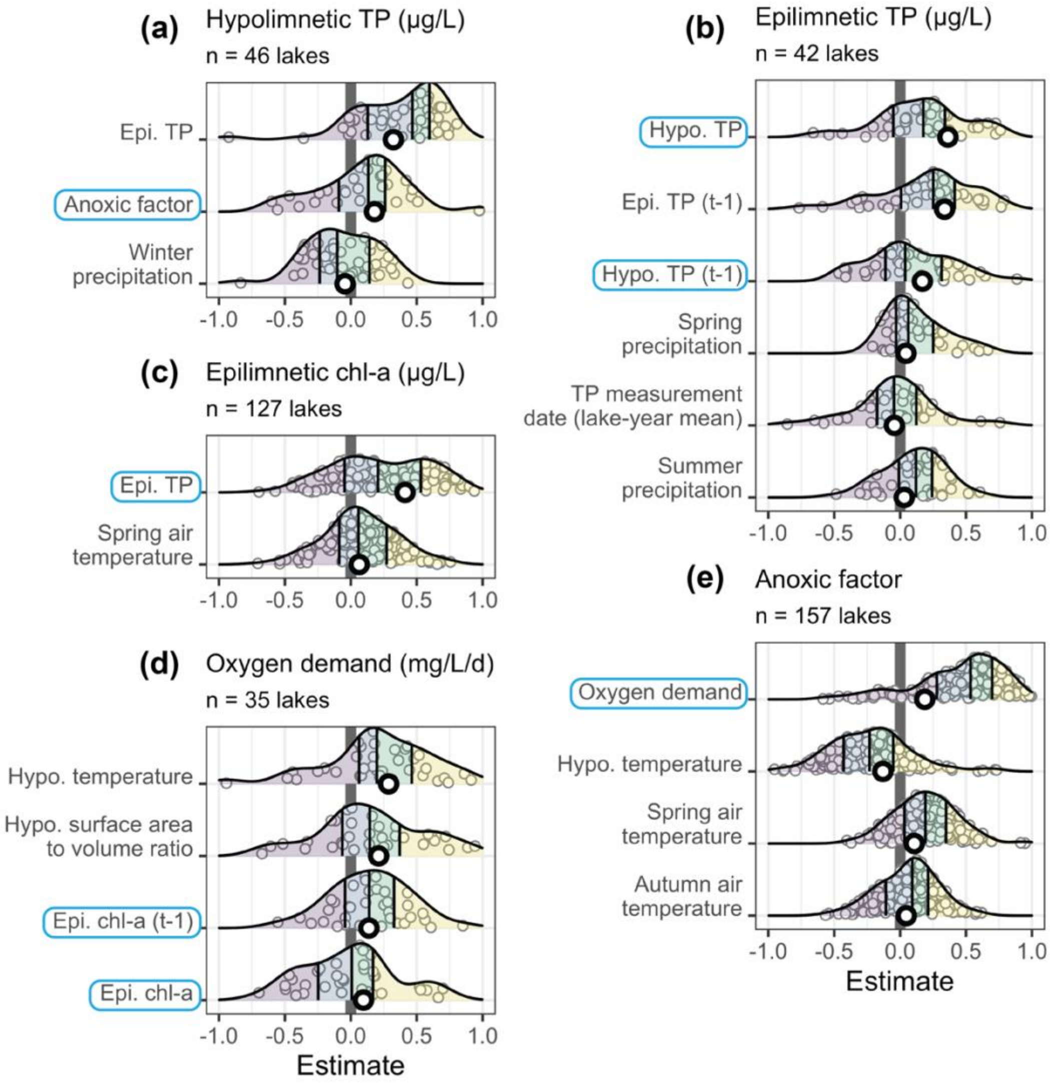

Figure 5: Linear regressions analyzing time series data within individual lakes provide further support for the proposed "anoxia begets anoxia" (ABA) feedback. Here, panel titles indicate the response variable for each panel and y-axis labels indicate explanatory variables. Individual points represent regression coefficients from within one lake. Density distributions describe the distribution of parameter values across lakes, with colors delineating the quartiles of the distribution (purple: 0-25%, blue: 25-50%, green: 50-75%, and yellow: 75-100%). Black and white circles at the bottom of each distribution mark the parameter estimate from the mixed

model analysis (Figure 4). The gray vertical lines in panels A-E denote a parameter estimate of zero. Blue rectangles highlight drivers in the hypothesized ABA feedback. Explanatory variables are ordered by the magnitude of the mixed-model parameter estimate for consistency with Figure 4. All x-axes range from -1 to 1 to enable comparison among panels.

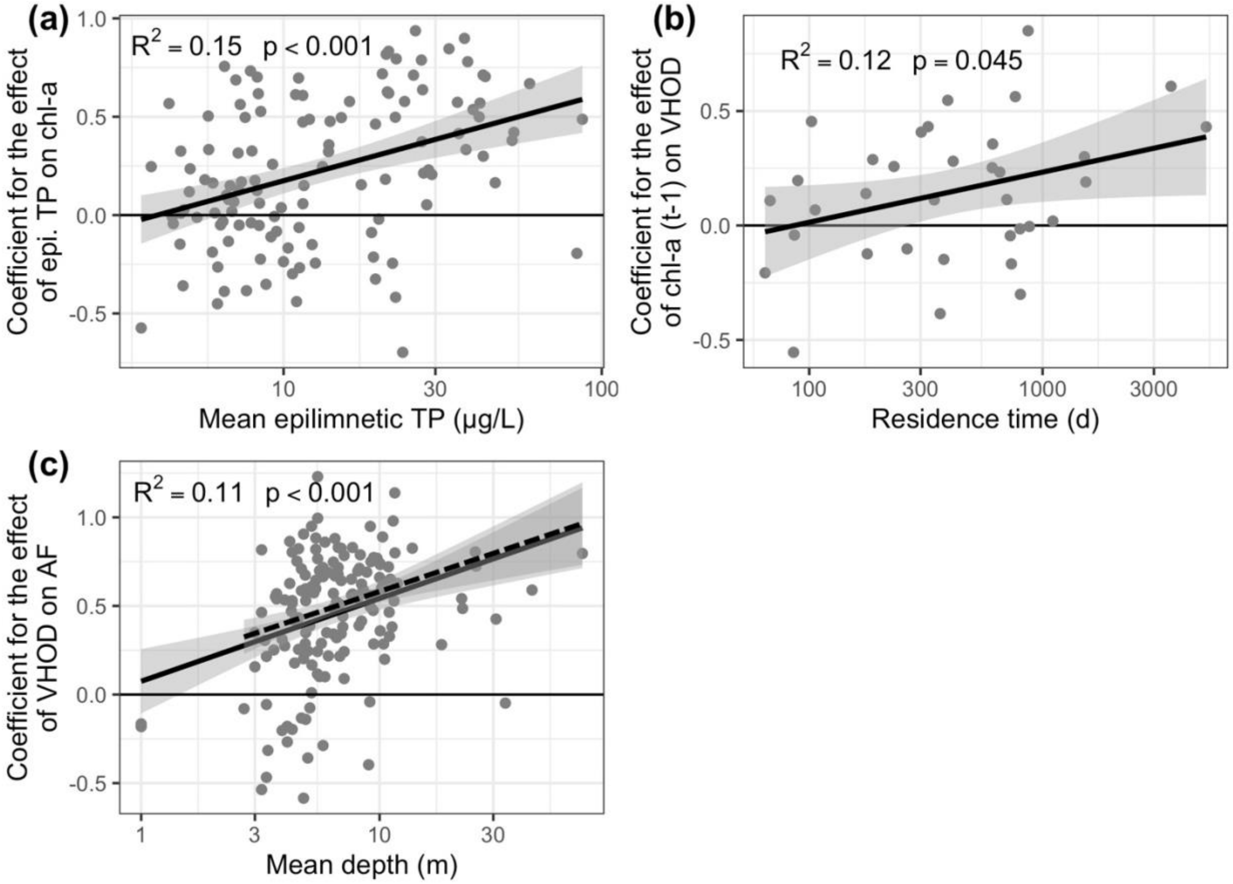

Figure 6: The strength of "anoxia begets anoxia" (ABA) feedback relationships may be modulated by lake characteristics. (a): The coefficient for the effect of epilimnetic total phosphorus (epi. TP) on chlorophyll-*a* (chl-a) was most positive in lakes with high mean epilimnetic TP. (b): The coefficient for the effect of the previous year's chlorophyll-*a* (chl-a) on volume-weighted hypolimnetic oxygen demand (VHOD) was most positive in lakes with long residence times. (c): The coefficient for the effect of VHOD on anoxic factor (AF) was most positive in lakes with deep mean depths. This relationship was robust to including all data (solid regression line) and excluding disproportionately influential points (i.e., Cook's distance greater than 3× the mean, *n* = 12 lakes; shown as a dashed line). Linear regressions are presented as solid lines.

Supporting Information for Chapter III

Appendix S1: Stratification

Contents

This document describes the depth-cutoff used for stratification (Text S1.1; Figure S1.1) and the methods by which the stratified period was calculated at each lake (Text S1.2; Figure S1.2).

Text S1.1: Effects of variation in depth cutoff

The proposed ABA cycle includes distinct epilimnetic and hypolimnetic processes. Consequently, we removed n = 158 lakes that are < 6.4 m deep from further analysis (of an initial 822 lakes; Lewis et al. 2023), as these lakes are less likely to experience stable seasonal stratification (Kirillin & Shatwell, 2016). To test the effect of variation in this depth threshold, we re-ran our mixed model results with a 3 m, rather than 6.4 m, depth cutoff. While the total number of lakes and lake-years increased with the 3 m threshold, results did not differ substantially from those identified using the 6.4 m threshold (Figure S1, compared to Figure 4 in the main manuscript).

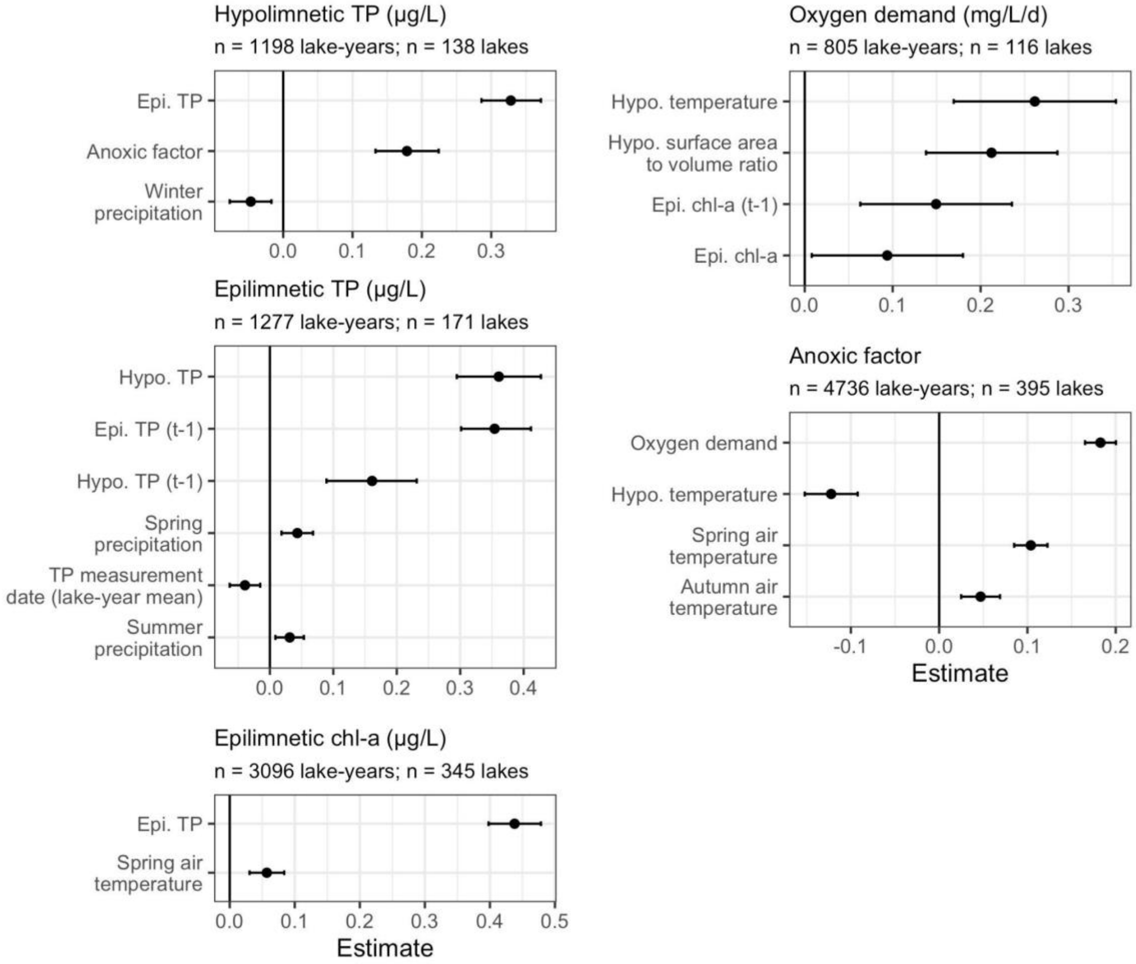

Figure S1.1: Mixed-model results using a 3 m depth cutoff did not differ substantially from those using a 6.4 m depth cutoff, as presented in Figure 4 of the main manuscript.

Text S1.2: Multiple summer time-periods of analysis

Stratified period

To calculate epilimnetic and hypolimnetic boundaries during the entire summer stratified period, we identified the date of the last non-stratified profile in the before August 1 (northern hemisphere) or February 1 (southern hemisphere) and the first non-stratified profile after this date (Figure S2). Non-stratified profiles were identified as those with a water-column density range of < 0.1 kg m^{-3} m^{-1} (Wilson et al., 2020). We then filtered the dataset to only include profiles collected between these two dates. The median Julian day of year for the latest non-stratified profile in spring was 110 (northern hemisphere), while the median day of year for the earliest non-stratified profile in fall was 291 (northern hemisphere; Figure S2). For consistency across lakes, we also removed any remaining profiles that were before March 1 (northern hemisphere) or September 1 (southern hemisphere) and after November 30 (northern hemisphere) or May 31 (southern hemisphere) from the “stratified period” calculations (Figure S2).

Late summer

To calculate epilimnetic and hypolimnetic boundaries during the late-summer period, we filtered all data to July 15 through August 31 in the northern hemisphere and January 15–February 28 in the southern hemisphere, following Jane et al. (2021). These dates were before the onset of fall mixing in the majority of lake-years (Figure S2). While the timing of fall mixing differed across years and lakes (Figure S2), using a standardized window of time to describe the late-summer period allowed us to account for variation in sampling timing across lakes and years (Jane et al., 2021). We identified and removed non-stratified profiles and removed lakes from further analysis if over 10% of the profiles during this interval were non-stratified (density range of < 0.1 kg m^{-3} m^{-1}; n = 25).

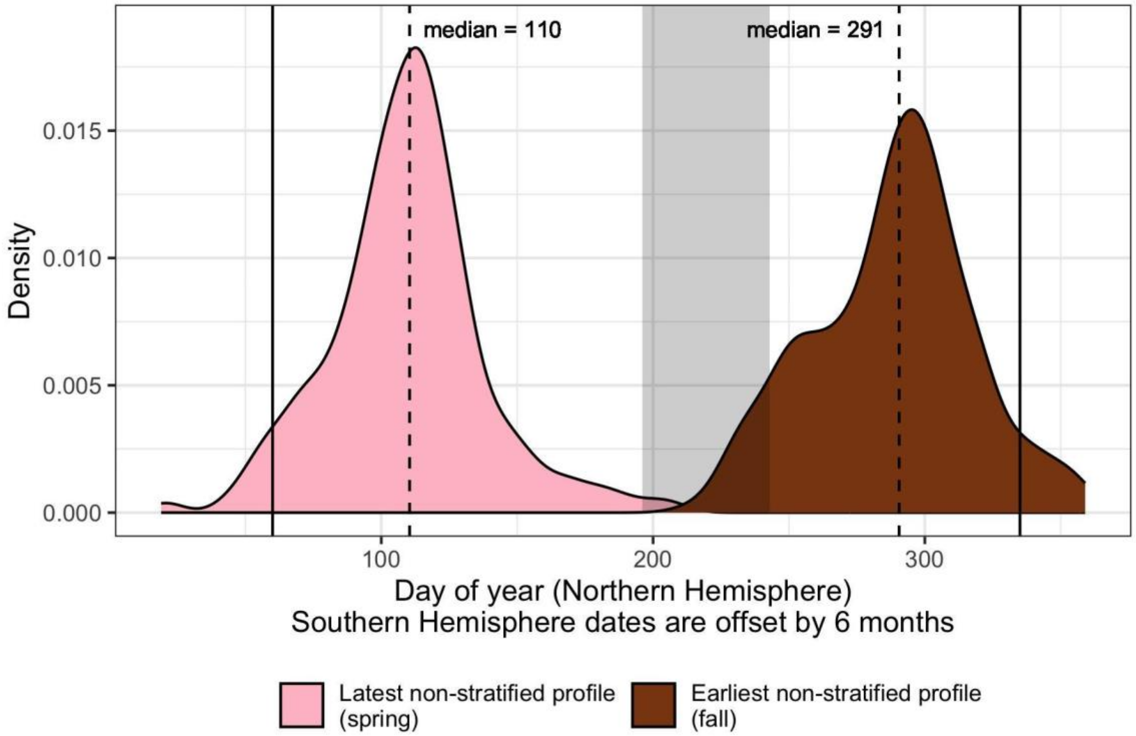

Figure S1.2: Across all lake-years, the latest non-stratified profile before the middle of summer tended to be in mid-April, while the earliest non-stratified profile tended to be in mid-October (Southern hemisphere dates are offset by 6 months). Density curves represent the distribution of dates across all lake-years. Solid lines indicate the date range considered as *potentially* part of the stratified period, which was then further constrained by sampling data from each lake-year. Dashed lines mark the median for each distribution. Grey shading indicates the period considered for late-summer analysis, which was before the end of stratification for most lakes.

References

Jane, S. F., Hansen, G., Kraemer, B., Leavitt, P., Mincer, J., North, R., Pilla, R., Stetler, J., Williamson, C., Woolway, R., Arvola, L., Chandra, S., DeGasperi, C., Diemer, L., Dunalska, J., Erina, O., Flaim, G., Grossart, H.-P., Hambright, K., & Rose, K. (2021). Widespread deoxygenation of temperate lakes. *Nature*, *594*. https://doi.org/10.1038/s41586-021-03550-y

Lewis, A.S., M. P. Lau, S. F. Jane, Y. Be’eri-Shlevin, S. H. Burnet, F. Clayer, H. Feuchtmayr, H. Grossart, D. W. Howard, H. Mariash, J. Delgado-Martin, R. L. North, I. Oleksy, R. M. Pilla, K. C. Rose, A. P. Smagula, R. Sommaruga, S. E. Steiner, P. Verburg, D. Wain, G. A. Weyhenmeyer, and C. C. Carey. 2023. Dissolved oxygen, temperature, chlorophyll-a, total phosphorus, total nitrogen, and dissolved organic carbon at multiple depths in 827 lakes from 1921-2022 ver 7. Environmental Data Initiative. https://portal-s.edirepository.org/nis/mapbrowse?scope=edi&identifier=1029&revision=7

Wilson, H. L., Ayala, A. I., Jones, I. D., Rolston, A., Pierson, D., de Eyto, E., Grossart, H.-P., Perga, M.-E., Woolway, R. I., & Jennings, E. (2020). Variability in epilimnion depth estimations in lakes. *Hydrology and Earth System Sciences*, *24*(11), 5559–5577. https://doi.org/10.5194/hess-24-5559-2020

Appendix S2: Dataset description

Contents

This document provides four supplemental figures characterizing the temporal (Figure S2.1) and spatial (Figures S2.2 and S2.3) extent of the multi-lake database, as well as the climatological variability across lakes and seasons (Figure S2.4).

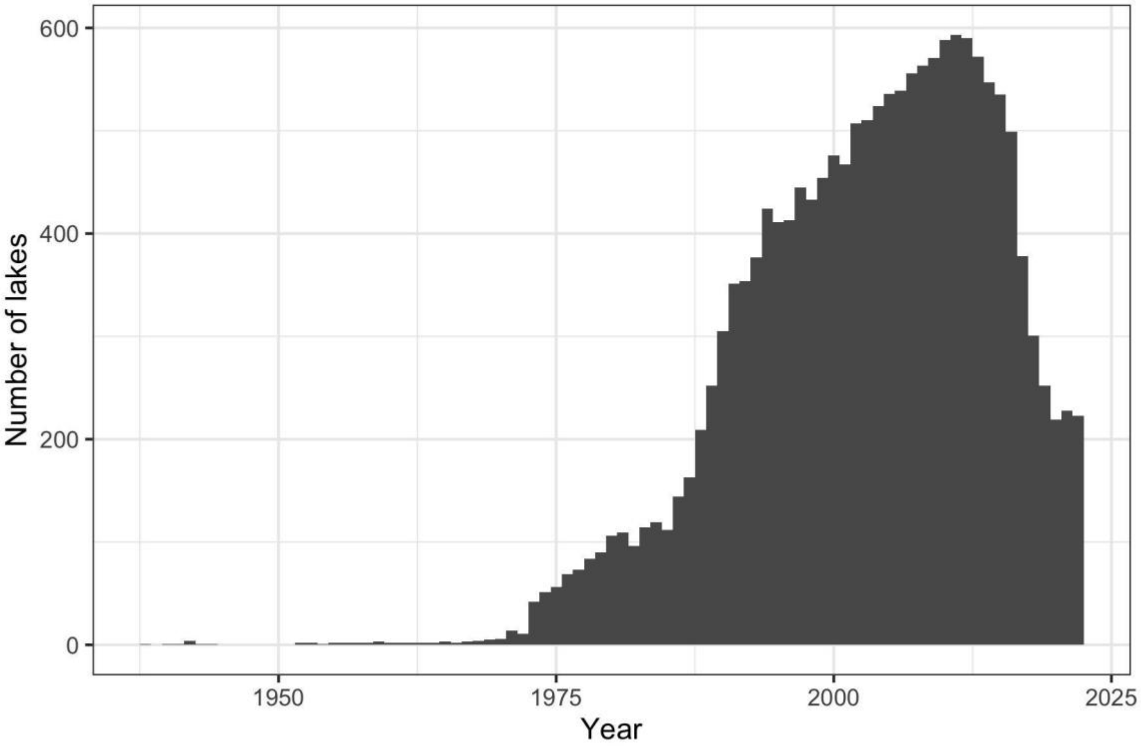

Figure S2.1: Total data availability extended from 1938–2022, with greatest coverage from ca. 1990–2020.

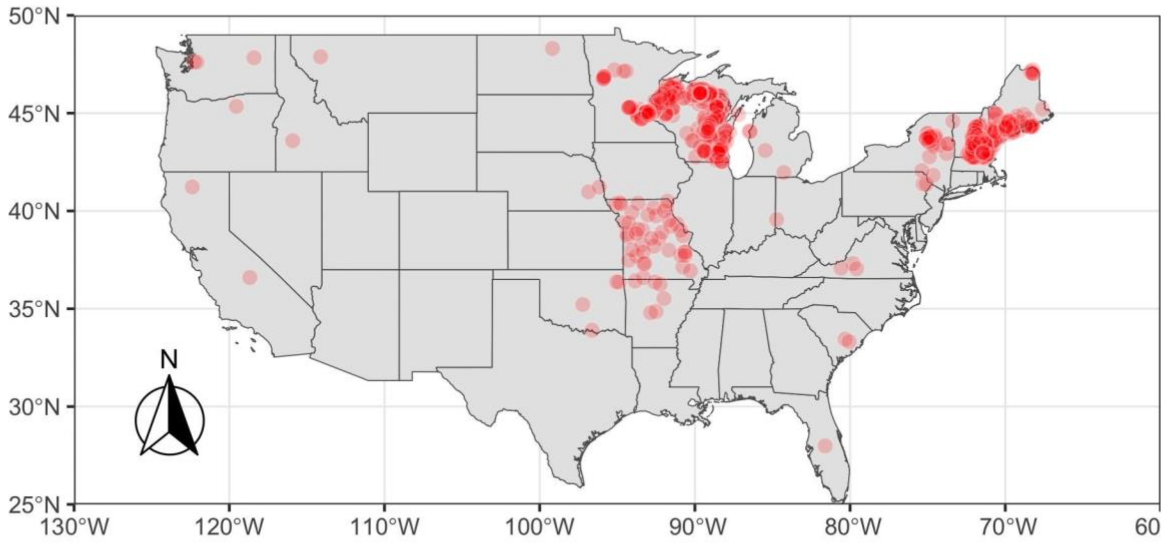

Figure S2.2: Detailed map of lake sites located in the United States of America that are used in this analysis. Points represent individual lakes. Map lines delineate study areas and do not necessarily depict accepted national boundaries.

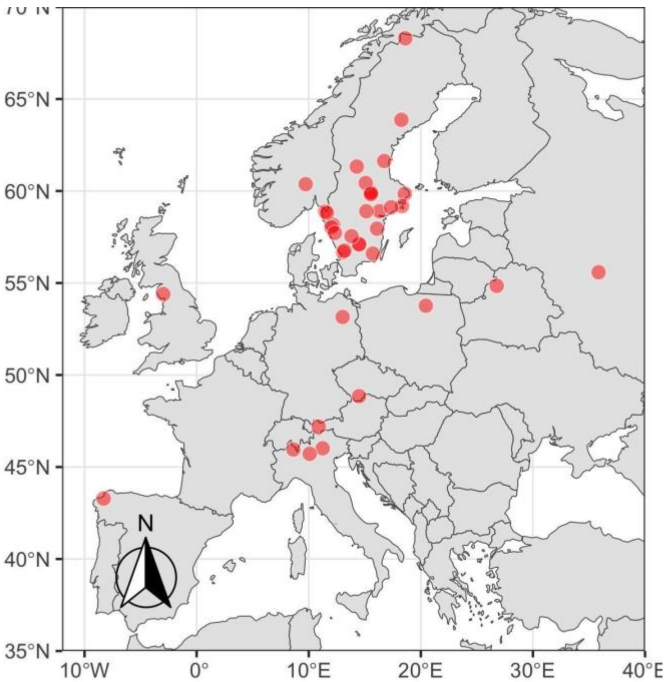

Figure S2.3: Detailed map of European lake sites used in this analysis. Points represent individual lakes. Map lines delineate study areas and do not necessarily depict accepted national boundaries.

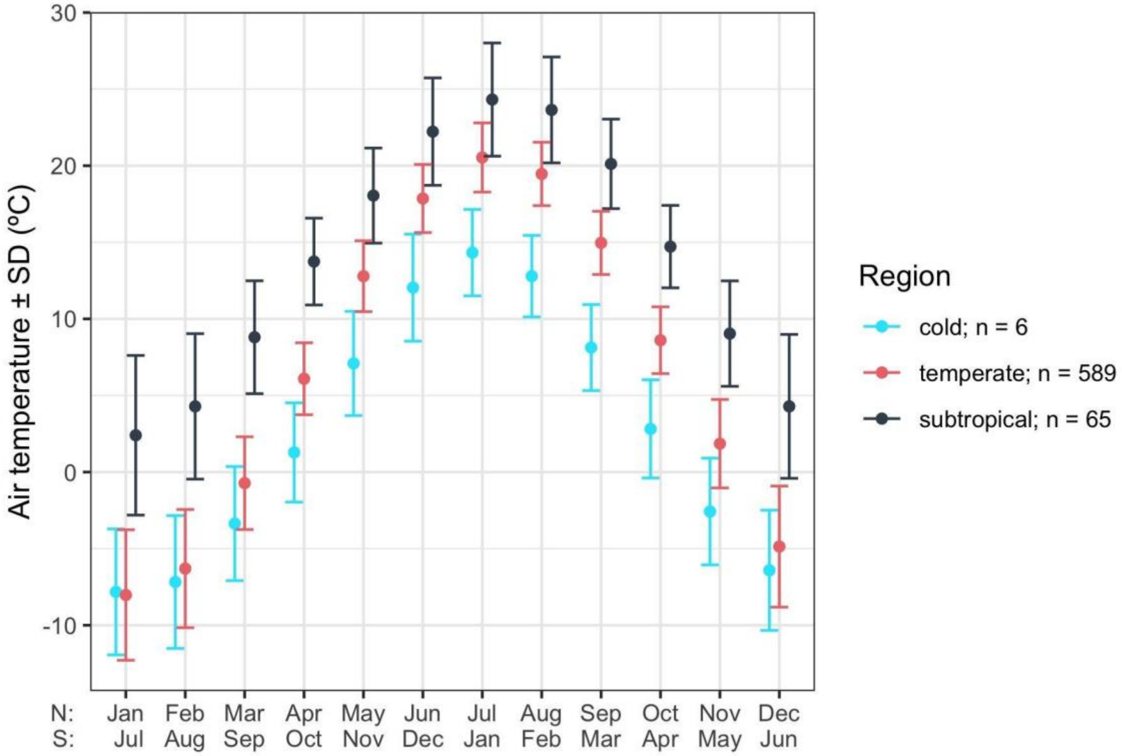

Figure S2.4: Mean monthly air temperature across study lakes. Here, lakes are separated into climate zones by latitude, where “cold” lakes are those between 60° – 90° absolute latitude, temperate lakes are those between 40° – 60° absolute latitude, and subtropical lakes are those between 23.5° – 40° absolute latitude.

Appendix S3: Depth Variation

Contents

This document provides text and one figure describing how temperature and oxygen profiles were filtered to remove profiles with outlying maximum depths.

Text S1

The deepest depth sampled for temperature and oxygen sometimes differed substantially among sampling dates within a lake. The reasons for this variability are manifold, including changes in lake water level or measurement protocol and errors in the dataset. Motivated by our focus on inter-annual patterns rather than extreme events, we implemented a standardized screening protocol to remove incomplete or abnormal temperature and oxygen profiles. First, we filtered out sampling days when only surface measurements were taken by removing profiles where the maximum sampling depth was under 2 m deep. We then removed profiles for which the maximum sampling depth was at least 30% above or below the reported maximum depth of the lake (i.e., deepest profile depth very shallow relative to maximum depth, or much greater than reported maximum depth). Lastly, for each lake, we identified and removed outlier temperature/oxygen profiles using the interquartile range outlier identification method (i.e., Tukey's boxplot). Following this cleaning procedure, the mean percentage of the water column sampled across lakes was 90.3% (Figure S3.1).

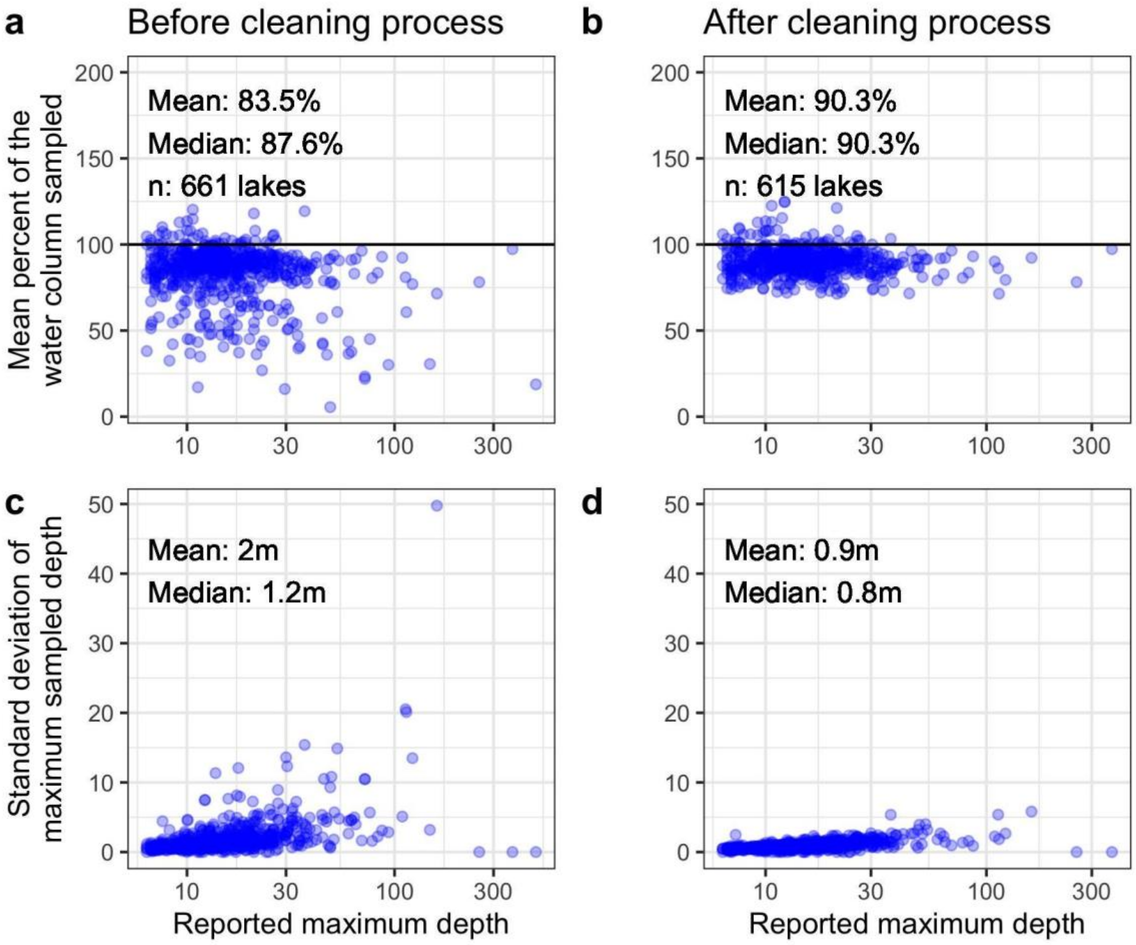

Figure S3.1: Our standardized filtering procedure successfully reduced variation in maximum sampling depths, both across (a, b) and within (c, d) lakes. Here each data point represents a given lake, with the reported maximum depth of the lake on the x-axis.

Appendix S4: Volume-weighted hypolimnetic oxygen demand

Contents

This document provides supplementary information describing methods used to calculate volume-weighted hypolimnetic oxygen demand (VHOD; Text S4.1 and S4.2) and temperature-corrected VHOD ($\mathrm{VHOD_{std\ 10^{o}C}}$; Text S4.3).

Text S4.1: Bathymetry modeling

Calculating VHOD requires an estimation of the bathymetric contours of the lake (Quinlan et al., 2005). Our dataset included measured hypsometry (area and depth intervals; e.g., using acoustic doppler current profiler data) for a small subset of lakes (n = 18). For these lakes, we interpolated from the measured bathymetric contours to 1 m intervals using a cubic spline function (Forsythe et al., 1977). Volume of each interval was calculated assuming a cylinder of 1 m height and surface area equal to the average of lake area above and below this interval. For all other lakes, we modeled bathymetric contours using maximum depth, mean depth, and surface area following Håkanson (2005). Briefly, a “shape-factor” was calculated based upon the ratio of mean to maximum depth, and this shape factor was used to estimate lake area in 1 m intervals from the surface to the bottom of the lake. Volume of each interval was then calculated as above (Lewis et al., 2023).

Text S4.2: VHOD calculation

We calculated VHOD for each lake-year in the dataset using interpolated dissolved oxygen (DO) profiles, hypolimnetic depths, and modeled bathymetry (Burns, 1995; Quinlan et al., 2005; Wetzel & Likens, 2000).

First, we calculated volume-weighted hypolimnetic DO concentrations for each sampling date during the summer stratified period. DO profiles were filtered to hypolimnetic depths, and the concentration of DO in each 1 m interval was multiplied by the volume of that interval to get total DO mass. Total DO mass was then summed across all hypolimnetic depths for a given date and divided by total hypolimnetic volume to calculate a volume-weighted DO concentration for this date.

Next, we restricted the data for each lake-year to the period of DO decline. If volume-weighted hypolimnetic DO concentrations decreased below 1 mg/L in any profiles from a given lake-year, we identified the first occurrence of DO < 1 mg/L and only considered profiles before this date within that lake-year. For all other lake-years, we filtered out any profiles after the date of minimum volume-weighted DO concentration within the lake-year, as these profiles likely indicate intrusion of epilimnetic DO associated with weakening stratification, impeding the calculation of DO demand.

For all lake-years with at least three DO depth-profiles remaining (n = 5385), we used linear regression to calculate the rate of decline in volume-weighted hypolimnetic DO concentrations within the summer, which we refer to as VHOD. To minimize the impact of confounding factors (e.g., DO measurement errors, uncertainty in hypolimnetic depth, physical mixing, or diffusion), we removed lake-years where time explained less than 50% of the variation in DO concentrations within the lake-year ($R^2 < 0.5$; 4.6% of lake-years, n = 246).

Following this filtering process, no lakes had positive rates of change in volume-weighted hypolimnetic DO concentrations throughout the stratified period, and we were left with VHOD measurements from 5140 lake-years and 414 lakes.

Text S4.3: Temperature-corrected VHOD

As a supplemental analysis, we estimated the change in VHOD that would be expected based upon established relationships between respiration and temperature by calculating temperature-corrected VHOD rates (VHOD$_{\text{std } 10^{\circ}\text{C}}$). We divided VHOD values for each lake-year by a correction factor based on the mean volume-weighted hypolimnetic temperature during the stratified period, following EQ1 (Pace & Prairie, 2005).

$$EQ1: \quad VHOD_{std\ 10^{\circ}C} = \frac{VHOD}{(Hypo.temperature/10)^{0.65}}$$

References

Burns, N. M. (1995). Using hypolimnetic dissolved oxygen depletion rates for monitoring lakes. *New Zealand Journal of Marine and Freshwater Research*, *29*(1), 1–11. https://doi.org/10.1080/00288330.1995.9516634

Forsythe, G. E., Malcolm, M. A., & Moler, C. B. (1977). *Computer Methods for Mathematical Computations*. Prentice Hall Professional Technical Reference.

Håkanson, L. (2005). The Importance of Lake Morphometry for the Structure and Function of Lakes. *International Review of Hydrobiology*, *90*(4), 433–461. https://doi.org/10.1002/iroh.200410775

Lewis, A. S. L., M. P. Lau, S. F. Jane, Y. Beeri-Shlevin, S. H. Burnet, F. Clayer, H. Feuchtmayr, H. Grossart, D. W. Howard, H. Mariash, J. Delgado-Martin, R. L. North, I. Oleksy, R. M. Pilla, K. C. Rose, A. P. Smagula, R. Sommaruga, S. E. Steiner, P. Verburg, D. Wain, G. A. Weyhenmeyer, and C. C. Carey. 2023. Dissolved oxygen, temperature, chlorophyll-a, total phosphorus, total nitrogen, and dissolved organic carbon at multiple depths in 822 lakes from 1921-2022 ver 9. Environmental Data Initiative. https://portal-s.edirepository.org/nis/mapbrowse?scope=edi&identifier=1029&revision=9

Pace, M. L., & Prairie, Y. T. (2005). Respiration in lakes. In P. del Giorgio & P. Williams (Eds.), *Respiration in Aquatic Ecosystems* (pp. 103–121). Oxford University Press. https://doi.org/10.1093/acprof:oso/9780198527084.003.0007

Quinlan, R., Paterson, A. M., Smol, J. P., Douglas, M. S. V., & Clark, B. J. (2005). Comparing different methods of calculating volume-weighted hypolimnetic oxygen (VWHO) in lakes. *Aquatic Sciences*, *67*(1), 97–103. https://doi.org/10.1007/s00027-004-0717-6

Wetzel, R. G., & Likens, G. E. (2000). Estimates of Whole Lake Metabolism: Hypolimnetic Oxygen Deficits and Carbon Dioxide Accumulation. In R. G. Wetzel & G. E. Likens (Eds.), *Limnological Analyses* (pp. 373–382). Springer. https://doi.org/10.1007/978-1-4757-3250-4_29

Appendix S5: Anoxic factor

Contents

This document describes the calculation of anoxic factor, with one text description (Text S5.1), one table (Table S5.1), and three figures (Figures S5.1–S5.3).

Text S5.1: Anoxic factor calculation

Anoxic factor (AF) describes the spatial and temporal extent of anoxia within a lake, and is calculated through the following equation (Nürnberg 1998):

EQ1:

$$AF = \frac{duration\ of\ anoxia\ *\ anoxic\ sediment\ area}{A_0}$$

where A_0 is the total sediment area of the lake.

The anoxic factor is typically calculated using distinct hypolimnetic layers to capture the dynamic spatial extent of anoxia throughout a summer stratified period. Here, we treated the entire hypolimnion as one layer. This approach corresponds with our treatment of total phosphorus and volume-weighted hypolimnetic oxygen demand (VHOD) throughout our analysis (e.g., *Section 2.2.2 Epilimnetic and hypolimnetic concentrations* of the main text). Comparison of AF calculated for the entire hypolimnion and for the hypolimnion divided in two layers showed close correspondence, though dividing the hypolimnion in two layers substantially reduced the number of lake-years where we were able to estimate AF (*n* = 5489 vs. *n* = 3665 lake-years; see below in *S1.3 Two Layers*).

S5.1.1 Duration of anoxia

We used two approaches to estimate the first day within a lake-year that exhibited anoxia (hereafter, anoxic onset). First, for lake-years when we multiple dissolved oxygen (DO) profiles within one week at the transition from oxic to anoxic conditions (defined as <1.8 mg/L; see Figure 4 in the main text), we interpolated between these profiles to determine the date of anoxic onset. Second, if we did not have multiple DO profiles within one week of anoxic onset but were able to calculate volume-weighted hypolimnetic oxygen demand (VHOD) for a given lake-year (see *Section 2.2.3 Volume-weighted hypolimnetic oxygen demand* in the main text), we then modeled the onset of anoxia as the date when volume-weighted DO was predicted to fall below our 1.8 mg/L threshold given the slope and intercept of the decline in hypolimnetic DO. For lake-years when we were able to calculate anoxic onset in both ways (i.e., interpolation between two profiles and using VHOD), these approaches were in very close agreement ($R^2 = 0.97$; Figure S5.1), and we preferentially used the profile-based measurements when available.

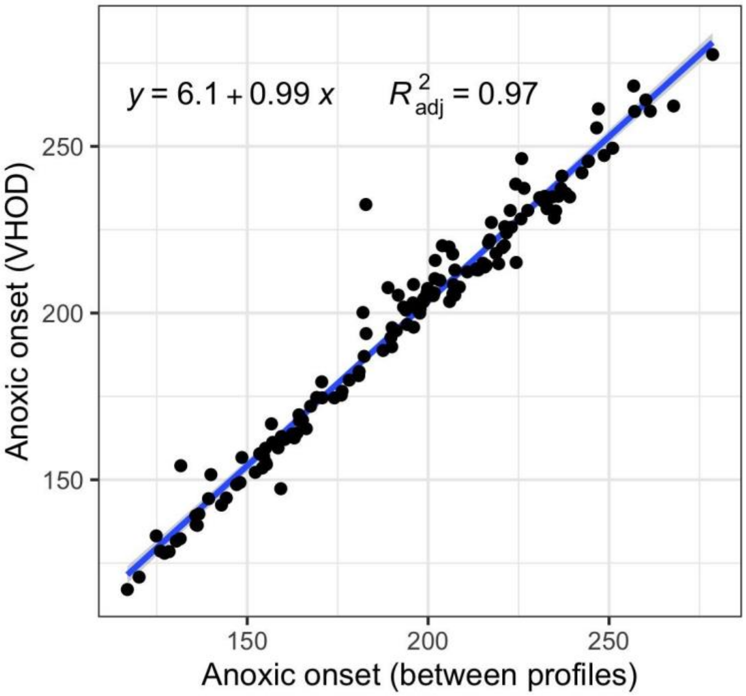

Figure S5.1: Correspondence between anoxic onset (given as day of year on both axes) identified using two methods: interpolation between two DO profiles (x-axis) and modeled using VHOD (y-axis).

We similarly used two approaches to estimate the end of anoxia (i.e., the first day of fall turnover). First, we identified all lake-years when we had water temperature profiles within one week surrounding turnover, and estimated the end of anoxia as being halfway between these profiles. For the remaining lake-years, we adapted the model from Nürnberg (1988, 2019) to predict the end of anoxia (i.e., end of stratification) based on hypolimnetic temperatures, mean lake depth, and latitude (EQ2). Because the duration of summer stratification is increasing in many lakes due to changing climate (Jane et al. 2023), we re-fit the model from Nürnberg (1988) using our data (*n* = 33 lakes; *n* = 66 lake-years) and using “year” as an additional factor in the regression. This produced a similar model output to that from Nürnberg (1988), with an additional, positive effect of analysis year, as expected (EQ3, Table S5.1). Both the modified and unmodified Nürnberg (1988) models explained a substantial portion of the variation in our estimated stratification end dates (Figure S5.2), though the modified model had greater explanatory power (modified $R^2 = 0.72$, unmodified $R^2 = 0.55$) and thus was included in subsequent analyses in our study.

EQ2 (Nürnberg, 1988):

$$\begin{aligned} log(stratification\ end\ date) = 2.62 &- 0.116 * log(hypo.temp) \\ &+ 0.042 * log(mean\ depth.) \\ &- 0.002 * latitude \end{aligned}$$

EQ3 (modified using our dataset):

$$\begin{aligned} log(stratification\ end\ date) = 1.56 &- 0.131 * log(hypo.temp) \\ &+ 0.007 * log(mean\ depth.) \\ &- 0.002 * latitude \\ &+ 0.0006 * year \end{aligned}$$

Table S5.1: Linear model results for the model formulation adapted from Nürnberg (1988).

Coefficient	Estimate	SE	T	p
Intercept	1.562	0.298	5.24	< **0.001**
Hypo. temp	-0.131	0.011	-11.33	< **0.001**
Mean depth	0.007	0.010	0.74	0.46
Latitude	-0.002	0.0003	-5.23	< **0.001**
Year	0.0006	0.0002	3.65	< **0.001**

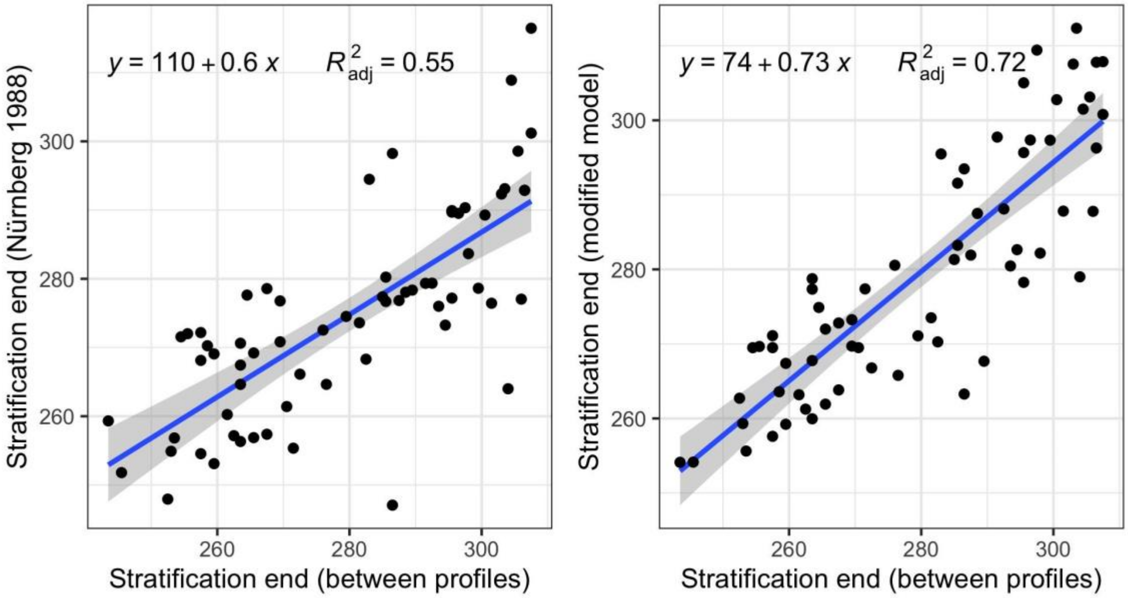

Figure S5.2: Comparison of two methods of estimating the last day of anoxia within a lake-year (given as day of year in both axes). Modifying the model from Nürnberg (1988; left) improved model fit (right). We note that the performance of both models is comparable to that of the original Nürnberg (1988) paper, where $R^2 = 0.67$.

S5.1.2 Sediment area

We calculated anoxic sediment area as the sediment area that corresponds to the thermocline depth for a given year (to correspond with our use of hypolimnetic average DO), using modeled bathymetry (Appendix S4).

S5.1.3 Split hypolimnion

To assess the magnitude of uncertainty that results from the treatment of the hypolimnion as one unified layer, we re-ran the calculation of AF using two distinct hypolimnetic layers in each lake. We split the hypolimnion into two layers of equal depth and calculated anoxic onset in each layer following the methods above (*S1.1 Duration of anoxia*). We used the same anoxic end date for both layers, and we calculated the area of the shallower layer as the surface area of the top of this layer minus the surface area of the bottom layer. If data were available to successfully estimate anoxic duration for *both* layers, we then calculated AF as the sum of AF in each individual layer (Nürnberg 1998).

Ultimately, the use of two hypolimnetic layers did not alter our AF calculations (Figure S5.3), though calculating AF with two hypolimnetic layers substantially reduced data availability from 5489 to 3665 lake-years. Consequently, to include as many lakes as possible in our study, we focused on the one-layer analysis for the manuscript.

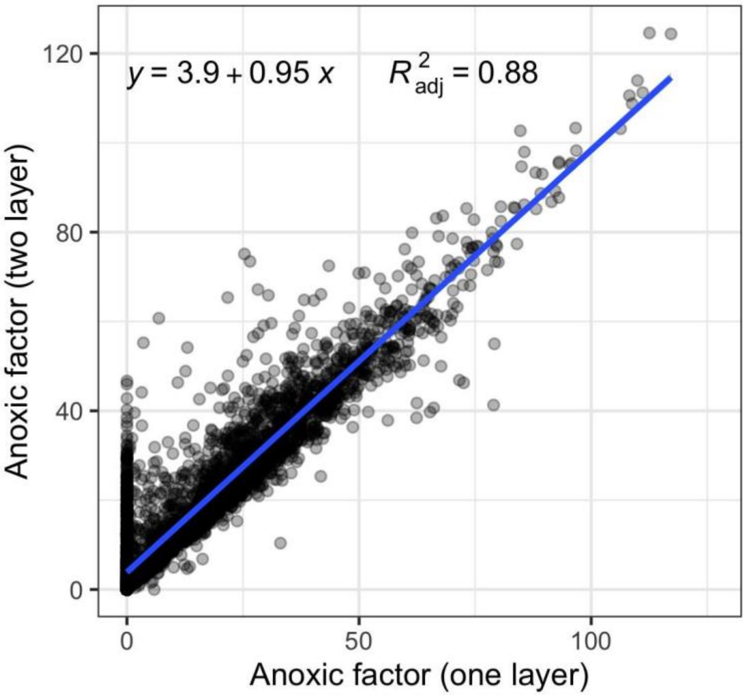

Figure S5.3: Correlation between anoxic factor values calculated using one and two hypolimnetic layers. Points represent individual lake-years.

References

Jane, S. F., J. L. Mincer, M. P. Lau, A. S. L. Lewis, J. T. Stetler, and K. C. Rose. 2023. Longer duration of seasonal stratification contributes to widespread increases in lake hypoxia and anoxia. Global Change Biology **29**: 1009–1023. doi:10.1111/gcb.16525

Nürnberg, G. K. 1988. A simple model for predicting the date of fall turnover in thermally stratified lakes. Limnology and Oceanography **33** 1190–1195. doi: 10.4319/lo.1988.33.5.1190

Nürnberg, G. K. 2019. Quantification of Anoxia and Hypoxia in Water Bodies. In *Encyclopedia of Water* (pp. 1–9). John Wiley & Sons, Ltd. https://doi.org/10.1002/9781119300762.wsts0081

Appendix S6: Oxygen breakpoints

Contents

This document provides:

1. Text description of the breakpoint analysis results for hypolimnetic dissolved oxygen (DO) and total phosphorus (TP; Text S6.1)
2. The driver analysis results for hypolimnetic dissolved oxygen (DO) concentrations in lakes that did not experience anoxia throughout the time series of data used in this study (hereafter oxic lakes; Text S6.2)
3. A supporting figure (Figure S6.1) and table (Table S6.1)

Text S6.1

As an operational definition of hypolimnetic anoxia, we calculated the breakpoint in the mixed model regression between hypolimnetic DO and hypolimnetic TP. Of the proposed explanatory variables for hypolimnetic TP (Table S6.1), the explanatory variables selected using AICc included hypolimnetic DO, epilimnetic TP, and winter precipitation. We ran a segmented regression using this model formulation, and the segmented regression identified a breakpoint of 1.8 mg/L DO.

Text S6.2

Of the proposed explanatory variables for hypolimnetic DO (Table S6.1), the selected explanatory variables included spring air temperature, oxygen demand, oxygen measurement date. Both across-lake mixed model analyses and within-lake regressions indicated that oxygen demand generally had a positive effect on late-summer hypolimnetic oxygen concentrations in oxic lakes (Figure S6.1). For the mixed model analysis, standard deviation of the random effect for lake ID was 0.82 and standard deviation of the residuals was 0.61.

Table S6.1: Proposed explanatory variables for late-summer hypolimnetic DO.

Response variable	Proposed explanatory variables	Time period	Motivation for inclusion
Late-summer hypolimnetic TP	Hypolimnetic DO	Late summer	ABA feedback
	Epi. TP	Stratified	Diffusion/sinking
	Maximum buoyancy frequency	Stratified	Diffusion
	Hypo. temp	Late summer	Temperature dependence of sediment flux
	Spring precipitation		Catchment inputs/flushing
	Summer precipitation		Catchment inputs/flushing
	Winter precipitation		Catchment inputs/flushing
	Mean TP measurement date	Late summer	Modeling control
Late-summer hypolimnetic DO	Oxygen demand	Stratified	ABA feedback
	Spring average air temp.		Stratification onset
	Summer average air temp.		Saturation
	Winter average air temp.		Ice dynamics
	Hypo. temperature	Late summer	Saturation
	Mean DO measurement date	Late summer	Modeling control

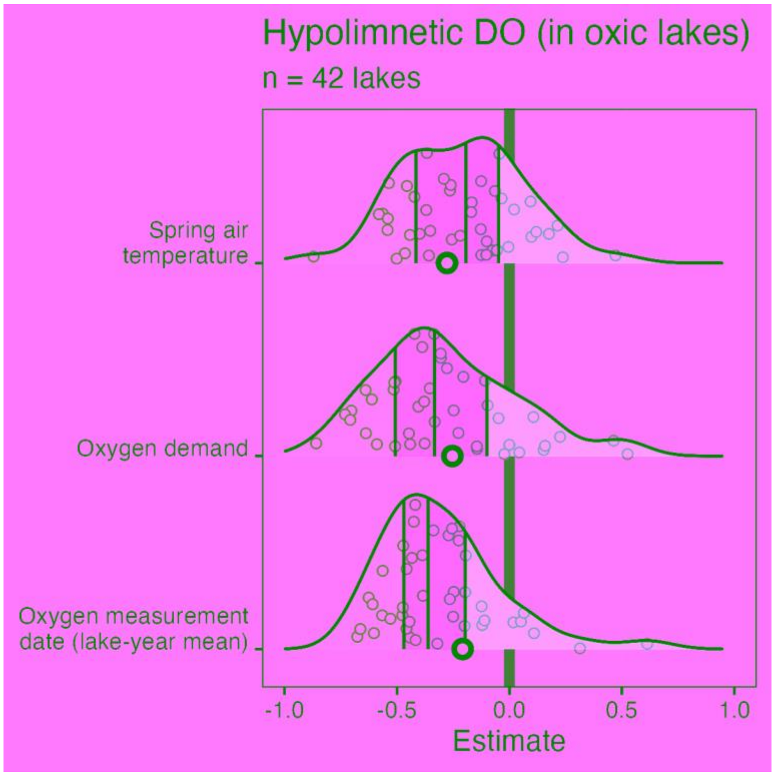

Figure S6.1: Oxygen demand tended to have a positive effect on late-summer hypolimnetic dissolved oxygen in oxic lakes. Here, y-axis labels indicate explanatory variables. Individual points represent regression coefficients from within one lake. Density distributions describe the distribution of parameter values across lakes, with colors delineating the quartiles of the distribution (purple: 0-25%, blue: 25-50%, green: 50-75%, and yellow: 75-100%). Black and white circles at the bottom of each distribution mark the parameter estimate from the mixed model analysis. The gray vertical line denotes a parameter estimate of zero.

Appendix S7: Lags, multicollinearity, and alternative model structures

Contents

This document provides a supplemental table about alternative model structures (Table S7.1), a supplemental table describing multicollinearity of model results (Table S7.2), and five supporting figures to illustrate the relevant lags of each relationship in the hypothesized ABA feedback (Figures S7.1–S7.5).

Table S7.1: Alternative models within 2 units AICc.

Response variable	Model selected	AICc	Other potential models (within 2 units AICc)	AICc
Anoxic factor	Oxygen demand + Spring average temp. + Autumn average temp. + Hypo. temperature	4754	None	
Late-summer hypo. TP	Anoxic factor + Epi. TP + Winter precipitation	870	Anoxic factor + Epi. TP	870
Stratified epi. TP	Hypo TP + Hypo. TP (t-1) + Epi. TP (t-1) + Spring precipitation + Summer precipitation + Mean TP measurement date	1131	Hypo TP + Hypo. TP (t-1) + Epi. TP (t-1) + Spring precipitation + Mean TP measurement date	1129
			Hypo TP + Hypo. TP (t-1) + Epi. TP (t-1) + Mean TP measurement date	1130
Stratified epi. chl-a	Epi. TP + Spring average air temp.	979	None	
Oxygen demand	Epi. chl-a + Epi. chl-a (t-1) + Hypolimnetic temp. + Hypo. surface area to volume ratio	1668	Epi. chl-a (t-1) + Hypolimnetic temp. + Hypo. surface area to volume ratio	1666

Table S7.2: Multicollinearity of explanatory variables from mixed model regression results, where VIF is the variance inflation factor.

Response variable	Explanatory variable	VIF
Anoxic factor	Oxygen demand	1.01
	Spring average temp.	1.11
	Autumn average temp.	1.01
	Hypo. temperature	1.12
Late-summer hypo. TP	Anoxic factor	1.01
	Epi. TP	1.01
	Winter precipitation	1.00
Stratified epi. TP	Hypo TP	2.73
	Hypo. TP (t-1)	3.09
	Epi. TP (t-1)	1.75
	Spring precipitation	1.03
	Summer precipitation	1.01
	Mean TP measurement date	1.04
Stratified epi. chl-a	Epi. TP	1.00
	Spring average air temp.	1.00
Oxygen demand	Epi. chl-a	1.27
	Epi. chl-a (t-1)	1.25
	Hypolimnetic temp.	1.10
	Hypo. surface area to volume ratio	1.04

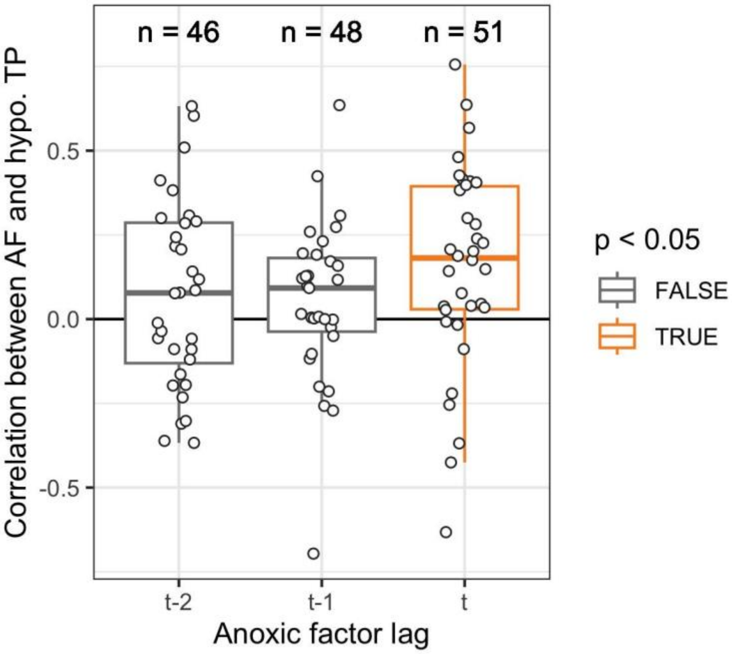

Figure S7.1: Hypolimnetic TP (hypo. TP) tended to be positively correlated with the current year’s anoxic factor (AF). Here, each data point indicates the spearman's correlation between hypo. TP and AF at the specified lag within a given lake. Correlations are calculated on an annual time step over the entire time series at the lake. Boxplot color indicates whether the mean correlation across all lakes is significantly different than 0 (wilcox test; $p < 0.05$), and the number of lakes included at each lag is indicated above the boxplot.

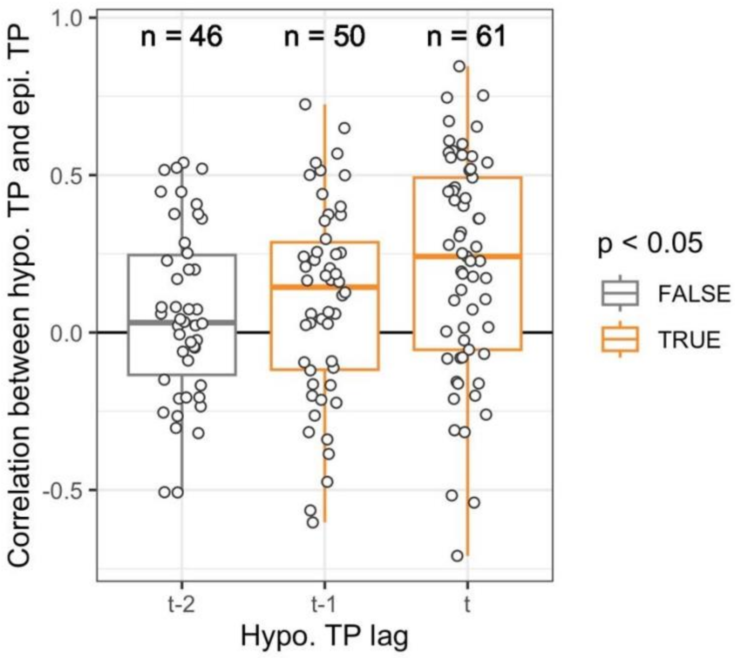

Figure S7.2: Epilimnetic total phosphorus (epi. TP) tended to be positively correlated with the current and previous years' (t and t-1) hypolimnetic total phosphorus (hypo. TP). Here, each data point indicates the spearman's correlation between epi. TP and hypo. TP at the specified lag within a given lake. Correlations are calculated on an annual time step over the entire time series at the lake. Boxplot color indicates whether the mean correlation across all lakes is significantly different than 0 (wilcox test; $p < 0.05$), and the number of lakes included at each lag is indicated above the boxplot.

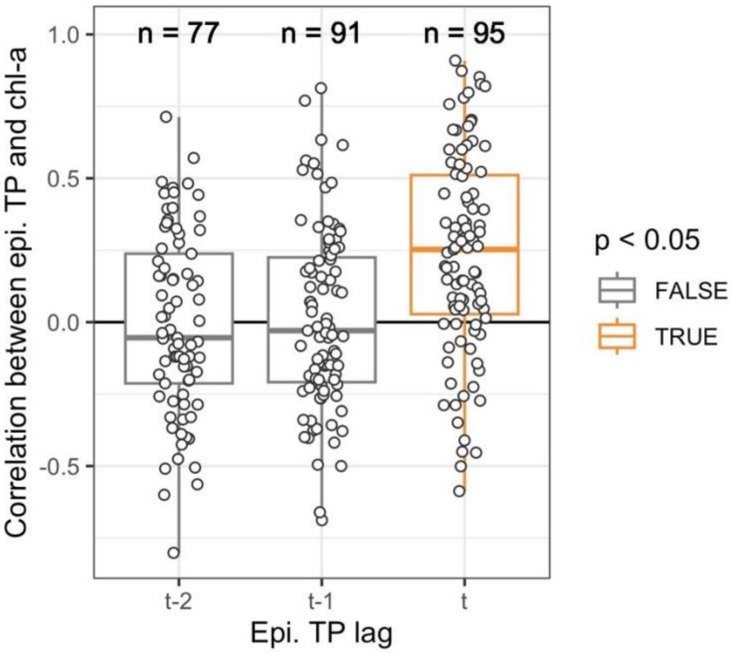

Figure S7.3: Epilimnetic chlorophyll-a (chl-a) tended to be positively correlated with the current year's epilimnetic total phosphorus (TP). Here, each data point indicates the spearman's correlation between chl-a and TP at the specified lag within a given lake. Correlations are calculated on an annual time step over the entire time series at the lake. Boxplot color indicates whether the mean correlation across all lakes is significantly different than 0 (wilcox test; $p < 0.05$), and the number of lakes included at each lag is indicated above the boxplot.

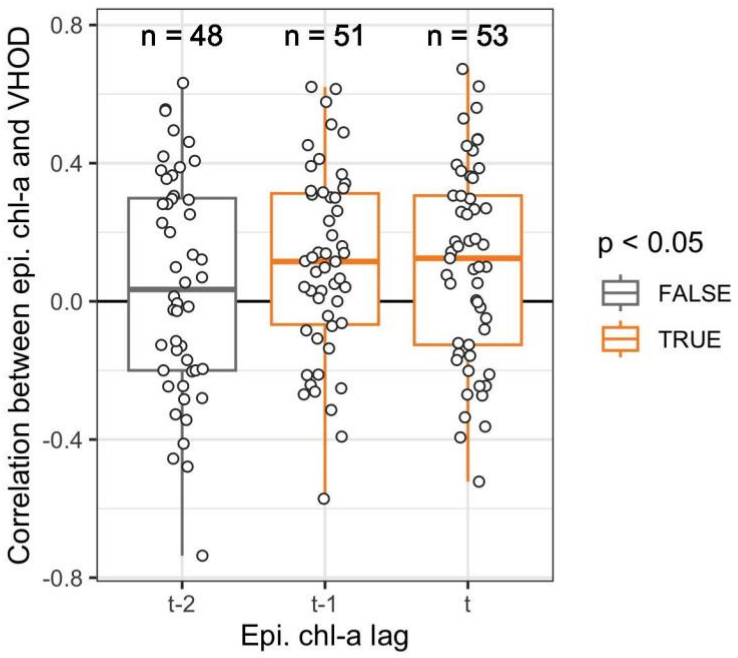

Figure S7.4: Volume-weighted hypolimnetic oxygen demand (VHOD) tended to be positively correlated with the current and previous years’ (t and t-1) epilimnetic chlorophyll-a (chl-a). Here, each data point indicates the spearman's correlation between VHOD and chl-a at the specified lag within a given lake. Correlations are calculated on an annual time step over the entire time series at the lake. Boxplot color indicates whether the mean correlation across all lakes is significantly different than 0 (wilcox test; $p < 0.05$), and the number of lakes included at each lag is indicated above the boxplot.

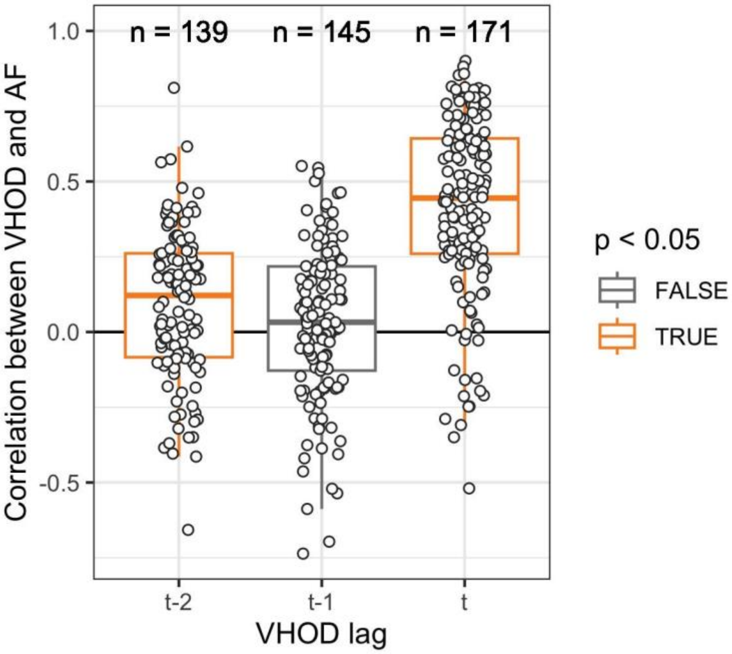

Figure S7.5: Anoxic factor (AF) tended to be positively correlated with the current and second lag (t and t-2) volume-weighted hypolimnetic oxygen demand (VHOD). Here, each data point indicates the spearman's correlation between AF and VHOD at the specified lag within a given lake. Correlations are calculated on an annual time step over the entire time series at the lake. Boxplot color indicates whether the mean correlation across all lakes is significantly different than 0 (wilcox test; $p < 0.05$), and the number of lakes included at each lag is indicated above the boxplot.

Appendix S8: Air temperature analysis

Contents

This document provides text description of the air temperature analysis methods (Text S8.1) and results (Text S8.2), including two figures (Figures S8.1, S8.2) and one table (Table S8.1).

Text S8.1: Methods

To analyze how variation in monthly air temperatures influences hypolimnetic dissolved oxygen (DO) concentrations, we calculated for each lake the partial Spearman correlation between monthly air temperature and four variables—hypolimnetic temperature, volume-weighted hypolimnetic oxygen demand (VHOD), hypolimnetic DO, and anoxic factor (AF)—while accounting for measurement year. These correlations were calculated for each lake with at least 10 years of paired data for monthly air temperature and the target variable of interest. Year of analysis was included in these partial correlation analyses to address independent and confounding temporal trends that influence air temperature and target variables. We calculated whether the mean of the resulting distribution of correlations was significantly different from zero using Wilcox tests with $\alpha = 0.001$, and we conducted analysis of variance (ANOVA) tests with Tukey post hoc tests when applicable to determine whether the distribution of correlations was significantly different between months.

To summarize climate effects on hypolimnetic DO, we calculated spring air temperature and hypolimnetic DO anomalies (value minus the lake-wise mean over the entire time series) for every lake-year in the dataset. We grouped air temperature anomalies into three approximately equal bins, then plotted the percentage of lake years in each bin that had DO anomalies < -0.2 mg/L, between -0.2 and 0.2 mg/L, and > 0.2 mg/L. Through this analysis, we aimed to assess the magnitude of the effect that increasing air temperatures can have in driving interannual variability of DO.

Text S8.2: Results

Across all lakes, spring air temperatures tended to be positively correlated with mean hypolimnetic temperature and VHOD, and negatively correlated with late-summer hypolimnetic DO (Figure S8.1). One-way ANOVA tests indicated significant differences in the distribution of correlations between months of air temperature data for all four variables (Table S8.1). Tukey post-hoc tests identified the northern hemisphere's March and April, and the southern hemisphere's September and October air temperatures as the months that were most strongly correlated with all three variables.

Analyzing across 477 lakes with available data, spring air temperature anomalies tended to be negatively correlated with hypolimnetic DO anomalies (Figure S8.2). Warm spring air temperatures (positive anomalies) were twice as likely to result in low hypolimnetic DO (negative anomalies) rather than high hypolimnetic DO (positive anomalies; Figure S8.2).

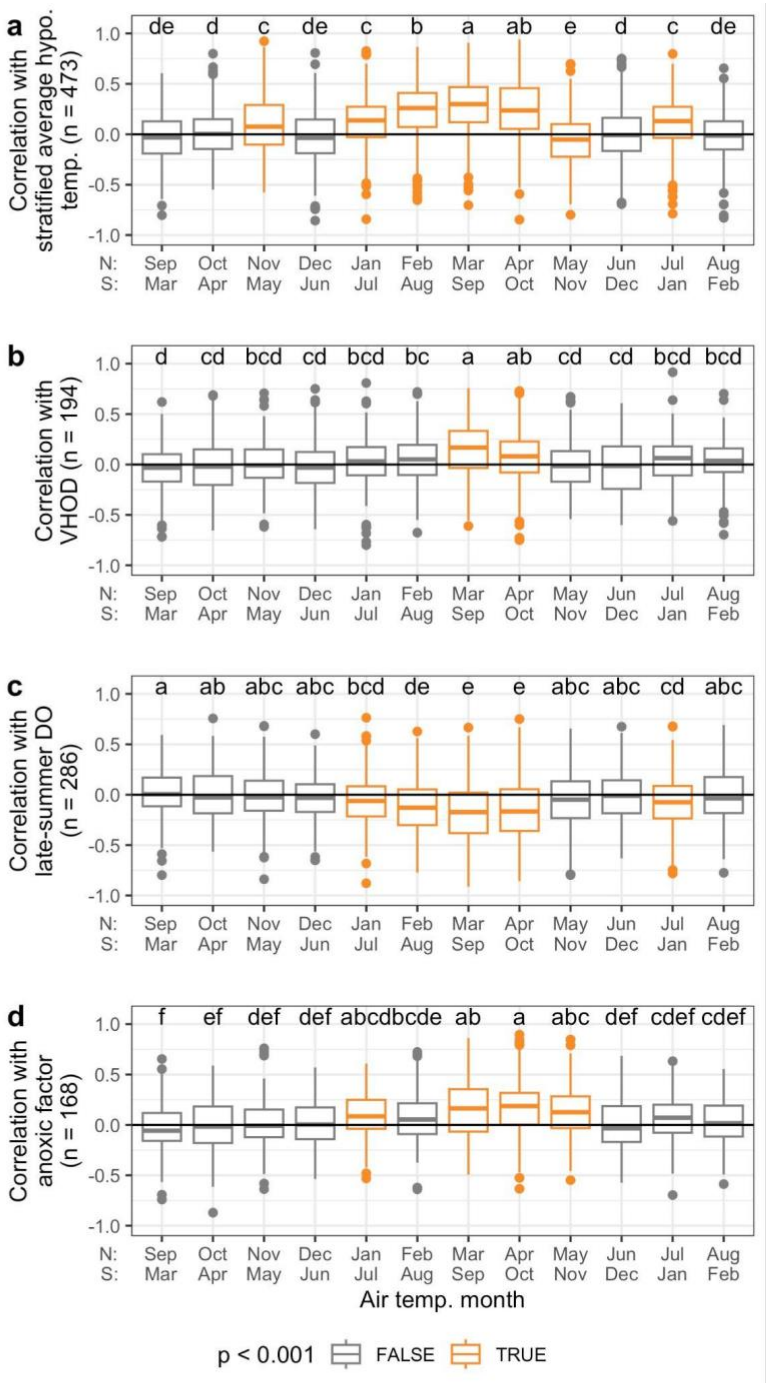

Figure S8.1: Across all lakes, spring air temperatures tended to be positively correlated with hypolimnetic temperatures (a), positively correlated with volume-weighted hypolimnetic oxygen demand (VHOD; b), negatively correlated with late-summer hypolimnetic dissolved oxygen (DO) concentrations (c), and positively correlated with

Anoxic Factor (AF; d). Here, each data point indicates the partial spearman's correlation between monthly air temperature and the specified variable (hypolimnetic temperature, VHOD, DO, or AF) while accounting for measurement year. Correlations are calculated on an annual time step over the entire time series at a given lake (number of lakes given in y axis title). Boxplot color indicates whether the distribution of correlations across all lakes is significantly different than zero (Wilcox test; $p < 0.001$). Letters above each boxplot delineate months with significantly distinct distributions (Tukey post hoc tests; $p < 0.05$). X-axis text indicates the air temperature month in either the Northern (N) or Southern (S) Hemisphere.

Table S8.1: ANOVA results describing differences in the across-lake distribution of correlations between monthly air temperature data and three focal variables. Tukey post hoc test results are presented in Figure S1.

Variable	*n* (lakes)	*df*	*F*	*p*
Hypolimnetic temperature (stratified period)	473	11	102.9	**<0.001**
Oxygen demand	194	11	8.358	**<0.001**
Late-summer DO	286	11	16.14	**<0.001**
Anoxic factor	168	11	10.56	**<0.001**

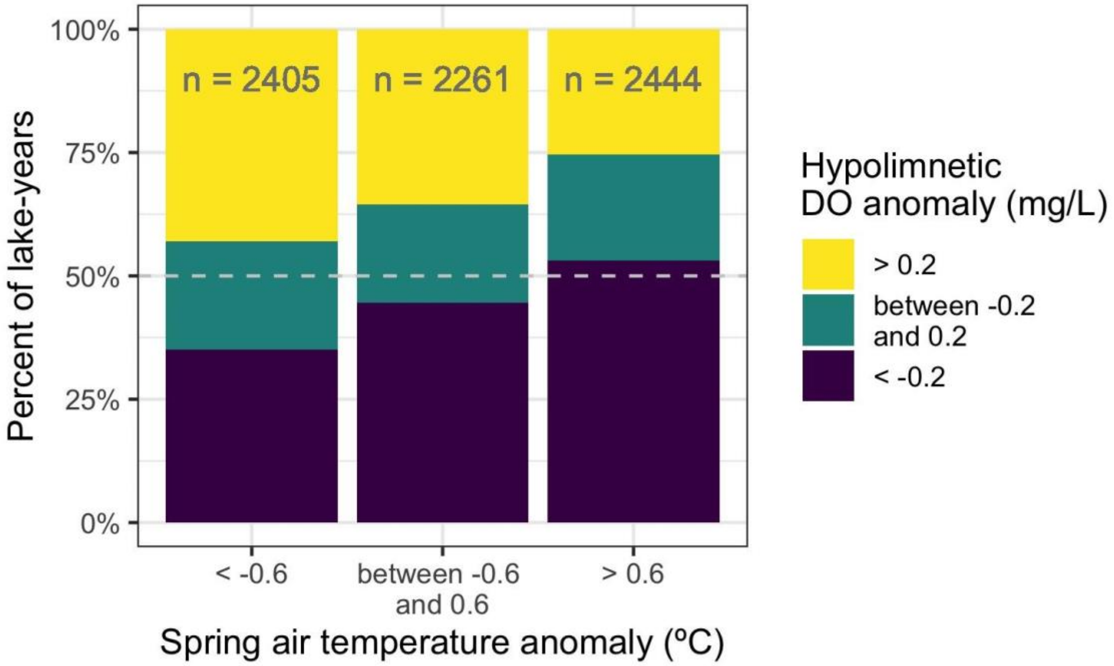

Figure S8.2: Using data available for 436 lakes, lake-years with positive spring air temperature anomalies were more likely to have negative hypolimnetic dissolved oxygen (DO) anomalies. Here, spring air temperatures are the mean air temperature combined across March and April (northern hemisphere) or September and October (southern hemisphere). Anomalies are calculated across all years at a given lake. The number of lake-years in each air temperature bracket is indicated at the top of the bar.

Appendix S9: First year of anoxia

Contents

This document provides one figure describing oxygen concentrations before and after the first year of anoxia (Figure S9.1).

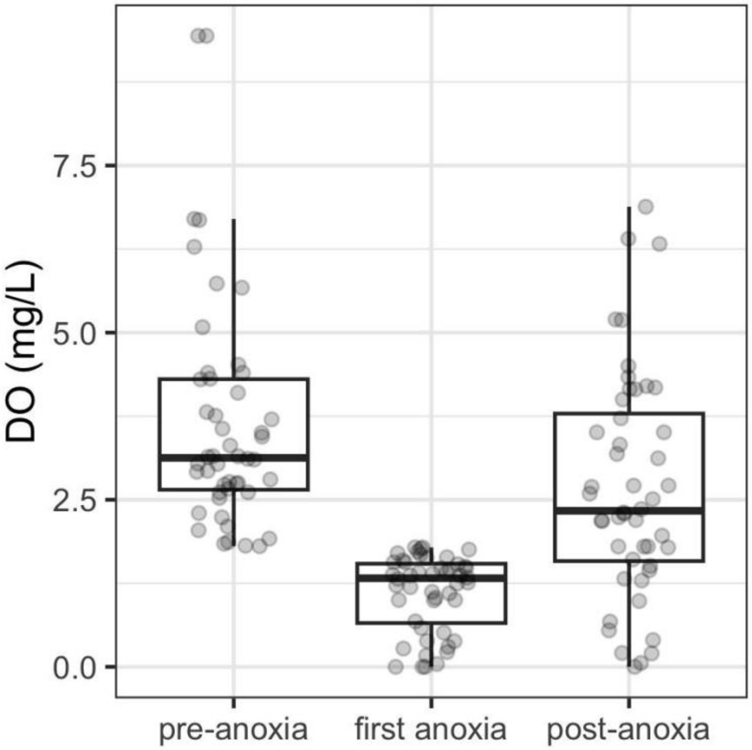

Figure S9.1: Oxygen concentrations tended to be lower in the year following the onset of anoxia (1.8 mg/L) than in the year prior to the first occurrence of anoxia. Here each point represents one lake. Only lakes with data for consecutive years of DO > 1.8 mg/L, DO < 1.8 mg/L, and the following year are presented (*n* = 48 lakes). All differences between groups are significant with $p < 0.01$ (two-way ANOVA based on oxygen status and lake ID; Tukey post hoc test).

Appendix S10: Temperature-corrected oxygen demand

Contents

This document provides text description of the driver analysis results for volume-weighted hypolimnetic oxygen demand standardized to 10ºC (Text S10.1), along with a supporting figure (Figure S10.1) and table (Table S10.1).

Text S10.1

Of the proposed explanatory variables for $\text{VHOD}_{\text{std 10ºC}}$ (Table S10.1), three model formulations were statistically similar:

1. Epi. chl-a (t-1): AICc = 2671
2. Epi. chl-a (t-1) + epi. chl-a: AICc = 2671
3. Epi. chl-a (t-1) + epi. chl-a + maximum buoyancy frequency: AICc = 2672

We used the third model for the analyses below, though we note that all model formulations indicated a positive effect of epi. chl-a on $\text{VHOD}_{\text{std 10ºC}}$. Using this model, both across-lake mixed model analyses and within-lake regressions indicated that chl-a had a positive effect on VHOD (Figure S10.1). For the mixed model analysis, standard deviation of the random effect for lake ID was 0.68 and standard deviation of the residuals was 0.67.

Table S10.1: Proposed explanatory variables for $\mathrm{VHOD}_{\mathrm{std}\ 10^{\circ}\mathrm{C}}$

Response variable	Proposed explanatory variables	Time period	Motivation for inclusion
$\mathrm{VHOD}_{\mathrm{std}\ 10^{\circ}\mathrm{C}}$	Epi. chl-a	Stratified	ABA cycle
	Epi. chl-a (t-1)	Stratified	ABA cycle
	Hypolimnetic temp.	Stratified	Temperature-dependence of respiration
	Hypo. DOC	Stratified	Organic matter for water-column mineralization
	Maximum buoyancy frequency	Late summer	Diffusion

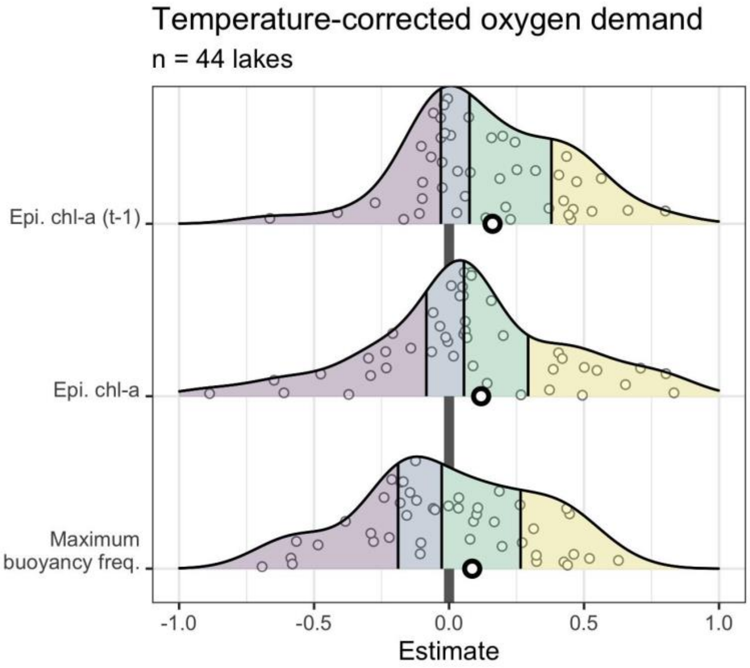

Figure S10.1: Chlorophyll-a tended to have a positive effect on VHOD$_{\text{std }10^{o}}$. Here, y-axis labels indicate explanatory variables. Individual points represent regression coefficients from within one lake. Density distributions describe the distribution of parameter values across lakes, with colors delineating the quartiles of the distribution (purple: 0-25%, blue: 25-50%, green: 50-75%, and yellow: 75-100%). Black and white circles at the bottom of each distribution mark the parameter estimate from the mixed model analysis. The gray vertical line denotes a parameter estimate of zero.

Appendix S11: Epilimnetic total phosphorus

Contents

This document provides two figures to describe the relationship between TP concentrations and chlorophyll-a in greater detail (Figures S11.1, S11.2).

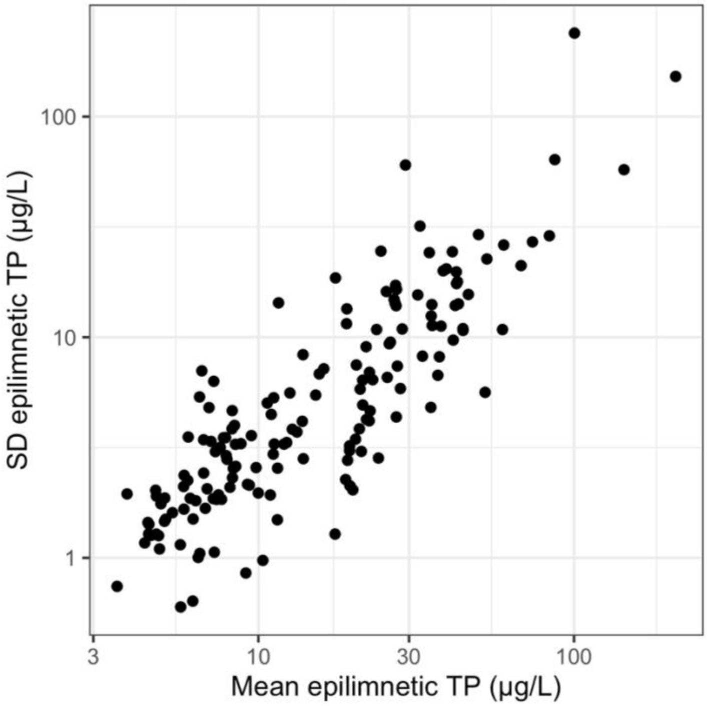

Figure S11.1: Lakes with high mean epilimnetic total phosphorus (epi. TP) tended to also have high variability (standard deviation; SD) in epi. TP concentrations. Here, each point represents one lake.

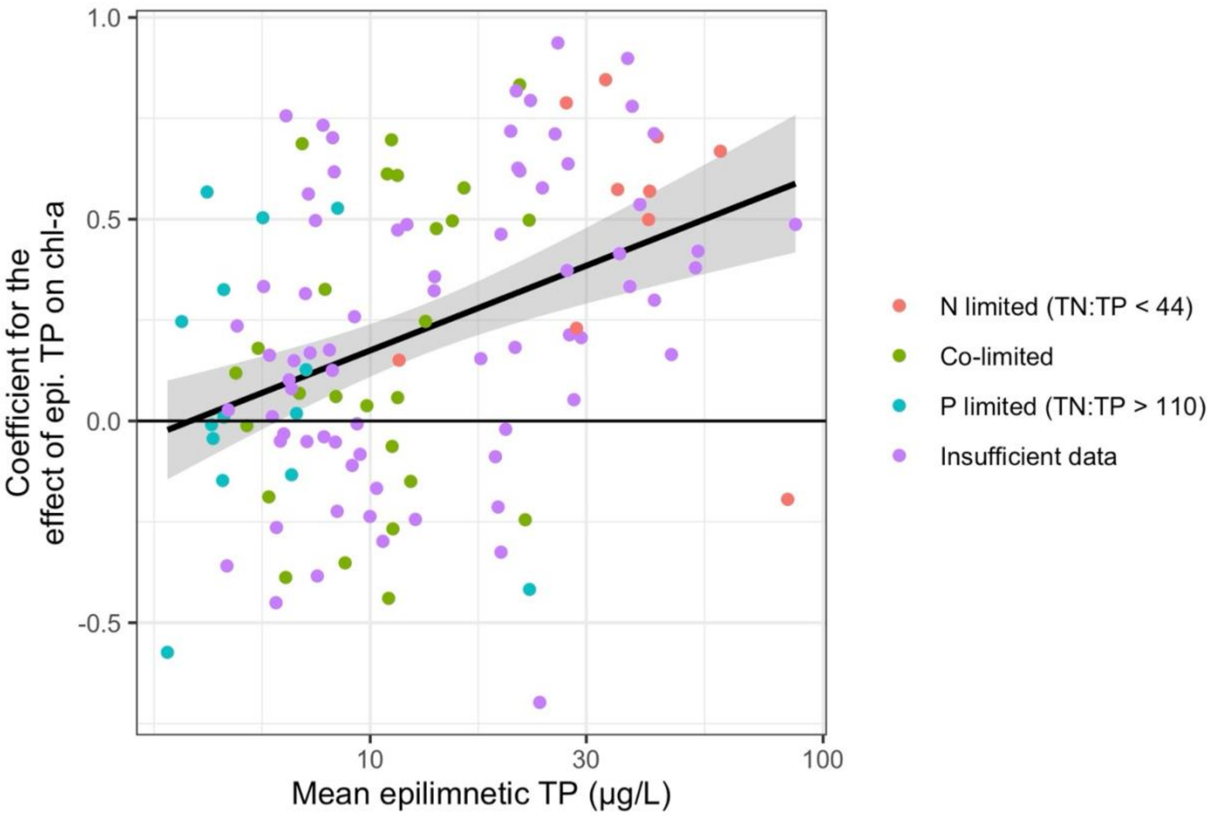

Figure S11.2: Lakes with low mean epilimnetic total phosphorus (TP) concentrations tended to have molar total nitrogen (TN) to total phosphorus (TP) ratios indicative of P limitation, though these lakes also showed the smallest effect of epilimnetic (epi.) TP on chlorophyll-a (chl-a). Molar ratios indicative of TN and TP limitation are drawn from Elser et al. (2009), following Lewis et al. (2020).

References

Elser, J. J., M. E. S. Bracken, E. E. Cleland, and others. 2007. Global analysis of nitrogen and phosphorus limitation of primary producers in freshwater, marine and terrestrial ecosystems. Ecology Letters **10**: 1135–1142. doi:10.1111/j.1461-0248.2007.01113.x

Lewis, A. S. L., B. S. Kim, H. L. Edwards, and others. 2020. Prevalence of phytoplankton limitation by both nitrogen and phosphorus related to nutrient stoichiometry, land use, and primary producer biomass across the northeastern United States. Inland Waters 1–9. doi:10.1080/20442041.2019.1664233

Chapter IV: Effects of hypoxia on coupled carbon and iron cycling differ between weekly and multiannual timescales in two freshwater reservoirs

Abigail S. L. Lewis[1], Madeline E. Schreiber[2], B. R. Niederlehner[1], Arpita Das[1], Nicholas W. Hammond[2], Mary E. Lofton[1], Heather L. Wander[1], Cayelan C. Carey[1]

[1] Department of Biological Sciences, Virginia Tech, Blacksburg, Virginia, USA

[2] Department of Geosciences, Virginia Tech, Blacksburg, Virginia, USA

Published in *Journal of Geophysical Research: Biogeosciences* with the citation:

Lewis, A. S. L., Schreiber, M. E., Niederlehner, B. R., Das, A., Hammond, N. W., Lofton, M. E., et al. (2023). Effects of hypoxia on coupled carbon and iron cycling differ between weekly and multiannual timescales in two freshwater reservoirs. Journal of Geophysical Research: Biogeosciences, 128, e2022JG007071. https://doi.org/10.1029/2022JG007071

Key Points

- A substantial fraction of sediment organic carbon (~30%) was bound to iron in two freshwater reservoirs
- Short-term (2–3 week) periods of hypoxia decreased iron-bound organic carbon and total organic carbon in reservoir sediments
- Multiannual periods of hypoxia increased total organic carbon in sediment, likely through decreased rates of respiration

Abstract

Freshwater lakes and reservoirs play a disproportionate role in the global organic carbon (OC) budget, as active sites for carbon processing and burial. Associations between OC and iron (Fe) are hypothesized to contribute substantially to the stabilization of OC in sediment, but the magnitude of freshwater Fe-OC complexation remains unresolved. Moreover, global declines in bottom-water oxygen concentrations have the potential to alter OC and Fe cycles in multiple ways, and the net effects of low-oxygen (hypoxic) conditions on OC and Fe are poorly characterized. Here, we measured the pool of Fe-bound OC (Fe-OC) in surficial sediments from two eutrophic reservoirs, and we paired whole-ecosystem experiments with sediment incubations to determine the effects of hypoxia on OC and Fe cycling over multiple timescales. Our experiments demonstrated that short (2–4 week) periods of hypoxia can increase aqueous Fe and OC concentrations while decreasing OC and Fe-OC in surficial sediment by 30%. However, exposure to seasonal hypoxia over multiple years was associated with a 57% increase in sediment OC and no change in sediment Fe-OC. These results suggest that the large

sediment Fe-OC pool (~30% of sediment OC in both reservoirs) contains both oxygen-sensitive and oxygen-insensitive fractions, and over multiannual timescales OC respiration rates may play a more important role in in determining the effect of hypoxia on sediment OC than Fe-OC dissociation. Consequently, we anticipate that global declines in oxygen concentrations will alter OC and Fe cycling, with the direction and magnitude of effects dependent upon the duration of hypoxia.

Plain Language Summary

Freshwater lakes and reservoirs (hereafter: lakes) play a remarkably important role in the global carbon cycle, as important sites for both carbon sequestration and greenhouse gas emissions. The extent to which lakes sequester carbon vs. release greenhouse gases depends upon many factors, including associations between carbon and iron that can help to preserve carbon in sediment. However, global declines in freshwater oxygen concentrations have the potential to affect these chemical complexes. Here, we added oxygen to the bottom waters of a lake to test how changes in oxygen concentration affect carbon and iron cycling. We found that over short timescales (weeks), low oxygen conditions decreased the amount of carbon in sediment by breaking apart associations between iron and carbon that help retain carbon in sediment. However, over long timescales (years), low oxygen conditions appeared to *increase* carbon burial by decreasing the rate at which carbon inputs were decomposed. These results suggest that declining oxygen concentrations in lakes around the world may have important effects on global carbon cycling, with the direction and magnitude of the impact depending on the duration of low oxygen conditions.

1. Introduction

Freshwater lakes and reservoirs are increasingly recognized as hotspots in the global carbon cycle (Bastviken et al., 2011; Battin et al., 2009; Carey, Hanson, et al., 2022; Raymond et al., 2013; Tranvik et al., 2018). Due to high organic carbon (OC) loading from the surrounding watershed, lakes and reservoirs likely bury more OC than coastal sediments each year (Dean & Gorham, 1998; Knoll et al., 2013; Mendonça et al., 2017; Pacheco et al., 2014; USGCRP 2018). Much of this OC remains sequestered in the sediments, especially in reservoirs, which may bury organic carbon at over six times higher rates than natural lakes (per unit area; Mendonça et al. 2017). However, OC inputs can also be respired to carbon dioxide and methane, making lakes and reservoirs a source of greenhouse gas emissions equivalent to 20% of the global emissions from fossil fuels (Deemer et al., 2016; DelSontro et al., 2018). The balance between carbon burial and emission in freshwater systems is controlled by numerous factors, notably including associations between OC and iron (Fe). To refine global carbon budgets and manage water resources in a changing world, it is critically important to quantify the role of Fe in OC cycling in lakes and reservoirs against the backdrop of rapidly-changing environmental conditions.

Recent research suggests that associations between OC and iron (Fe) may play a critical role in OC sequestration, though the importance of Fe in freshwater OC dynamics is currently unresolved. Fe can promote OC stability through multiple mechanisms, including occlusion of OC in aggregates, which can result in physical inaccessibility to microbial degradation and subsequent burial of OC in deeper soil or sediment horizons (Kleber et al., 2015 and references therein). Consequently, protection of OC through complexation with Fe may facilitate OC sequestration over decades to millennia (Kleber et al., 2015; Lalonde et al., 2012 and references therein). To date, most research on OC-Fe cycling has focused on terrestrial and marine environments, where it has been shown that Fe-OC complexation can serve as an important mechanism for stabilizing OC, the so-called “rusty carbon sink” (e.g., Barber et al. 2017; Hemingway et al., 2019; Kramer & Chadwick, 2018; Lalonde et al., 2012). In contrast to terrestrial and marine ecosystems, only a few studies have explicitly examined Fe-OC in freshwater lakes and reservoirs. Peter and Sobek (2018) analyzed Fe-OC in surficial sediment from five boreal lakes that spanned a gradient of oxygen conditions and found that less than 11% of sediment OC was bound to Fe, in comparison with ~20% across a range of primarily marine sediments (Lalonde et al., 2012). Furthermore, Peter and Sobek (2018) found no association between Fe-OC content in sediment and oxygen in overlying water when comparing across lakes. However, it should be noted that the lakes in that study were particularly high in dissolved OC (DOC) concentrations (9–42 mg/L DOC) and may not be representative of all freshwater ecosystems. Bai et al. (2021) studied Fe-OC along a salinity gradient in a subtropical tidal wetland and similarly found that freshwater areas had lower levels of sediment Fe-OC (18% of sediment OC in freshwater and 29% in saltwater), but these results were attributed primarily to wetland plant characteristics, which may not be relevant in the bottom waters of lakes and reservoirs. Differences in sediment Fe-OC between freshwater and saltwater environments may be expected based on water column characteristics, as increasing ionic strength can increase aggregation and flocculation of Fe, with differential effects depending on the quantity and quality of organic matter (Heerah and Reader, 2022; Beauvois et al. 2021; Herzog et al. 2020).

Despite limited research on Fe-OC in freshwater sediments, there are multiple reasons to expect that Fe may play an important role in OC sequestration in some freshwater ecosystems. Concentrations of Fe and DOC are strongly correlated in many freshwaters (Björnerås et al., 2017; von Wachenfeldt et al., 2008; Weyhenmeyer et al., 2014), and aqueous Fe concentrations are correlated with sediment OC accumulation in boreal lakes (Einola et al., 2011). Moreover, it is well-documented that DOC can be released from lake sediments under low-oxygen conditions, and this sediment flux is often attributed to reductive dissolution of Fe(III) (Brothers et al., 2014; Yang et al. 2014; Kim & Kim, 2020; Lau & del Giorgio, 2020; Peter et al., 2017). Still, few studies have examined whether reactions involving Fe-OC complexes are the driving force for observed correlations between dissolved Fe and OC (but see Peter et al. 2018). Furthermore, it remains unknown how the Fe-OC cycling occurring on sub-annual time scales may affect OC sequestration on the multi-annual timescales relevant for global carbon budgets.

Over short timescales (days to weeks), Fe-bound OC (Fe-OC) complexes are sensitive to the redox conditions of the surrounding environment (Figure 1). Fe-OC complexes form under oxic conditions (Riedel et al., 2013), as Fe(III) is more effective at complexing with organic matter than Fe(II) (Nierop et al., 2002). Under hypoxic conditions (low oxygen, defined here as < 2 mg/L following, e.g., Yang et al. 2014), OC can be released from Fe-OC complexes through Fe(III) reduction and dissolution (e.g., Pan et al., 2016; Patzner et al., 2020; Skoog & Arias-Esquivel, 2009), which can either result directly from hypoxia or from redox-driven increases in pH that promote OC release (Kirk, 2004; Thompson et al., 2006). Given these conflicting patterns—i.e., that

Fe-OC complexes can be preserved over decades to millennia and yet may be unstable under the reducing conditions which commonly occur on day to month timescales in aquatic sediments—it remains unclear how changing oxygen dynamics will affect coupled OC and Fe cycling in freshwater ecosystems.

Currently, the duration of bottom-water hypoxia is increasing in many lakes and reservoirs around the world (Bartosiewicz et al., 2019; Jane et al., 2021; Jenny et al., 2016; Williamson et al., 2015), which could have varying consequences for OC sequestration (Figure 1). In many dimictic lakes and reservoirs, bottom-water hypoxia is interrupted by oxic conditions during spring mixing and fall turnover, resulting in dynamic oxygen conditions on the week to month scale. Combined, these short-term patterns sum to determine the net role of lakes and reservoirs in the global carbon cycle over multiannual timescales. Periods of hypoxia have the potential to decrease OC sequestration through reductive dissolution of Fe(III) in Fe-OC complexes (Chen et al., 2020; Huang et al., 2021; Patzner et al., 2020). However, hypoxia also has the potential to increase OC sequestration by decreasing the rate of OC respiration (Carey et al., 2018; Carey, Hanson, et al., 2022; Hargrave, 1969; Peter et al., 2017; Sobek et al., 2009; Walker & Snodgrass, 1986), particularly if Fe-OC complexes are resistant to, or protected from, changes in oxygen concentrations in overlying water. Decreased OC respiration rates under hypoxic conditions is thought to occur primarily because respiration is less thermodynamically favorable in the absence of oxygen (e.g., Arndt et al., 2013; LaRowe & Van Cappellen, 2011). Because reductive dissolution of Fe(III) in Fe-OC complexes and decreased OC respiration under hypoxic conditions would have divergent effects on total OC sequestration, understanding the relative importance of these two processes across multiple timescales is critical for predicting the effect of hypoxia on OC sequestration in the bottom waters of lakes and reservoirs (Figure 1).

Analyzing the complex effects of oxygen on coupled OC and Fe cycling requires multiple experimental approaches. Field surveys have been effective at identifying correlations between OC and Fe (Björnerås et al., 2017; von Wachenfeldt et al., 2008; Weyhenmeyer et al., 2014). However, these observational approaches have limited capacity for identifying causal relationships. Whole-ecosystem experiments may be highly effective at identifying real-world impacts of freshwater oxygen on Fe and OC dynamics, while allowing for important ecosystem-scale processes such as turbulence and external loading (Carpenter, 1996; Dzialowski et al., 2014; Schindler, 1998). However, high levels of variability on a whole-ecosystem scale may limit the detection of subtle changes in OC and Fe processing. Small-scale incubations may be particularly useful for identifying changes that result from hypoxia (i.e., increased DOC and Fe release from sediment, decreased levels of Fe-OC, changes in sediment OC). However, small-scale incubations are limited by fouling and changes in microbial communities, among other microcosm effects, and do not reflect the full suite of processes that interact to control OC and Fe cycling in lakes and reservoirs. Consequently, integrating multiple approaches can provide complementary information on Fe-OC dynamics across spatial and temporal scales and overcome the limitations of single-approach studies.

To analyze how hypoxia impacts OC and Fe cycling over multiple scales, this study paired whole-ecosystem oxygen manipulations with laboratory incubations. We had two objectives: (1) characterize Fe-OC (operationally defined as dithionite-extractable OC) levels in sediment of two iron-rich reservoirs, and (2) analyze how hypoxia affects coupled OC and Fe cycling over both short-term (2–4 week) and multiannual timescales. Through this work, we aimed to provide insight on how increasing prevalence and duration of hypoxia in lakes and reservoirs may affect the critical role of these ecosystems in the global carbon cycle.

2. Methods

2.1 Study Sites: Falling Creek and Beaverdam Reservoirs

Falling Creek Reservoir (FCR; 37.30ºN, 79.84ºW) and Beaverdam Reservoir (BVR; 37.31ºN, 79.81ºW) are small (FCR: 0.12 km^2, 9.3 m deep; BVR: 0.39 km^2, 11 m deep), eutrophic drinking water reservoirs located in southwestern Virginia, USA (Hounshell et al., 2021; Figure 2). Both reservoirs are located in deciduous forested catchments, and both are dimictic, with summer stratified periods that typically last from May to October. BVR is located 3 km upstream of FCR and serves as the primary inflow source for FCR. Fe levels are high in surface water and groundwater from this region as a result of weathering and erosion of Fe-rich metamorphic rocks (53,466 mg/kg dry weight in sediment; Krueger et al., 2020; Chapman et al., 2013; Woodward, 1932). The bedrock underlying both reservoirs is layered pyroxene granulite (Virginia Division of Mineral Resources, 2003), and the primary soil series in the reservoir catchments is Edneytown Loam (Soil Survey Staff). The Köppen-Geiger climate designation of this region is Cfa: humid subtropical climate (Kottek et al. 2006). Both reservoirs have been owned and operated for drinking water provision by the Western Virginia Water Authority (WVWA) since their construction (FCR: 1898, BVR: 1872; Gerling et al., 2016; Hamre et al., 2018).

A suite of variables are routinely sampled in FCR and BVR as part of a long-term monitoring program; all data analyzed in this manuscript are available in the Environmental Data Initiative (EDI) repository with detailed metadata (Carey, Lewis, McClure, et al., 2022; Carey, Wander, Howard, et al., 2022; Carey, Wander, McClure, et al., 2022; Lewis et al., 2022; Lewis, Schreiber, et al., 2022; Schreiber et al., 2022).

2.2 Whole-ecosystem oxygenation experiments

In 2012, FCR was equipped with a side-stream supersaturation hypolimnetic oxygenation (HOx) system to improve water quality in the reservoir (Gerling et al., 2014). This type of HOx system functions by withdrawing water from the bottom of the reservoir, adding concentrated, pressurized oxygen gas (95% purity) to supersaturate the water with dissolved oxygen (DO), and then returning the oxygenated water at the same depth and temperature. Previous work in FCR has shown that the HOx system effectively increases DO concentrations throughout the hypolimnion without altering temperature or decreasing thermal stability (see Gerling et al., 2014). From 2013–2019, the HOx system in FCR was operated at variable rates, maintaining an oxygenated hypolimnion for at least part of the summer (Carey, Thomas, et al., 2022). Conversely, oxygenation was reduced in 2020 and 2021, resulting in median hypolimnetic DO concentrations < 1 mg/L throughout the summer stratified period. To assess the effects of multiannual changes in oxygen availability on OC and Fe-OC in sediment, we compared sediment core and sedimentation trap data from summer 2019 (which had a history of high-oxygen conditions during the preceding six years) to summer 2021 (which followed a summer of hypoxic conditions in 2020; Figure S1). Sediment data were not collected in 2020 due to the Covid-19 pandemic.

To assess how short-term changes in hypolimnetic DO concentrations impact Fe-OC on a whole-ecosystem scale, we operated the HOx in FCR on a variable schedule throughout the summer of 2019 (Carey, Thomas, et al., 2022). Oxygen was added in approximately two-week intervals at a rate of 25 kg O_2 day^{-1} to the whole hypolimnion. Between oxygenation periods, we allowed the hypolimnion to become hypoxic over periods of at least two weeks without oxygenation. Because hypolimnetic volume varied throughout the summer (generally decreasing throughout the summer as the thermocline deepened), the mean concentration of oxygen added to the whole hypolimnion throughout an oxygenation period in 2019 ranged from 0.80 mg L^{-1} day^{-1} to 0.90 mg L^{-1} day^{-1}.

BVR does not have a HOx system and experiences seasonal hypoxia from May through November (Hounshell et al., 2021). Consequently, BVR serves as a reference ecosystem to analyze the effects of oxygenation in FCR.

2.2.1 Oxygen

We monitored DO concentrations throughout the full water column approximately two times per week in FCR and one time per week in BVR (Carey, Lewis, McClure, et al., 2022). High-resolution (~1 cm) depth profiles were taken using a conductivity, temperature, and depth profiler (CTD; Sea-Bird, Bellevue, Washington, USA) equipped with a DO sensor (SBE 43; Carey, Lewis, McClure, et al., 2022) from the reservoir’s surface to the sediments. We also measured dissolved oxygen using a YSI

ProODO DO probe when the CTD was not available due to maintenance (YSI Inc. Yellow Springs, Ohio, USA; Carey, Wander, McClure, et al., 2022). YSI measurements were taken at discrete 1 m depth intervals. For a comparison of YSI and CTD measurements, see Carey et al. (2022).

2.2.2 Hypolimnetic Fe and DOC

We collected water samples for DOC and Fe analysis at the deepest site in each reservoir with a 4-L Van Dorn sampler (Wildlife Supply Company, Yulee, FL, USA). Samples were collected once per week at seven depths in FCR (0.1, 1.6, 3.8, 5.0, 6.2, 8.0, and 9.0 m), which corresponded to the reservoir's extraction depths, and five depths in BVR (0.1, 3.0, 6.0, 9.0, and 11.0 m). In 2019, we conducted a limited amount of additional sampling in FCR on a second day each week, and these measurements included DOC from 0.1, 1.6, 5.0, and 9.0 m depths.

We analyzed DOC by filtering water samples through a 0.7-µm glass fiber filter into an acid-washed bottle, which was rinsed with the filtered water three times before sample collection. The filtered samples were frozen for less than six months before analysis on an OC analyzer (Elementar Vario TOC cube, following APHA standard method 5310B; American Public Health Association, 2018b).

We collected both total and dissolved (filtered through 0.45-µm filters) samples for Fe. Samples were preserved in the field using trace metal grade nitric acid and analyzed using ICP-MS (Thermo Electron X-Series, Waltham, MA, USA) following APHA Standard Method 3125-B (American Public Health Association, 2018a; Krueger et al., 2020; Munger et al., 2019; Schreiber et al., 2022).

2.2.3 Fe-OC in sediments

We analyzed the concentration of Fe-OC in surficial sediments from both FCR and BVR on multiple dates throughout the summer stratified periods of 2019 and 2021. In 2019, sediment cores in FCR were collected immediately before the HOx system was turned on or off, resulting in the most oxic or hypoxic conditions during that SSS activation or deactivation interval, respectively. Sediment cores at BVR were taken once in the middle of summer and once approximately two weeks before fall turnover in 2019. In 2021, sediment core samples were taken from both reservoirs on the same dates, approximately once per month. Additional sediment core samples were collected in March 2021, when both reservoirs were unstratified and had oxic hypolimnia.

On each sampling date, we collected four replicate hypolimnetic sediment cores using a K-B gravity sediment corer (Wildlife Supply Company, Yulee, FL, USA). Cores were collected in the deepest part of each reservoir, approximately 20 m from where water samples were taken. In 2019, each core was capped and kept on ice while transported back to the lab, where the top 1 centimeter of sediment from each core was immediately extruded, collected, and frozen in scintillation vials for future analysis. In 2021, cores were extruded in the field, and the samples were kept on ice while being transported back to the lab.

2.2.4 Sediment traps

To determine the amount of Fe-OC and total OC in samples of material settling from the water column (i.e., not estimate deposition rates), we deployed 19-L buckets approximately 1 m above the sediments at the deepest point of each reservoir (8 m at FCR and 10 m at BVR). These sediment traps were deployed from June–December 2021 and sampled every two weeks by slowly bringing the bucket to the surface, decanting and discarding water from the bucket, collecting up to 5 L of the remaining water and particulate matter, and transporting this material back to the lab on ice. Upon arriving at the lab, we allowed the particulates to settle for approximately 5 minutes before decanting and discarding as much water as possible and filling four 50-mL centrifuge tubes with the remaining material. The samples were centrifuged for 10 minutes at 3100 rpm, then combined into one vial and frozen for later analysis. No sediment traps were deployed for Fe-OC analysis in 2019.

2.3 Microcosm incubations

To isolate the effects of oxygen from other interacting factors that affect Fe and OC on a whole-ecosystem scale, we conducted six-week microcosm incubations using hypolimnetic sediment and water from FCR. Incubations were conducted in 177-mL glass jars with two-piece gasket-sealed lids (Verones brand; Figure S2), after extensive pilot testing revealed that these jars were highly effective at maintaining hypoxic conditions when sealed (DO concentrations < 0.5 mg/L in this experiment) and oxic conditions when uncapped. We started the experiment with 102 microcosms split evenly into oxic (uncapped) and hypoxic (capped) treatments. After two weeks (similar to the 2019 whole-ecosystem HOx manipulation), we switched the treatment of approximately half of the remaining microcosms, generating two additional oxygen regimes: hypoxic-to-oxic and oxic-to-hypoxic. Starting on week two, there were consequently a total of four oxygen regimes: hypoxic, oxic, hypoxic-to-oxic, and oxic-to-hypoxic.

To set up the experiment, we collected sediment and water from the deepest site in FCR on 30 June 2021, when the hypolimnetic DO concentrations were < 0.5 mg/L. Water was collected from 9 m depth using a Van Dorn sampler, and sediment was collected from the same location using an Ekman sampler. Samples were transported on ice back to the lab, then homogenized by stirring and shaking. We used a syringe to add the sediment slurry (20 mL) to each jar, then slowly added 150 mL of hypolimnetic water, making an effort to minimize sediment disturbance. We stored the microcosms in an unlit incubation chamber at 15 ºC for the duration of the experiment, which corresponded to warm, end-of-summer conditions in the hypolimnion of FCR (Carey, Lewis, McClure, et al., 2022).

2.3.1 Microcosm sampling

Microcosms were sampled destructively for DO, total and dissolved Fe, total and dissolved OC, pH, sediment OC, and sediment Fe-OC. For the continuous oxic and hypoxic treatments, we sampled 3–6 replicates two times per week for four weeks (6 replicates: days 2, 6, 9, 13; 3 replicates: days 16, 20, 23). We added additional sampling for the hypoxic-to-oxic and oxic-to-hypoxic treatments: these treatments were sampled for the first three days after switching the oxygen regime (days 14, 15, 16), twice the following week (days 20, 23), and one more time a total of four weeks from when treatments were switched (day 34), with three replicates analyzed per sampling event. All microcosms under a hypoxic treatment were sampled in an anaerobic chamber which maintained mean ambient oxygen conditions <200 ppm (Coy Laboratory, Grass Lake, MI, USA) to reduce oxygen exposure during sampling.

To begin sampling a microcosm, DO was measured using a YSI DO probe. While measuring DO, we used the probe to gently swirl the water in the microcosm, homogenizing the water sample while minimizing sediment disturbance. Next, we used an acid-washed syringe to withdraw 30 mL of water for total OC (TOC), 13 mL for total Fe, 30 mL of water for DOC, and 13 mL for dissolved Fe analyses. DOC samples were filtered through a 0.7-µm glass fiber filter, and dissolved Fe samples were filtered through 0.45-µm filters. After taking samples for Fe and DOC, we withdrew as much water as possible without disturbing the sediment and measured pH from this sample in a separate container using an Ohaus Starter 300 pH probe (Parsippany, NJ, USA). Finally, we swirled the sediment with remaining water (approximately 1–5 mL) and poured this mixture into a 20 mL glass EPA vial, which we then froze for Fe-OC analysis. Hypoxic microcosms were stored in the anaerobic chamber for approximately two hours before analysis to ensure oxygen concentrations in the chamber were sufficiently low before opening the jars. Oxic microcosms were sampled immediately after removal from the incubator.

All microcosm samples were analyzed following standard methods. We stored TOC and DOC samples in bottles that had been acid-washed and rinsed three times with the sample water. All DOC and TOC samples were frozen for <6 months prior to analysis on an OC analyzer (Elementar Vario TOC cube, following Standard Method 5310B; American Public Health Association, 2018b) Fe samples were preserved using trace metal grade nitric acid and analyzed using the ferrozine method (Gibbs, 1979). We also analyzed Fe samples from days 16 and 23 using inductively coupled plasma mass spectrometry (ICP-MS). All microcosm data are published with complete metadata in the Environmental Data Initiative repository (Lewis et al., 2022).

2.4 Fe-OC analysis

We analyzed the amount of Fe-OC in both the whole-ecosystem and microcosm sediment samples using the citrate bicarbonate dithionite (CBD) method (Figure S3). This method was first described for marine systems by Lalonde et al. (2012) and has since been adapted for freshwater lakes by Peter and Sobek (2018). It is important to note that our measurement of Fe-OC as the percentage of OC that is extractable using the CBD method is an operational definition (Fisher et al., 2021). CBD extractions have documented inefficiencies when extracting crystalline hematite (Thompson et al. 2019; Adhikiri & Yang, 2015) and carboxyl-rich compounds (Fisher et al. 2020). While Fe is the primary reducible metal that associates with OC, other metals, including aluminum (Al) and calcium (Ca), may also release OC during CBD extractions. However, previous work in soils found that CBD-extracted aluminum was approximately an order of magnitude lower than CBD-extracted Fe, and therefore quantitatively much less important (Sondheim and Standish, 1983). Moreover, we found that Fe was present in much (≥ 5 times) higher quantities than Al and Ca in water samples across all of our sediment incubation treatments (Lewis et al., 2022), further justifying our use of the operational term Fe-OC. We used the CBD method to enable comparisons both between oxygen treatments and with other published work that used the same general approach (e.g., Lalonde et al., 2012; Peter & Sobek, 2018).

Following the CBD method, each sediment sample was freeze-dried and divided into three treatments: initial, reduction, and control (Figure S3). “Initial” samples received no treatment and were used to measure the OC content of the sediment. “Reduction” samples were treated with a metal-complexing agent (trisodium citrate) and reducing agent (sodium dithionite) in a buffered solution (sodium bicarbonate) to measure how much Fe and OC were released as a result of Fe reduction. Control samples were used to account for the release of OC in the reduction treatment that resulted from processes other than Fe reduction. They were treated with the same buffer (sodium bicarbonate) and sodium chloride in the same ionic strength as the trisodium citrate and sodium dithionite of the reduction treatment.

For both the control and reduction treatments, we measured 100 mg of homogenized, freeze-dried sediment into 15-mL polypropylene centrifuge tubes (Falcon Blue, Corning Inc., Corning, NY, USA). We then added 6 mL of either control or reduction buffer solution (0.11 M sodium bicarbonate) to each tube. The reduction buffer contained 0.27 M trisodium citrate, while the control buffer contained 1.6 M sodium chloride. After heating samples to 80ºC in an oven, 0.1 g sodium dithionite was added to the reduction samples and 0.088 g sodium chloride was added to control samples. Samples were kept at 80ºC for an additional 15 min, then centrifuged for 10 min at 3100 RPM. The supernatant was discarded. This extraction process was repeated two more times for both treatments, resuspending the sediment pellet each time by vortexing with buffer solution (Peter and Sobek, 2018).

Following the extraction step, samples were rinsed three times using OC- and Fe-free artificial lake water. Artificial lake water was prepared by diluting Artificial Hard

Water from Marking and Dawson (1973) to 12.5% with Type I reagent grade water. We added 3 mL of artificial lake water to each tube and resuspended the sediment pellet using a vortex. Samples were then centrifuged for 10 min at 3100 RPM, and the supernatant was discarded.

After extraction and rinsing, all sediment samples (including those in the initial treatment) were dried and acid-fumigated for 48 hours to remove remaining citrate and bicarbonate (Harris et al., 2001). Samples were then run on a CN analyzer (Elementar VarioMax, Ronkonkoma, NY, USA) to determine the amount of OC per unit mass of sediment. In these calculations, we adjusted sediment mass to account for Fe loss during control and reduction treatments (Lewis et al., 2022; Lewis, Schreiber et al., 2022; Peter and Sobek, 2018; Text S1). The amount of OC removed with Fe reduction (CBD-extractable OC) was calculated as the difference between the OC content of the control and reduction samples and expressed as a percentage of the initial OC content of the sediment.

2.5 Data analysis

All analyses were performed in R (version 4.0.3; R core team 2020) using packages tidyverse (Wickham et al., 2019), lubridate (Grolemund & Wickham, 2011), ggpubr (Kassambara, 2020), egg (Auguie, 2019), rstatix (Kassambara, 2021), akima (Akima et al., 2022), colorRamps (Keitt, 2022), rLakeAnalyzer (Winslow et al., 2019), and tseries (Trapletti et al., 2022). All novel analysis code is archived as a Zenodo repository (Lewis, 2022).

2.5.1 Sediment Fe-OC characterization

We calculated summary statistics to describe iron-bound organic carbon and total organic carbon in surficial sediment (2019 and 2021) and settling particulate material (2021 only) across both reservoirs. We then pooled data from both reservoirs to analyze the difference between settling material and surficial sediments using Welch's t-tests. Because data were unavailable for settling material in 2019, the comparison of settling material to surficial sediment was limited to 2021 data only.

2.5.2 Whole-ecosystem experiments: short-term responses

We used Welch's t-tests to assess whether sediment properties differed between the two-week periods of HOx activation compared to HOx deactivation during summer 2019 in FCR. Sediment time series did not exhibit significant temporal autocorrelation, justifying this approach (Lewis, Schreiber, et al., 2022).

To qualitatively assess whether oxygenation experiments led to differences in water column chemistry, we overlayed plots of DOC and Fe from the deepest sampling depth in each reservoir with dissolved oxygen at the same depths throughout the summer stratified period of 2019.

2.5.3 Whole-ecosystem experiments: interannual differences

We assessed whether there were significant differences in sediment properties among the four reservoir-years—BVR in 2019 (hypoxic), BVR in 2021 (hypoxic), FCR in 2019 (oxic) and FCR in 2021 (hypoxic). First, we used Levene tests to assess homogeneity of variance among reservoir-years (Table S1). While Fe-OC (both per unit sediment and as a percentage of sediment OC) met the ANOVA assumption of homogeneous variance, total sediment OC did not. Consequently, we used one-way ANOVAs and Tukey post hoc tests for Fe-OC metrics but used Welch one-way ANOVAs and Games-Howell post-hoc tests, both of which account for unequal variances, for sediment OC (Tables S2 and S3).

2.5.4 Microcosm incubations

We used one-way ANOVAs and Tukey post-hoc tests to assess whether sediment properties differed between microcosm treatments, after testing for homogeneity of variance using Levene tests (Table S4). For this analysis, we used data from days 20 and 23 (pooled together because replicates were sampled destructively), as these were the final days when data were available for all treatments.

Equilibrium speciation-solubility calculations were conducted for day 23 of the microcosm experiments using the Spece8 module of Geochemists' Workbench (GWB; Aquatic Solutions LLC, Champaign, IL, USA) and the wateq4f thermodynamic database (Ball & Nordstrom, 1991). The goal of the calculations was to assess the predicted speciation of Fe in the presence of OC under the environmental conditions of each microcosm treatment (following Oyewumi & Schreiber, 2017). Environmental conditions considered in this analysis included pH, DO, temperature, DOC, major cations (Ca, Na, K), Fe, and major anions (Cl, SO_4; bicarbonate was not measured so we calculated bicarbonate concentrations via charge balance). Data for major cations and anions were drawn from ICP-MS analyses (described in 2.3.1 Microcosm sampling). We assumed that

DOC consisted primarily of humic acids (operationally defined within the wateq4f database) for the calculations.

3. Results

3.1 Fe-OC comprised a substantial portion of sediment OC and a smaller proportion of OC in settling particulate matter

A substantial proportion of sediment OC was associated with Fe in both FCR and BVR. In FCR (averaged across 2019 and 2021), one gram of surficial sediment contained a mean of 481 µmol Fe-OC (±138, 1 SD), 31±8% of the total sediment OC pool (n=30). BVR had slightly lower Fe-OC than FCR on average, and one gram of surficial sediment contained a mean of 418±121 µmol Fe-OC, 24±7% of the total sediment OC pool (n=20). Total OC comprised 9±3% of sediment mass in FCR and 10±1% of sediment mass in BVR.

Levels of Fe-OC, both as a fraction of sediment mass and as a fraction of total sediment OC, were significantly higher in sediment core samples than in settling material collected in hypolimnetic traps (Figure 3). In 2021, averaged across both reservoirs, one gram of the hypolimnetic surficial sediments contained a mean of 443±133 µmol of Fe-OC (n=28), 69% higher than settling material collected in the traps, which contained a mean of 262±143 µmol Fe-OC (n=17; t_{32}=-4.24, p<0.001; Figure 3a). A mean of 24±6% of the total sediment OC pool was bound to Fe in sediments (n=28), while only 9±4% of sediment OC was bound to Fe in settling material (n=17; t_{43}=-10.44, p<0.001; Figure 3c). Total OC was 60% higher in settling material (µ=16.5±3.3) than in surficial sediments (µ=10.3±1.6; t_{20}=7.33, p<0.001; Figure 3b).

3.2 Short-term hypoxia decreased sediment OC and Fe-OC on a whole-ecosystem scale

Intermittent activation of the HOx in FCR in 2019 was associated with substantial changes in sediment characteristics. The amount of Fe-OC per g sediment was 30% lower during hypoxic ($\mu=394\pm173$, n=9) compared to oxic ($\mu=560\pm70$, n=7) periods in 2019 ($t_{11}=-2.6$, p=0.02; Figure 4b). Likewise, the total amount of OC (as a percentage of sediment mass) decreased by 30% during hypoxic ($\mu=6.0\pm1.55$, n=11) compared to oxic periods ($\mu=8.5\pm0.8$, n=7; $t_{15}=-4.6$, $p<0.001$; Figure 4b). Fe-OC as a percentage of total sediment OC did not significantly change with variation in oxygen during these experiments (oxic: $\mu=36.7\pm3.8$, n=7; hypoxic: $\mu=35.7\pm7.9$, n=9; $t_{12}=-0.3$, p=0.747; Figure 4c).

In the hypolimnion of FCR, total Fe concentrations tended to increase as oxygen decreased and decrease as oxygen increased (Figure 5b). Consequently, Fe concentrations were generally lower in FCR compared to the unoxygenated reference reservoir (BVR) in 2019. Trends in DOC were more variable, though DOC concentrations were typically highest when oxygen concentrations were low in FCR (Figure 5).

3.3 Multiannual hypoxia was associated with increased sediment OC

Activation of the oxygenation system increased summer hypolimnetic DO concentrations in FCR from 2014 through 2019, and lower oxygen addition rates allowed for primarily hypoxic conditions in 2020 and 2021 (Figure S1). BVR exhibited summer hypolimnetic hypoxia throughout the duration of the study (Figure S1).

In FCR, the amount of OC in surficial sediment increased by 57% as DO concentrations decreased from 2019 to 2021 (Figure 6b; Table S1, S2). Consequently, total OC was lower in FCR than BVR in 2019, but not in 2021 (Figure 6b; Table S1, S2). However, the amount of Fe-OC per gram of sediment did not change (Figure 6a; Table S1). As a result, the percentage of sediment OC that was bound to Fe decreased from 2019 to 2021 in FCR (Figure 6c; Table S1, S3). None of these three sediment characteristics differed between 2019 and 2021 in BVR (Figure 6d–f; Table S1, S2, S3).

3.4 Experimental microcosm incubations revealed rapid effects of hypoxia on Fe and OC

Experimental microcosm incubations successfully established four distinct oxygen regimes. DO concentrations increased rapidly when hypoxic microcosms were unsealed and decreased rapidly when microcosms were sealed (Figure 7). At the transition from hypoxic-to-oxic conditions, DO concentrations increased to approximately the same level as the continuous oxygen treatment (~7 mg/L) within one day. At the transition from oxic-to-hypoxic conditions, DO concentrations decreased below 1 mg/L within one day and declined to 0 mg/L by the end of the experiment.

Changes in oxygen conditions were associated with clear but asynchronous changes in aqueous OC and Fe. As microcosms switched from hypoxic-to-oxic conditions, TOC, DOC, and total Fe decreased near synchronously, while dissolved Fe decreased below detection within one day of oxygen exposure. At the transition from oxic-to-hypoxic conditions, DOC and TOC rapidly increased to the same level as microcosms that had experienced continuous hypoxia (~10 mg/L; Figure 7). However, concentrations of both dissolved and total Fe only began to increase after three weeks of hypoxia (Figure 7). Measured DOC and TOC were strongly and linearly correlated, with DOC representing a mean of 96±14% of TOC (Figure S5); thus, we focus our discussion on DOC hereafter, but the same trends apply to TOC.

At the end of the experiment, sediment OC differed significantly among treatments (one-way ANOVA: $F_{3,20}=9.09$, $p<0.001$). Sediment OC was significantly higher in microcosms that started under oxic conditions (oxic: $\mu=4.6\pm0.3$, oxic-to-hypoxic: $\mu=4.5\pm0.3$) than microcosms that started under hypoxic conditions (hypoxic: $\mu=4.0\pm0.0$, hypoxic-to-oxic: $\mu=4.1\pm0.2$; Figure 8). Fe-OC did not differ significantly between treatments as a proportion of sediment mass ($F_{3,20}=0.51$, $p=0.683$) or as a proportion of sediment OC ($F_{3,20}=2.40$, $p=0.098$).

Speciation calculations (Table S5) based upon observed solution chemistry (Figure S6) suggest that oxygen conditions had primary control over Fe speciation, with a lesser impact on Fe-OC. The experiments that were maintained under hypoxic conditions had dominant Fe species of Fe(II), $FeHCO_3^+$, $FeCO_3$, and $FeSO_4$ (all of these species contained Fe in its reduced state, Fe(II)). For all of the microcosms that were exposed to oxygen at any time (hypoxic-to-oxic, oxic-to-hypoxic, oxic), the dominant Fe species were $Fe(OH)_3$, $Fe(OH)_2^+$, $Fe(OH)_4^-$, $FeOH_2^+$ and $FeHumate^+$ (all of these species contained Fe in the oxidized state, Fe(III)). pH remained circumneutral across all treatments (Figure S7). These results indicate that 1) exposure to oxic conditions at any time in the experiment shifted the dominant oxidation state to Fe(III); 2) under oxic conditions, and to a lesser extent, hypoxic conditions, Fe complexed with DOC.

4. Discussion

Results from our whole-ecosystem manipulations suggest that oxygen affects coupled OC and Fe cycling differently over short-term (weekly) compared to long-term (multiannual) timescales (Figure 9). Short periods of hypoxia decreased total OC and Fe-OC in surficial sediment and increased concentrations of DOC and Fe in overlying water, indicating that a portion of the sediment Fe-OC pool is sensitive to changes in oxygen. However, over longer timescales, low oxygen conditions in FCR from 2019–2021 were associated with a 57% increase in sediment OC, indicating that the effects of hypoxia on Fe-OC (i.e., dissociation of Fe-OC complexes) may be outweighed by decreases in respiration rates under hypoxic conditions. Microcosm incubations composed of slightly deeper sediment layers showed no significant change in sediment Fe-OC in response to hypoxia, suggesting that buried Fe-OC may be resistant to the effects of hypoxia. Notably, Fe-OC comprised nearly one-third of surficial sediment OC in both FCR and BVR—regardless of oxygen status—which is more than previously reported for freshwater lakes (Peter & Sobek, 2018). Below, we discuss short-term (section 4.1) and multiannual (section 4.2) results in the context of previous work, analyze net processing rates across the sediment-water interface (section 4.3), and discuss why Fe-OC levels may be higher in these reservoirs than other freshwater systems (section 4.4).

4.1 Short-term periods of hypoxia lead to release of Fe-protected OC and decrease total sediment OC

Both whole-ecosystem and microcosm experiments suggest that short-term periods (i.e., weeks) of hypoxia can dramatically alter OC and Fe cycling. Whole-ecosystem experiments revealed changes in hypolimnetic DOC and Fe, sediment OC, and sediment Fe-OC associated with water-column oxygenation (Figures 4, 5, 9), while microcosm incubations showed clear differences in aqueous Fe, and DOC and sediment OC among treatments (Figures 7, 8). The magnitude of these effects was substantial: on a whole-ecosystem scale, two weeks of hypoxic conditions decreased both sediment Fe-OC and total sediment OC by a mean of 30%. Declining Fe-OC and total OC in sediment, as well as concomitant increases in Fe and OC in overlying water, are consistent with the expectation that hypoxia causes reductive dissolution of Fe(III) in Fe-OC complexes, releasing soluble Fe and DOC on day to week scales (e.g., Carey et al., 2018; Pan et al., 2016; Patzner et al., 2020; Peter et al., 2016; Skoog & Arias-Esquivel, 2009; Figures 1, 9).

Our results contribute to an accumulating body of evidence that short-term fluctuations in oxygen concentrations have important effects on OC storage in soils and sediment. Previous research has shown that recently-formed Fe-OC associations may be particularly prone to hypoxic release, and reduction of Fe(III) in Fe-OC compounds can increase OC respiration rates during hypoxic conditions (Chen et al., 2020). As a result of these and other processes, periodic fluctuations in oxygen conditions may sustain or stimulate respiration rates relative to both constant oxic and constant hypoxic conditions

(Bastviken et al., 2004; Huang et al., 2021). Furthermore, while OC released from Fe is likely to be aromatic and therefore potentially resistant to respiration (e.g., Riedel et al., 2013), this OC is susceptible to photo-oxidation upon release as DOC to the water column. Here, we found substantial decreases in sediment OC and Fe-OC following two weeks of hypoxia, with restored OC and Fe-OC after two weeks of oxic conditions (Figure 4, S3), suggesting that at least a fraction of the sediment Fe-OC pool is sensitive to short-term changes in oxygen concentrations in overlying water on a whole-ecosystem scale.

While sediment Fe-OC responded to oxygenation on a whole-ecosystem scale, Fe-OC did not vary significantly among oxygen treatments in experimental incubations, and observed changes in aqueous Fe and DOC in microcosms were asynchronous. These observations suggest that Fe may not be driving the observed oxygen-dependent changes in OC in microcosm sediments. We expect that this difference between microcosm and whole-ecosystem results may derive at least in part from the sediments we analyzed: whole-ecosystem samples were composed of the top 1 cm of sediment from sediment cores, while sediment for the experimental incubations was sampled using an Ekman grab sampler, and therefore included deeper layers of sediment. In soil, deeper horizons are thought to have more stable Fe-OC aggregates (Rumpel & Kögel-Knabner, 2011). Our results suggest that the same pattern may be true in sediments, resulting in burial of stable Fe-OC compounds in deeper sediments over time.

Formation and dissociation of Fe-OC complexes are two of many ways in which Fe and OC are impacted by hypoxia; both Fe and OC can also respond independently to changes in DO concentrations. Fe is oxidized from Fe(II) (soluble) to Fe(III) minerals (insoluble) both biotically and abiotically under oxic conditions (Kappler et al., 2021). Increased microbial biomass may be partially responsible for the increase in sediment OC under oxic conditions in experimental microcosms, as we observed the formation of orange (likely Fe-oxidizing) biofilms on top of the sediment layer in oxic microcosms (Figure S2). Fe reduction is also often associated with an increase in pH, which may increase the solubility of OC (Tavakkoli et al., 2015). However, pH did not differ consistently between microcosm treatments in this study and remained circumneutral on a whole-ecosystem scale (Figure S7 and S8). Likewise, other metals (e.g., aluminum, calcium, manganese) may release OC from sediment under hypoxic conditions, though the influence of these alternative metals on OC release is likely less quantitatively important than Fe (e.g., Wang et al. 2021). While these alternative mechanisms likely play a role in Fe and OC release, the decrease in Fe-OC and total OC following inactivation of the oxygenation system in FCR suggests that, at least for some surficial sediments, short (~2 week) periods of hypoxia can cause Fe-OC complexes to dissociate and decrease sediment OC burial on a whole-ecosystem scale.

4.2 Over multiannual timescales, OC respiration rates play a greater role than Fe-OC in determining the net effect of hypoxia on sediment OC content

Over multiannual timescales (2019–2021), exposure to seasonal hypoxia increased the amount of OC in sediments from FCR by 57% without changing the amount of Fe-OC (Figure 6). This clearly contrasts with short-term experimental results, which showed decreased OC content following short periods of hypoxia (section 4.3). While many factors could affect OC and Fe-OC over multiannual timescales, the fact that no comparable effects were seen in the unoxygenated reference reservoir (BVR) suggests that these changes may be attributed to changes in DO concentrations in overlying water. Over two years of summer hypoxia, OC levels in sediment from FCR increased to the extent that they were no longer significantly different from the hypoxic reference reservoir (Figure 6), suggesting that legacy effects of oxygen conditions on total sediment OC may diminish after a two-year interval.

Increases in sediment OC content with increased hypoxic duration are consistent with a reduction in sediment OC respiration rates under hypoxic conditions (Carey et al., 2018; Hargrave, 1969; Walker & Snodgrass, 1986). OC respiration rates decrease under hypoxic conditions because OC must be broken down using alternative electron acceptors, which produce a lower energy yield (Bastviken et al., 2003, 2004). Previous work conducted in BVR found that CO2 was the dominant terminal electron acceptor in the hypolimnion during hypoxic summer conditions (producing CH4), and CO2 has one of the lowest energy yields of alternate electron acceptors (McClure et al., 2021). As less OC is respired in hypoxic hypolimnetic water and sediments, OC can consequently accumulate more quickly in surficial sediments. Our results suggest that over multiannual timescales, this process (decreased respiration under hypoxic conditions) outweighs the counteracting decrease in Fe protection of OC that we observed during short periods of hypoxia.

Sediment Fe-OC content (per g sediment mass) did not significantly change after two years of hypoxic conditions in FCR (Figure 6), indicating that at least a fraction of these compounds are able to withstand fluctuations in environmental redox conditions. Long-term stability of Fe-OC complexes can be promoted by the formation of strong chemical bonds between OC and mineral surfaces, and these bonds continue to form over time through the rearrangement of organic molecules (Kaiser et al., 2007). Likewise, associations between Fe and OC can help to maintain a pool of small (high surface area) Fe particles that are particularly likely to associate with OC, as associations with OC can inhibit the conversion of these particles into larger, more crystalline Fe forms (called Ostwald ripening; e.g., Hiemstra et al. 2019; Zhao et al. 2022). Decreased accessibility to microbial decomposition (e.g., through burial) may further increase the ability of Fe-OC compounds to persist over time (Kaiser & Guggenberger, 2003; Kleber et al., 2015). In FCR, the history of oxic conditions (2013–2019) may have contributed to the formation of particularly stable Fe-OC complexes in sediment, which were then able to withstand two summers of hypoxia.

Importantly, much of the OC that accumulated under hypoxic conditions did not end up being bound to Fe. This result may be due to Fe oxidation state, as sorptive associations between DOC and Fe in sediment are much less likely to form if Fe is in a reduced state (Fe(II); Nierop et al., 2002). Changes in oxygen conditions are also likely to affect the composition of organic matter in sediments and in the water column (e.g., Riedel et al., 2013), potentially altering the capacity to associate with Fe. Because total OC increased following hypoxia and Fe-OC did not change, Fe-OC as a percentage of sediment OC was significantly lower after two years of hypoxia than before this hypoxic period. Declines in the percentage of OC that is bound to Fe may have important implications for ecosystem-scale carbon cycling, as OC that is associated with Fe is comparatively more protected from respiration (e.g., Chen et al., 2018, 2020; Hemingway et al., 2019; Kleber et al., 2005). Increased stocks of OC that are not associated with Fe may increase rates of methane production and OC release from the sediment to the water column (e.g., Hounshell et al., 2021), and could increase aerobic respiration rates under subsequent oxic periods (e.g., Chen et al., 2020; Huang et al., 2021).

4.3 Substantial OC and Fe cycling occurs at the sediment-water interface

Notably, the OC content of the top 1 cm of sediment was significantly lower than that of settling particulate material in both FCR and BVR, and nearly three times as much of this OC was bound to Fe in sediments compared to settling material (Figure 3). These results imply a substantial level of OC and Fe processing at the sediment-water interface, and they reinforce previous research in suggesting that the sediment-water interface is a hotspot for biogeochemical cycling freshwater lakes and reservoirs (e.g., Dadi et al., 2017; Hanson et al., 2015; Krueger et al., 2020).

From a mass-balance perspective, the difference in Fe-OC between settling material and surficial sediments suggests that Fe-OC complexes are either formed or preferentially preserved (compared to OC that is not associated with Fe) in sediments. Preferential preservation of Fe-OC is well-supported, as complexation with Fe has been shown to decrease OC turnover rates across multiple ecosystems (Eusterhues et al., 2014; Kaiser & Guggenberger, 2003; Kalbitz et al., 2005; Kleber et al., 2005; Lalonde et al., 2012; Mikutta & Kaiser, 2011). However, the difference in Fe-OC between settling material and surficial sediments likely also results in large part from Fe-OC associations formed in sediment (e.g., through adsorption of organic matter onto existing Fe minerals and Fe-OC complexes), as Fe(III) levels are much higher in sediments (e.g., Davison et al., 1991) and the composition of OC in sediments may be more preferable for complexation with Fe. While we did not measure OC quality in this study, we anticipate that settling material may have higher autochthonous OC levels and be more rapidly respired, while sediment OC may be enriched in allochthonous aromatic OC, which preferentially associates with Fe (Kramer et al., 2012; Riedel et al., 2013; Shields et al., 2016 ; Luo et al. 2022). Documenting changes in Fe-OC throughout the process of sediment diagenesis enhances our understanding of OC sequestration, as few if any previous studies have quantified the difference between Fe-OC inputs and stocks in aquatic sediments.

4.4 High Fe-OC levels reflect site-specific characteristics

On average, nearly one-third of surficial sediment OC was bound to Fe (dithionite-extractable) across two years in FCR and BVR (Figure 6). This percentage is far greater than that documented by Peter et al. (2018), where Fe-OC comprised ≤11% of total sediment OC across five boreal lakes. Furthermore, the levels of Fe-OC recorded here are higher than the mean of 21.5±8.6% reported for a broad range of marine sediments (Lalonde et al. 2012). With few other studies analyzing Fe-OC in freshwater lakes and reservoirs to date, our analysis provides new evidence that Fe-OC may play an important role in carbon sequestration in some freshwaters.

Despite having higher Fe-OC levels (as a percentage of total sediment OC) than most aquatic sediments studied to date, other sediment characteristics in FCR and BVR are within the range of those measured in other locations. FCR and BVR have much lower sediment OC content than the boreal lakes analyzed by Peter and Sobek (2018; 14–38% of sediment mass), but higher sediment OC than the primarily marine sediments analyzed by Lalonde et al. (2012; 0–7% of sediment mass). Fe concentrations are high in sediment from FCR and BVR, with a mean of 53,466 mg/kg dry weight (Krueger et al., 2020). However, Peter and Sobek (2018) observed low Fe-OC as a percentage of sediment OC (μ=6.7%) in one extremely high-Fe lake (Övre Skärsjön; 226,172 mg/kg reducible Fe in sediment). Likewise, pH in FCR and BVR is circumneutral (Figure S8), well within the range of 5.4–7.6 reported by Peter and Sobek (2018), and both Peter and Sobek (2018) and Lalonde et al. (2012) included a range of oxic and hypoxic sediments in their analyses.

Differences in the percentage of organic matter that is bound to Fe may result from numerous site-specific factors. For example, increasing ratios of Fe:OC and increasing absolute concentrations of Fe and OC can all increase the amount of Fe-OC coprecipitation (Chen et al., 2016; Kleber et al., 2015 and references therein). Likewise, differing Fe forms, Fe-weathering rates, OC quality, and pH may also impact the formation and stability of Fe-OC complexes (Curti et al., 2021; Kaiser et al., 2007; Kaiser & Guggenberger, 2003; Kleber et al., 2015; Luo et al. 2022); these differences may derive from contrasting geology, catchment vegetation, and trophic status, among many other factors. Disentangling the multiple interacting factors that can influence Fe-OC dynamics across sites will require Fe-OC characterization at a greater number and diversity of lakes and reservoirs. Such research will be essential to understanding how freshwater OC sequestration may be affected by global changes in Fe concentrations (Weyhenmeyer et al., 2014), water temperatures (Dokulil et al., 2021; O'Reilly et al., 2015), and pH (Garmo et al., 2014; Gavin et al., 2018; Stoddard et al., 1999), among other factors.

5. Conclusions

Results from this study help reconcile previous Fe-OC research and shed light on how declining oxygen concentrations may impact the role of lakes and reservoirs in the global carbon cycle. Research across terrestrial soils and marine sediments has provided contradictory evidence that Fe-OC complexes are (1) readily dissociated under hypoxic conditions and (2) capable of promoting sediment OC burial into deeper (hypoxic) layers over the course of decades to millennia. Here, we find that the timescale of analysis plays a critical role in understanding the net effect of hypoxia on sediment OC and Fe-OC. Specifically, a portion of the Fe-OC pool in surficial sediment is highly responsive to hypoxia in overlying water on a weekly timescale, resulting in decreased sediment OC. However, over longer timescales, the decrease in OC that results from dissociation of Fe-OC complexes is outweighed by the increase in sediment OC that results from slower respiration rates under hypoxia, and Fe-OC complexes buried in deeper sediment layers may be particularly resistant to hypoxic release. At both timescales, our results reinforce that Fe may serve as one of several important controls over OC cycling and sediment preservation of OC in freshwater ecosystems. As the duration of hypoxia increases in lakes and reservoirs, our results suggest that OC dynamics will respond non-linearly. While short periods of hypoxia may decrease OC burial, increasing prevalence and duration of hypoxia over multiannual timescales has the potential to increase OC burial in freshwater sediment, intensifying the role of freshwaters as sinks in the global carbon cycle.

223

Acknowledgements

We are grateful for ongoing partnerships with the Western Virginia Water Authority that facilitated this research. Additionally, we thank the Virginia Tech Reservoir Group for helping to collect these data, particularly Adrienne Breef-Pilz for organizing the 2021 field season and helping to collect sediment cores in 2021, James Maze and Dexter Howard for helping to collect sediment cores in 2019, Ryan McClure for leading CTD data collection before 2019, and Alex Hounshell for organizing the 2019 field season. We thank Whitney Woelmer for making the map of study sites (Figure 2), Chip Frazier and Jeb Barrett for providing access to laboratory equipment, and Jeff Parks in the VT ICP-MS lab for analyzing Fe samples. This work is supported by the Institute for Critical Science and Applied Technology at Virginia Tech and the U.S. National Science Foundation (NSF) foundation grants DGE-1651272, DEB-1753639, SCC-1737424, DBI-1933016, and DBI-1933102.

Author Contributions

ASL conceptualized this study with CCC and MES. ASL performed chemical Fe-OC extractions, analyzed data, developed figures, and wrote this manuscript with MES, MEL, and CCC. BRN led analytical chemistry methods development and performed DOC analyses. NWH and MES oversaw whole-ecosystem Fe sampling, analysis, and data collation. MES performed speciation-solubility calculations. AD helped to design and run the microcosm experiment and process sediment samples. HLW collated and processed whole-ecosystem DOC and YSI data and reviewed code for this manuscript.

CCC oversaw whole-ecosystem experiments. All authors edited and approved the final manuscript.

Open Research

All data used in this study are available in the Environmental Data Initiative (Carey et al., 2021; Carey, Lewis, Howard, et al., 2022; Carey, Lewis, McClure, et al., 2022; Carey, Wander, McClure, et al., 2022; Lewis et al., 2022; Lewis, Schreiber, et al., 2022; Schreiber et al., 2022). Code to reproduce results in this manuscript is available in a Zenodo repository (Lewis, 2022).

Chapter IV References

Adhikari, D., & Yang, Y. (2015). Selective stabilization of aliphatic organic carbon by iron oxide. *Scientific Reports*, *5*(1), 11214. https://doi.org/10.1038/srep11214

Akima, H., Gebhardt, A., Petzold, T., Maechler, M., & code), bilinear. (2022). akima: Interpolation of Irregularly and Regularly Spaced Data (Version 0.6-3.4). Retrieved from https://CRAN.R-project.org/package=akima

American Public Health Association. (2018a). 3125 metals by inductively coupled plasma-mass spectrometry. In *Standard Methods For the Examination of Water and Wastewater*. American Public Health Association. https://doi.org/10.2105/smww.2882.048

American Public Health Association. (2018b). 5310 total organic carbon (toc). In *Standard Methods For the Examination of Water and Wastewater*. American Public Health Association. https://doi.org/10.2105/SMWW.2882.104

Arndt, S., Jørgensen, B. B., LaRowe, D. E., Middelburg, J. J., Pancost, R. D., & Regnier, P. (2013). Quantifying the degradation of organic matter in marine sediments: A review and synthesis. *Earth-Science Reviews*, *123*, 53–86. https://doi.org/10.1016/j.earscirev.2013.02.008

Auguie, B. (2019). egg: Extensions for “ggplot2”: Custom Geom, Custom Themes, Plot Alignment, Labelled Panels, Symmetric Scales, and Fixed Panel Size (Version 0.4.5). Retrieved from https://CRAN.R-project.org/package=egg

Bai, J., Luo, M., Yang, Y., Xiao, S., Zhai, Z., & Huang, J. (2021). Iron-bound carbon increases along a freshwater−oligohaline gradient in a subtropical tidal wetland.

Soil Biology and Biochemistry, *154*, 108128. https://doi.org/10.1016/j.soilbio.2020.108128

Ball, J. W., & Nordstrom, D. K. (1991). User's manual for WATEQ4F, with revised thermodynamic data base and text cases for calculating speciation of major, trace, and redox elements in natural waters (USGS Numbered Series No. 91–183). User's manual for WATEQ4F, with revised thermodynamic data base and text cases for calculating speciation of major, trace, and redox elements in natural waters (Vol. 91–183). U.S. Geological Survey. https://doi.org/10.3133/ofr91183

Barber, A., Brandes, J., Leri, A., Lalonde, K., Balind, K., Wirick, S., et al. (2017). Preservation of organic matter in marine sediments by inner-sphere interactions with reactive iron. *Scientific Reports*, *7*(1), 366. https://doi.org/10.1038/s41598-017-00494-0

Bartosiewicz, M., Przytulska, A., Lapierre, J.-F., Laurion, I., Lehmann, M. F., & Maranger, R. (2019). Hot tops, cold bottoms: Synergistic climate warming and shielding effects increase carbon burial in lakes. *Limnology and Oceanography Letters*, *4*(5), 132–144. https://doi.org/10.1002/lol2.10117

Bastviken, D., Olsson, M., & Tranvik, L. (2003). Simultaneous measurements of organic carbon mineralization and bacterial production in oxic and anoxic lake sediments. *Microbial Ecology*, *46*(1), 73–82. https://doi.org/10.1007/s00248-002-1061-9

Bastviken, D., Persson, L., Odham, G., & Tranvik, L. (2004). Degradation of dissolved organic matter in oxic and anoxic lake water. *Limnology and Oceanography*, *49*(1), 109–116. https://doi.org/10.4319/lo.2004.49.1.0109

Bastviken, D., Tranvik, L. J., Downing, J. A., Crill, P. M., & Enrich-Prast, A. (2011). Freshwater methane emissions offset the continental carbon sink. *Science*, *331*(6013), 50–50. https://doi.org/10.1126/science.1196808

Battin, T. J., Luyssaert, S., Kaplan, L. A., Aufdenkampe, A. K., Richter, A., & Tranvik, L. J. (2009). The boundless carbon cycle. *Nature Geoscience*, *2*(9), 598–600. https://doi.org/10.1038/ngeo618

Beauvois, A., Vantelon, D., Jestin, J., Bouhnik-Le Coz, M., Catrouillet, C., Briois, V., et al. (2021). How crucial is the impact of calcium on the reactivity of iron-organic matter aggregates? Insights from arsenic. *Journal of Hazardous Materials*, *404*, 124127. https://doi.org/10.1016/j.jhazmat.2020.124127

Björnerås, C., Weyhenmeyer, G. A., Evans, C. D., Gessner, M. O., Grossart, H.-P., Kangur, K., et al. (2017). Widespread increases in iron concentration in European and North American freshwaters. *Global Biogeochemical Cycles*, *31*(10), 1488–1500. https://doi.org/10.1002/2017GB005749

Brothers, S., Köhler, J., Attermeyer, K., Grossart, H. P., Mehner, T., Meyer, N., et al. (2014). A feedback loop links brownification and anoxia in a temperate, shallow lake. *Limnology and Oceanography*, *59*(4), 1388–1398. https://doi.org/10.4319/lo.2014.59.4.1388

Carey, C. C., Doubek, J. P., McClure, R. P., & Hanson, P. C. (2018). Oxygen dynamics control the burial of organic carbon in a eutrophic reservoir. *Limnology and Oceanography Letters*, *3*(3), 293–301. https://doi.org/10.1002/lol2.10057

Carey, C. C., Wander, H. L., Woelmer, W. M., Lofton, M. E., Breef-Pilz, A., Doubek, J. P., et al. (2021). Water chemistry time series for Beaverdam Reservoir, Carvins

Cove Reservoir, Falling Creek Reservoir, Gatewood Reservoir, and Spring Hollow Reservoir in southwestern Virginia, USA 2013-2020 [Data set]. Environmental Data Initiative. https://doi.org/10.6073/PASTA/6343E979A970E8A2590B4A450E851DD2

Carey, C. C., Hanson, P. C., Thomas, R. Q., Gerling, A. B., Hounshell, A. G., Lewis, A. S. L., et al. (2022). Anoxia decreases the magnitude of the carbon, nitrogen, and phosphorus sink in freshwaters. *Global Change Biology*, *28*(16), 4861–4881. https://doi.org/10.1111/gcb.16228

Carey, C.C., A.S. Lewis, D.W. Howard, W.M. Woelmer, P.A. Gantzer, K.A. Bierlein, J.C. Little, and WVWA. 2022. Bathymetry and watershed area for Falling Creek Reservoir, Beaverdam Reservoir, and Carvins Cove Reservoir ver 1. Environmental Data Initiative. https://doi.org/10.6073/pasta/352735344150f7e77d2bc18b69a22412 (Accessed 2022-11-21).

Carey, C. C., Thomas, R. Q., & Hanson, P. C. (2022). General Lake Model-Aquatic EcoDynamics model parameter set for Falling Creek Reservoir, Vinton, Virginia, USA 2013-2019 [Data set]. Environmental Data Initiative. https://doi.org/10.6073/PASTA/9F7D037D9A133076A0A0D123941C6396

Carey, C. C., Wander, H. L., McClure, R. P., Lofton, M. E., Hamre, K. D., Doubek, J. P., et al. (2022). Secchi depth data and discrete depth profiles of photosynthetically active radiation, temperature, dissolved oxygen, and pH for Beaverdam Reservoir, Carvins Cove Reservoir, Falling Creek Reservoir, Gatewood Reservoir, and Spring Hollow Reservoir in southwestern Virginia, USA 2013-2021 [Data set].

Environmental Data Initiative. https://doi.org/10.6073/PASTA/887D8AB8C57FB8FDF3582507F3223CD6

Carey, C. C., Lewis, A. S. L., McClure, R. P., Gerling, A. B., Breef-Pilz, A., & Das, A. (2022). Time series of high-frequency profiles of depth, temperature, dissolved oxygen, conductivity, specific conductance, chlorophyll a, turbidity, pH, oxidation-reduction potential, photosynthetic active radiation, and descent rate for Beaverdam Reservoir, Carvins Cove Reservoir, Falling Creek Reservoir, Gatewood Reservoir, and Spring Hollow Reservoir in Southwestern Virginia, USA 2013-2021 [Data set]. Environmental Data Initiative. https://doi.org/10.6073/PASTA/C4C45B5B10B4CB4CD4B5E613C3EFFBD0

Carey, C. C., Wander, H. L., Howard, D. W., Niederlehner, B. R., Woelmer, W. M., Lofton, M. E., et al. (2022). Water chemistry time series for Beaverdam Reservoir, Carvins Cove Reservoir, Falling Creek Reservoir, Gatewood Reservoir, and Spring Hollow Reservoir in southwestern Virginia, USA 2013-2021 [Data set]. Environmental Data Initiative. https://doi.org/10.6073/PASTA/7BD797155CDBB5F1ACDF0547C6BA9023

Carpenter, S. R. (1996). Microcosm experiments have limited relevance for community and ecosystem ecology. *Ecology*, *77*(3), 677–680. https://doi.org/10.2307/2265490

Chapman, M. J., Cravotta III, C. A., Szabo, Z., & Lindsey, B. D. (2013). Naturally occurring contaminants in the Piedmont and Blue Ridge crystalline-rock aquifers and Piedmont Early Mesozoic basin siliciclastic-rock aquifers, eastern United

States, 1994–2008. Retrieved June 25, 2022, from https://pubs.er.usgs.gov/publication/sir20135072

Chen, C., Meile, C., Wilmoth, J., Barcellos, D., & Thompson, A. (2018). Influence of pO2 on Iron Redox Cycling and Anaerobic Organic Carbon Mineralization in a Humid Tropical Forest Soil. *Environmental Science & Technology*, *52*(14), 7709–7719. https://doi.org/10.1021/acs.est.8b01368

Chen, C., Hall, S. J., Coward, E., & Thompson, A. (2020). Iron-mediated organic matter decomposition in humid soils can counteract protection. *Nature Communications*, *11*(1), 2255. https://doi.org/10.1038/s41467-020-16071-5

Chen, K.-Y., Chen, T.-Y., Chan, Y.-T., Cheng, C.-Y., Tzou, Y.-M., Liu, Y.-T., & Teah, H.-Y. (2016). Stabilization of Natural Organic Matter by Short-Range-Order Iron Hydroxides. *Environmental Science & Technology*, *50*(23), 12612–12620. https://doi.org/10.1021/acs.est.6b02793

Curti, L., Moore, O. W., Babakhani, P., Xiao, K.-Q., Woulds, C., Bray, A. W., et al. (2021). Carboxyl-richness controls organic carbon preservation during coprecipitation with iron (oxyhydr)oxides in the natural environment. *Communications Earth & Environment*, *2*(1), 1–13. https://doi.org/10.1038/s43247-021-00301-9

Dadi, T., Wendt-Potthoff, K., & Koschorreck, M. (2017). Sediment resuspension effects on dissolved organic carbon fluxes and microbial metabolic potentials in reservoirs. *Aquatic Sciences*, *79*(3), 749–764. https://doi.org/10.1007/s00027-017-0533-4

Davison, W., Grime, G. W., Morgan, J. a. W., & Clarke, K. (1991). Distribution of dissolved iron in sediment pore waters at submillimetre resolution. *Nature*, *352*(6333), 323–325. https://doi.org/10.1038/352323a0

Dean, W. E., & Gorham, E. (1998). Magnitude and significance of carbon burial in lakes, reservoirs, and peatlands, 4.

Deemer, B. R., Harrison, J. A., Li, S., Beaulieu, J. J., DelSontro, T., Barros, N., et al. (2016). Greenhouse gas emissions from reservoir water surfaces: A new global synthesis. *BioScience*, *66*(11), 949–964. https://doi.org/10.1093/biosci/biw117

DelSontro, T., Beaulieu, J. J., & Downing, J. A. (2018). Greenhouse gas emissions from lakes and impoundments: Upscaling in the face of global change. *Limnology and Oceanography Letters*, *3*(3), 64–75. https://doi.org/10.1002/lol2.10073

Dokulil, M. T., de Eyto, E., Maberly, S. C., May, L., Weyhenmeyer, G. A., & Woolway, R. I. (2021). Increasing maximum lake surface temperature under climate change. *Climatic Change*, *165*(3), 56. https://doi.org/10.1007/s10584-021-03085-1

Dzialowski, A. R., Rzepecki, M., Kostrzewska-Szlakowska, I., Kalinowska, K., Palash, A., & Lennon, J. T. (2014). Are the abiotic and biotic characteristics of aquatic mesocosms representative of in situ conditions? *Journal of Limnology*, *73*(3). https://doi.org/10.4081/jlimnol.2014.721

Einola, E., Rantakari, M., Kankaala, P., Kortelainen, P., Ojala, A., Pajunen, H., et al. (2011). Carbon pools and fluxes in a chain of five boreal lakes: A dry and wet year comparison. *Journal of Geophysical Research: Biogeosciences*, *116*(G3). https://doi.org/10.1029/2010JG001636

Eusterhues, K., Neidhardt, J., Hädrich, A., Küsel, K., & Totsche, K. U. (2014). Biodegradation of ferrihydrite-associated organic matter. *Biogeochemistry, 119*(1–3), 45–50. https://doi.org/10.1007/s10533-013-9943-0

Fisher, B. J., Moore, O. W., Faust, J. C., Peacock, C. L., & März, C. (2020). Experimental evaluation of the extractability of iron bound organic carbon in sediments as a function of carboxyl content. Chemical Geology, 556, 119853. https://doi.org/10.1016/j.chemgeo.2020.119853

Fisher, B. J., Faust, J. C., Moore, O. W., Peacock, C. L., & März, C. (2021). Technical Note: Uncovering the influence of methodological variations on the extractability of iron bound organic carbon, 20.

Garmo, Ø. A., Skjelkvåle, B. L., de Wit, H. A., Colombo, L., Curtis, C., Fölster, J., et al. (2014). Trends in surface water chemistry in acidified areas in Europe and North America from 1990 to 2008. *Water, Air, & Soil Pollution*, *225*(3), 1880. https://doi.org/10.1007/s11270-014-1880-6

Gavin, A. L., Nelson, S. J., Klemmer, A. J., Fernandez, I. J., Strock, K. E., & McDowell, W. H. (2018). Acidification and climate linkages to increased dissolved organic carbon in high-elevation lakes. *Water Resources Research*, *54*(8), 5376–5393. https://doi.org/10.1029/2017WR020963

Gerling, A. B., Browne, R. G., Gantzer, P. A., Mobley, M. H., Little, J. C., & Carey, C. C. (2014). First report of the successful operation of a side stream supersaturation hypolimnetic oxygenation system in a eutrophic, shallow reservoir. *Water Research*, *67*, 129–143. https://doi.org/10.1016/j.watres.2014.09.002

Gerling, A. B., Munger, Z. W., Doubek, J. P., Hamre, K. D., Gantzer, P. A., Little, J. C., & Carey, C. C. (2016). Whole-catchment manipulations of internal and external loading reveal the sensitivity of a century-old reservoir to hypoxia. *Ecosystems, 19*(3), 555–571. https://doi.org/10.1007/s10021-015-9951-0

Gibbs, M. M. (1979). A simple method for the rapid determination of iron in natural waters. *Water Research*, *13*(3), 295–297. https://doi.org/10.1016/0043-1354(79)90209-4

Grolemund, G., & Wickham, H. (2011). Dates and Times Made Easy with lubridate. *Journal of Statistical Software*, *40*, 1–25. https://doi.org/10.18637/jss.v040.i03

Hamre, K. D., Lofton, M. E., McClure, R. P., Munger, Z. W., Doubek, J. P., Gerling, A. B., et al. (2018). In situ fluorometry reveals a persistent, perennial hypolimnetic cyanobacterial bloom in a seasonally anoxic reservoir. *Freshwater Science, 37*(3), 483–495. https://doi.org/10.1086/699327

Hanson, P. C., Pace, M. L., Carpenter, S. R., Cole, J. J., & Stanley, E. H. (2015). Integrating landscape carbon cycling: research needs for resolving organic carbon budgets of lakes. *Ecosystems*, *18*(3), 363–375. https://doi.org/10.1007/s10021-014-9826-9

Hargrave, B. T. (1969). Similarity of oxygen uptake by benthic communities. *Limnology and Oceanography*, *14*(5), 801–805. https://doi.org/10.4319/lo.1969.14.5.0801

Harris, D., Horwáth, W. R., & Kessel, C. van. (2001). Acid fumigation of soils to remove carbonates prior to total organic carbon or CARBON-13 isotopic analysis. *Soil Science Society of America Journal*, *65*(6), 1853–1856. https://doi.org/10.2136/sssaj2001.1853

Heerah, K. M., & Reader, H. E. (2022). Towards the identification of humic ligands associated with iron transport through a salinity gradient. *Scientific Reports*, *12*(1), 15545. https://doi.org/10.1038/s41598-022-19618-2

Hemingway, J. D., Rothman, D. H., Grant, K. E., Rosengard, S. Z., Eglinton, T. I., Derry, L. A., & Galy, V. V. (2019). Mineral protection regulates long-term global preservation of natural organic carbon. *Nature*, *570*(7760), 228–231. https://doi.org/10.1038/s41586-019-1280-6

Herzog, S. D., Gentile, L., Olsson, U., Persson, P., & Kritzberg, E. S. (2020). Characterization of Iron and Organic Carbon Colloids in Boreal Rivers and Their Fate at High Salinity. *Journal of Geophysical Research: Biogeosciences*, *125*(4), e2019JG005517. https://doi.org/10.1029/2019JG005517

Hiemstra, T., Mendez, J. C., & Li, J. (2019). Evolution of the reactive surface area of ferrihydrite: time, pH, and temperature dependency of growth by Ostwald ripening. Environmental Science: Nano, 6(3), 820–833. https://doi.org/10.1039/C8EN01198B

Hounshell, A. G., McClure, R. P., Lofton, M. E., & Carey, C. C. (2021). Whole-ecosystem oxygenation experiments reveal substantially greater hypolimnetic methane concentrations in reservoirs during anoxia. *Limnology and Oceanography Letters*, *6*(1), 33–42.

Huang, W., Wang, K., Ye, C., Hockaday, W. C., Wang, G., & Hall, S. J. (2021). High carbon losses from oxygen-limited soils challenge biogeochemical theory and model assumptions. *Global Change Biology*, *27*(23), 6166–6180. https://doi.org/10.1111/gcb.15867

Jane, S., Hansen, G., Kraemer, B., Leavitt, P., Mincer, J., North, R., et al. (2021). Widespread deoxygenation of temperate lakes. *Nature*, *594*. https://doi.org/10.1038/s41586-021-03550-y

Jenny, J.-P., Francus, P., Normandeau, A., Lapointe, F., Perga, M.-E., Ojala, A., et al. (2016). Global spread of hypoxia in freshwater ecosystems during the last three centuries is caused by rising local human pressure. *Global Change Biology*, *22*(4), 1481–1489. https://doi.org/10.1111/gcb.13193

Kaiser, K., & Guggenberger, G. (2003). Mineral surfaces and soil organic matter. *European Journal of Soil Science*, *54*(2), 219–236. https://doi.org/10.1046/j.1365-2389.2003.00544.x

Kaiser, K., Mikutta, R., & Guggenberger, G. (2007). Increased stability of organic matter sorbed to ferrihydrite and goethite on aging. *Soil Science Society of America Journal*, *71*(3), 711–719. https://doi.org/10.2136/sssaj2006.0189

Kalbitz, K., Schwesig, D., Rethemeyer, J., & Matzner, E. (2005). Stabilization of dissolved organic matter by sorption to the mineral soil. *Soil Biology and Biochemistry*, *37*(7), 1319–1331. https://doi.org/10.1016/j.soilbio.2004.11.028

Kappler, A., Bryce, C., Mansor, M., Lueder, U., Byrne, J. M., & Swanner, E. D. (2021). An evolving view on biogeochemical cycling of iron. *Nature Reviews Microbiology*, 1–15. https://doi.org/10.1038/s41579-020-00502-7

Kassambara, A. (2020). ggpubr: “ggplot2” Based Publication Ready Plots (Version 0.4.0). Retrieved from https://CRAN.R-project.org/package=ggpubr

Kassambara, A. (2021). rstatix: Pipe-Friendly Framework for Basic Statistical Tests (Version 0.7.0). Retrieved from https://CRAN.R-project.org/package=rstatix

Keitt, T. (2022). colorRamps: Builds Color Tables (Version 2.3.1). Retrieved from https://CRAN.R-project.org/package=colorRamps

Kim, J., & Kim, T.-H. (2020). Distribution of Humic Fluorescent Dissolved Organic Matter in Lake Shihwa: the Role of the Redox Condition. *Estuaries and Coasts*, *43*(3), 578–588. https://doi.org/10.1007/s12237-018-00491-0

Kirk, G. (2004). Reduction and Oxidation. In G. Kirk (Ed.), *The Biogeochemistry of Submerged Soils* (pp. 93–134). John Wiley & Sons, Ltd. https://doi.org/10.1002/047086303X.ch4

Kleber, M., Mikutta, R., Torn, M. S., & Jahn, R. (2005). Poorly crystalline mineral phases protect organic matter in acid subsoil horizons. *European Journal of Soil Science*, *56*(6), 717–725. https://doi.org/10.1111/j.1365-2389.2005.00706.x

Kleber, M., Eusterhues, K., Keiluweit, M., Mikutta, C., Mikutta, R., & Nico, P. S. (2015). Chapter One - Mineral–Organic Associations: Formation, Properties, and Relevance in Soil Environments. In D. L. Sparks (Ed.), *Advances in Agronomy* (Vol. 130, pp. 1–140). Academic Press. https://doi.org/10.1016/bs.agron.2014.10.005

Knoll, L. B., Vanni, M. J., Renwick, W. H., Dittman, E. K., & Gephart, J. A. (2013). Temperate reservoirs are large carbon sinks and small CO2 sources: Results from high-resolution carbon budgets. *Global Biogeochemical Cycles*, *27*(1), 52–64. https://doi.org/10.1002/gbc.20020

Kottek, M., Grieser, J., Beck, C., Rudolf, B., & Rubel, F. (2006). World Map of the Köppen-Geiger climate classification updated. *Meteorologische Zeitschrift*, 259–263. https://doi.org/10.1127/0941-2948/2006/0130

Kramer, M. G., & Chadwick, O. A. (2018). Climate-driven thresholds in reactive mineral retention of soil carbon at the global scale. *Nature Climate Change*, *8*(12), 1104–1108. https://doi.org/10.1038/s41558-018-0341-4

Kramer, M. G., Sanderman, J., Chadwick, O. A., Chorover, J., & Vitousek, P. M. (2012). Long-term carbon storage through retention of dissolved aromatic acids by reactive particles in soil. *Global Change Biology*, *18*(8), 2594–2605. https://doi.org/10.1111/j.1365-2486.2012.02681.x

Krueger, K. M., Vavrus, C. E., Lofton, M. E., McClure, R. P., Gantzer, P., Carey, C. C., & Schreiber, M. E. (2020). Iron and manganese fluxes across the sediment-water interface in a drinking water reservoir. *Water Research*, *182*, 116003. https://doi.org/10.1016/j.watres.2020.116003

Lalonde, K., Mucci, A., Ouellet, A., & Gélinas, Y. (2012). Preservation of organic matter in sediments promoted by iron. *Nature*, *483*(7388), 198–200. https://doi.org/10.1038/nature10855

LaRowe, D. E., & Van Cappellen, P. (2011). Degradation of natural organic matter: A thermodynamic analysis. *Geochimica et Cosmochimica Acta*, *75*(8), 2030–2042. https://doi.org/10.1016/j.gca.2011.01.020

Lau, M. P., & del Giorgio, P. (2020). Reactivity, fate and functional roles of dissolved organic matter in anoxic inland waters. *Biology Letters*, *16*(2), 20190694. https://doi.org/10.1098/rsbl.2019.0694

Lewis, A. S. L. (2022). Effects of hypoxia on coupled carbon and iron cycling in two freshwater reservoirs v1.1.0. Zenodo. https://doi.org/10.5281/zenodo.7527419

Lewis, A. S. L., Niederlehner, B. R., Das, A., Wander, H. L., Schreiber, M. E., & Carey, C. C. (2022). Experimental microcosm incubations assessing the effect of hypoxia on aqueous iron and organic carbon, pH, sediment organic carbon, and sediment iron-bound organic carbon. Environmental Data Initiative. https://doi.org/10.6073/pasta/60a7784acef3038d3c8a16776a5b5746

Lewis, A. S. L., Schreiber, M. E., Niederlehner, B. R., Das, A., & Carey, C. C. (2022). Total organic carbon, total nitrogen, and iron-bound organic carbon in surficial sediment and settling particulate material from Falling Creek and Beaverdam Reservoirs in 2019 and 2021. Environmental Data Initiative. https://doi.org/10.6073/pasta/a1d49c266b57465daa863cde4b1d4b4e

Luo, C., Wen, S., Lu, Y., Dai, J., & Du, Y. (2022). Coprecipitation of humic acid and phosphate with Fe(III) enhances the sequestration of carbon and phosphorus in sediments. *Chemical Geology*, 588, 120645. https://doi.org/10.1016/j.chemgeo.2021.120645

Marking, L. L., & Dawson, V. K. (1973). Toxicity of quinaldine sulfate to fish (Report No. 48) (pp. 0–8). La Crosse, WI. Retrieved from http://pubs.er.usgs.gov/publication/2001015

McClure, R. P., Schreiber, M. E., Lofton, M. E., Chen, S., Krueger, K. M., & Carey, C. C. (2021). Ecosystem-Scale Oxygen Manipulations Alter Terminal Electron Acceptor Pathways in a Eutrophic Reservoir. *Ecosystems*, *24*(6), 1281–1298. https://doi.org/10.1007/s10021-020-00582-9

Mendonça, R., Müller, R. A., Clow, D., Verpoorter, C., Raymond, P., Tranvik, L. J., & Sobek, S. (2017). Organic carbon burial in global lakes and reservoirs. *Nature Communications*, *8*(1), 1694. https://doi.org/10.1038/s41467-017-01789-6

Mikutta, R., & Kaiser, K. (2011). Organic matter bound to mineral surfaces: Resistance to chemical and biological oxidation. *Soil Biology and Biochemistry*, *43*(8), 1738–1741. https://doi.org/10.1016/j.soilbio.2011.04.012

Munger, Z. W., Carey, C. C., Gerling, A. B., Doubek, J. P., Hamre, K. D., McClure, R. P., & Schreiber, M. E. (2019). Oxygenation and hydrologic controls on iron and manganese mass budgets in a drinking-water reservoir. *Lake and Reservoir Management*, *35*(3), 277–291. https://doi.org/10.1080/10402381.2018.1545811

Nierop, K. G. J., Jansen, B., & Verstraten, J. M. (2002). Dissolved organic matter, aluminium and iron interactions: precipitation induced by metal/carbon ratio, pH and competition. *The Science of the Total Environment*, *300*(1–3), 201–211. https://doi.org/10.1016/s0048-9697(02)00254-1

O'Reilly, C. M., Sharma, S., Gray, D. K., Hampton, S. E., Read, J. S., Rowley, R. J., et al. (2015). Rapid and highly variable warming of lake surface waters around the globe. *Geophysical Research Letters*, *42*(24), 10,773-10,781. https://doi.org/10.1002/2015GL066235

Oyewumi, O., & Schreiber, M. E. (2017). Using column experiments to examine transport of As and other trace elements released from poultry litter: Implications for trace element mobility in agricultural watersheds. *Environmental Pollution*, *227*, 223–233. https://doi.org/10.1016/j.envpol.2017.04.063

Pacheco, F. S., Roland, F., & Downing, J. A. (2014). Eutrophication reverses whole-lake carbon budgets. *Inland Waters*, *4*(1), 41–48. https://doi.org/10.5268/IW-4.1.614

Pan, W., Kan, J., Inamdar, S., Chen, C., & Sparks, D. (2016). Dissimilatory microbial iron reduction release DOC (dissolved organic carbon) from carbon-ferrihydrite association. *Soil Biology and Biochemistry*, *103*, 232–240. https://doi.org/10.1016/j.soilbio.2016.08.026

Patzner, M. S., Mueller, C. W., Malusova, M., Baur, M., Nikeleit, V., Scholten, T., et al. (2020). Iron mineral dissolution releases iron and associated organic carbon during permafrost thaw. *Nature Communications*, *11*(1), 6329. https://doi.org/10.1038/s41467-020-20102-6

Peter, S., & Sobek, S. (2018). High variability in iron-bound organic carbon among five boreal lake sediments. *Biogeochemistry*, *139*(1), 19–29. https://doi.org/10.1007/s10533-018-0456-8

Peter, S., Isidorova, A., & Sobek, S. (2016). Enhanced carbon loss from anoxic lake sediment through diffusion of dissolved organic carbon. *Journal of Geophysical Research: Biogeosciences*, *121*(7), 1959–1977. https://doi.org/10.1002/2016JG003425

Peter, S., Agstam, O., & Sobek, S. (2017). Widespread release of dissolved organic carbon from anoxic boreal lake sediments. *Inland Waters*, *7*(2), 151–163. https://doi.org/10.1080/20442041.2017.1300226

Raymond, P. A., Hartmann, J., Lauerwald, R., Sobek, S., McDonald, C., Hoover, M., et al. (2013). Global carbon dioxide emissions from inland waters. *Nature*, *503*(7476), 355–359. https://doi.org/10.1038/nature12760

Riedel, T., Zak, D., Biester, H., & Dittmar, T. (2013). Iron traps terrestrially derived dissolved organic matter at redox interfaces. *Proceedings of the National Academy of Sciences*, *110*(25), 10101–10105. https://doi.org/10.1073/pnas.1221487110

Rumpel, C., & Kögel-Knabner, I. (2011). Deep soil organic matter—a key but poorly understood component of terrestrial C cycle. *Plant and Soil*, *338*(1), 143–158. https://doi.org/10.1007/s11104-010-0391-5

Schindler, D. W. (1998). Whole-ecosystem experiments: replication versus realism: the need for ecosystem-scale experiments. *Ecosystems*, *1*(4), 323–334. https://doi.org/10.1007/s100219900026

Schreiber, M. E., Hammond, N. W., Krueger, K. M., Munger, Z. W., Ming, C. L., Breef-Pilz, A., & Carey, C. C. (2022). Time series of total and soluble iron and manganese concentrations from Falling Creek Reservoir and Beaverdam Reservoir in southwestern Virginia, USA from 2014 through 2021 [Data set]. Environmental Data Initiative. https://doi.org/10.6073/PASTA/7CDF3D7A234963B265F09B7D6D08F357

Shields, M. R., Bianchi, T. S., Gélinas, Y., Allison, M. A., & Twilley, R. R. (2016). Enhanced terrestrial carbon preservation promoted by reactive iron in deltaic sediments. *Geophysical Research Letters*, *43*(3), 1149–1157. https://doi.org/10.1002/2015GL067388

Skoog, A. C., & Arias-Esquivel, V. A. (2009). The effect of induced anoxia and reoxygenation on benthic fluxes of organic carbon, phosphate, iron, and manganese. *Science of The Total Environment*, *407*(23), 6085–6092. https://doi.org/10.1016/j.scitotenv.2009.08.030

Sobek, S., Durisch-Kaiser, E., Zurbrügg, R., Wongfun, N., Wessels, M., Pasche, N., & Wehrli, B. (2009). Organic carbon burial efficiency in lake sediments controlled by oxygen exposure time and sediment source. *Limnology and Oceanography*, *54*(6), 2243–2254. https://doi.org/10.4319/lo.2009.54.6.2243

Soil Survey Staff, Natural Resources Conservation Service, United States Department of Agriculture. Soil Series Classification Database. Available online. Accessed [11/21/2022].

Sondheim, M. W., & Standish, J. T. (1983). Numerical analysis of a chronosequence including an assessment of variability. *Canadian Journal of Soil Science, 63*(3), 501–517. https://doi.org/10.4141/cjss83-052

Stoddard, J. L., Jeffries, D. S., Lükewille, A., Clair, T. A., Dillon, P. J., Driscoll, C. T., et al. (1999). Regional trends in aquatic recovery from acidification in North America and Europe. *Nature, 401*(6753), 575–578. https://doi.org/10.1038/44114

Tavakkoli, E., Rengasamy, P., Smith, E., & McDonald, G. K. (2015). The effect of cation–anion interactions on soil pH and solubility of organic carbon. *European Journal of Soil Science*, *66*(6), 1054–1062. https://doi.org/10.1111/ejss.12294

Thompson, A., Chadwick, O. A., Rancourt, D. G., & Chorover, J. (2006). Iron-oxide crystallinity increases during soil redox oscillations. *Geochimica et Cosmochimica Acta*, *70*(7), 1710–1727. https://doi.org/10.1016/j.gca.2005.12.005

Thompson, J., Poulton, S. W., Guilbaud, R., Doyle, K. A., Reid, S., & Krom, M. D. (2019). Development of a modified SEDEX phosphorus speciation method for ancient rocks and modern iron-rich sediments. *Chemical Geology*, 524, 383–393. https://doi.org/10.1016/j.chemgeo.2019.07.003

Tranvik, L. J., Cole, J. J., & Prairie, Y. T. (2018). The study of carbon in inland waters—from isolated ecosystems to players in the global carbon cycle. *Limnology and Oceanography Letters*, *3*(3), 41–48. https://doi.org/10.1002/lol2.10068

Trapletti, A., Hornik, K., & code), B. L. (BDS test. (2022). tseries: Time Series Analysis and Computational Finance (Version 0.10-51). Retrieved from https://CRAN.R-project.org/package=tseries

USGCRP, 2018: Second State of the Carbon Cycle Report (SOCCR2): A Sustained Assessment Report. [Cavallaro, N., G. Shrestha, R. Birdsey, M. A. Mayes, R. G. Najjar, S. C. Reed, P. Romero-Lankao, and Z. Zhu (eds.)]. U.S. Global Change Research Program, Washington, DC, USA, 878 pp., doi: 10.7930/SOCCR2.2018

Virginia Division of Mineral Resources. (2003). Digital representation of the 1993 geologic map of Virginia.

von Wachenfeldt, E., Sobek, S., Bastviken, D., & Tranvik, L. J. (2008). Linking allochthonous dissolved organic matter and boreal lake sediment carbon sequestration: The role of light-mediated flocculation. *Limnology and Oceanography*, *53*(6), 2416–2426. https://doi.org/10.4319/lo.2008.53.6.2416

Walker, R. R., & Snodgrass, W. J. (1986). Model for sediment oxygen demand in lakes. *Journal of Environmental Engineering*, *112*(1), 25–43. https://doi.org/10.1061/(ASCE)0733-9372(1986)112:1(25)

Wang, S., Jia, Y., Liu, T., Wang, Y., Liu, Z., & Feng, X. (2021). Delineating the Role of Calcium in the Large-Scale Distribution of Metal-Bound Organic Carbon in Soils.

Geophysical Research Letters, *48*(10), e2021GL092391. https://doi.org/10.1029/2021GL092391

Weyhenmeyer, G. A., Prairie, Y. T., & Tranvik, L. J. (2014). Browning of boreal freshwaters coupled to carbon-iron interactions along the aquatic continuum. *PloS One*, *9*(2), e88104. https://doi.org/10.1371/journal.pone.0088104

Wickham, H., Averick, M., Bryan, J., Chang, W., McGowan, L. D., François, R., et al. (2019). Welcome to the Tidyverse. *Journal of Open Source Software*, *4*(43), 1686. https://doi.org/10.21105/joss.01686

Williamson, C. E., Overholt, E. P., Pilla, R. M., Leach, T. H., Brentrup, J. A., Knoll, L. B., et al. (2015). Ecological consequences of long-term browning in lakes. *Scientific Reports*, *5*(1), 1–10. https://doi.org/10.1038/srep18666

Winslow, L., Read, J., Woolway, R., Brentrup, J., Leach, T., Zwart, J., et al. (2019). rLakeAnalyzer: Lake Physics Tools (Version 1.11.4.1). Retrieved from https://CRAN.R-project.org/package=rLakeAnalyzer

Woelmer, W., Hounshell, A. G., Lofton, M. E., Wander, H. L., Lewis, A. S. L., Scott, D., & Carey, C. C. (2022, June 25). The importance of time and space in biogeochemical heterogeneity and processing along the reservoir ecosystem continuum. Earth and Space Science Open Archive. https://doi.org/10.1002/essoar.10511710.1

Woodward, H. P. (1932). Geology and Mineral Resources of the Roanoke Area, Virginia.

Yang, L., Choi, J. H., & Hur, J. (2014). Benthic flux of dissolved organic matter from lake sediment at different redox conditions and the possible effects of biogeochemical processes. *Water Research*, *61*, 97–107. https://doi.org/10.1016/j.watres.2014.05.009

Chapter IV Figures

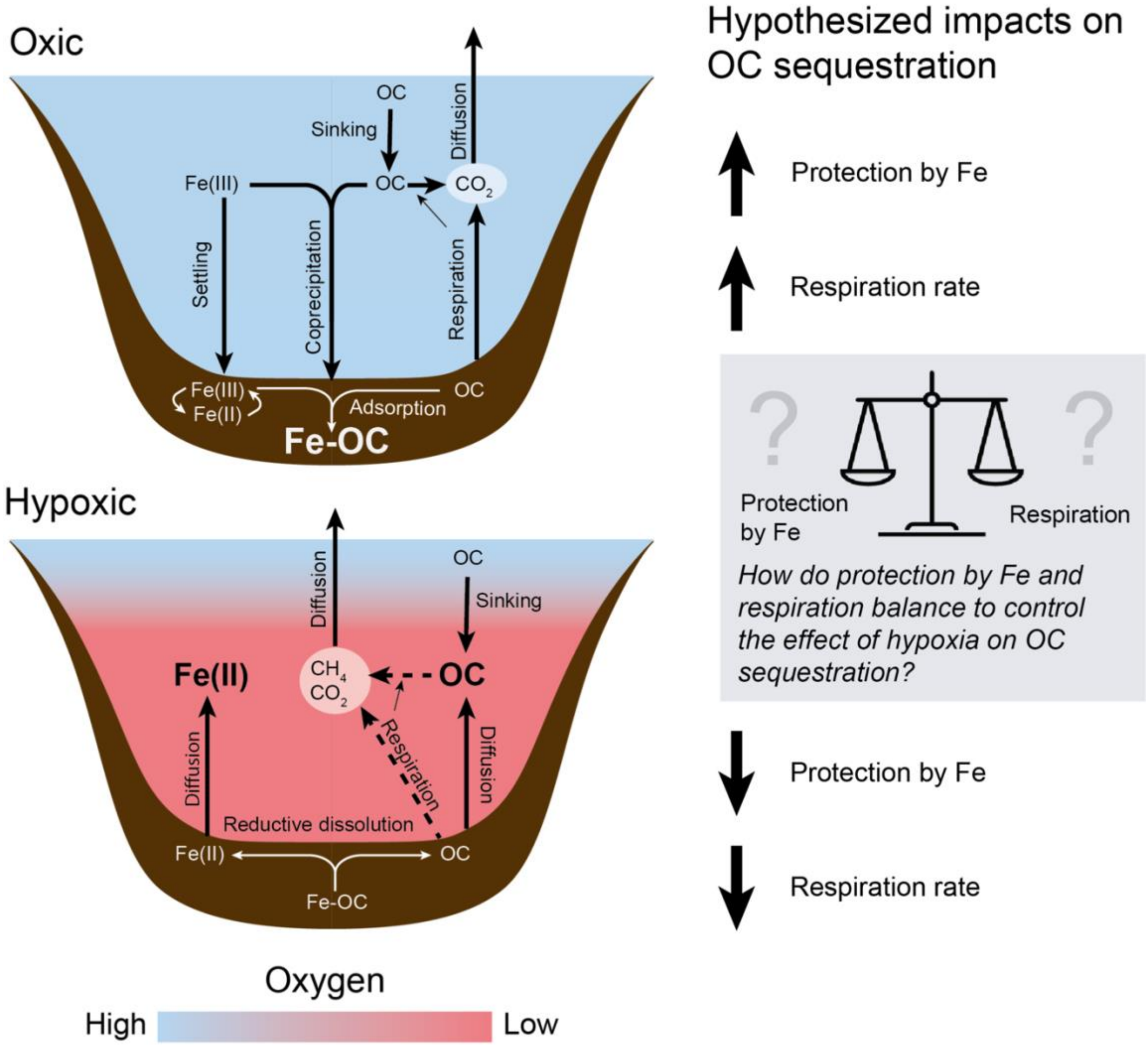

Figure 1: Conceptual diagram describing the hypothesized effects of changing oxygen conditions on coupled iron (Fe) and organic carbon (OC) interactions in a lake or reservoir. Under oxic conditions (top), complexation of Fe and OC (both through coprecipitation and adsorption) leads to increased concentrations of Fe-OC in sediments (increased Fe-OC protection), though oxic conditions may also lead to increased OC respiration rates. Under hypoxic conditions, reductive dissolution of Fe(III) in Fe-OC

complexes increases dissolved concentrations of Fe(II) and OC in the water column while decreasing the amount of Fe-OC in sediment (decreasing Fe-OC protection), though hypoxia may also decrease OC respiration rates. The net effect of these processes on OC sequestration remains unknown, motivating this study. This figure is a simplification of complex interactions happening on a whole-ecosystem scale, and focuses on hypothesized dominant processes operating on the timescale of days to years.

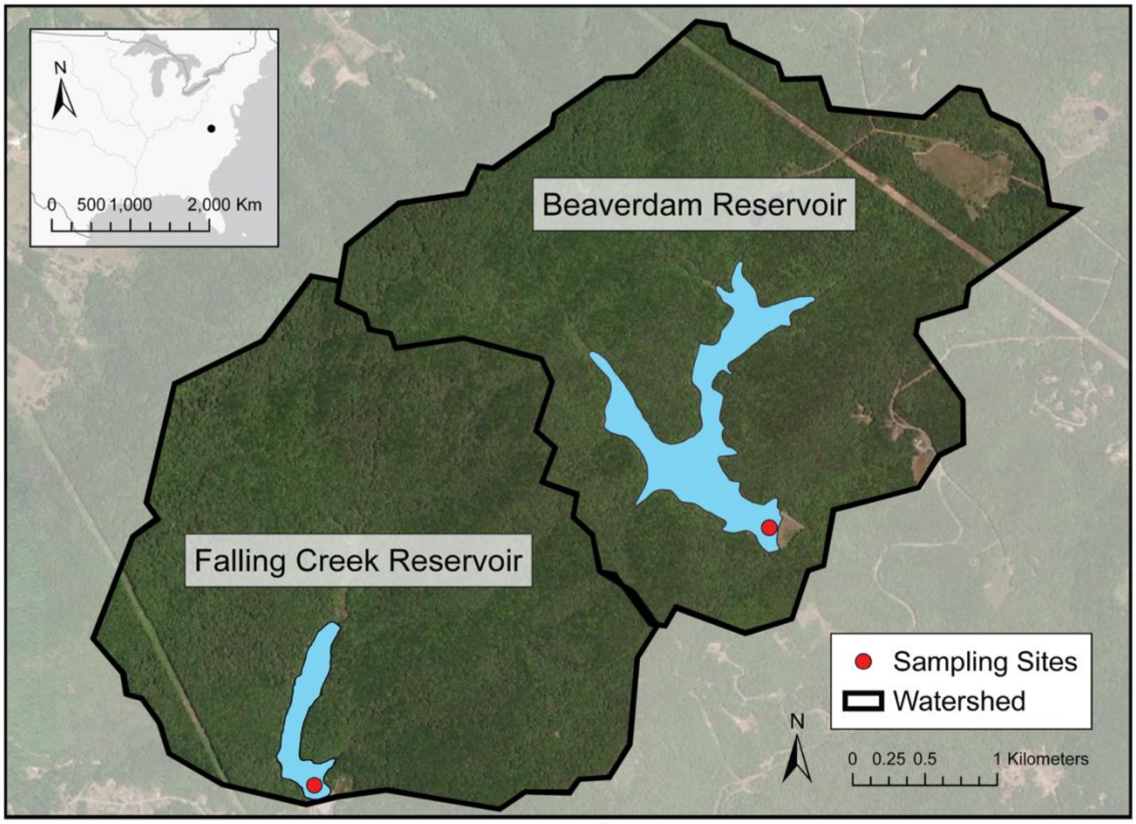

Source: Esri, Maxar, Earthstar Geographics, and the GIS User Community

Figure 2: Falling Creek Reservoir (FCR; 37.30ºN, 79.84ºW) and Beaverdam Reservoir (BVR; 37.31ºN, 79.81ºW) are eutrophic drinking water reservoirs located in southwest Virginia, USA (data from Carey, Lewis, Howard et al. 2022, following Woelmer et al. 2022).

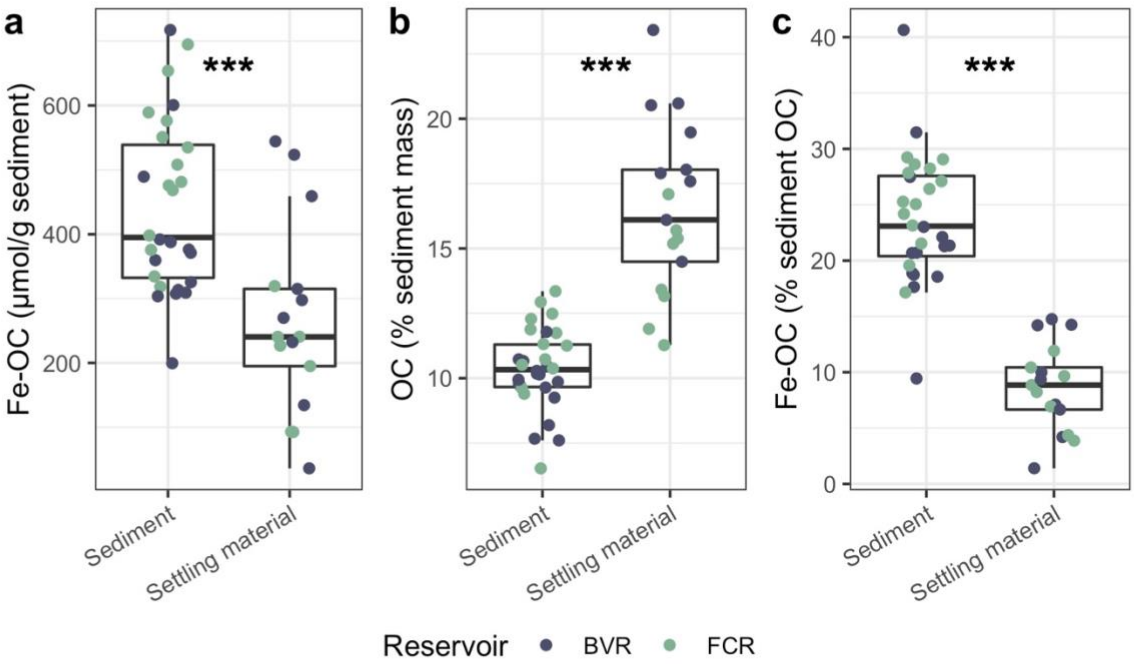

Figure 3: Iron-bound organic carbon (Fe-OC; a), total sediment organic carbon (b), and Fe-OC as a percentage of sediment OC (c) all differed significantly between surficial sediment and settling particulate matter. Asterisks indicate statistical significance of the difference between surficial sediment and sediment traps: *** indicates $p < 0.001$ (Welch's ANOVA). Note that only 2021 data are presented because settling particulate material was not collected in 2019.

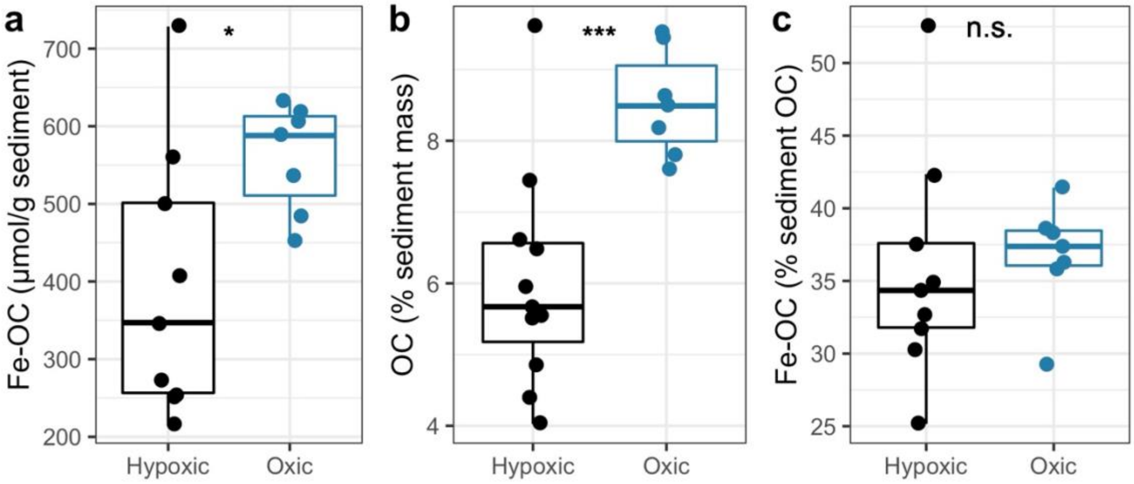

Figure 4: Iron-bound organic carbon (Fe-OC; a) and total organic carbon (b) in sediment were significantly higher under oxic compared to hypoxic conditions in Falling Creek Reservoir (FCR) during the summer stratified period of 2019. Fe-OC as a percentage of sediment OC did not differ significantly between hypoxic and oxic conditions. Here, oxic and hypoxic conditions are classified based upon mean oxygen levels during the two weeks preceding sampling (Figures 5, S4). Statistical significance of differences between oxic and hypoxic periods is indicated using asterisks: * indicates $p < 0.05$, *** indicates $p < 0.001$.

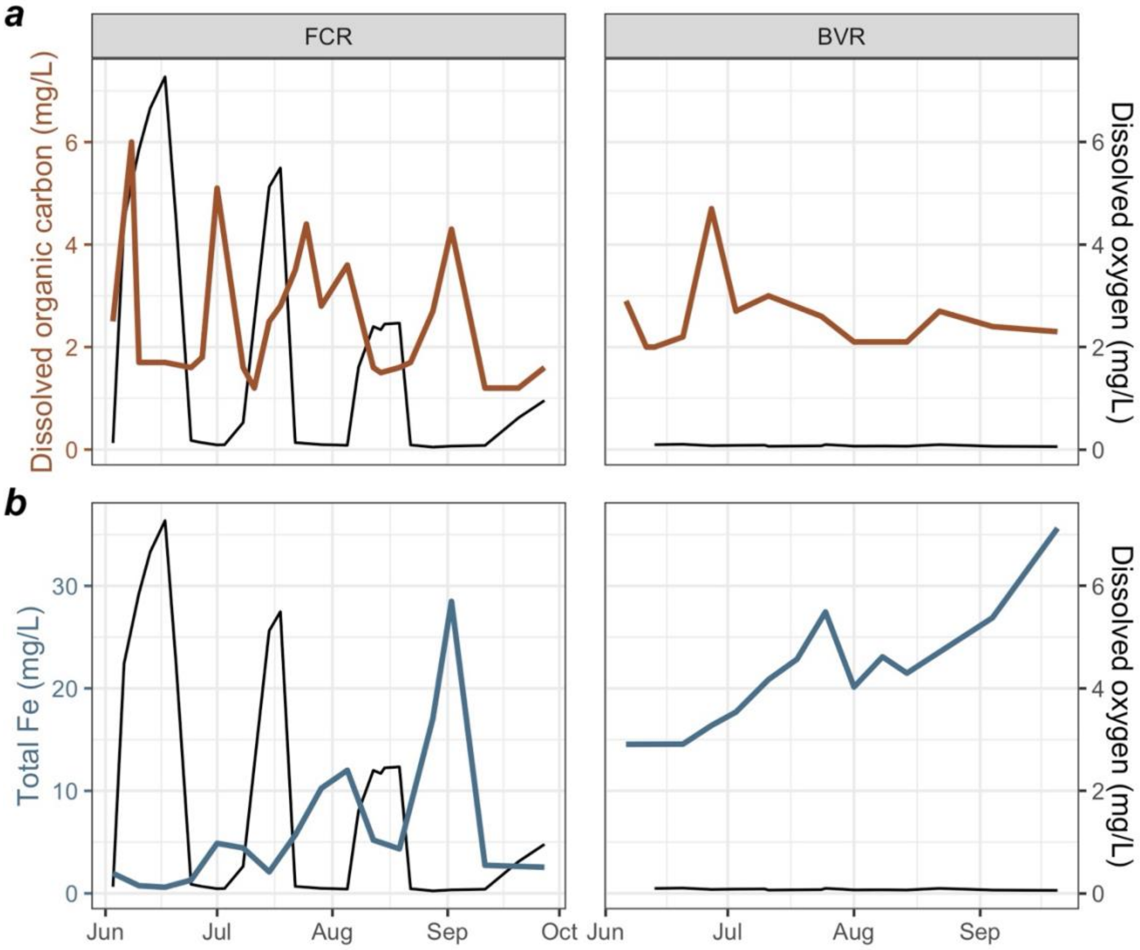

Figure 5: Increased dissolved oxygen concentrations (black lines) were associated with decreased dissolved organic carbon (brown lines; a) and total iron (Fe; slate blue lines; b) in the hypolimnia of Falling Creek Reservoir (FCR; left) and Beaverdam Reservoir (BVR; right) during the summer stratified period of 2019. All data presented are from the deepest sampling depth in each reservoir (9 m in FCR and 11 m in BVR).

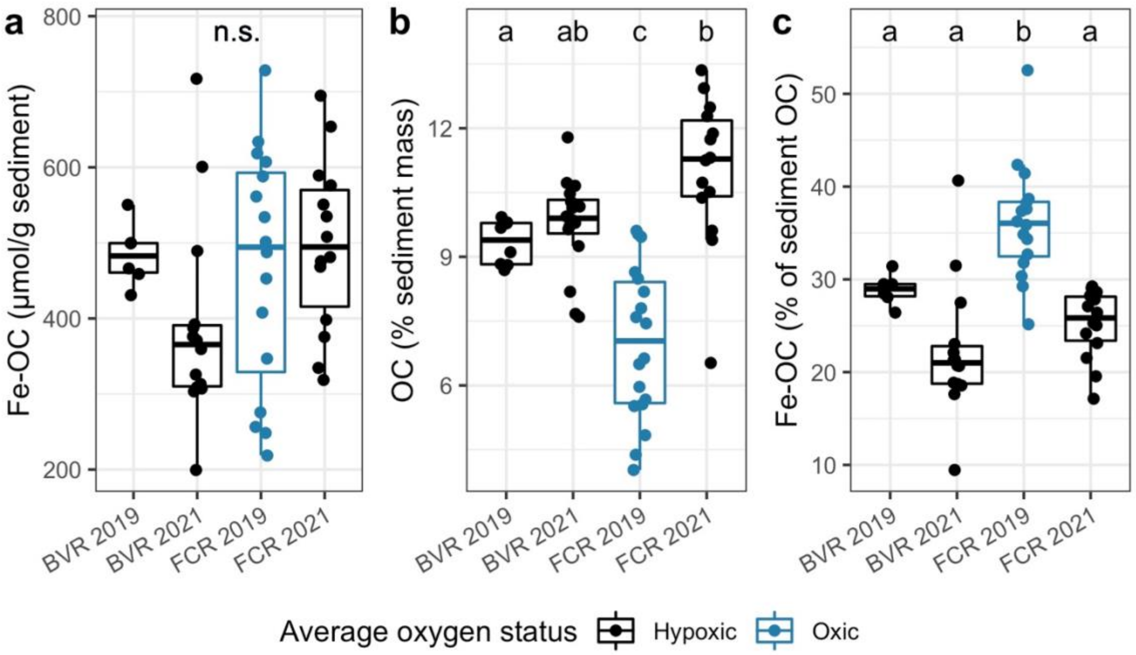

Figure 6: Sediment organic carbon metrics differed significantly in association with oxygen on a multiannual scale. Metrics assessed include iron-bound organic carbon (Fe-OC) (a), total sediment organic carbon (OC; b), and Fe-OC as a percentage of OC (c) in Falling Creek Reservoir (FCR) and Beaverdam Reservoir (BVR). Blue color indicates the reservoir-year with the highest mean oxygen (2019 in FCR) and letters delineate groups that are significantly different ($p < 0.05$; Table S1, S2, S3).

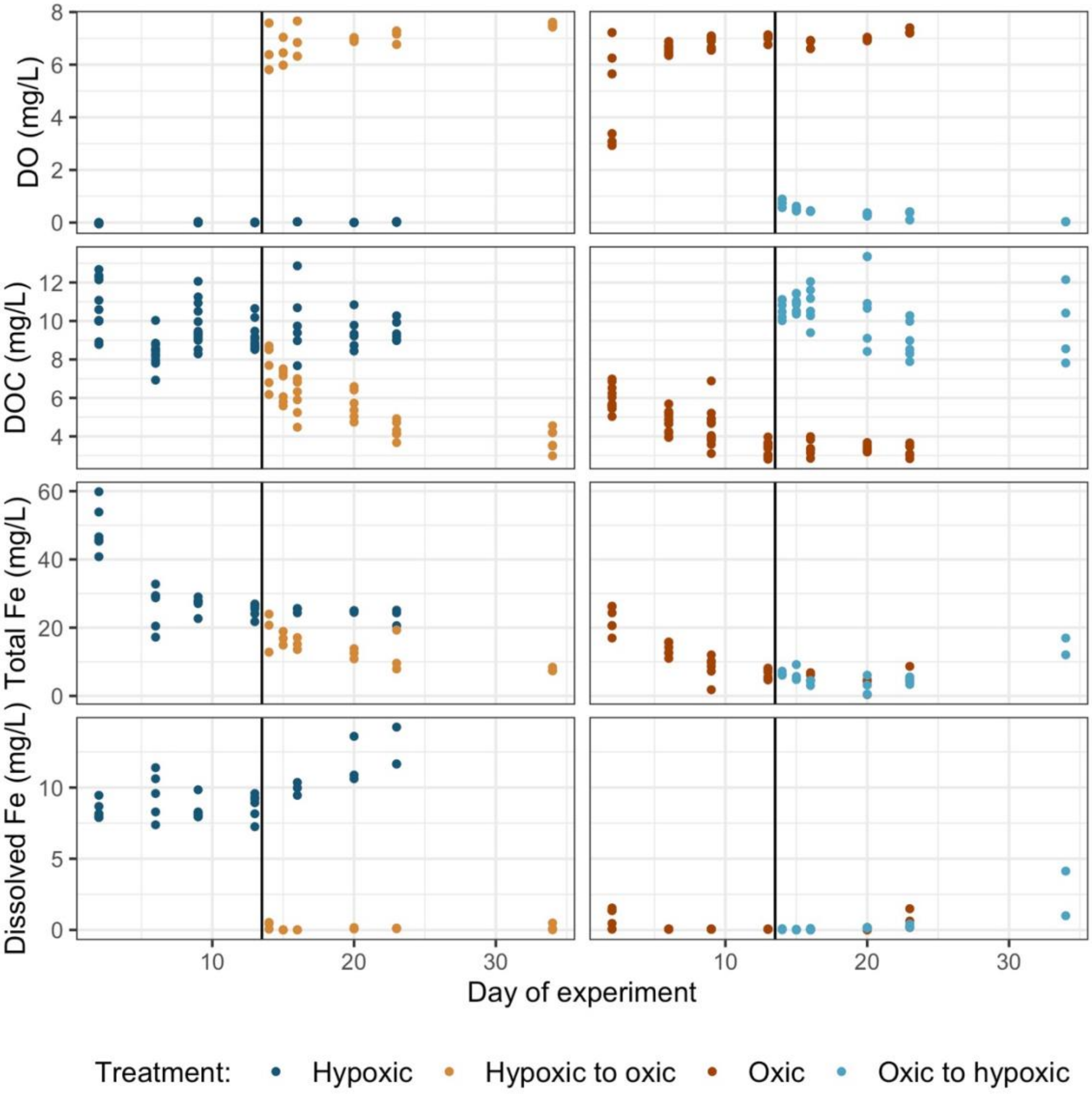

Figure 7: Varied oxygen regimes led to differences in water chemistry among experimental microcosm treatments. Metrics assessed include dissolved oxygen (DO), dissolved organic carbon (DOC), total iron (Fe), and dissolved Fe concentrations in microcosms that were sampled destructively over the course of 34 days. Vertical lines indicate when oxygen conditions were switched, creating the oxic-to-hypoxic and hypoxic-to-oxic treatments.

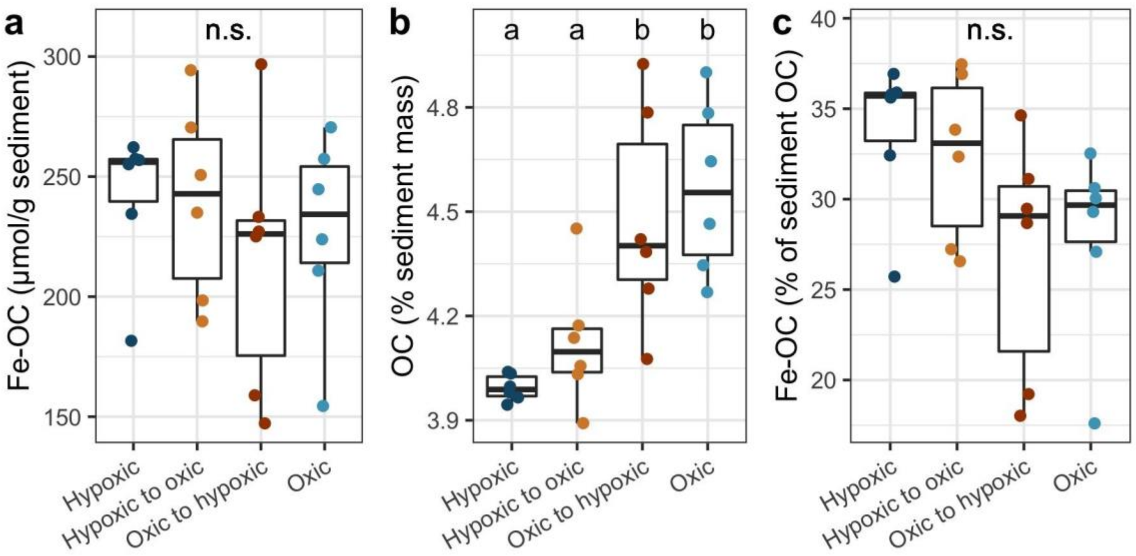

Figure 8: Experimental oxygen microcosm treatments altered some, but not all, sediment properties. Metrics assessed include moles of iron-bound organic carbon (Fe-OC) per unit sediment mass (a), total sediment organic carbon (b), and Fe-OC as a percentage of sediment OC (c). Letters delineate treatments that are significantly different ($p < 0.05$): no treatments were significantly different for Fe-OC metrics (a, c). Days 20 and 23 were chosen for statistical comparisons as the last days in the experiment when data were available from all treatments.

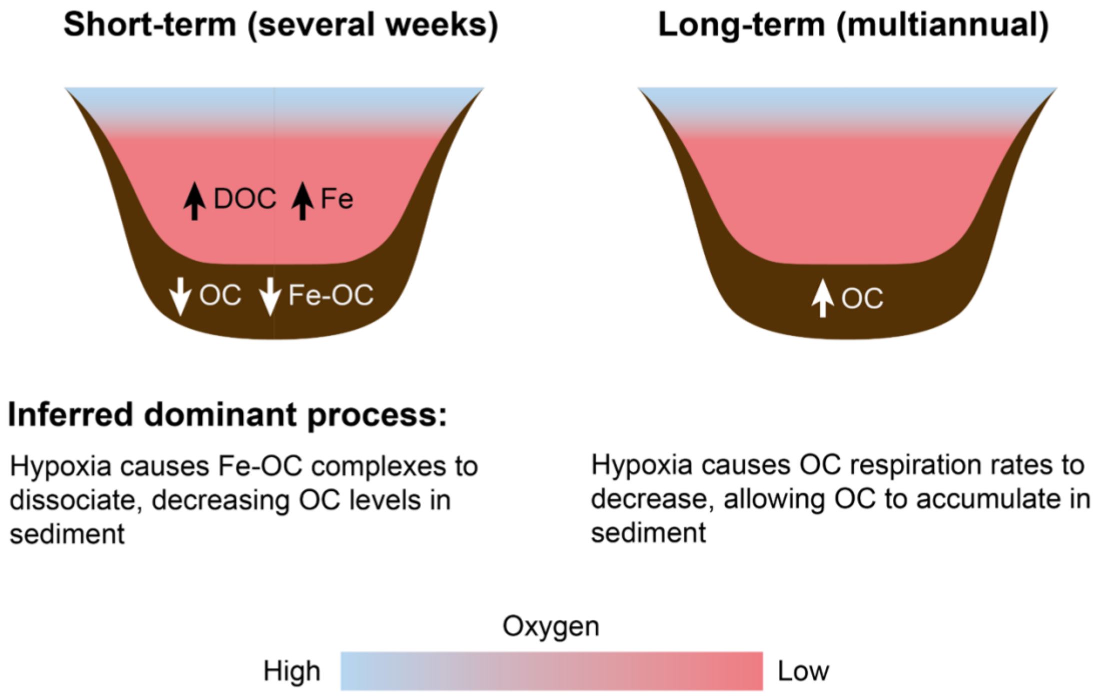

Figure 9: Experimental results suggest that the dominant process through which hypoxia affects sediment organic carbon differs between weekly and multiannual timescales. Left: in microcosm incubations, short-term (weeks) periods of hypoxia led to increased DOC and aqueous Fe, while decreasing sediment OC. On a whole-ecosystem scale, hypolimnetic Fe was closely correlated with oxygen concentrations, and short periods of hypoxia decreased both Fe-OC and OC in sediment. Consequently, Fe-OC protection appears to be a more dominant control on sediment OC sequestration than respiration on short timescales. Right: two years of summer hypoxia in FCR led to increased OC in sediment on a whole-ecosystem scale, suggesting that respiration may be a more dominant control on OC sequestration than protection by Fe on this timescale.

Supporting Information for Chapter IV

Contents

- Text S1
- Figures S1 to S7
- Tables S1 to S5

Introduction

This supporting information document includes one text section, seven figures, and five tables that are referenced throughout the manuscript.

Text S1: Description of the calculations used to account for mass loss during control and reduction treatments.

First, we calculated a correction factor based upon the difference between the initial dry mass of sediment added to the tubes (~100 mg) and the final mass of sediment remaining after extraction and drying (EQ 1). We then multiplied the mass of sediment used for CN analysis by this correction factor and added the product to the mass of sediment used for CN analysis again, yielding an estimate of what the total sample mass for CN analysis would have been if mass had not been lost during extractions (EQ 2). Next, we divided the measured OC mass from CN analysis by the corrected sediment mass and multiplied by 100 to get a corrected value for organic carbon as a percentage of sediment mass (EQ 3). To determine what percentage of sediment OC was associated with Fe (dithionite-extractable), we subtracted the corrected OC % in the reduction treatment from the corrected OC % in the control treatment, then divided by the OC % (uncorrected) in the initial sediment sample (EQ 4).

EQ 1:

$$correction\ factor = \frac{initial\ sediment\ mass - final\ sediment\ mass}{final\ sediment\ mass}$$

EQ 2:

$$\begin{aligned} &corrected\ sample\ mass \\ &\qquad = mass\ used\ for\ CN\ analysis\ (mg) \\ &\qquad + (mass\ used\ for\ CN\ analysis\ (mg) * correction\ factor) \end{aligned}$$

EQ 3:

$$corrected\ OC\ (\%) = \frac{measured\ OC\ (mg)}{corrected\ sed\ mass} * 100$$

EQ 4:

$$\text{Fe-OC (\%)} = \frac{corrected\ OC\ \%\ (control) - corrected\ OC\ \%\ (reduction)}{OC\ \%\ (initial)} * 100$$

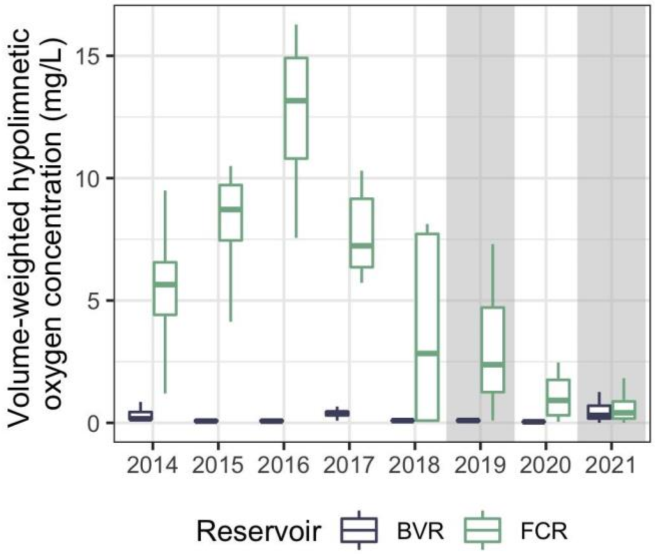

Figure S1. Volume-weighted hypolimnetic oxygen concentrations were higher during the summer stratified periods (June–September) of 2014–2019 than 2020 and 2021 in Falling Creek Reservoir (FCR). Volume-weighted summer hypolimnetic oxygen concentrations were near zero in Beaverdam Reservoir (BVR), the hypoxic reference reservoir. Boxplots present the median, 75th quartile, and 25th quartile of dissolved oxygen concentrations that have been interpolated to a daily timestep.

Figure S2. Photo illustrating experimental microcosm set-up, with visual differences between treatments on day 13 of the experiment. Left: an oxic microcosm. Right: a hypoxic (sealed) microcosm. Note that the oxic microcosm has an orange biofilm overlying sediment, suggestive of oxidized Fe, while sediments and water in the hypoxic microcosm are darker, suggestive of reduced Fe. Microcosm containers were 177 mL glass jars with two-piece gasket-sealed lids (Verones brand).

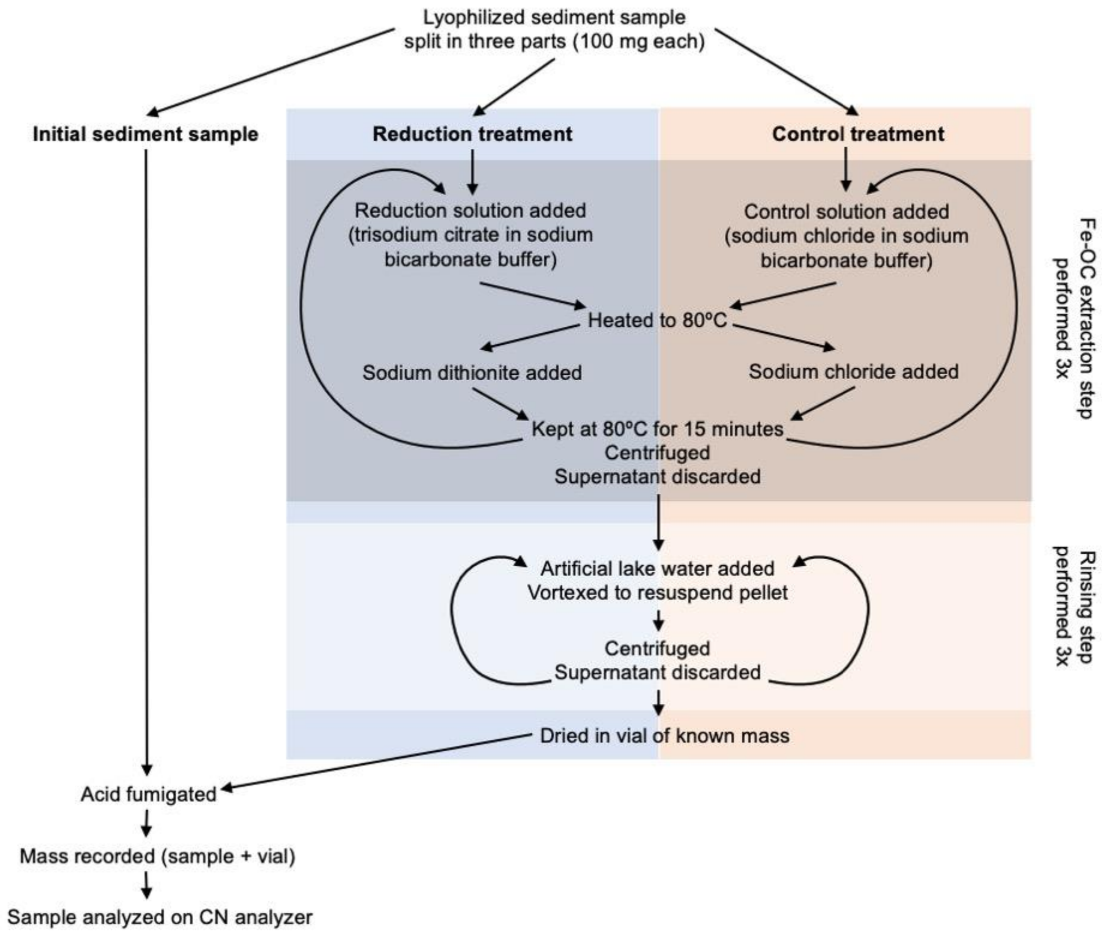

Figure S3. Conceptual workflow for the citrate Bicarbonate Dithionite (CBD) method of Fe-OC analysis. Lyophilized sediment samples were divided into three treatments: initial, reduction, and control. “Initial” samples were used to measure the OC content of the sediment. “Reduction” samples were treated with a metal-complexing agent (trisodium citrate) and reducing agent (sodium dithionite) in a buffered solution (sodium bicarbonate) to measure how much Fe and OC were released as a result of Fe reduction. Control samples were treated with sodium chloride and the same buffer to account for release of OC that resulted from processes other than Fe reduction. Methods are described in more detail in the main text.

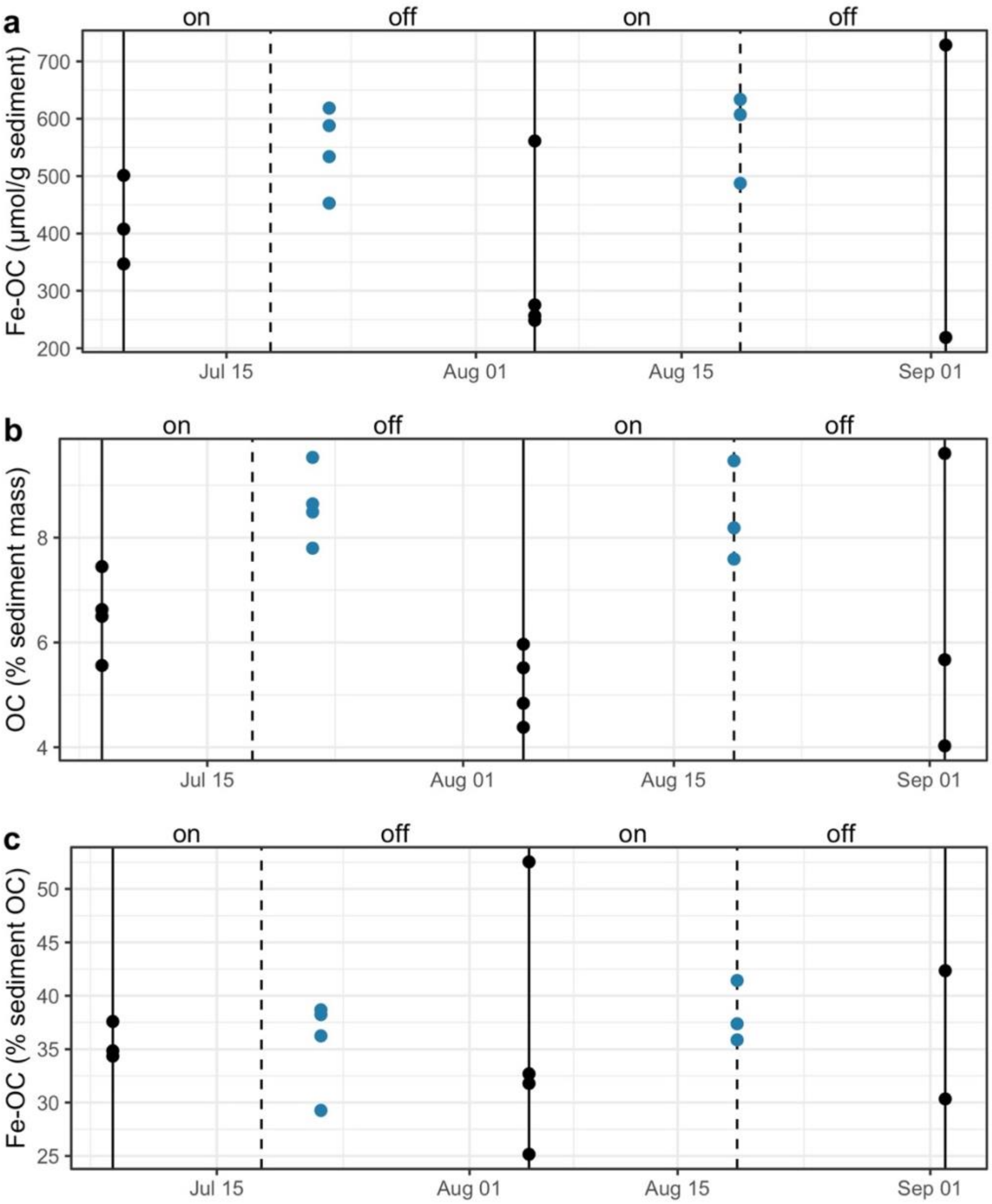

Figure S4. Intermittent operation of the hypolimnetic oxygenation system in Falling Creek Reservoir was associated with changes in sediment characteristics during the summer stratified period of 2019. Solid lines and dashed lines indicate activation and inactivation of the oxygenation system, respectively. Blue and black point colors indicate oxic and hypoxic conditions during the preceding two weeks, respectively. We note that on one occasion (mid-July), the oxygenation system shut off prematurely and sediment samples were collected three days after the oxygenated period—these samples still experienced oxic conditions during the preceding two weeks and are therefore classified as “oxic.”

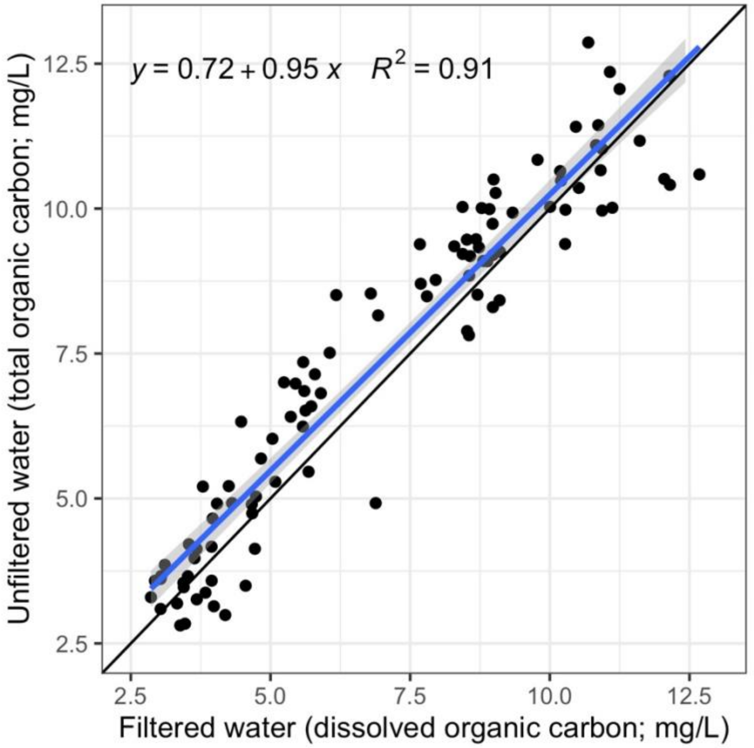

Figure S5. Measured dissolved organic carbon (DOC) and measured total organic carbon (TOC) were closely correlated in microcosm samples. The black diagonal line represents a 1:1 relationship between DOC and TOC. Linear regression results are shown by the blue line, with the equation and R^2 of the regression presented in the top right corner.

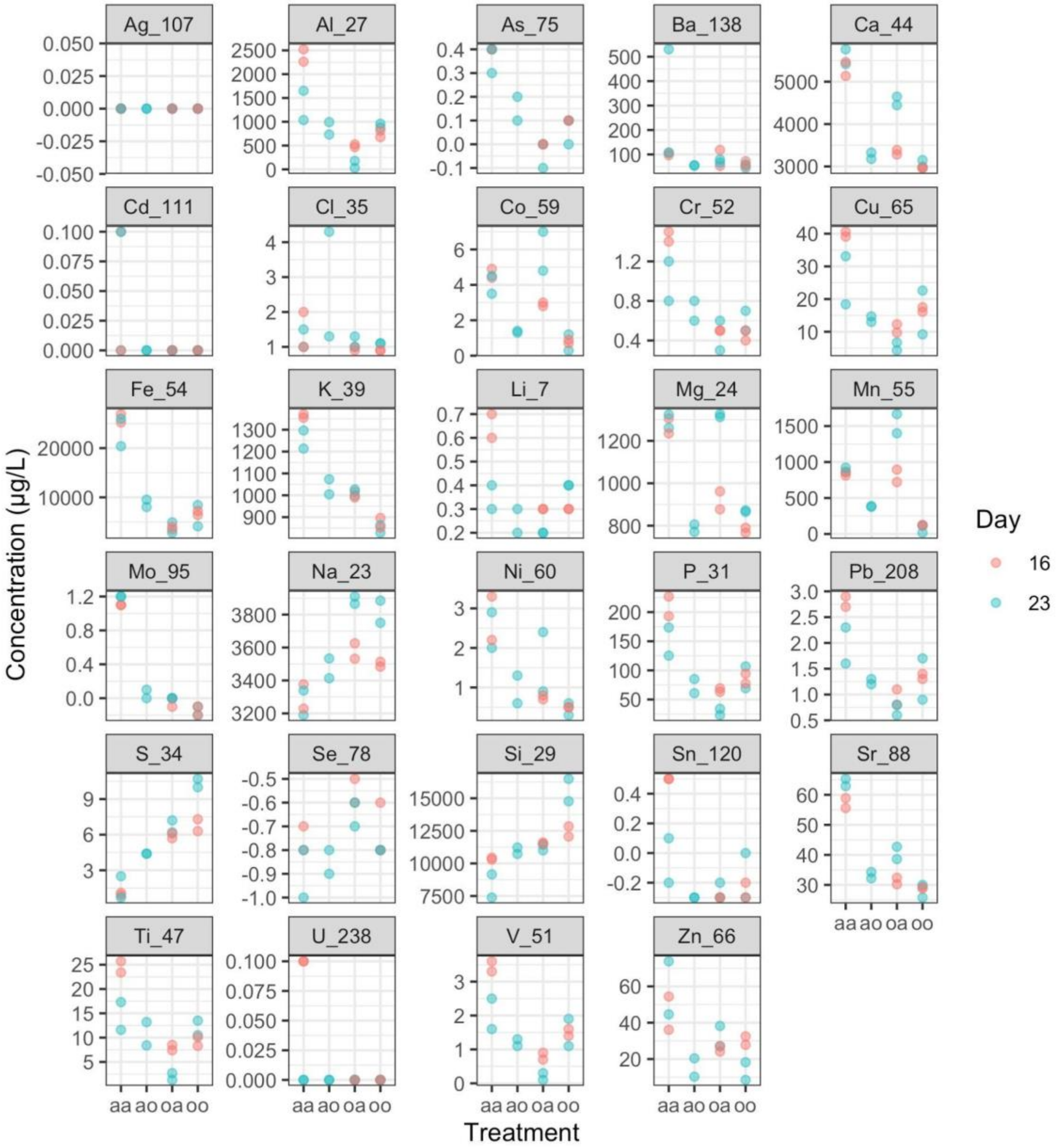

Figure S6. Experimental oxygen treatments led to differences in the concentrations of many elements. Data graphed here are unfiltered samples from microcosms sampled on day 16 (red) and 23 (blue). The x-axis represents experimental treatment, where aa = Hypoxic, ao = Hypoxic-to-oxic, oa = Oxic-to-hypoxic, and oo = Oxic. Each panel is labeled with the elemental abbreviation, followed by the isotope measured.

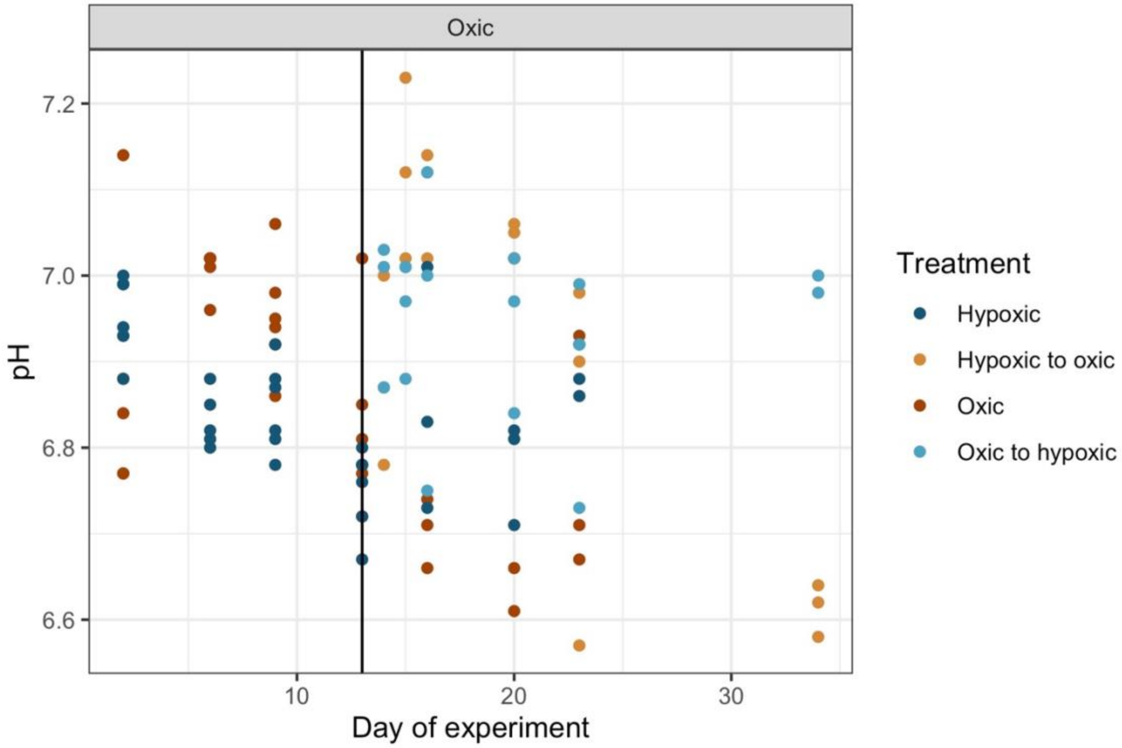

Figure S7. pH remained circumneutral (6.5 – 7.3) across all experimental treatments throughout the duration of the microcosm incubations. Vertical lines indicate when experimental treatments were switched, creating the Oxic-to-hypoxic and Hypoxic-to-oxic treatments.

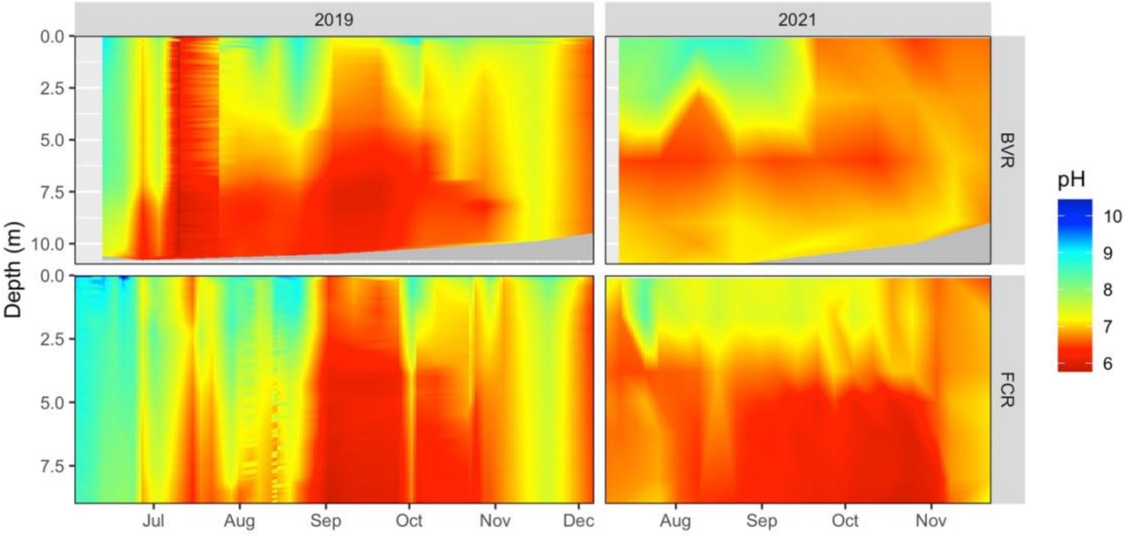

Figure S8. Hypolimnetic pH remained circumneutral (6–8) in the hypolimnia of both Beaverdam (BVR; top) and Falling Creek (FCR; bottom) Reservoirs throughout the duration of this study (2019 and 2021). Heatmaps present data from weekly (BVR) or twice-weekly (FCR) depth profiles that have been interpolated to a daily timestep and among measurement depths. In 2019, high-resolution (~1 cm interval) depth profiles were taken using a conductivity, temperature, and depth profiler (CTD; Sea-Bird, Bellevue, Washington, USA). In 2021, pH measurements were taken at seven discrete depths in FCR (0.1, 1.6, 3.8, 5.0, 6.2, 8.0, and 9.0 m), which corresponded to the reservoir's extraction depths, and five depths in BVR (0.1, 3.0, 6.0, 9.0, and 11.0 m).

Table S1. Levene tests and ANOVA results describing differences in sediment characteristics between BVR in 2019, BVR in 2021, FCR in 2019, and FCR in 2021. Values in bold were statistically significant (p<0.05)

	Levene statistic	Levene p-value	Test used	F	df	ANOVA p-value
Fe-OC (% of sediment OC)	1.21	0.32	ANOVA	17.2	3, 46	< 0.001
OC (% of sediment mass)	3.69	0.017	Welch's ANOVA	14.6	3, 28	< 0.001
Fe-OC (µmol/g sediment)	2.21	0.10	ANOVA	1.8	3, 46	0.16

Table S2. Games Howell post-hoc tests analyzing differences in sediment OC (% of sediment mass) among reservoir-years. Values in bold were statistically significant ($p<0.05$).

Comparison	Difference	Lower 95% CI	Upper 95% CI	p-value
BVR 2019-BVR 2021	0.41	-0.51	1.34	0.61
BVR 2019-FCR 2019	-2.34	-3.62	-1.06	<0.001
BVR 2019-FCR 2021	1.70	0.27	3.13	0.017
BVR 2021-FCR 2019	-2.75	-4.13	-1.37	<0.001
BVR 2021-FCR 2021	1.28	-0.23	2.80	0.12
FCR 2019-FCR 2021	4.04	2.32	5.76	<0.001

Table S3. Tukey post-hoc tests analyzing differences in Fe-OC (% of sediment OC) among reservoir-years. Values in bold were statistically significant (p<0.05)

Comparison	Difference	Lower 95% CI	Upper 95% CI	p-value
BVR 2021-BVR 2019	-6.61	-13.94	0.73	0.09
FCR 2019-BVR 2019	7.28	0.08	14.47	0.046
FCR 2021-BVR 2019	-3.73	-11.06	3.61	0.53
FCR 2019-BVR 2021	13.89	8.39	19.39	<0.001
FCR 2021-BVR 2021	2.88	-2.80	8.56	0.54
FCR 2021-FCR 2019	-11.00	-16.50	-5.51	<0.001

Table S4. Levene tests assessing homogeneity of variance among microcosm treatments at the end of the experiment (days 20 and 23)

	df	Levene statistic	Levene p-value
Fe-OC (% of sediment OC)	3, 20	0.39	0.76
OC (% of sediment mass)	3, 20	2.81	0.07
Fe-OC (µmol/g sediment)	3, 20	0.51	0.68

Table S5. Log activity of Fe species in each of four treatments on day 23 of the microcosm experiments. Speciation calculations were conducted using SPECE8 module of Geochemist's Workbench, using the wateq4 thermodynamic database. Bolded values show the top 5 highest activities for each condition.

	Hypoxic	Hypoxic to oxic	Oxic to hypoxic	Oxic
Fe^{2+}	-3.7599	-14.9723	-14.0942	-14.223
$FeHCO_3^+$	-4.8094	-16.7332	-15.5919	-16.0846
$FeCO_3$	-5.8983	-17.7821	-16.6208	-17.3635
$FeOH^+$	-6.3186	-17.5723	-16.6742	-17.053
$FeSO_4$	-6.4408	-17.1044	-15.9887	-15.9106
$Fe(OH)_2^+$	-7.1404	-6.1546	-5.7579	-5.632
$Fe(OH)_3$	-7.2287	-6.1446	-5.7279	-5.852
$FeCl^+$	-8.0724	-18.7584	-18.4746	-18.4399
$Fe(OH)_4^-$	-9.4087	-8.2846	-7.8479	-8.222
$FeOH^{2+}$	-10.5786	-9.5746	-9.1979	-8.822
$Fe(OH)_2$	-10.6099	-21.7423	-20.8242	-21.453
$FeHumate^+$	-11.2688	-10.6659	-9.8711	-9.7085
$FeHSO_4^+$	-12.483	-23.1866	-22.0909	-21.7628
$Fe(OH)_3^-$	-14.1799	-25.2723	-24.3342	-25.213
Fe^{3+}	-15.2486	-14.2846	-13.9278	-13.302
$FeSO_4^+$	-16.1395	-14.6267	-14.0324	-13.1996
$FeCl^{2+}$	-18.2211	-16.7307	-16.9682	-16.1788
$Fe_2(OH)_2^{4+}$	-19.7273	-17.7192	-16.9657	-16.214
$Fe(SO_4)_2^-$	-19.7305	-17.6688	-16.8369	-15.7972
$FeCl_2^+$	-22.0236	-20.0068	-20.8385	-19.8857
$FeHSO_4^{2+}$	-22.5717	-21.0989	-20.5246	-19.4418
$Fe_3(OH)_4^{5+}$	-24.6059	-21.5538	-20.4036	-19.5259
$FeCl_3$	-27.476	-24.9329	-26.3589	-25.2426
$Fe(HS)_2$	-85.2473	-290.9054	-281.5707	-288.86
$Fe(HS)_3^-$	-128.4289	-300	-300	-300

Chapter V: Increased adoption of best practices in ecological forecasting enables comparisons of forecastability

Abigail S. L. Lewis[1], Whitney M. Woelmer[1], Heather L. Wander[1], Dexter W. Howard[1], John W. Smith[2], Ryan P. McClure[1], Mary E. Lofton[1], Nicholas W. Hammond[3], Rachel S. Corrigan[4], R. Quinn Thomas[4], Cayelan C. Carey[1]

[1]Department of Biological Sciences, Virginia Tech, Blacksburg, Virginia, USA

[2]Department of Statistics, Virginia Tech, Blacksburg, Virginia, USA

[3]Department of Geosciences, Virginia Tech, Blacksburg, Virginia, USA

[4]Department of Forest Resources and Environmental Conservation, Virginia Tech, Blacksburg, Virginia, US

Published in *Ecological Applications* with the citation:

Lewis, A. S. L., W. M. Woelmer, H. L. Wander, D. W. Howard, J. W. Smith, R. P. McClure, M. E. Lofton, N. W. Hammond, R. S. Corrigan, R. Q. Thomas, and C. C. Carey. 2022. Increased adoption of best practices in ecological forecasting enables comparisons of forecastability. Ecological Applications 32(2):e02500. 10.1002/eap.2500

Abstract

Near-term iterative forecasting is a powerful tool for ecological decision support and has the potential to transform our understanding of ecological predictability. However, to this point, there has been no cross-ecosystem analysis of near-term ecological forecasts, making it difficult to synthesize diverse research efforts and prioritize future developments for this emerging field. In this study, we analyzed 178 near-term (≤10-year forecast horizon) ecological forecasting papers to understand the development and current state of near-term ecological forecasting literature and compare forecast accuracy across scales and variables. Our results indicate that near-term ecological forecasting is widespread and growing: forecasts have been produced for sites on all seven continents and the rate of forecast publication is increasing over time. As forecast production has accelerated, a number of best practices have been proposed and application of these best practices is increasing. In particular, data publication, forecast archiving, and workflow automation have all increased significantly over time. However, adoption of proposed best practices remains low overall: for example, despite the fact that uncertainty is often cited as an essential component of an ecological forecast, only 45% of papers included uncertainty in their forecast outputs. As the use of these proposed best practices increases, near-term ecological forecasting has the potential to make significant contributions to our understanding of forecastability across scales and variables. In this study, we found that forecastability (defined here as realized forecast accuracy) decreased in predictable patterns over 1–7 day forecast horizons. Variables that were closely related (i.e., chlorophyll and phytoplankton) displayed very similar trends in forecastability, while more distantly related variables (i.e., pollen and evapotranspiration) exhibited

significantly different patterns. Increasing use of proposed best practices in ecological forecasting will allow us to examine the forecastability of additional variables and timescales in the future, providing a robust analysis of the fundamental predictability of ecological variables.

Introduction

Nearly 90 years ago, Hodgson (1932) published what was arguably the first near-term ecological forecast, using demographic trends to predict herring age structure one year into the future. Hodgson concluded by stating "... we hope that before long these prognostications will be issued with the same confidence as those which are broadcast daily by the Meteorological Office, and, once they are received with confidence by the trade, they should be of considerable financial value" (p. 118). During the past 90 years, advances in data availability, computational power, and statistical methodologies have enabled a substantial increase in the development and application of near-term ecological forecasts (Luo et al. 2011, Petrovskii and Petrovskaya 2012, Hampton et al. 2013, LaDeau et al. 2017). Near-term ecological forecasting has become an increasingly powerful tool for ecological decision support (Dietze 2017a, Henden et al. 2020, Carey et al. 2021) and has the potential to provide new insights into fundamental questions about ecological functioning and predictability (Petchey et al. 2015, Dietze 2017b, Dietze et al. 2018). However, to this point, there has been no systematic analysis of the development or current state of near-term ecological forecasting literature, making it difficult to synthesize diverse research efforts and prioritize future developments for this emerging field.

Throughout the development of near-term ecological forecasting, there have been numerous calls for the adoption of standardized best practices (e.g., Clark et al. 2001, Pielke and Conant 2003, Harris et al. 2018, Dietze et al. 2018, White et al. 2019, Hobday et al. 2019, Carey et al. 2021). Developing and adhering to best practices advances the contributions of forecasting to both basic and applied research, as it allows for comparisons of forecast accuracy across forecast horizons (the amount of time into the future for which predictions are made) and increases the reliability of forecast products as decision support tools (Armstrong 2001). Recent interest in establishing best practices for ecological forecasting follows similar efforts in meteorology and economics, disciplines in which forecasting is well-established (Armstrong 2001, Hyndman and Athanasopoulos 2018).

While proposed best practices for near-term ecological forecasting differ among papers, a number of common themes related to forecast development, assessment, archiving, and decision support can be identified (Box 1; Appendix S1). As ecological forecasting has developed over the past several decades, we expect that adherence to these proposed best practices is increasing. However, without a comprehensive review of published ecological forecasts, it is difficult to assess which of the proposed best practices have been adopted and which should be prioritized for further advancement of the field (e.g., see Payne et al. 2017 for marine ecological forecasting). Ideally, best practices should evolve using a community-driven approach to enable buy-in and robustness to many applications (following Hanson et al. 2016); consequently, the list of proposed best practices in Box 1 is not exhaustive, and some of the practices may not be appropriate for every forecasting application. However, these practices provide a framework to begin analyzing the state of the field.

Adoption of these proposed best practices in near-term ecological forecasting may be particularly important to improving our understanding of forecastability across scales and variables. As the number of published near-term ecological forecasts has increased over the past several decades (Luo et al. 2011, Dietze et al. 2018), we now have an unprecedented opportunity to compare across studies and analyze the relative forecastability (defined here as realized forecast accuracy) of environmental variables at varying forecast horizons. Understanding ecological predictability is a fundamental goal in ecology (e.g., Gleason 1926, Clements 1936, Sutherland et al. 2013, Godfray and May 2014, Houlahan et al. 2017, and references therein) and provides valuable information regarding the nature of ecological processes (Petchey et al. 2015). Ecological forecasting can be a particularly powerful test of predictability, as forecasting requires predicting beyond the range of observed data (Dietze et al. 2018). Thus, comparisons of forecastability complement and extend existing theoretical and modeling-based work that has predicted how various factors (e.g., forecast horizon, computational irreducibility) influence the relative predictability of ecological variables (Beckage et al. 2011, Petchey et al. 2015).

In this study, we performed a systematic analysis of near-term ecological forecasting papers to examine the use of our proposed best practices over time (Box 1). To illustrate how proposed best practices can enable insights into fundamental ecological understanding, we then compared forecast accuracy across scales and variables. We discuss the implications of our findings for further development and adoption of best practices within the near-term ecological forecasting research community.

Methods

We systematically reviewed literature on near-term ecological forecasting to determine how proposed best practices have been implemented over time and compare forecastability across ecosystems. First, we searched the Web of Science^{TM} Core Collection [v.5.34] database (Clarivate Analytics, Philadelphia, USA) and reviewed abstracts to identify papers that reported near-term ecological forecasts (described in *Literature search* below). Two reviewers then independently read and analyzed each selected paper using a standardized matrix of criteria (*Matrix analysis*) and recorded forecast accuracy when reported. Once collated, we analyzed the full dataset to understand the development and current state of ecological forecasting (*Dataset description* and *Assessment of forecasting best practice adoption*). Finally, we analyzed forecast evaluation data to assess how forecast performance varied with forecast horizon for ecological variables with sufficient data (*Comparing forecast accuracy across ecosystem and models*).

Literature search

Creating an all-encompassing search query to identify near-term ecological forecasts presented three challenges: first, the term “near-term” was neither universally defined nor used in all papers that report near-term forecasts; second, there was no one search term that can match all papers describing ecological variables; and third, many papers used the word “forecast” when talking about implications of their research, despite not actually reporting forecasting results in the paper. To address these challenges, we began by querying the Web of Science Core Collection [v.5.34] for “forecast*” in the title, abstract, or keywords of papers published in 301 ecological journals, then manually screened abstracts of all resulting papers. We conducted the Web of Science search on 18 May 2020 and limited the search to articles and proceedings papers (hereafter, ‘papers’) published in English. This yielded 2711 results (Figure 1).

We screened the abstracts of all 2711 papers and selected those that met three criteria:

1. Papers had to include at least one forecast, which we defined as a prediction of future conditions from the perspective of the model; forecasts could be developed retroactively (i.e., “hindcasts”) but could only use driver data that were available before the forecast date (e.g., forecasted or time-lagged driver variables).
2. The forecast had to be near-term, which we defined as predicting ≤10 years into the future (following Dietze et al. 2018).
3. The forecast had to be ecological, which we defined as predicting a biogeochemical, population, or community response variable. This definition therefore excluded physical (e.g., streamflow or water temperature) and meteorological forecasts. Forecasts of human disease were only included if there was an animal vector.

If the abstract indicated that the paper met all three criteria, it was moved to the second round of screening. Here, a second reviewer read the full paper to ensure that at least one forecast in the paper met all three criteria.

By the end of this screening process, we identified 142 near-term ecological forecasting papers out of the 2711 Web of Science results (Figure 1a, 1b). The initial Web of Science search did well at identifying studies with ecological focal variables, as 74% of the initial search results were marked as 'ecological' during our review process. However, only 36% of papers from this search actually included forecasts (predicting future conditions from the perspective of the forecast model). Furthermore, of the ecological forecasts identified in this search (n = 669), only 21% met our near-term criteria by including forecast horizons that were ≤10 years; the majority of forecasts predicted ecological changes over multidecadal timescales (Figure 1b).

Because ecological forecasts may be published in journals that are not categorized as “ecological” by Web of Science, we then searched all papers that were cited by the 142 near-term ecological forecast papers we identified, as well as all papers that cited these studies. From the citing and cited papers, we selected those that were published in English and included “forecast*” in the title, abstract, or keywords, then screened the abstracts using our three criteria described above. Finally, a second reviewer read all papers that passed the abstract screening to confirm that at least one forecast in the paper met all three criteria. Searching the papers that cite and are cited by the near-term ecological forecasting papers from our initial search yielded proportionally more ecological forecasting papers than the initial Web of Science search. Of the 472 search results, 112 (24%) of these papers were identified as near-term ecological forecasts after two rounds of review (Figure 1a, 1c). Furthermore, this search highlighted predominantly near-term forecasts; 73% of the ecological forecasts identified in this search included forecast horizons that were ≤10 years (Figure 1c). After combining our initial search with the citing and cited papers, 254 papers were included in our dataset for matrix review (Figure 1a).

Matrix analysis

We analyzed each of the 254 papers using a standardized matrix of questions (Appendix S2). This matrix was co-developed over several months of iteration and discussion by all authors within an Ecological Forecasting graduate seminar at Virginia Tech (January–May 2020). The final matrix used for this study included 58 fields of information about the forecast paper's model(s), evaluation, cyberinfrastructure, archiving, and decision support (Lewis et al. 2021).

During the graduate seminar, we read and analyzed 10 papers as a group, ensuring that all reviewers understood how to interpret and answer questions in a consistent manner. Prior to the start of this analysis, reviewers also screened several papers independently and checked their responses with another reviewer, helping to ensure consistency between reviewers. For the matrix analysis described in this paper, all 254 papers were read and analyzed independently by two reviewers, and reviewers then compared any differing answers to reach consensus on a final set of responses for each paper.

During the matrix analysis, 76 papers were determined to not meet our criteria of being near-term ecological forecasts, despite having passed the initial rounds of screening. These papers typically used one or more data sources that became available after the forecast issue date, which was difficult to identify without reading the entire text, including all supplementary information, in detail. These papers were excluded from the analysis, leaving 178 papers in the final dataset (Figure 1a).

Dataset description

To characterize the current state of near-term ecological forecasting, we began by analyzing the distribution of forecasts presented in the 178 papers across geographical locations, variables, and time scales, as described below.

We classified the spatial scale of each forecast into five categories: point (localized to one discrete site, such as pollen forecasts for a city or algal forecasts for a lake), multipoint (several distinct forecast locations, such as three different lakes), regional (localized to a broad geographic region, such as coral bleaching forecasts that span a sea), national (spanning all of one nation, such as nationwide production of an agricultural crop), or global (such as coral bleaching stress in world oceans), and we calculated the percentage of forecasting papers within each of these categories. We recorded latitude and longitude of the forecast site(s) for point or multipoint forecasts or of the approximate centroid of the site for regional and national forecasts.

Forecast variables were divided into two categories: organismal (population and community; e.g., white-tailed deer populations) and biogeochemical (e.g., evapotranspiration), and each paper was classified within one of 11 ecosystem types: forest, grassland, freshwater, marine, desert, tundra, atmosphere, agricultural, urban, global, other, where "other" included any ecosystem types that could not be classified within one of the other 10 categories (e.g., plant phenology across the entire United States). We recorded the number of years of data used to create each forecasting paper (summed across model development, training, evaluation, etc.) and calculated the percentage of papers that used long-term datasets in their analysis, using the definition of long-term as any dataset with more than 10 years of data (Lindenmayer et al. 2012).

Assessment of forecasting best practice adoption

We synthesized proposed best practices for ecological forecasting from four recent papers—Harris et al. (2018), Hobday et al. (2019), Carey et al. (2021), and White et al. (2019), then selected all practices that were mentioned in at least two of these papers (Appendix S1). To analyze how adherence to the nine selected best practices has changed over time, we performed binary logistic regressions assessing how adoption of each best practice (binary yes/no) varied with publication year. Hodgson (1932) was excluded from this best practice analysis as a temporal outlier, leaving a dataset of papers published between 1980 and 2020. We used the following criteria in the matrix analysis to assess which proposed best practices (Box 1) were included in each forecasting paper:

Forecast Requirements

1. "Include uncertainty": uncertainty was included in forecast outputs
2. "Report forecast accuracy": any form of forecast evaluation was reported (this includes Figures that compare forecasts and observations, as well as any evaluation metric)

Decision Support

3. "Identify an end user": A specific end user was mentioned
4. "Make iterative forecasts": Forecasts were made repeatedly, incorporating new data over time. For this practice, we included all types of data assimilation,

including those that only updated the initial conditions of the forecast. As a separate analysis, we also determined whether the use of data assimilation methods that updated the parameters of the model (not just initial conditions) have increased over time

5. "Automate forecasting workflows": at least one source of new driver and/or observation data was made available to the model in real time (<24 hours from collection) without any manual effort when the forecasting system was working as intended

Research

6. "Make data available": Data availability was specified
7. "Archive forecasts": Text specified that forecasts were archived and available
8. "Use null model comparisons": Forecasts were compared to a null model (e.g., a persistence or climatology null model)
9. “Compare modeling approaches”: At least two modeling approaches that have different model structures (not including null models) were compared

All analyses were performed using R version 4.0.3 (R Core Team 2020).

Comparison of forecast performance across scales and variables

To compare forecast performance across forecast variables, sites, and scales, it was necessary to identify an evaluation metric that is not dependent on the units or range of the forecast variable. For reasons discussed below, we chose R^2 as our metric of forecast performance in this analysis. Petchey et al. (2015) recommend using the length of time until a forecast performs no better than a relevant threshold value as one way of comparing between papers. However, this type of analysis would require that a threshold value be determined equitably for each forecast variable, which would be challenging across the numerous variables in our dataset. Performance of null models offers one objective way of determining these threshold values, but null models were not commonly reported in this dataset. Another means of comparing forecast performance would be to directly compare forecast accuracy using a standardized statistical score. Commonly used forecast evaluation metrics include root mean squared error (RMSE), mean absolute error (MAE), the coefficient of determination (R^2), and bias (Petchey et al. 2015, Dietze 2017a). To fully assess probabilistic forecasts, the continuous ranked probability score (CRPS) and ignorance can also be used (Roulston and Smith 2002, Gneiting et al. 2005). Among these, only R^2 allows comparisons between forecasts that have different native units or forecasts for the same variable in very different ranges. Furthermore, more papers reported Pearson's r or R^2 (n = 56, 42%) than any other forecast performance metric in this dataset: for comparison, only 34% included RMSE and 20% included MAE. While the fact that R^2 is typically bias-corrected makes it an imperfect metric of forecast performance, it remains widely reported and uniquely suited to inter-study comparisons.

We recorded all R^2 and Pearson's r data reported in papers in the dataset. Pearson's r values were squared to yield R^2 (following Rousso et al. 2020). We selected all forecast variables that had at least three papers and three forecast horizons represented, and we plotted forecast performance (in R^2) as a function of forecast horizon for these variables. To allow comparability between variables, we limited the analysis to forecast horizons between one and seven days, which were reported for all variables selected. Because some papers reported R^2 individually for each plot, site, or year and others reported one overall evaluation per model, we averaged all R^2 across sites and years for forecasts that used the same model within each paper.

We used indicator variable analysis (Draper and Smith 1998) to compare the slope of R^2 values over 1–7 day horizons among forecast variables by performing a 50% quantile regression that predicted R^2 based upon indicator ("dummy") predictors for all forecast variables, as well as terms for the interaction between all forecast variables and forecast horizon. Quantile regression was used rather than standard linear regression to account for heteroscedasticity and non-normal data distribution. The regression was performed using the package "quantreg" in R (Koenker et al. 2021). Indicator analysis compares the slope and intercept of the first indicator ("reference" indicator) to all subsequent indicators (Draper and Smith 1998). In this case, chlorophyll was used as the reference indicator to enable comparisons between phytoplankton and chlorophyll, two closely related forecast variables. We analyzed which terms were significant in the model to determine how patterns in forecast performance over time differed among forecast variables: significance was determined using the "wild" bootstrapping method to account for heteroskedasticity (Feng et al. 2011).

Results

Dataset description

The number of ecological forecasts published each year has increased substantially over time: more papers were published in the last seven years of the dataset (2014–2020) than in the first 82 years (1932–2013; Figure 2). Forecast sites for these papers were located on all seven continents (Fig 3a). The majority of forecast sites were located in the northern hemisphere (n = 211, 91%), especially the United States, China, and Western Europe (Figure 3a). The geographic scale of the forecasts was most often either point (n = 66, 37%), or regional (n = 66, 37%; Figure 3b).

More ecological forecasts predicted organismal (population and community) variables than biogeochemical variables. Very few papers included forecasts for both biogeochemical and organismal focal variables (organismal: n = 146, 82%; biogeochemical: n = 43, 24%; both: n = 11, 6%; Figure 3c). The majority of papers predicted ecological processes in either marine (n = 49, 28%), freshwater (n = 41, 23%), or agricultural (n = 34, 19%) ecosystems (Figure 3). In particular, many papers predicted fish taxa (n = 25), phytoplankton taxa (n = 20), chlorophyll (n = 14), evapotranspiration (n = 14), pollen (n = 10), and crop yield (n = 9).

Papers in this dataset included forecasts at a wide range of forecast horizons and were developed using diverse time steps, forecast horizons, and datasets. Among the forecasts surveyed in this analysis, 75% of papers predicted within one year into the future (n = 130; Figure 4). In particular, many papers either predicted 2–7 days into the future on a daily time step (n = 39, 23% of all papers) or one year into the future on a yearly time step (n = 30, 17%; Figure 4). The median temporal duration of data used to create a forecasting paper (summed over model development, training, evaluation, etc.) was 15 years (min. = 17 days, mean = 19.2 years, max. = 145 years; Figure 5), and 60% of papers (n = 107) used more than 10 years of data in the forecast paper.

The 178 papers included in this analysis were published in 114 unique journals and conference proceedings (103 journals, 11 conferences). The journal with the greatest number of papers represented in the dataset was *Ecological Applications*, which published a total of 14 near-term ecological forecasting papers.

Adoption of proposed best practices is low but increasing over time

Overall rates of best practice use are low but may be increasing. On average, papers used three of the proposed nine best practices (median and mode = 3, mean = 2.83), but there was considerable variation: seven papers did not use any of the best practices, and one paper used eight of the best practices. The percentage of papers that demonstrated a given best practice did not exceed 50% for any practice except “Report forecast accuracy” (Figure 6). All but one (“Use null model comparisons”) of our proposed best practices have been increasingly adopted over time. However, the increase in adoption with time was only statistically significant ($p < 0.05$) for three practices: “Automate forecasting workflows,” “Archive forecasts,” and “Make data available” (Figure 6; Table 1).

Of the *Forecast Requirement* best practices, “Include uncertainty” was demonstrated in 45% of papers and “Report forecast accuracy” was demonstrated in 75% of papers. Both of the *Forecast Requirement* best practices show a positive trend in adoption, though neither had a statistically significant relationship with publication year (Figure 6; Table 1). When uncertainty was included in forecasts (n = 80), the most commonly included uncertainty sources were observation uncertainty (48%), process uncertainty (40%), and parameter uncertainty (35%). Driver uncertainty was included in 23% of papers that report uncertainty, and initial condition uncertainty was included in 18%. Of the 80 papers that reported uncertainty, 55% did not specify a data-driven origin of this uncertainty (e.g., ensemble model parameters, forecasted meteorological driver data) in the text. Only three papers partitioned uncertainty sources (Caughlin et al. 2019, Geremia et al. 2014, Dietze 2017b), and all of these papers were published in or after 2014. All three papers quantified the influence of process, initial condition, and parameter uncertainty, and one partitioned driver uncertainty. Process uncertainty dominated total uncertainty for two papers (Geremia et al. 2014, Dietze 2017b), while initial condition uncertainty dominated in the third paper (Caughlin et al. 2019). Over 70% of forecasts that did not report forecast evaluation in the text (n = 44) predicted at forecast horizons of at least one year; in comparison, 47% predicted at forecast horizons of at least one year in the dataset as a whole. As noted in the Methods, the most commonly reported metric of forecast performance was R^2.

Overall, 20% of papers identified a specific end user, 39% of papers made iterative forecasts, and 11% of papers included automated forecasting workflows. All three of these proposed best practices ("Identify an end user", "Make iterative forecasts", "Automate forecasting workflows") in the *Decision Support* tier showed positive relationships with publication year, but only "Automate forecasting workflows" significantly increased over time (Figure 6, Table 1). Of the papers that mentioned a specific end user (n = 35), 31% mentioned that the end user aided in forecast development and 46% mentioned that forecasts were in use by the end user. Data assimilation for iterative forecasts most often updated initial conditions but not parameters of the model (67% of the 69 iterative forecasts only updated initial conditions). However, data assimilation methods that updated the parameters of the model (not just initial conditions) have increased significantly over time (Table 1).

Overall, there was a wide range in the percentage of papers that used *Research* tier best practices. “Make data available” was demonstrated in 25% of papers, “Archive forecasts” was demonstrated in 8% of papers, “Use null model comparisons” was demonstrated in 12% of papers, and “Compare modeling approaches” was demonstrated in 47% of papers. Two of the five *Research* tier practices have increased significantly over time (“Make data available” and “Archive forecasts”; Table 1). “Use null model comparisons” was the only practice that has decreased in adoption over time (Figure 6). For papers that described forecast archiving (n = 15), the most common repository for archived forecasts was Zenodo (used in 20% of papers that archive forecasts); other papers used websites or other archives specific to the forecasting project. Only two of the seven papers that mentioned archiving forecasts on a website had links that were still functional as of 14 Jun 2021. Of the papers that used null models in this study (n = 21), 62% used persistence null models and 48% used climatology null models. Two papers used both persistence and climatology null models. Of the papers that compared multiple modeling approaches (n = 84), a median of 3 different approaches were included (not including null models; mean = 5.4, max. = 49).

Declines in forecast performance over increasing forecast horizons differ between variables

Forecast accuracy data (R^2) from at least three papers on 1–7 day forecast horizons were available for four forecast variables: chlorophyll, phytoplankton taxa, pollen, and evapotranspiration (ET). Forecast performance decreased with increasing forecast horizon for all forecast variables (Figure 7, Table 2). The slope and intercept of forecast accuracy over increasing forecast horizons differed between variables, as revealed in our indicator analysis: the intercepts for pollen and ET were significantly lower than for chlorophyll, the reference indicator. In comparison to chlorophyll, forecast accuracy for pollen and ET decreased significantly more slowly over time. Unsurprisingly, the intercept and slope of phytoplankton were not significantly different from the intercept and slope of chlorophyll, the reference indicator (Figure 7, Table 2).

Discussion

Our systematic analysis of 178 near-term ecological forecasting papers demonstrates that the field of near-term ecological forecasting is widespread and growing: forecasts have been produced on all seven continents, and the rate of forecast publication is increasing over time. Although the overall implementation of proposed best practices is low, best practice use is increasing. In particular, the use of automated forecasting workflows, making data available, and archiving forecasts are all increasing significantly over time. We used this dataset of published studies to compare forecast accuracy across scales and variables, and we found that forecast accuracy decreased in consistent patterns over 1–7 day forecast horizons. Variables that were closely related (i.e., chlorophyll and phytoplankton) displayed very similar trends in predictability over increasing forecast horizons, while more distantly related variables (i.e., pollen, evapotranspiration) exhibited significantly different patterns.

Near-term ecological forecasting: state of the field

As publication of near-term ecological forecasts continues to accelerate, evaluating the state of the field now can provide critical insight to help prioritize areas of improvement moving forward. Below, we discuss aspects of near-term ecological forecasting that are well-developed, those that are improving over time, and areas that may need improvement based upon the results of this analysis.

Well-developed practices in near-term ecological forecasting: high rates of forecast assessment and model comparison

Only one out of the nine proposed best practices was demonstrated in more than half of the papers in this analysis: report forecast accuracy. In this study, high rates of forecast assessment and reporting allowed us to compare forecast performance across scales and variables. While R^2 was the most commonly reported forecast evaluation metric and served as an effective accuracy score for this preliminary analysis, it would be preferable to use a metric of forecast performance that is not bias-corrected. Other scale-independent metrics of forecast performance include percentage errors (e.g., mean absolute percentage error; MAPE) or scaled errors (e.g., mean absolute scaled error; MASE; Hyndman and Athanasopoulos 2018). Percentage errors are not universally applicable because they penalize a lack of precision more heavily in a range closer to zero (in the units of the forecast), which is not valid for a number of forecast variables (e.g., temperature in units of Fahrenheit or Celsius, net ecosystem exchange of carbon dioxide; Hyndman and Athanasopoulos 2018). Scaled errors may present the most effective means of comparing forecasts with different ranges and units, however, they require choosing a relevant null model (Hyndman and Athanasopoulos 2018), which is currently not common in near-term ecological forecasting literature (Figure 6).

Of the papers that did not assess and report any metric of forecast accuracy, many (77%) predicted at forecast horizons greater than or equal to one year, suggesting that part of the reason these papers did not assess forecast accuracy may be the long time lag before data would be available for forecast evaluation. In cases when the forecast horizon is too far into the future to evaluate results, researchers could consider making and evaluating additional forecasts at short horizons to provide at least an intermediate evaluation of their forecasting system (Harris et al. 2018). Assessing hindcasts may also provide a means of evaluating the forecasting system, given sufficient historical data.

Notably, many papers that included forecast assessment also compared multiple modeling approaches; 47% of papers in the dataset included model comparisons, despite the fact that this is a *Research* tier practice and may not be relevant to all applications. These high rates of model comparison may facilitate future analyses that determine relevant model structures for a variety of ecological applications (e.g., see Rousso et al. 2020).

Developments in near-term ecological forecasting: increasing automation and use of open science practices

Over time, near-term ecological forecasting is becoming increasingly automated, creating forecast products that enable real-time decision support (Dietze et al. 2018). Forecast automation can be beneficial to decision support because it decreases the amount of manual effort required to create each forecast once the automated system is set up and thereby increases the sustainability of iterative forecasting workflows (White et al. 2019, Hobday et al. 2019, Carey et al. 2021). However, it is important to note that automated forecasting workflows may still require significant human effort to maintain cyberinfrastructure over time (Carey et al. 2021). While the increase in use of iterative forecasts over time was not statistically significant, the percentage of papers that use iterative workflows to update model parameters rather than just the initial conditions of the forecast has increased significantly (Table 1). Updating model parameters as new data are incorporated allows the forecasting system to learn over time and potentially make more accurate predictions in the future (Luo et al. 2011, Niu et al. 2014, Zwart et al. 2019).

Another area of promise is in the adoption of open scientific practices: both data publication and forecast archiving have increased significantly over the past 40 years. These advances likely reflect a broader movement for open scientific practices that has gained momentum over the past decade in response to intersecting needs for greater reproducible science, knowledge dissemination, and collaboration (e.g., Reichman et al. 2011, Fecher and Friesike 2013, Beardsley 2014, Wilkinson et al. 2016, Munafò et al. 2017, Powers and Hampton 2019). Further increases in the use of open scientific practices have the potential to increase the reproducibility of published forecasting literature while fostering collaboration and accelerating the development of the field.

Priorities for the future development of near-term ecological forecasting: uncertainty, end user engagement, and null models

One of the most notable gaps identified in this analysis is the lack of specified uncertainty in published forecasts. Meaningful representations of uncertainty are considered so critical to forecast interpretation and evaluation that many definitions of ecological forecasts include uncertainty as an essential component (e.g., Clark et al. 2001, Luo et al. 2011, Harris et al. 2018, Dietze et al. 2018, Carey et al. 2021). However, only 45% of papers included uncertainty in their forecasts. Lack of forecast uncertainty can be problematic in decision support because when uncertainty is not specified in a forecast output, forecast users create their own, often inaccurate, expectations of forecast uncertainty (Morss et al. 2008, Joslyn and Savelli 2010).

Moving beyond specifying uncertainty to partitioning uncertainty into its component parts (e.g., initial condition, driver, parameter, and process uncertainty) provides information to help forecast developers prioritize improvements to their forecasting system and allows researchers to understand the constraints to predictability for a given ecological variable (Dietze 2017b). It is well established that forecasting meteorological conditions is a fundamentally chaotic problem, dominated by initial condition uncertainty (Kalnay 2003). Due to stabilizing feedbacks in ecological systems (e.g., carrying capacity, functional redundancy), other components of uncertainty are hypothesized to dominate ecological forecasts (Dietze 2017b). This hypothesis is partially supported by our dataset: initial condition uncertainty was the dominant source of forecast uncertainty in only one of three papers that partitioned uncertainty in this analysis. However, because uncertainty partitioning is a relatively new development in ecological forecasting, the small number of studies that partition uncertainty currently prevents us from making conclusions about the limiting factors for predictability across variables and forecast horizons.

While not all of the near-term ecological forecasts described in our dataset were designed for decision support, approximately 20% of papers mentioned a specific end user for their forecasts. Of these, nearly half specify that the forecasting system was in use by the specified end user (e.g., drinking water management organization, coral reef conservation agency, etc.). Designing forecasts for end users involves a variety of ethical considerations, including equity for end users, communication of forecast accuracy, and stakeholder education (Hobday et al. 2019). However, it was rare for a paper to include any explicit mention of ethical considerations made in designing the forecast (5% of papers overall; 25% of forecasts that are in use by an end user). Given the power of forecasts to inform decision support, education on how to navigate engagement with end users, and particularly any ethical considerations that must be made, may be useful in improving the utility of forecasts for stakeholder use.

In this study, we found that the use of null model comparisons remains low and has not increased in adoption over time, despite the importance of this practice for contextualizing forecast skill (Harris et al. 2018, Dietze et al. 2018, White et al. 2019). For meteorological forecasting, comparing forecasts to a climatological null model has proved useful as a means of analyzing the limit of predictive skill and the comparative performance of weather forecasts across spatial and temporal scales (Buizza and Leutbecher 2015). Parallel advances in ecological forecasting may be enabled through increased use of null model comparisons in the future (Petchey et al. 2015, Hyndman and Athanasopoulos 2018).

Published forecasts provide insight into forecastability across scales and variables

Analyzing forecastability across variables, we found that aquatic chlorophyll and phytoplankton taxa were more predictable than pollen and evapotranspiration at the shortest forecast horizons (chlorophyll: 1–5 days; phytoplankton: 1–7 days). However, the predictability of chlorophyll and phytoplankton decayed faster over increasing forecast horizons than that of evapotranspiration and pollen. Similar patterns in forecast performance for chlorophyll and phytoplankton likely result from the fact that these two ecological variables are closely related. Greater predictability of chlorophyll and phytoplankton than evapotranspiration and pollen at short forecast horizons likely indicates a greater degree of autocorrelation in these processes (Reynolds 2006), but predictability quickly decays over time due to bloom dynamics (e.g., Rigosi et al. 2011, Recknagel et al. 2016). The consistency of these patterns across 3–10 different papers for each forecast variable suggests that the relationship between forecast performance and forecast horizon could be a robust indicator of the predictability of other ecological processes.

While this is a preliminary analysis limited to four ecological variables, it is among the first comparative tests that have analyzed forecastability across scales and variables, building on two previously published studies. Ward et al. (2014) analyzed the ability of multiple time-series models to predict 2379 vertebrate population datasets. They found that increased forecast performance (measured using MASE) was correlated with long lifespans and large body size for fish and high trophic level for birds over 1–5 year forecast horizons. Additionally, Rousso et al. (2020) performed a systematic review of cyanobacterial bloom forecasting literature and analyzed the relationship between forecast performance (R^2) and forecast horizon for three types of models: artificial neural networks, decision trees, and genetic programming. They found that forecast performance decreased over 1–30 day forecast horizons, and forecasts created using greater amounts of historical data had superior forecast performance. Altogether, these first analyses of the forecastability of ecological variables highlight the growing applicability of forecasting to inform our understanding of ecological predictability.

Accelerating forecast publication and increased adoption of proposed best practices will increase the statistical strength of future analyses to detect trends in forecast performance over increasing forecast horizons, including possible non-linear patterns. In particular, increased assessment and reporting of forecast accuracy ensures that published papers can be included in a meta-analysis of predictability; increased data publication allows reevaluation of forecasts; increased forecast archiving addresses publication biases in forecast results; increased use of null models allows researchers to analyze how the maximum length of time until a forecast performs no better than the null differs among variables; and increased quantification of uncertainty allows researchers to compare how uncertainty sources differ across scales and variables.

Literature search process: observations and limitations

While the rates of adoption of these proposed best practices (Box 1) are low overall, they are not necessarily unexpected. Different forecasting applications likely require different best practices; in this analysis, we have divided our selected best practices among three categories: *Forecast Requirements*, *Decision Support*, and *Research*. However, this is a coarse delineation, and the last two tiers are not mutually exclusive: *Decision Support* practices can also be important for ecological understanding and vice versa. Ecological forecasting is an emerging discipline and many of these methods are still in development; notably, our list of proposed best practices was derived from papers that were all published within the last four years of the dataset (Harris et al. 2018, Dietze et al. 2018, White et al. 2019, Hobday et al. 2019, Carey et al. 2021; Appendix S1). Ideally, best practices should evolve using a community-driven approach to enable buy-in and robustness to many applications (following Hanson et al. 2016). Armstrong (2001) proposed as many as 139 principles for forecasting at large, all of which could be relevant to ecological forecasting applications. If one had to wait to publish a forecast until it satisfied all potential best practices, it is likely that no forecasting papers would ever be published. Increasing the number of published ecological forecasts benefits the field of ecological forecasting even if forecasts do not follow all proposed best practices because the research community gains increasingly more information about the forecastability of ecological variables and the tools and techniques needed to make effective forecasts (Dietze et al. 2018). Still, as near-term ecological forecasting continues to grow, assessing the rate of best practice adoption now allows researchers to identify and prioritize areas for growth and education, simultaneously advancing the basic and applied value of ecological forecasting.

Results from our literature search process highlight the decentralized nature of near-term ecological forecasting and the challenges associated with systematically reviewing this literature. The 178 near-term ecological forecasting papers in this analysis came from 114 unique journals and conference proceedings, and no one journal published more than 15 near-term ecological forecasts papers in this analysis. Decentralized forecast publications may present a barrier to those interested in this literature, particularly because there is no one search term that comprehensively surveys the current near-term ecological forecasting literature. Many papers do not explicitly use the terms “near-term” or “ecological” when describing forecasts for a particular application, and only 5% of the results from our initial search for the term “forecast*” in ecology-related journal articles were identified as near-term ecological forecasts after two rounds of review (Figure 1). By systematically reviewing and synthesizing near-term ecological forecasting literature published to date, we aim to begin addressing this gap.

Importantly, this comprehensive analysis of near-term ecological forecasting literature is limited to published forecast results. Operational forecasting systems that have not been described in peer-reviewed literature were not included (e.g., the U.S. National Oceanic and Atmospheric Administration, NOAA, has multiple operational forecasting systems for harmful algal blooms, fisheries, and coral reef bleaching that are available via websites). We anticipate that this exclusion may affect results in at least three ways: first, because unpublished operational forecasting systems are often used for decision support, the percentage of forecasting systems that connect to a specific end user is likely underrepresented in published literature. Second, both the need to refine forecasting models prior to paper submission and reviewer requests for forecast revisions may make it difficult to publish genuine forecasts. Because of this, most papers in this study are likely hindcasts or forecast reanalyses. Third, because of publication biases

(Dickersin 1990, Mlinarić et al. 2017), we anticipate that average forecast performance is artificially inflated in published literature relative to unpublished operational forecasts. As coordination within the near-term ecological forecasting discipline increases, surveying and comparing operational forecasts may become increasingly possible over time.

Future needs in near-term ecological forecasting

Looking to the future, advancing the field of near-term ecological forecasting will involve a suite of technological, organizational, and educational advances. First, the low level of adoption of the proposed best practices suggests that increased coordination within the ecological forecasting research community for developing common forecasting standards (e.g., Dietze et al. 2021), best practices, and vocabulary will advance near-term ecological forecasting. Second, we find that incorporation of uncertainty and use of null models are critical gaps in ecological forecasting literature where education may be needed. The creation of additional educational resources will enable more forecasts to be created and facilitate the adoption of best practices in ecological forecasting. Third, our analysis strongly suggests that long-term data are an important resource for near-term ecological forecast development and assessment. In our dataset, 60% of published near-term ecological forecasting studies used >10 years of ecological data when developing, calibrating, and assessing their forecasts (Figure 5). Long-term support for data collection will likely be necessary to advance the field. Finally, our analysis indicates that near-term ecological forecasting may be disproportionately centered in the northern hemisphere, particularly the United States of

America, Western Europe, and China. This result follows the disproportionate representation of these geographic regions across all sciences (UNESCO 2015). Lack of forecast locations in other countries, particularly in the southern hemisphere, is a detriment to the field as a whole, as the full diversity of ecological systems is not represented in ecological forecasting research to date.

While there are a variety of challenges and opportunities facing the development of near-term ecological forecasting, the literature indicates that the field has grown significantly over the past 90 years. Near-term ecological forecasting is now widespread, and the rate of forecast publication continues to increase over time. Moving forward, near-term ecological forecasting is well-positioned to transform ecological management and provide critical insight into the predictability of ecological variables.

Acknowledgements

We thank members of the Ecological Forecasting Initiative (EFI), particularly the Theory working group and the EFI Research Coordination Network (RCN) Steering Committee, for productive discussions throughout the process of writing this paper, and we thank two anonymous reviewers for their helpful revisions. We are also grateful for the assistance of Arpita Das in helping compile R^2 values and the Virginia Tech libraries in planning this review and accessing the papers in the analysis. This project was supported by U.S. National Science Foundation (NSF) grants 1737424, 1926050, 1926388, 1933016, and 1933102, as well as NSF Graduate Research Fellowships to ASL and WMW (DGE-1651272).

Author contributions

This paper originated in an Ecological Forecasting graduate seminar at Virginia Tech led by CCC and RQT; all authors participated in the seminar and co-developed the matrix used for this analysis. Conceptualization of the project was led by ASL, CCC, JS, RPM, RQT, and WMW. ASL, CCC, MEL, and WMW led the development of methods for the project. All authors contributed to abstract screening and paper review. Data analysis was led by ASL, with input from CCC, HLW, and WMW. ASL, CCC, DWH, HLW, MEL, RPM, and WMW contributed to initial development of the manuscript, which was written by ASL. All authors edited and approved the final manuscript.

Open Research

All data, metadata, and analysis code are provided as a published data package in the Environmental Data Initiative (EDI) repository (Lewis et al. 2021). Additionally, analysis code is archived with this publication (Data S1).

Chapter V References

Armstrong, J. S. 2001. Principles of forecasting: a handbook for researchers and practitioners. Springer Science & Business Media, New York.

Beardsley, T. M. 2014. Are you ready for open data? BioScience 64:855–855.

Beckage, B., L. J. Gross, and S. Kauffman. 2011. The limits to prediction in ecological systems. Ecosphere 2:art125.

Buizza, R., and M. Leutbecher. 2015. The forecast skill horizon. Quarterly Journal of the Royal Meteorological Society 141:3366–3382.

Carey, C. C., W. M. Woelmer, M. E. Lofton, R. J. Figueiredo, B. J. Bookout, R. S. Corrigan, V. Daneshmand, A. G. Hounshell, D. W. Howard, A. S. L. Lewis, R. P. McClure, H. L. Wander, N. K. Ward, and R. Q. Thomas. 2021. Advancing lake and reservoir water quality management with near-term, iterative ecological forecasting. Inland Waters. doi: 10.1080/20442041.2020.1816421

Caughlin T. T., E. I. Damschen, N. M. Haddad, D. J. Levey, C. Warneke, and L. A. Brudvig. 2019. Landscape heterogeneity is key to forecasting outcomes of plant reintroduction. Ecological Applications 29:e01850.

Clark, J. S., S. R. Carpenter, M. Barber, S. Collins, A. Dobson, J. A. Foley, D. M. Lodge, M. Pascual, R. Pielke, W. Pizer, C. Pringle, W. V. Reid, K. A. Rose, O. Sala, W. H. Schlesinger, D. H. Wall, and D. Wear. 2001. Ecological forecasts: an emerging imperative. Science 293:657–660.

Clements, F. E. 1936. Nature and structure of the climax. Journal of ecology, 24:252–284.

Dickersin, K. 1990. The existence of publication bias and risk factors for its occurrence. JAMA 263:1385–1389.

Dietze, M. C. 2017a. Ecological forecasting. Princeton University Press, Princeton.

Dietze, M. C. 2017b. Prediction in ecology: a first-principles framework. Ecological Applications 27:2048–2060.

Dietze, M. C., A. Fox, L. M. Beck-Johnson, J. L. Betancourt, M. B. Hooten, C. S. Jarnevich, T. H. Keitt, M. A. Kenney, C. M. Laney, L. G. Larsen, H. W. Loescher, C. K. Lunch, B. C. Pijanowski, J. T. Randerson, E. K. Read, A. T. Tredennick, R. Vargas, K. C. Weathers, and E. P. White. 2018. Iterative near-term ecological forecasting: Needs, opportunities, and challenges. Proceedings of the National Academy of Sciences 115:1424–1432.

Dietze, M. C., R. Q. Thomas, J. Peters, C. Boettiger, A. N. Shiklomanov, J. Ashander. 2021. A Community Convention for Ecological Forecasting: Output Files and Metadata. EcoEvoRxiv. doi: 10.32942/osf.io/9dgtq

Draper, N. R., and H. Smith. 1998. Applied regression analysis. John Wiley & Sons.

Fecher, B., and S. Friesike. 2013. Open science: one term, five schools of thought.

Feng, X., X. He, and J. Hu. 2011. Wild bootstrap for quantile regression. Biometrika 98:995–999.

Geremia, C., P. J. White, J. A. Hoeting, R. L. Wallen, F. G. R. Watson, D. Blanton, and N. T. Hobbs. 2014. Integrating population- and individual-level information in a movement model of Yellowstone bison. Ecological Applications 24:346–362.

Gleason, H. A. 1926. The individualistic concept of the plant association. Bulletin of the Torrey botanical club 7–26.

Gneiting, T., A. E. Raftery, A. H. Westveld, and T. Goldman. 2005. Calibrated probabilistic forecasting using ensemble model output statistics and minimum CRPS estimation. Monthly Weather Review 133:1098–1118.

Godfray, H. C. J., and R. M. May. 2014. Open questions: are the dynamics of ecological communities predictable? BMC Biology 12:22.

Hampton, S. E., C. A. Strasser, J. J. Tewksbury, W. K. Gram, A. E. Budden, A. L. Batcheller, C. S. Duke, and J. H. Porter. 2013. Big data and the future of ecology. Frontiers in Ecology and the Environment 11:156–162.

Hanson, P. C., K. C. Weathers, and T. K. Kratz. 2016. Networked lake science: how the Global Lake Ecological Observatory Network (GLEON) works to understand, predict, and communicate lake ecosystem response to global change. Inland Waters 6:543–554.

Harris, D. J., S. D. Taylor, and E. P. White. 2018. Forecasting biodiversity in breeding birds using best practices. PeerJ 6:e4278.

Henden, J.-A., R. A. Ims, N. G. Yoccoz, E. J. Asbjørnsen, A. Stien, J. P. Mellard, T. Tveraa, F. Marolla, and J. U. Jepsen. 2020. End-user involvement to improve predictions and management of populations with complex dynamics and multiple drivers. Ecological Applications 30:e02120.

Hobday, A. J., J. R. Hartog, J. P. Manderson, K. E. Mills, M. J. Oliver, A. J. Pershing, and S. Siedlecki. 2019. Ethical considerations and unanticipated consequences associated with ecological forecasting for marine resources. ICES Journal of Marine Science 76:1244–1256.

Hodgson, W. C. 1932. The forecasting of the East Anglian herring fishery. Journal of Animal Ecology 1:108–118.

Houlahan, J. E., S. T. McKinney, T. M. Anderson, and B. J. McGill. 2017. The priority of prediction in ecological understanding. Oikos 126:1–7.

Hyndman, R. J., and G. Athanasopoulos. 2018. Forecasting: principles and practice. OTexts.

Joslyn, S., and S. Savelli. 2010. Communicating forecast uncertainty: public perception of weather forecast uncertainty. Meteorological Applications 17:180–195.

Kalnay, E. 2003. Atmospheric modeling, data assimilation and predictability. Cambridge University Press, New York.

Koenker, R., S. Portnoy, P. T. Ng, B. Melly, A. Zeileis, P. Grosjean, C. Moler, Y. Saad, V. Chernozhukov, I. Fernandez-Val, and B. D. Ripley. 2021. quantreg: Quantile Regression.

LaDeau, S. L., B. A. Han, E. J. Rosi-Marshall, and K. C. Weathers. 2017. The next decade of big data in ecosystem science. Ecosystems 20:274–283.

Lewis, A. S. L., W. M. Woelmer, H. L. Wander, D. W. Howard, J. W. Smith, R. P. McClure, M. E. Lofton, N. W. Hammond, R. S. Corrigan, R. Q. Thomas, and C. C. Carey. 2021. Systematic review of near-term ecological forecasting literature published between 1932 and 2020. Environmental Data Initiative. https://doi.org/10.6073/pasta/c4bea94f100f39a6b73c7b9a577df214

Lindenmayer, D. B., G. E. Likens, A. Andersen, D. Bowman, C. M. Bull, E. Burns, C. R. Dickman, A. A. Hoffmann, D. A. Keith, M. J. Liddell, A. J. Lowe, D. J. Metcalfe,

S. R. Phinn, J. Russell-Smith, N. Thurgate, and G. M. Wardle. 2012. Value of long-term ecological studies. Austral Ecology 37:745–757.

Luo, Y., K. Ogle, C. Tucker, S. Fei, C. Gao, S. LaDeau, J. S. Clark, and D. S. Schimel. 2011. Ecological forecasting and data assimilation in a data-rich era. Ecological Applications 21:1429–1442.

Mlinarić, A., M. Horvat, and V. Šupak Smolčić. 2017. Dealing with the positive publication bias: why you should really publish your negative results. Biochemia Medica 27:447–452.

Morss, R. E., J. L. Demuth, and J. K. Lazo. 2008. Communicating uncertainty in weather forecasts: a survey of the U.S. public. Weather and Forecasting 23:974–991.

Munafò, M. R., B. A. Nosek, D. V. M. Bishop, K. S. Button, C. D. Chambers, N. Percie du Sert, U. Simonsohn, E.-J. Wagenmakers, J. J. Ware, and J. P. A. Ioannidis. 2017. A manifesto for reproducible science. Nature Human Behaviour 1:1–9.

Niu, S., Y. Luo, M. C. Dietze, T. F. Keenan, Z. Shi, J. Li, and F. S. C. Iii. 2014. The role of data assimilation in predictive ecology. Ecosphere 5:art65.

Payne, M. R., , A. J. Hobday, B. R. MacKenzie, D. Tommasi, D. P. Dempsey, S. M. M. Fässler, A. C. Haynie, R. Ji, G. Liu, P. D. Lynch, D. Matei, A. K. Miesner, K. E. Mills, K. O. Strand, and E. Villarino. 2017. Lessons from the first generation of marine ecological forecasts. Frontiers in Marine Science 4:289.

Pennekamp, F., A. C. Iles, J. Garland, G. Brennan, U. Brose, U. Gaedke, U. Jacob, P. Kratina, B. Matthews, S. Munch, M. Novak, G. M. Palamara, B. C. Rall, B. Rosenbaum, A. Tabi, C. Ward, R. Williams, H. Ye, and O. L. Petchey. 2019. The intrinsic predictability of ecological time series and its potential to guide forecasting. Ecological Monographs 89:e01359.

Petchey, O. L., M. Pontarp, T. M. Massie, S. Kéfi, A. Ozgul, M. Weilenmann, G. M. Palamara, F. Altermatt, B. Matthews, J. M. Levine, D. Z. Childs, B. J. McGill, M. E. Schaepman, B. Schmid, P. Spaak, A. P. Beckerman, F. Pennekamp, and I. S. Pearse. 2015. The ecological forecast horizon, and examples of its uses and determinants. Ecology Letters 18:597–611.

Petrovskii, S., and N. Petrovskaya. 2012. Computational ecology as an emerging science. Interface Focus 2:241–254.

Pielke, R. A., and R. T. Conant. 2003. Best practices in prediction for decision-making: lessons from the atmospheric and earth sciences. Ecology 84:1351–1358.

Powers, S. M., and S. E. Hampton. 2019. Open science, reproducibility, and transparency in ecology. Ecological Applications 29:e01822.

R Core Team. 2020. R: A language and environment for statistical computing. R Foundation for Statistical Computing, Vienna, Austria.

Recknagel, F., R. Adrian, J. Köhler, and H. Cao. 2016. Threshold quantification and short-term forecasting of Anabaena, Aphanizomenon and Microcystis in the polymictic eutrophic Lake Müggelsee (Germany) by inferential modelling using the hybrid evolutionary algorithm HEA. Hydrobiologia 778:61–74.

Reichman, O. J., M. B. Jones, and M. P. Schildhauer. 2011. Challenges and opportunities of open data in ecology. Science 331:703–705.

Reynolds, C. S. 2006. The ecology of phytoplankton. Cambridge University Press.

Rigosi, A., R. Marcé, C. Escot, and F. J. Rueda. 2011. A calibration strategy for dynamic succession models including several phytoplankton groups. Environmental Modelling & Software 26:697–710.

Roulston, M. S., and L. A. Smith. 2002. Evaluating probabilistic forecasts using information theory. Monthly Weather Review 130:1653–1660.

Rousso, B. Z., E. Bertone, R. Stewart, and D. P. Hamilton. 2020. A systematic literature review of forecasting and predictive models for cyanobacteria blooms in freshwater lakes. Water Research 182:115959.

Sutherland, W. J., R. P. Freckleton, H. C. J. Godfray, S. R. Beissinger, T. Benton, D. D. Cameron, Y. Carmel, D. A. Coomes, T. Coulson, M. C. Emmerson, R. S. Hails, G. C. Hays, D. J. Hodgson, M. J. Hutchings, D. Johnson, J. P. G. Jones, M. J. Keeling, H. Kokko, W. E. Kunin, X. Lambin, O. T. Lewis, Y. Malhi, N. Mieszkowska, E. J. Milner-Gulland, K. Norris, A. B. Phillimore, D. W. Purves, J. M. Reid, D. C. Reuman, K. Thompson, J. M. J. Travis, L. A. Turnbull, D. A. Wardle, and T. Wiegand. 2013. Identification of 100 fundamental ecological questions. Journal of Ecology 101:58–67.

Ward, E. J., E. E. Holmes, J. T. Thorson, and B. Collen. 2014. Complexity is costly: a meta-analysis of parametric and non-parametric methods for short-term population forecasting. Oikos 123:652–661.

White, E. P., G. M. Yenni, S. D. Taylor, E. M. Christensen, E. K. Bledsoe, J. L. Simonis, and S. K. M. Ernest. 2019. Developing an automated iterative near-term forecasting system for an ecological study. Methods in Ecology and Evolution 10:332–344.

Wilkinson, M. D., M. Dumontier, I. J. Aalbersberg, G. Appleton, M. Axton, A. Baak, N. Blomberg, J.-W. Boiten, L. B. da Silva Santos, P. E. Bourne, J. Bouwman, A. J. Brookes, T. Clark, M. Crosas, I. Dillo, O. Dumon, S. Edmunds, C. T. Evelo, R. Finkers, A. Gonzalez-Beltran, A. J. G. Gray, P. Groth, C. Goble, J. S. Grethe, J. Heringa, P. A. C. 't Hoen, R. Hooft, T. Kuhn, R. Kok, J. Kok, S. J. Lusher, M. E. Martone, A. Mons, A. L. Packer, B. Persson, P. Rocca-Serra, M. Roos, R. van Schaik, S.-A. Sansone, E. Schultes, T. Sengstag, T. Slater, G. Strawn, M. A. Swertz, M. Thompson, J. van der Lei, E. van Mulligen, J. Velterop, A. Waagmeester, P. Wittenburg, K. Wolstencroft, J. Zhao, and B. Mons. 2016. The FAIR Guiding Principles for scientific data management and stewardship. Scientific Data 3:160018.

Zwart, J. A., O. Hararuk, Y. T. Prairie, S. E. Jones, and C. T. Solomon. 2019. Improving estimates and forecasts of lake carbon dynamics using data assimilation. Limnology and Oceanography: Methods 17:97–111.

Box 1: Proposed best practices for ecological forecasting, drawn from peer-reviewed literature: Harris et al. (2018), White et al. (2019), Hobday et al. (2019), and Carey et al. (2021). *Forecast Requirements* include traits of forecasting systems that are essential to the development of a forecast. *Decision Support* practices are those that are particularly helpful if the forecast will be applied as a decision support tool. *Research* practices include characteristics of a forecasting system that are particularly suited to enabling the advancement of fundamental ecological understanding across studies. Importantly, these last two tiers are not mutually exclusive: *Decision Support* practices can also be important for ecological understanding and vice versa.

Forecast Requirements

1. Include uncertainty
   a. Meaningful representations of uncertainty are important to forecast interpretation and evaluation, so much so that uncertainty is identified as an essential component of many ecological forecast definitions (Clark et al. 2001, Luo et al. 2011, Harris et al. 2018, Dietze et al. 2018, Carey et al. 2021).
2. Report forecast accuracy
   a. Assessing and reporting forecast accuracy allows end users to understand the reliability of the forecasting system (Harris et al. 2018, Hobday et al. 2019) and provides the near-term ecological forecasting research community with increased insight into the tools and techniques needed to produce effective forecasts (Dietze et al. 2018). Furthermore, assessing and reporting forecast accuracy contributes to our understanding of ecological predictability by facilitating comparisons of forecast accuracy across scales and variables (Beckage et al. 2011, Petchey et al. 2015).

   Decision Support

3. Identify an end user
   a. One of the goals of ecological forecasting is to aid in decision-making. The first step in this process is to identify a specific end user and consider their needs throughout forecast development (Dietze et al. 2018, Hobday et al. 2019, Carey et al. 2021).
4. Make iterative forecasts
   a. Iterative forecasts incorporate new data as they become available, providing updated predictions that can aid in continuous decision-making and forecast improvement (Dietze et al. 2018, Hobday et al. 2019, Carey et al. 2021).

5. Automate forecasting workflows
    a. End-to-end automation of the forecasting workflow (from data processing to forecast communication) allows for more frequent forecast outputs and more sustainable forecasting infrastructure (Dietze et al. 2018, White et al. 2019, Hobday et al. 2019, Carey et al. 2021). This practice is particularly relevant for forecasts with horizons of days to months that are rerun often to provide updated information.

Research

6. Make data available
    a. To ensure full forecast reproducibility and allow future research to build off of existing forecasting workflows, all data and code used to create forecasts should be findable, accessible, interoperable, and reusable (FAIR; Wilkinson et al. 2016, Harris et al. 2018, Dietze et al. 2018, White et al. 2019, Carey et al. 2021).
7. Archive forecasts
    a. Archiving forecasts as they are created provides a means of demonstrating when forecasts were made and tracking forecast improvement over time (Harris et al. 2018, Dietze et al. 2018, White et al. 2019, Carey et al. 2021).
8. Use null model comparisons
    a. Comparing forecasts to simple, standard baselines (e.g., persistence or climatology null models) allows researchers to compare forecastability across systems (Petchey et al. 2015) and evaluate the amount of information contained in the forecasts (Harris et al. 2018, Dietze et al. 2018, White et al. 2019).
9. Compare modeling approaches
    a. Comparing multiple modeling approaches (e.g., process-based and empirical approaches, alternative model drivers, alternative mathematical representations of mechanistic processes) can provide insight into the nature of ecological processes and develop a better understanding of the circumstances under which different modeling approaches are most effective (Harris et al. 2018, White et al. 2019).

Chapter V Tables

Table 1: Logistic regression results for each proposed best practice based on n = 177 papers (one paper from 1932 was excluded from this analysis). Statistically significant p values are in bold. In addition to the nine proposed best practices, statistics are included for the use of iterative forecasting to update model parameters.

	Estimate	Standard error	Z value	P value
Include uncertainty				
Intercept	-7.615	35.157	-0.217	0.83
Year	0.004	0.017	0.211	0.83
Report forecast accuracy				
Intercept	-59.665	38.486	-1.550	0.12
Year	0.030	0.019	1.579	0.11
Identify an end user				
Intercept	-86.809	52.611	-1.650	0.10
Year	0.042	0.026	1.624	0.10
Make iterative forecasts				
Intercept	-14.147	36.152	-0.391	0.70
Year	0.007	0.018	0.379	0.71
Make iterative forecasts (updating model parameters)				
Intercept	-182.741	85.680	-2.133	**0.03**
Year	0.090	0.043	2.111	**0.04**
Automate forecasting workflows				
Intercept	-237.502	100.550	-2.362	**0.02**
Year	0.117	0.050	2.344	**0.02**
Make data available				
Intercept	-252.217	69.775	-3.615	**<0.001**
Year	0.125	0.035	3.602	**<0.001**
Archive forecasts				
Intercept	-308.891	136.546	-2.262	**0.02**
Year	0.152	0.068	2.247	**0.03**
Use null model comparisons				
Intercept	33.795	50.388	0.671	0.50
Year	-0.018	0.025	-0.710	0.48
Compare modeling approaches				
Intercept	-41.332	35.718	-1.157	0.25
Year	0.021	0.018	1.154	0.25

Table 2: Indicator variable analysis results comparing the slope of R^2 values over 1–7 day horizons among forecast variables. Chlorophyll was treated as the reference variable for the analysis. Statistically significant p values are in bold.

	Estimate	SE	t	P value
Chlorophyll (reference; n = 68 data points from 8 papers)				
Intercept	0.98	0.025	39.53	**<0.001**
Horizon	-0.08	0.012	-6.78	**<0.001**
Phytoplankton (n = 33 data points from 8 papers)				
Intercept	0.04	0.055	0.71	0.48
Horizon	0.02	0.016	1.06	0.29
Pollen (n = 110 data points from 3 papers)				
Intercept	-0.29	0.043	-6.62	**<0.001**
Horizon	0.05	0.014	3.94	**<0.001**
Evapotranspiration (n = 113 data points from 10 papers)				
Intercept	-0.26	0.059	-4.40	**<0.001**
Horizon	0.05	0.015	3.46	**<0.001**

Chapter V Figures

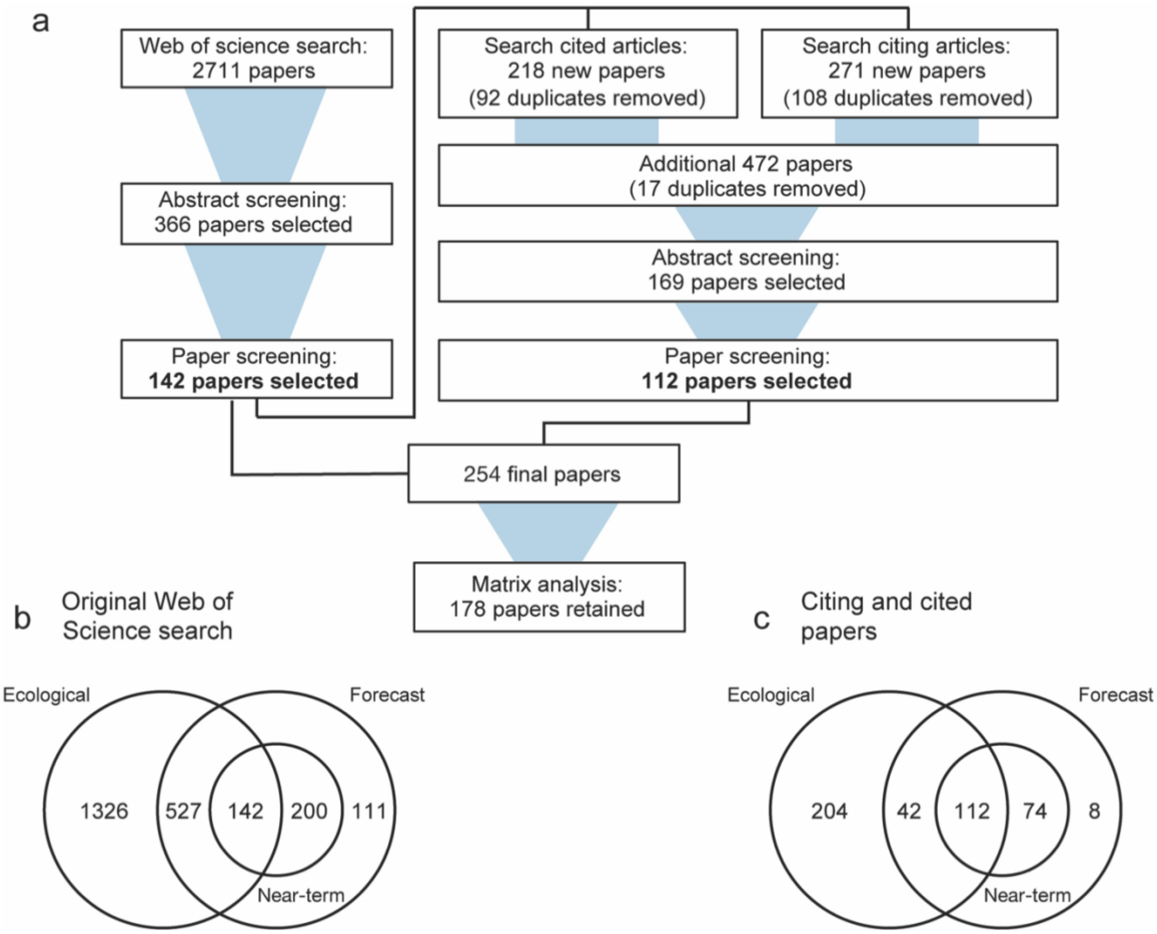

Figure 1: Systematic literature analysis methods. a: Flow chart of literature review process. b and c: Venn diagrams illustrating the number of studies that met each of our three criteria after two rounds of review (abstract and paper reviews) for our original Web of Science search (b) and a search of citing and cited papers (c).

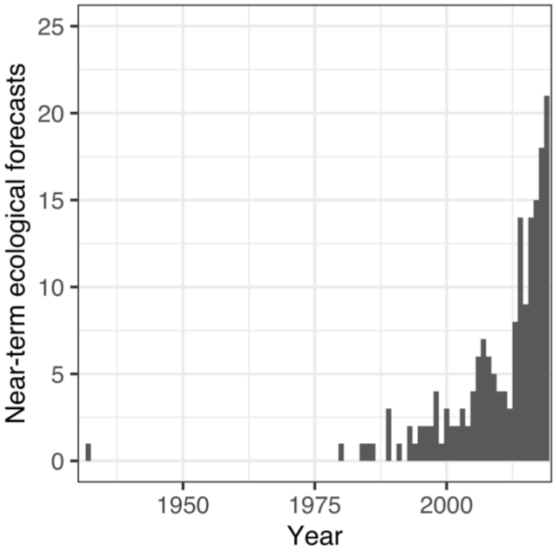

Figure 2: Number of near-term ecological forecasts published per year. Five papers from the final year (2020) are not plotted because data for this year are incomplete: only papers indexed on Web of Science by the date of our search (18 May 2020) were included in this study.

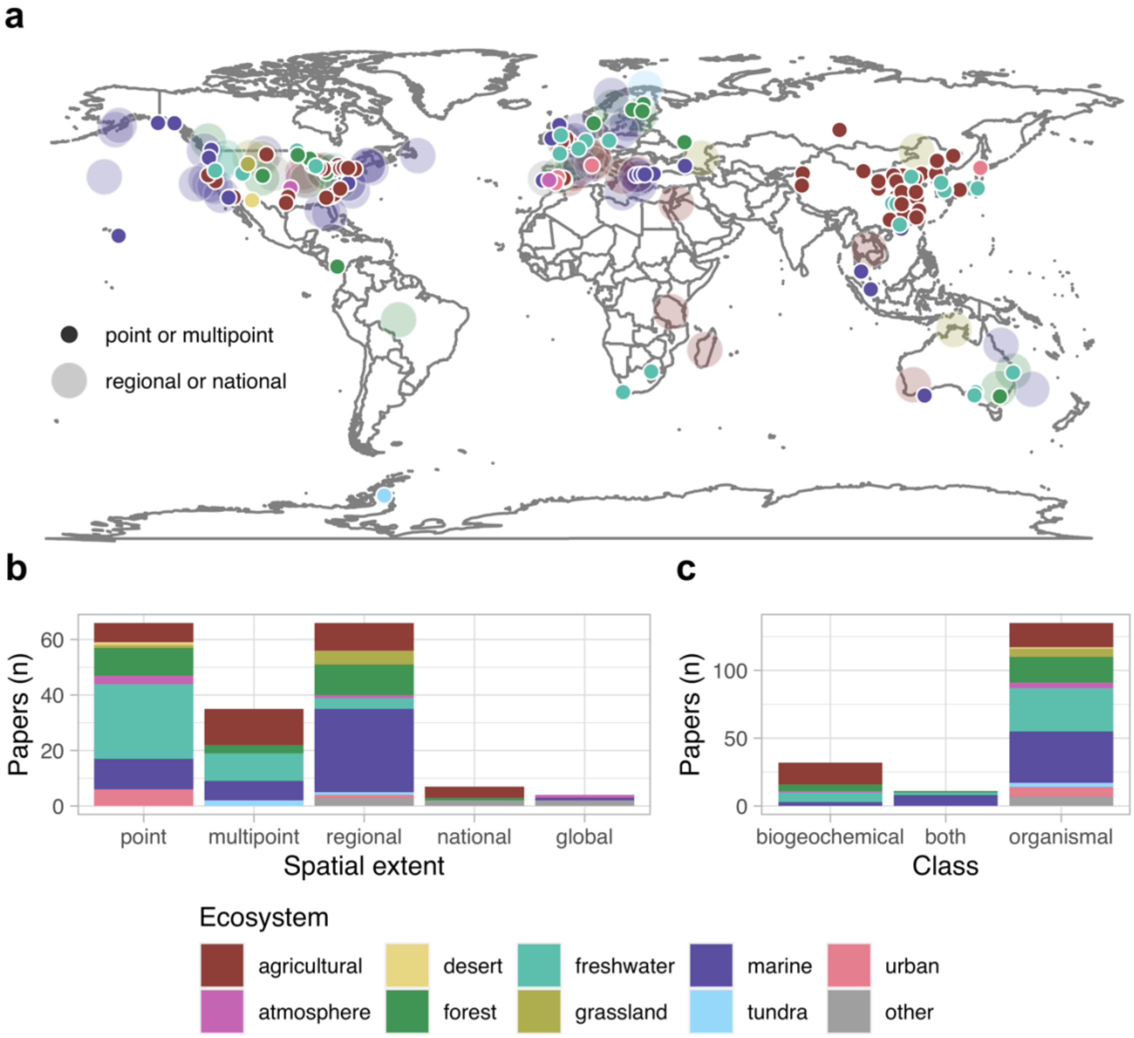

Figure 3: Description of ecological forecasting papers identified in this study. a: Map of all forecasts: regional and national studies are shown in large transparent points near the center of the forecast region, while point and multipoint forecasts are shown in small opaque points. b: Bar chart illustrating the spatial extent of the forecast for each paper—point, multipoint (several distinct points), regional (a broad region that does not follow national bounds), national, or global (for details about how spatial extent was determined, see Lewis et al. 2021). c: Bar chart illustrating the class—organismal (population or community) or biogeochemical—of the forecast variable for each paper. Fill colors

illustrate ecosystem type. Forecasts that could not be matched to one of our nine ecosystem types have been labeled “other.”

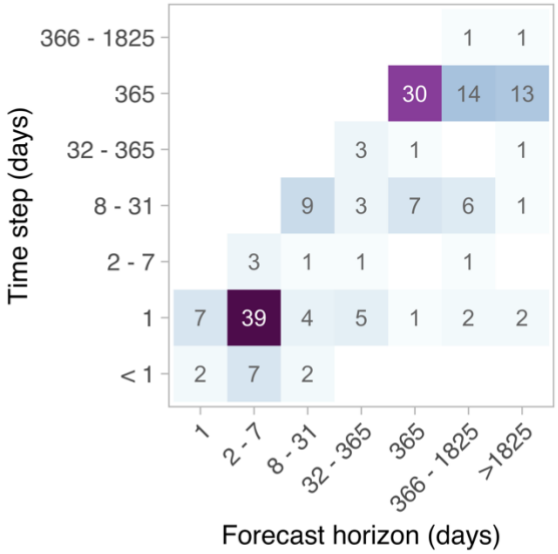

Figure 4: Relationship between time step and forecast horizon of forecasting papers. Colors and numbers within each square indicate the number of papers corresponding to that combination of time step and forecast horizon (darker colors indicate more common combinations). White areas indicate combinations of time step and horizon that were not represented in the dataset. Papers that did not have a defined horizon (e.g., predicting end of summer harvest) or that did not specify time step/horizon were omitted (n = 10).

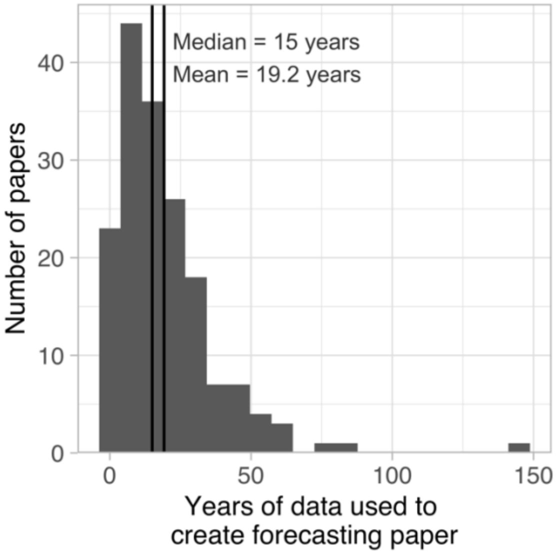

Figure 5: Histogram illustrating the total number of years of data used to develop each forecasting paper, summed across model development, training, evaluation, etc. Vertical lines represent the median (left) and mean (right) number of years used.

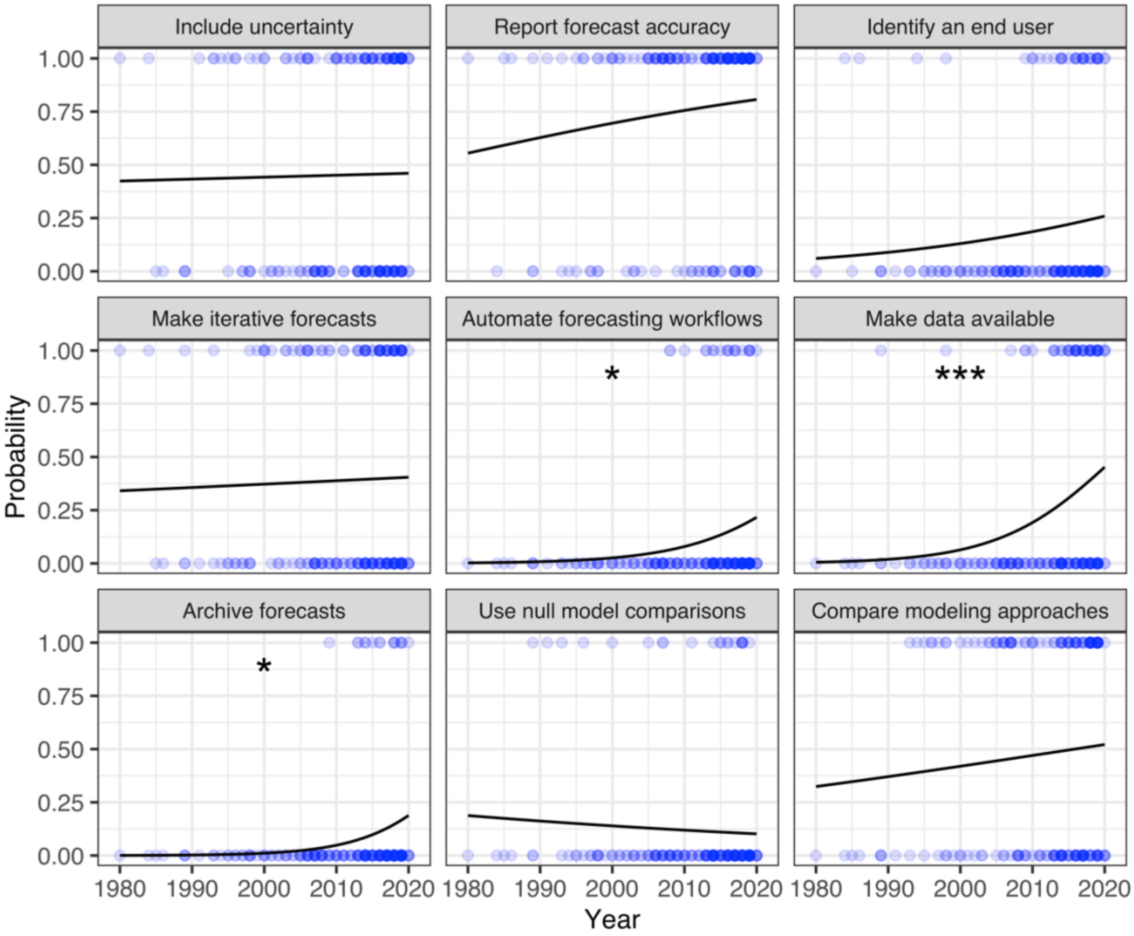

Figure 6: Best practice adoption over time. Points demarcate whether or not an individual paper demonstrated the best practice (1 = observed, 0 = not observed), and lines represent logistic regression results. Significance of the year term in the regression is indicated using asterisks: * indicates $p < 0.05$, *** indicates $p < 0.001$. One paper from 1932 was excluded from this analysis.

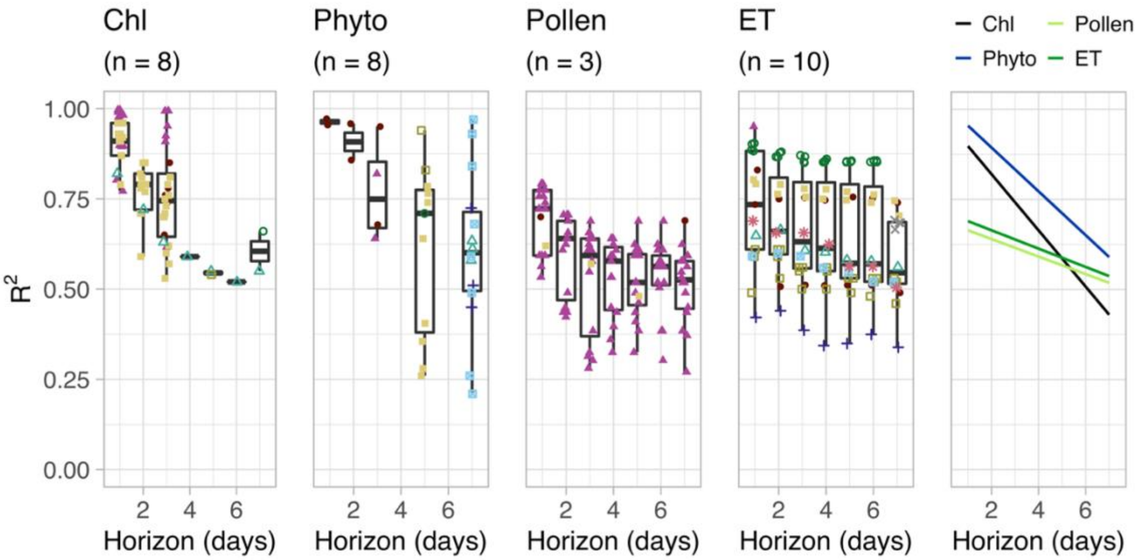

Figure 7: Relationship between forecast performance and forecast horizon (Horiz) for four forecast variables: chlorophyll (Chl), phytoplankton (Phyto), pollen, and evapotranspiration (ET). Different papers are indicated by points of different colors and shapes. Within a paper, forecasts using the same model were averaged (across sites, years, etc.). Rightmost panel: model predictions from the quantile regression indicator analysis.

Supporting Information for Chapter V

Appendix S1: Table of best practices referenced in previous publications

Table S1: Proposed best practices for ecological forecasting. Each column lists the practices that are specifically outlined in a given paper, and practices are aligned into rows with the same or similar proposed practices. We note that White et al. (2019) synthesized many of the best practices mentioned by Dietze et al. (2018). The Dietze et al. (2018) paper is not included here because it did not provide a defined list of practices (as provided by the four other papers in this table).

Reference	This manuscript	Harris et al. (2018)	White et al. (2019)	Hobday et al. (2019)	Carey et al. (2021)
Title	Increased adoption of best practices in ecological forecasting enables comparisons of forecastability	Forecasting biodiversity in breeding birds using best practices.	Developing an automated iterative near-term forecasting system for an ecological study	Ethical considerations and unanticipated consequences associated with ecological forecasting for marine resources	Advancing lake and reservoir water quality management with near-term, iterative ecological forecasting
Description	Proposed best practices	Best practices for making and evaluating ecological forecasts	Key practices for automated iterative near-term ecological forecasting	Principles for ethical forecasting	Lessons learned from iterative near-term forecasting for management

Include uncertainty	Pay attention to uncertainty	Focus on uncertainty	Representation of uncertainty	
Assess and report forecast skill	Validate using hindcasting		Skill assessment	
Identify an end user			Engagement and education	Human-centered design improves the utility of forecasts for managers
Make iterative forecasts			Delivery failures	Sustainability plans are needed for short- and long-term forecasting system maintenance
Automate forecasting workflows		Automated end-to-end reproducibility	Ongoing delivery	Cyberinfrastructure is not trivial
Make data available		Rapid data release under open licenses		Forecasts should be reproducible and archived
Archive forecasts	Publicly archive forecasts	Publicly archive forecasts		Forecasts should be reproducible and archived
Use null model comparisons	Compare multiple modeling approaches (specifically	Compare forecasts to simple baselines		

	mentions null models)			
Compare modeling approaches	Compare multiple modeling approaches	Compare and combine multiple modelling approaches		
	Use time-series data when possible			
	Use predictors related to the question			
	Address unknown or unmeasured predictors			
	Include an observation model			
	Assess how forecast accuracy changes with time-lag			
		Frequent data collection		
		Best practices in data structure		

		Best practices in software development		
		Support easy inclusion of new models		
			Conflicts of interest	
			Ecosystem health	
			Equity for end users	
			Unintended consequences	
			Review of performance	
				Uncertainty partitioning informs forecast interpretation and forecast improvement
				Building and maintaining a forecasting system takes an interdisciplinary,

				highly coordinated team
				Let your forecasting goals guide your modeling approach

References

Carey, C. C., W. M. Woelmer, M. E. Lofton, R. J. Figueiredo, B. J. Bookout, R. S. Corrigan, V. Daneshmand, A. G. Hounshell, D. W. Howard, A. S. L. Lewis, R. P. McClure, H. L. Wander, N. K. Ward, and R. Q. Thomas. 2021. Advancing lake and reservoir water quality management with near-term, iterative ecological forecasting. Inland Waters. doi: 10.1080/20442041.2020.1816421

Dietze, M. C., A. Fox, L. M. Beck-Johnson, J. L. Betancourt, M. B. Hooten, C. S. Jarnevich, T. H. Keitt, M. A. Kenney, C. M. Laney, L. G. Larsen, H. W. Loescher, C. K. Lunch, B. C. Pijanowski, J. T. Randerson, E. K. Read, A. T. Tredennick, R. Vargas, K. C. Weathers, and E. P. White. 2018. Iterative near-term ecological forecasting: Needs, opportunities, and challenges. Proceedings of the National Academy of Sciences 115:1424–1432.

Harris, D. J., S. D. Taylor, and E. P. White. 2018. Forecasting biodiversity in breeding birds using best practices. PeerJ 6:e4278.

Hobday, A. J., J. R. Hartog, J. P. Manderson, K. E. Mills, M. J. Oliver, A. J. Pershing, and S. Siedlecki. 2019. Ethical considerations and unanticipated consequences associated with ecological forecasting for marine resources. ICES Journal of Marine Science 76:1244–1256.

White, E. P., G. M. Yenni, S. D. Taylor, E. M. Christensen, E. K. Bledsoe, J. L. Simonis, and S. K. M. Ernest. 2019. Developing an automated iterative near-term forecasting system for an ecological study. Methods in Ecology and Evolution 10:332–344.

Appendix S2: List of standardized criteria used to assess each paper

1. Paper title
2. Digital object identifier (doi)
3. Author list
4. Year of publication
5. Journal or conference in which the paper was published
6. Forecast spatial scale, classified into five categories
7. Geographic coordinates of the forecast site using decimal degrees. Locations for regional and national forecasts are approximately the center of the forecast area
8. Forecast ecosystem: forest, grassland, freshwater, marine, desert, tundra, atmosphere, agricultural, urban, global, other
9. Forecast class: biogeochemical or organismal (population or community)
10. Identity of forecast variables
11. Model dimension: 0D, 1D, 2D, 3D
12. Model type: empirical (dependent on correlative or statistical relationships) or process-based (explicitly simulating ecological processes). For forecasting workflows that involve a pipeline of multiple models, this refers to the “final” model that forecasts the forecast variable of interest
13. If specified: more detailed description of model: for example, Bayesian hierarchical, machine learning, named model (e.g., PROTECH), etc.
14. Are meteorological covariates used in this forecast? 1 = yes, 0 = no
15. Are physical covariates (e.g., streamflow) used in this forecast? 1 = yes, 0 = no
16. Are biological covariates used in this forecast? 1 = yes, 0 = no

17. Are chemical covariates used in this forecast? 1 = yes, 0 = no
18. Does the paper include an ensemble forecast (ensemble within model)? 1 = yes, 0 = no
19. Number of ensemble members
20. Does the paper use an ensemble of models to produce one output? 1 = yes, 0 = no
21. How many models in the ensemble model
22. Are multiple models with different model structures compared (NOT including null models)? 1 = yes, 0 = no
23. How many models with different structures are compared?
24. Was a forecast null model (persistence or climatology) included? 1 = yes, 0 = no
25. How many null models?
26. What type of null model (climatology or persistence)?
27. Maximum time into the future that the forecast predicts in this paper, described in days
28. Time step of forecast output. For example, a forecast that gives predictions for the next 16 days but was only run once a week would have a time step of one day (not one week)
29. Are the forecasts described in the papers iterative (i.e., data updating forecasts iteratively)? Any form of iteration counts here: updating initial conditions with new data, refitting the model to incorporate new data, updating parameter values, etc. State updating via the autoregressive term counts as data assimilation for autoregressive models

30. What technique of data assimilation was used? For example, KF, enKF, refit, update IC, etc.
31. Extent to which uncertainty is included in the forecast, classified within 5 categories:
    a. no (this model does not contain uncertainty)
    b. contains (the model contains uncertainty, but uncertainty is not derived from data; e.g. uncertainty comes from spin-up initial conditions or hand-tuned parameters)
    c. data_driven (the model contains data-driven uncertainty; e.g. uncertainty in meteorological drivers)
    d. propagates (the model propagates some source of uncertainty)
    e. assimilates (the model iteratively updates uncertainty through data assimilation)
    f. NOTE: this is assumed to be a hierarchy (e.g. if the forecast contains data driven uncertainty and propagates that uncertainty, it would be marked "propagates")
32. What sources of uncertainty were incorporated?
33. Was observation uncertainty included? 1 = yes, 0 = no
34. Are at least two different sources of uncertainty quantified and compared? 1 = yes, 0 = no. NOTE: the two sources may be in the same category of uncertainty—e.g. two forms of driver data)
35. Initial condition uncertainty partitioned? 1 = yes, 0 = no
36. Driver uncertainty partitioned? 1 = yes, 0 = no

37. Parameter uncertainty partitioned? 1 = yes, 0 = no
38. Process uncertainty partitioned? 1 = yes, 0 = no
39. Other partitioned sources of uncertainty? 1 = yes, 0 = no
40. If at least two categories of uncertainty were partitioned, what was the dominant source of uncertainty?
41. If the dominant source varies by forecast horizon, season, etc. please describe here
42. Paper states that forecast was evaluated? 1 = yes, 0 = no
43. Forecast evaluation results reported in paper? 1 = yes, 0 = no
44. List all skill metrics used (e.g. R2, RMSE, bias, MAE). SD and Bayesian credible intervals are not skill metrics
45. Is forecast performance assessed at multiple forecast horizons (results must be reported in paper/supplemental info)? 1 = yes, 0 = no
46. Maximum forecast horizon such that the forecast was better than the null model (out of any models used)
47. Temporal coverage of data used to create this forecasting paper
48. Was new data (driver and/or observations) available to the model in real time (<24 hours from collection) without any manual effort when the system was working as intended? 1 = yes, 0 = no
49. Forecast archiving described in text? 1 = yes, 0 = no
50. Repository in which forecasts are archived
51. Archiving website is still accessible via the link in the paper as of 14 Jun 2021? 1 = yes, 0 = no

52. Text specifies that driver data are publicly available to reproduce the forecasts? 1 = yes, 0 = no
53. Specific end user identified (proper noun)? 1 = yes, 0 = no
54. Partnership with the end user in forecast development mentioned in paper? 1 = yes, 0 = no
55. Forecast being used by the end user according to paper? 1 = yes, 0 = no
56. Forecast delivery method identified? 1 = yes, 0 = no
57. Forecast delivery method?
58. Any ethical considerations mentioned? 1 = yes, 0 = no

Chapter VI: Synthesis

Overview

Anthropogenic climate and land use change have profoundly impacted lakes worldwide, disrupting both local ecosystem services and global biogeochemical cycling. Throughout my dissertation, I used diverse analyses to build a predictive understanding of how bottom-water dissolved oxygen may mediate water quality in the face of global change (Chapter 1 Figure 1). My dissertation demonstrates that increasing prevalence and duration of summer bottom-water anoxia may be driven in part by increased spring air temperature and the legacy effects of previous years of anoxia (Chapters II and III). In turn, bottom-water anoxia has important consequences for the biogeochemical cycling of iron, phosphorus, and organic carbon in the bottom waters and sediments of temperate lakes (Chapters III and IV). Ultimately, predicting future changes in bottom-water biogeochemistry will require both fundamental ecological understanding and rigorous conceptual and methodological frameworks for the quantitative prediction of future ecosystem states (Clark et al., 2001; Dietze et al., 2018; Luo et al., 2011). In Chapter V, I explored the emerging field of near-term ecological forecasting as one approach to meet this need. I documented that near-term ecological forecasting is widespread and growing, and the application of proposed best practices is increasing over time. Through these four chapters, my dissertation provides mechanistic characterization of the effects of climate change on water quality in lakes worldwide, laying the foundation for forecasts that can be used to anticipate, mitigate, and preempt future water quality declines.

Several themes emerged across the chapters of my dissertation, which I describe in more detail throughout the six sections of this Synthesis (section names are italicized below). First, on a high level, my dissertation demonstrates the importance of characterizing summer bottom-water biogeochemistry in lakes (See: *Importance of bottom water analysis*, below). Second and third, I identified multiple *Drivers of bottom-water dissolved oxygen dynamics* and *Consequences of bottom-water dissolved oxygen declines* throughout Chapters II–IV. Synthesizing across these three chapters provides complementary insight into biogeochemical dynamics in the bottom waters of temperate lakes. Fourth, both the drivers and consequences of bottom-water anoxia appear to be influenced in large part by antecedent conditions prior to the onset of anoxia, which I discuss in *Ecological memory and legacy*. Fifth, the four chapters of my dissertation span multiple scales of analysis; individually, each of these scales provides an important but limited perspective on ecological function, and combining research across multiple scales can provide more comprehensive insight into biogeochemical dynamics (*Strengths and limitations of dissertation approaches*). Lastly, I hope that my dissertation research can contribute to the development of future analyses on lake ecosystem function. In the section *Future Research*, I highlight three directions that I anticipate could be particularly important avenues of future research building upon my dissertation.

Importance of bottom-water analysis

While surface-water dynamics may be characterized across hundreds of thousands of widespread lakes using remote sensing (Khandelwal et al., 2022; Topp et al., 2021; Yang et al., 2022), bottom-water data collection is often more resource-intensive, logistically challenging, and expensive. Bottom-water data collection typically entails either physically traveling to the waterbody and conducting manual profiles from a boat or purchasing and maintaining in situ sensors. As a result, there are substantial disparities in data availability for surface- vs. bottom-water variables. In Chapters II and III, I compiled and analyzed one of the largest existing databases that include both surface and bottom-water temperature and dissolved oxygen data in lakes, and I was only able to characterize ~600 lakes (Lewis et al., 2024). Conversely, remote sensing and other technologies have enabled studies of surface water quality across >600,000 lakes worldwide (Khandelwal et al., 2022).

Despite these disparities, my dissertation research highlights the critical importance of studying bottom water conditions to understand whole-lake dynamics. For example, Chapter II demonstrates that if we expected bottom-water temperature and dissolved oxygen to be driven by the same factors as surface water temperature (i.e., spring vs. summer air temperature), we would overestimate trends in bottom-water temperature and dissolved oxygen by a factor of four. This mischaracterization of bottom-water temperature and dissolved oxygen would in turn have important implications because of the whole-ecosystem effects of bottom-water dissolved oxygen dynamics on carbon and nutrient cycling (Chapters III and IV). As climate and land use change continues to alter lake ecosystem function (e.g., Jane et al., 2021; Jenny et al., 2016; O’Reilly et al., 2015), my dissertation research highlights the importance of continuing and expanding data collection for bottom-water processes.

Drivers of bottom-water dissolved oxygen dynamics

Multiple factors can contribute to variation in summer bottom-water dissolved oxygen concentrations over time, as identified in Chapters II and III of my dissertation.

Understanding the relative importance of these drivers may help predict where and when lakes are likely to experience the negative effects of hypoxia and anoxia. Both Chapters II and III highlight that spring air temperature is one particularly important driver of bottom-water dissolved oxygen concentrations. Increased spring air temperature may contribute to oxygen declines by prolonging summer stratification (Jane et al., 2023; Woolway et al., 2021), as well as by increasing hypolimnetic temperatures, which will in turn drive increased rates of respiration and increased oxygen demand (Chapters II and III; Pace & Prairie, 2005; Yvon-Durocher et al., 2012). Notably, the importance of spring air temperature as a driver of bottom-water dissolved oxygen is likely to be particularly pronounced in large, stably-stratified lakes, where we observed stronger seasonal ecological memory for bottom water temperature and dissolved oxygen (Chapter II).

In addition to air and water temperature (e.g., Jane et al., 2023; Pace & Prairie, 2005), variation in bottom-water dissolved oxygen may also result from changes in organic matter availability (e.g., Bastviken et al., 2003, 2004; Müller et al., 2012). Specifically, in Chapter III, we found that summer bottom-water oxygen demand was positively associated with surface chlorophyll-a (a metric of phytoplankton biomass) during both the current and previous summer. Averaged across all lakes, bottom-water temperature played a relatively greater role than chlorophyll-a in determining the rate of summer oxygen demand. However, the relative importance of chlorophyll-a as a driver of summer oxygen demand increased with longer residence time across lakes (i.e., accounting for bottom-water temperature and other factors; Chapter III). Notably, we found that spring air temperatures had a positive effect on both summer chlorophyll-a and summer bottom-water temperatures (Chapters II and III), indicating that increased spring air temperature may contribute to increased summer bottom-water oxygen demand via multiple potential mechanisms. Ultimately, variation in both bottom-water temperature and surface phytoplankton biomass will likely be most influential in driving anoxia in deep lakes, as the effect of oxygen demand on the spatial and temporal extent of anoxia (i.e., “anoxic factor”; Nürnberg, 1995, 2019) increased with greater mean lake depth (Chapter III). In sum, Chapters II and III highlight that multiple drivers can contribute to interannual variability in summer bottom-water dissolved oxygen, and the relative importance of these factors may vary across lakes as a result of both lake morphometry and residence time.

Consequences of bottom-water dissolved oxygen declines

In Chapters III and IV, I assessed how anoxia may alter ecological functioning in lakes by mediating the flux of phosphorus (Chapter III) and organic carbon (Chapter IV) across the sediment-water interface. Decades of research using both sediment core incubations and whole-ecosystem oxygenation have established that anoxia can increase total phosphorus (TP) accumulation in bottom waters, at least in part through reductive dissolution of Fe(III) in Fe-bound phosphorus (Fe-P) complexes (Beutel & Horne, 1999; Einsele, 1936; Mortimer, 1942; Orihel et al., 2017 and references therein). However, Fe can also form redox-sensitive complexes with organic carbon (OC; Barber et al., 2017; Hemingway et al., 2019; Lalonde et al., 2012; Moorhead et al., 1999), which have been less examined than Fe-P in freshwater sediments. The discrepancy between the fundamental characterization of Fe-P and Fe-OC motivated divergent scales of analysis for two of my dissertation chapters: whereas Chapter III built upon previous experimental work to assess how anoxic TP dynamics shape water quality on an international scale (i.e., across >600 lakes on five continents), Chapter IV focused on a more fundamental characterization of Fe-OC using microcosm and whole-ecosystem experiments across two reservoirs. Ultimately, these two chapters provide complementary insight that contributes to a more robust understanding of bottom-water biogeochemistry under dynamic oxygen conditions.

Synthesizing freshwater Fe-OC research (e.g., Chapter IV) with previous research on Fe-P highlights that these two types of biogeochemical complexes exhibit similar dynamics, despite often being studied separately. Notably, the total pools of Fe-P and Fe-OC both appear to include substantial fractions that are stable under reducing conditions, despite containing some redox-sensitive fractions in surficial sediment (Chapter IV; Hupfer & Lewandowski, 2008; Li et al., 2015; Peter & Sobek, 2018; Wen et al., 2020). Short-term experiments and laboratory incubations often document reductive dissolution of surficial Fe complexes, resulting in release of Fe, phosphate, and DOC from sediment (Albright & Wilkinson, 2022; Orihel et al., 2017; Peter et al., 2017 and references therein). However, factors other than Fe binding may play an equal or greater role in governing long-term TP and OC retention in sediments (e.g., Hupfer & Lewandowski, 2008; Katsev et al., 2006; Li et al., 2015; Peter & Sobek, 2018). For example, we found in Chapter IV that total OC in sediment increased in sediment following multiple years of summer anoxia, likely due to decreased respiration rates under anoxic conditions. Conversely, if the main driver of sediment OC had been Fe-OC complexation, we would have expected to see decreased total OC in sediments following multiple years of anoxia due to reductive dissolution of Fe(III) in Fe-OC compounds. Research on Fe-P has similarly shown that the rate of TP input to sediments and organic P speciation may play a greater role than Fe-TP dynamics in determining net TP retention in sediments (Joshi et al., 2015; Reitzel et al., 2007). Despite these findings, redox conditions in bottom waters likely still play an important role in governing the accumulation of TP within the water column. For example, in Chapter III, we found that the anoxic factor (i.e., the spatial and temporal extent of anoxia; Nürnberg, 1995) was significantly correlated with bottom-water TP concentrations both across lakes and within lakes over time.

Importantly, one driver that likely regulates both Fe-P and Fe-OC dynamics across lakes is the availability of Fe in sediments. In Chapter IV, we found that a much higher fraction of sediment organic carbon was bound to iron in two iron-rich, low-DOC freshwater reservoirs (~30%), compared to the high-DOC systems that had been studied previously (0–11%; Peter & Sobek, 2018). Motivated by similar findings for Fe-TP, addition of Fe-based compounds has been used as a water quality remediation approach to increase the retention of TP in sediments (e.g., Cooke et al., 2005; Münch et al., 2024). When Fe is limiting, phosphate appears to have an inhibitory effect on the complexation of Fe and OC, as TP and OC compete for both coprecipitation with Fe and adsorption on Fe(III) mineral surfaces (Luo et al., 2022). However, Fe, OC, and TP can also co-precipitate to create ternary OC-P-Fe compounds, enhancing sediment retention of both P and OC (Luo et al., 2022).

In sum, synthesizing my Ph.D. research in combination with previous literature, it appears that (1) anoxia can contribute to increased bottom-water TP and DOC concentrations in lakes, (2) these relationships are driven in part by complexation with Fe, and (3) other factors may have equal or greater importance in governing TP and OC retention in sediment over multiannual timescales. Furthermore, the effects of anoxia on OC and TP are not only similar across the two compounds but directly shaped by interactions between OC and TP (e.g., ternary OC-P-Fe compounds, competition for binding with Fe). Consequently, future analyses that consider both Fe-OC and Fe-P will likely be helpful to better understand the biogeochemical dynamics of both compounds under varying oxygen conditions.

Ecological memory and legacy

Across ecosystems and variables, ecological memory and legacy effects have gained increasing attention in recent decades to describe the influential role that antecedent conditions can play in driving changes in population, community, and ecosystem dynamics (e.g., Dugan, 2021; Hanson et al., 2023; Ogle et al., 2015; Pilla et al., 2023; Van Meter et al., 2018). Memory and legacy are variably defined across analyses (e.g., Moorhead et al., 1999; Ogle et al., 2015), and my dissertation chapters illustrate the breadth of these terms. In particular, Ogle et al. (2015) differentiate between exogenous and endogenous ecological memory, where exogenous memory describes the effects of antecedent external factors (e.g., meteorology) on an ecosystem, and endogenous memory describes the effects of historical states internal to the ecological variable of interest. Through Chapters II and III, we show that both exogenous and endogenous ecological memory govern summer bottom-water oxygen dynamics: exogenous memory of spring air temperature influences summer dissolved oxygen concentrations (Chapter II), as does endogenous memory of dissolved oxygen concentrations the previous summer (Chapter III). Notably, whereas ecological memory often exerts a secondary influence relative to current conditions, bottom-water dynamics in lakes represent an interesting case study for a system in which exogenous ecological memory of spring air temperatures plays a more important role than current summer air temperatures in shaping summer bottom-water dissolved oxygen concentrations (Chapter II).

Differences in ecological memory among lake variables may have implications for future efforts to forecast water quality. While forecast performance is expected to degrade across increasing forecast horizons for all variables (Chapter V), ecological memory may play a role in regulating the degradation rate. For example, because summer surface water temperatures are more strongly influenced by summer air temperature than spring air temperature, season-ahead forecasts of summer surface water temperature made at the start of summer stratification may be limited by the performance of season-ahead meteorological forecasts of summer air temperature (Bauer et al. 2015). Consequently, we would expect a relatively rapid rate of degradation in the performance of surface water temperature forecasts over the seasonal forecast horizon. Conversely, a season-ahead forecast of bottom-water temperature made at the start of summer stratification may be expected to perform comparatively better throughout the duration of summer stratification, as summer bottom-water temperature is more strongly influenced by the known (i.e., recently observed) spring air temperature than the forecasted summer air temperature (Chapter II). We would expect this pattern to occur specifically in forecast models that include air temperature as a covariate, which is likely necessary for accurate predictions of both surface and bottom-water temperature (Chapter II). Ultimately, testing the relationship between ecological memory and predictability will require the production and comparison of forecasts for multiple lake variables that are differentially governed by antecedent vs. concurrent conditions.

Strengths and limitations of dissertation approaches

Throughout my dissertation, I used multiple methods and scales of analysis to characterize fundamental biogeochemical mechanisms, assess the ecosystem-level relevance of these mechanisms, and identify future ecological research priorities. Each approach (i.e., microcosm incubations, whole-ecosystem experiments, analysis of observational data from many lakes, and synthetic literature review) has distinct strengths and limitations, and combining multiple approaches provided complementary insight into bottom-water dissolved oxygen dynamics. Below, I describe each of the four major approaches I used in my dissertation, with their corresponding strengths and caveats.

First, investigations on microcosm scales have provided insight into the fundamental drivers and consequences of oxygen declines, both in my dissertation and across previous research (e.g., Bastviken et al., 2004; Peter & Sobek, 2018; Chapter IV). However, microcosm incubations are limited by potential fouling and changes in microbial communities, among other abstractions, and microcosms inherently do not reflect the full range of processes that interact to control oxygen dynamics in lakes and reservoirs (e.g., Carpenter, 1996; Schindler, 1998). Notably, in Chapter IV, our microcosm results likely had limited applicability on a whole-ecosystem scale, as we observed microbial biofilms in oxic microcosms, which altered microcosm OC dynamics. Similar biofilms were never observed at the study reservoir on a whole-ecosystem scale, likely due to turbulence near the sediment, among other factors. Despite this limitation, the microcosm incubations were ultimately still valuable as a means of identifying that Fe-OC compounds buried in deeper sediment may be more resistant to reductive dissolution than newly-formed surficial Fe-OC in reservoir sediments.

Second, whole-ecosystem experiments provide an excellent means of testing the effects of altered environmental conditions in a real-world environmental context (Carpenter, 1996; Dzialowski et al., 2014; Schindler, 1998). However, variability on a whole-ecosystem scale may limit the capacity to detect subtle changes that could be better identified by microcosm-scale research (Drenner & Mazumder, 1999), and whole-ecosystem experiments are often limited by the fact that they can be intensive and difficult to replicate. In Chapter IV, whole-ecosystem experiments allowed us to characterize the effects of dynamic oxygen conditions on biogeochemical cycling over multiple timescales. However, we were only able to include two oxic periods and three hypoxic periods during a summer of intermittent oxygenation, and we were only able to characterize these dynamics in two reservoirs (one oxygenated reservoir and one reference reservoir), which are not representative of all freshwater systems. Consequently, additional approaches are needed to assess whether the results from our whole-ecosystem experiments will be applicable to other waterbodies.

Third, field surveys and observational analyses across many lakes are useful for demonstrating the broad applicability of mechanisms identified in more localized research. In Chapters II and III, we built upon previous small-scale experimental analyses to assess support for seasonal ecological memory and the Anoxia Begets Anoxia feedback across >600 widespread lakes. A fundamental goal of both projects was to identify whether the strength of these interactions varied depending on the characteristics of the lake (e.g., lake size), which would not be possible without analysis of many lakes worldwide. However, observational analyses of widespread lakes are fundamentally limited in their ability to assess causal relationships. In Chapter II, we partially addressed this gap by using hydrodynamic model output from 42 lakes in our dataset, which provided further support for the seasonal ecological memory effect in the bottom waters of temperate lakes. However, future research will be required to partition the relative importance of ice dynamics, mixing period duration, and stratification onset date, among other factors in shaping summer bottom-water dynamics across lakes. Importantly, the datasets used for analysis of widespread lakes rarely provide a comprehensive or unbiased representation of ecosystems worldwide. In the database analyzed in Chapters II and III, the majority (82%) of lakes were in temperate climate zones, primarily in the United States; consequently, results are likely not generalizable to the global population of lakes, and more research is needed to characterize DO dynamics in a broader, representative range of ecosystems.

Finally, prioritizing and leveraging these diverse research approaches requires thoughtful consideration of the broader state of existing knowledge. As such, literature review can also be a useful means of helping to understand ecological dynamics. In Chapter V, our systematic review of 178 near-term ecological forecasting papers allowed us to analyze progress in this emerging field, identify spatial biases in existing forecast sites, and help prioritize future directions. Comparing multiple published forecasting studies also allowed us to identify that the rate of decline in forecast performance differed among ecological variables over 1–7 day ahead forecast horizons. However, this analysis (as with many other meta-analyses) was notably limited by the fact that we only considered published literature, and operational forecasting systems that had not been described in peer-reviewed literature were excluded from our study. Future trans-disciplinary research and collaborations will be needed to characterize operational ecological forecasting infrastructure that is unpublished or only available in gray literature. Altogether, microcosm incubations, whole-ecosystem experiments, large-scale observational analyses, and literature review all provide important but limited perspectives on ecological function, and studies across multiple scales and approaches are needed to provide complementary insight into the processes governing biogeochemical dynamics in lakes worldwide.

Future research

The chapters of my dissertation lay the foundation for future analyses of freshwater biogeochemical dynamics across multiple scales. In particular, there are three research directions that I consider to be particularly important ways of building upon the strengths and limitations of my dissertation research: (1) building forecasts of bottom-water dissolved oxygen dynamics, (2) characterizing spatiotemporal scales of variability in bottom-water dynamics, and (3) quantifying trends in bottom-water carbon cycling dynamics across widespread lakes. Below, I outline existing progress and research questions for each of these three directions.

Building towards forecasts

Forecasting future anoxia may be critical to lake management amidst global change. In particular, my research highlights that management to preempt the first occurrence of anoxia in a lake may be substantially more effective than management to restore ecological function after oxygen concentrations have already declined (i.e., due to the ABA feedback; Chapter III). In Chapter V, I explored near-term ecological forecasting as an emerging field focused on addressing this need for anticipatory predictions. Motivated by this body of work, a key next step will be to develop scalable near-term forecasts for bottom-water dissolved oxygen in lakes, which can aid in both understanding and managing lake ecosystem function.

My dissertation highlights several covariates that will likely be important to include in models for generating summer bottom-water dissolved oxygen forecasts. Specifically, spring air temperature just prior to the onset of summer stratification appears to be a key covariate for predicting summer bottom-water temperature and dissolved oxygen (Chapter II). Likewise, chlorophyll-a concentrations during both the forecasted summer and the previous year have the potential to affect the rate of oxygen demand, with concentrations the previous year being marginally more important (Chapter III). In Chapter V, we found that the performance of chlorophyll-a forecasts decreases rapidly over 1–7 day forecast horizons, indicating that it may be difficult to use forecasted chlorophyll-a as a driver of dissolved oxygen beyond one week in the future. However, year-ahead forecasts of bottom-water dissolved oxygen that are able to assimilate observed (i.e., rather than forecasted) chlorophyll-a data may be especially useful and effective. More broadly, dissolved oxygen forecasts may be expected to perform well over longer horizons than chlorophyll-a given the strong role of ecological memory in governing summer bottom-water dissolved oxygen (Chapters II and III). As these forecasts are developed, it will likely be important to engage with end users early on and compare multiple modeling approaches, following our proposed best practices in near-term ecological forecasting (Chapter V). Ultimately, the development and evaluation of bottom-water dissolved oxygen forecasts has the potential to contribute to both fundamental understanding of bottom-water dynamics and near-term ecological management goals.

Spatiotemporal scales of variability in surface- and bottom-water dynamics

A second avenue for future research would be to explicitly characterize landscape-scale spatial relationships that drive variation in surface- and bottom-water biogeochemistry. In Chapters II and III, I analyzed a large database of many lakes worldwide. Following many previous lake studies (e.g., Jane et al., 2021; Pilla et al., 2020), I treated each lake as an independent replicate in these analyses. However, catchment- to regional-scale factors likely drive spatial autocorrelation in biogeochemical dynamics among lakes (e.g., Pham et al., 2008) and synchrony in how in-lake biogeochemical variables change over time within a region (Lottig et al., 2017; Magnuson et al., 2004; Walter et al., 2017), potentially confounding these analyses. In general, the assumption of independence may be more justified for bottom-water vs. surface-water processes due to seasonal stratification, which partially isolates bottom-waters from regional variation in terrestrial and atmospheric processes. However, my dissertation also highlights that bottom-water biogeochemistry is shaped by regionally consistent changes in spring air temperature and nutrient loading (Chapters II and III). Therefore, characterizing spatial autocorrelation and synchrony in both surface-water and bottom-water biogeochemical variables across many lakes is necessary as a first step to clarify the relative importance of in-lake vs. external drivers of change. This initial characterization can then be used to inform the development of future models that couple catchment and in-lake data to predict changes in bottom-water biogeochemistry across space and time.

Trends in bottom-water carbon cycling dynamics across widespread lakes

Climate-driven changes in bottom-water dissolved oxygen dynamics have the potential to alter carbon cycling processes in lakes worldwide (e.g., Chapter IV), which may feed back to alter the global carbon cycling processes that shape Earth’s climate (Chapter 1 Figure 1). However, limited characterization of bottom-water greenhouse gas dynamics across regional to global scales has prevented the mechanistic incorporation of these processes to more accurately predict greenhouse gas emissions from lakes amidst global change. Future efforts to (1) compile data for bottom-water dissolved organic carbon, carbon dioxide, and methane and (2) characterize patterns in bottom-water carbon cycling across space and time will help advance our understanding of how changes in bottom-water dissolved oxygen are altering freshwater carbon cycling worldwide.

Existing research suggests that declining oxygen concentrations may increase dissolved organic carbon flux out of sediment (Chapter IV; Carey et al., 2022; Peter et al., 2017), decrease respiration rates (Chapter IV; Carey et al., 2018; Hargrave, 1969; Sobek et al., 2009; Walker & Snodgrass, 1986), and disproportionately promote the accumulation of methane, vs. carbon dioxide, in bottom waters (Hounshell et al., 2021; Juutinen et al., 2009; Soued & Prairie, 2022). Consequently, based on oxygen declines alone, there may be reason to expect that dissolved organic carbon concentrations are increasing, carbon dioxide concentrations are decreasing, and methane concentrations are increasing in the bottom waters of widespread lakes. Importantly, however, bottom-water carbon dynamics are also strongly influenced by numerous other factors including water temperature, dissolved organic matter inputs, stratification duration, and mineral availability, all of which are also changing over time in many lakes (Björnerås et al., 2017; Jane et al., 2023; Monteith et al., 2007; O'Reilly et al., 2015; Pilla et al., 2020; Weyhenmeyer et al., 2014). Altogether, understanding the dynamic role of lakes in the global carbon cycle will require integrated approaches, including long-term monitoring data on a global scale.

Conclusion

Throughout my dissertation, I built a predictive understanding of how bottom-water dissolved oxygen may mediate water quality in lakes amidst global change. I characterized both causes (e.g., increased spring air temperature) and consequences (e.g., altered biogeochemical cycling) of changes in bottom-water dissolved oxygen across multiple scales of analysis, and I analyzed the development of near-term ecological forecasting as an emerging subdiscipline that may aid in management of future water quality dynamics.

My dissertation highlights that water quality management needs may vary over short- and long-term timescales, with local to global scope. Over short-term timescales (e.g., days to years), local adaptation measures may be useful for maintaining sufficient water quality to support drinking water, recreation, and other ecosystem services, which may be aided by the use of near-term ecological forecasts. Local and regional catchment management can also be useful in helping to decrease nutrient inputs to lakes, though lake water quality improvement may take years to decades due to legacies of historical nutrient loading. Ultimately, climate change has been identified in my dissertation and previous research as one of the most important factors governing lake oxygen declines across recent decades (e.g., 1950–present). Addressing climate change will require concerted efforts on a global scale. While it may take centuries to see the impacts of climate mitigation on lakes, these efforts are profoundly important for conserving ecological function across freshwater ecosystems.

Chapter VI References

Albright, E. A., & Wilkinson, G. M. (2022). Sediment phosphorus composition controls hot spots and hot moments of internal loading in a temperate reservoir. Ecosphere, 13(8), e4201. https://doi.org/10.1002/ecs2.4201

Barber, A., Brandes, J., Leri, A., Lalonde, K., Balind, K., Wirick, S., Wang, J., & Gélinas, Y. (2017). Preservation of organic matter in marine sediments by inner-sphere interactions with reactive iron. Scientific Reports, 7(1), 366. https://doi.org/10.1038/s41598-017-00494-0

Bastviken, D., Olsson, M., & Tranvik, L. (2003). Simultaneous measurements of organic carbon mineralization and bacterial production in oxic and anoxic lake sediments. Microbial Ecology, 46(1), 73–82. https://doi.org/10.1007/s00248-002-1061-9

Bastviken, D., Persson, L., Odham, G., & Tranvik, L. (2004). Degradation of dissolved organic matter in oxic and anoxic lake water. Limnology and Oceanography, 49(1), 109–116. https://doi.org/10.4319/lo.2004.49.1.0109

Bauer, P., Thorpe, A., & Brunet, G. (2015). The quiet revolution of numerical weather prediction. *Nature*, *525*(7567), 47–55. https://doi.org/10.1038/nature14956

Beutel, M. W., & Horne, A. J. (1999). A Review of the Effects of Hypolimnetic Oxygenation on Lake and Reservoir Water Quality. Lake and Reservoir Management, 15(4), 285–297. https://doi.org/10.1080/07438149909354124

Björnerås, C., Weyhenmeyer, G. A., Evans, C. D., Gessner, M. O., Grossart, H.-P., Kangur, K., Kokorite, I., Kortelainen, P., Laudon, H., Lehtoranta, J., Lottig, N., Monteith, D. T., Nõges, P., Nõges, T., Oulehle, F., Riise, G., Rusak, J. A., Räike, A., Sire, J., Sterling, S., & Kritzberg, E. S. (2017). Widespread increases in iron concentration in European and North American freshwaters. Global Biogeochemical Cycles, 31(10), 1488–1500. https://doi.org/10.1002/2017GB005749

Carey, C. C., Doubek, J. P., McClure, R. P., & Hanson, P. C. (2018). Oxygen dynamics control the burial of organic carbon in a eutrophic reservoir. Limnology and Oceanography Letters, 3(3), 293–301. https://doi.org/10.1002/lol2.10057

Carey, C. C., Hanson, P. C., Thomas, R. Q., Gerling, A. B., Hounshell, A. G., Lewis, A. S. L., Lofton, M. E., McClure, R. P., Wander, H. L., Woelmer, W. M., Niederlehner, B. R., & Schreiber, M. E. (2022). Anoxia decreases the magnitude of the carbon, nitrogen, and phosphorus sink in freshwaters. Global Change Biology, 28(16), 4861–4881. https://doi.org/10.1111/gcb.16228

Carpenter, S. R. (1996). Microcosm experiments have limited relevance for community and ecosystem ecology. Ecology, 77(3), 677–680. https://doi.org/10.2307/2265490

Clark, J. S., Carpenter, S. R., Barber, M., Collins, S., Dobson, A., Foley, J. A., Lodge, D. M., Pascual, M., Pielke, R., Pizer, W., Pringle, C., Reid, W. V., Rose, K. A., Sala, O., Schlesinger, W. H., Wall, D. H., & Wear, D. (2001). Ecological Forecasts: An Emerging Imperative. Science, 293(5530), 657–660. https://doi.org/10.1126/science.293.5530.657

Cooke, G. D., Welch, E. B., Peterson, S., & Nichols, S. A. (2005). Restoration and Management of Lakes and Reservoirs (3rd ed.). Boca Raton: CRC Press. https://doi.org/10.1201/9781420032109

Dietze, M. C., Fox, A., Beck-Johnson, L. M., Betancourt, J. L., Hooten, M. B., Jarnevich, C. S., Keitt, T. H., Kenney, M. A., Laney, C. M., Larsen, L. G., Loescher, H. W., Lunch, C. K., Pijanowski, B. C., Randerson, J. T., Read, E. K., Tredennick, A. T., Vargas, R., Weathers, K. C., & White, E. P. (2018). Iterative near-term ecological forecasting: Needs, opportunities, and challenges. Proceedings of the National Academy of Sciences, 115(7), 1424–1432. https://doi.org/10.1073/pnas.1710231115

Drenner, R. W., & Mazumder, A. (1999). Microcosm Experiments Have Limited Relevance for Community and Ecosystem Ecology: Comment. Ecology, 80(3), 1081–1085. https://doi.org/10.2307/177042

Dugan, H. A. (2021). A Comparison of Ecological Memory of Lake Ice-Off in Eight North-Temperate Lakes. Journal of Geophysical Research: Biogeosciences, 126(6), e2020JG006232. https://doi.org/10.1029/2020JG006232

Dzialowski, A. R., Rzepecki, M., Kostrzewska-Szlakowska, I., Kalinowska, K., Palash, A., & Lennon, J. T. (2014). Are the abiotic and biotic characteristics of aquatic mesocosms representative of in situ conditions? Journal of Limnology, 73(3). https://doi.org/10.4081/jlimnol.2014.721

Einsele, W. (1936). Über die Beziehungen des Eisenkreislaufs zum Phosphatkreislauf im eutrophen See. Archiv Für Hydrobiologie, 29, 664–686.

Hanson, P. C., Ladwig, R., Buelo, C., Albright, E. A., Delany, A. D., & Carey, C. C. (2023). Legacy Phosphorus and Ecosystem Memory Control Future Water Quality in a Eutrophic Lake. Journal of Geophysical Research: Biogeosciences, 128(12), e2023JG007620. https://doi.org/10.1029/2023JG007620

Hargrave, B. T. (1969). Similarity of oxygen uptake by benthic communities. Limnology and Oceanography, 14(5), 801–805. https://doi.org/10.4319/lo.1969.14.5.0801

Hemingway, J. D., Rothman, D. H., Grant, K. E., Rosengard, S. Z., Eglinton, T. I., Derry, L. A., & Galy, V. V. (2019). Mineral protection regulates long-term global preservation of natural organic carbon. Nature, 570(7760), 228–231. https://doi.org/10.1038/s41586-019-1280-6

Hounshell, A. G., McClure, R. P., Lofton, M. E., & Carey, C. C. (2021). Whole-ecosystem oxygenation experiments reveal substantially greater hypolimnetic methane concentrations in reservoirs during anoxia. Limnology and Oceanography Letters, 6(1), 33–42.

Hupfer, M., & Lewandowski, J. (2008). Oxygen Controls the Phosphorus Release from Lake Sediments – a Long-Lasting Paradigm in Limnology. International Review of Hydrobiology, 93(4–5), 415–432. https://doi.org/10.1002/iroh.200711054

Jane, S. F., Hansen, G., Kraemer, B., Leavitt, P., Mincer, J., North, R., Pilla, R., Stetler, J., Williamson, C., Woolway, R., Arvola, L., Chandra, S., DeGasperi, C., Diemer, L., Dunalska, J., Erina, O., Flaim, G., Grossart, H.-P., Hambright, K., & Rose, K. (2021). Widespread deoxygenation of temperate lakes. Nature, 594. https://doi.org/10.1038/s41586-021-03550-y

Jane, S. F., Mincer, J. L., Lau, M. P., Lewis, A. S. L., Stetler, J. T., & Rose, K. C. (2023). Longer duration of seasonal stratification contributes to widespread increases in lake hypoxia and anoxia. Global Change Biology, 29(4), 1009–1023. https://doi.org/10.1111/gcb.16525

Jenny, J.-P., Francus, P., Normandeau, A., Lapointe, F., Perga, M.-E., Ojala, A., Schimmelmann, A., & Zolitschka, B. (2016). Global spread of hypoxia in freshwater ecosystems during the last three centuries is caused by rising local human pressure. Global Change Biology, 22(4), 1481–1489. https://doi.org/10.1111/gcb.13193

Joshi, S. R., Kukkadapu, R. K., Burdige, D. J., Bowden, M. E., Sparks, D. L., & Jaisi, D. P. (2015). Organic matter remineralization predominates phosphorus cycling in the mid-Bay sediments in the Chesapeake Bay. Environmental Science & Technology, 49(10), 5887–5896. https://doi.org/10.1021/es5059617

Juutinen, S., Rantakari, M., Kortelainen, P., Huttunen, J. T., Larmola, T., Alm, J., Silvola, J., & Martikainen, P. J. (2009). Methane dynamics in different boreal lake types. Biogeosciences, 6(2), 209–223. https://doi.org/10.5194/bg-6-209-2009

Katsev, S., Tsandev, I., L'Heureux, I., & Rancourt, D. G. (2006). Factors controlling long-term phosphorus efflux from lake sediments: Exploratory reactive-transport modeling. Chemical Geology, 234(1), 127–147. https://doi.org/10.1016/j.chemgeo.2006.05.001

Khandelwal, A., Karpatne, A., Ravirathinam, P., Ghosh, R., Wei, Z., Dugan, H. A., Hanson, P. C., & Kumar, V. (2022). ReaLSAT, a global dataset of reservoir and lake surface area variations. Scientific Data, 9(1), 356. https://doi.org/10.1038/s41597-022-01449-5

Lalonde, K., Mucci, A., Ouellet, A., & Gélinas, Y. (2012). Preservation of organic matter in sediments promoted by iron. Nature, 483(7388), 198–200. https://doi.org/10.1038/nature10855

Lewis, A. S. L., Lau, M. P., Jane, S. F., Rose, K. C., Be’eri-Shlevin, Y., Burnet, S. H., Clayer, F., Feuchtmayr, H., Grossart, H.-P., Howard, D. W., Mariash, H., Delgado Martin, J., North, R. L., Oleksy, I., Pilla, R. M., Smagula, A. P., Sommaruga, R., Steiner, S. E., Verburg, P., Wain, D., Weyhenmeyer, G. A., & Carey, C. C. (2024). Anoxia begets anoxia: A positive feedback to the deoxygenation of temperate lakes. Global Change Biology, 30(1), e17046. https://doi.org/10.1111/gcb.17046

Li, W., Joshi, S. R., Hou, G., Burdige, D. J., Sparks, D. L., & Jaisi, D. P. (2015). Characterizing Phosphorus Speciation of Chesapeake Bay Sediments Using Chemical Extraction, 31 P NMR, and X-ray Absorption Fine Structure Spectroscopy. Environmental Science & Technology, 49(1), 203–211. https://doi.org/10.1021/es504648d

Lottig, N. R., Tan, P.-N., Wagner, T., Cheruvelil, K. S., Soranno, P. A., Stanley, E. H., Scott, C. E., Stow, C. A., & Yuan, S. (2017). Macroscale patterns of synchrony identify complex relationships among spatial and temporal ecosystem drivers. Ecosphere, 8(12), e02024. https://doi.org/10.1002/ecs2.2024

Luo, C., Wen, S., Lu, Y., Dai, J., & Du, Y. (2022). Coprecipitation of humic acid and phosphate with Fe(III) enhances the sequestration of carbon and phosphorus in sediments. Chemical Geology, 588, 120645. https://doi.org/10.1016/j.chemgeo.2021.120645

Luo, Y., Ogle, K., Tucker, C., Fei, S., Gao, C., LaDeau, S., Clark, J. S., & Schimel, D. S. (2011). Ecological forecasting and data assimilation in a data-rich era. Ecological Applications, 21(5), 1429–1442. https://doi.org/10.1890/09-1275.1

Magnuson, J. J., Benson, B. J., & Kratz, T. K. (2004). Patterns of coherent dynamics within and between lake districts at local to intercontinental scales. BOREAL ENVIRONMENT RESEARCH, 9.

Monteith, D. T., Stoddard, J. L., Evans, C. D., de Wit, H. A., Forsius, M., Høgåsen, T., Wilander, A., Skjelkvåle, B. L., Jeffries, D. S., Vuorenmaa, J., Keller, B., Kopácek, J., & Vesely, J. (2007). Dissolved organic carbon trends resulting from changes in atmospheric deposition chemistry. Nature, 450(7169), 537–540. https://doi.org/10.1038/nature06316

Moorhead, D. L., Doran, P. T., Fountain, A. G., Lyons, W. B., McKnight, D. M., Priscu, J. C., Virginia, R. A., & Wall, D. H. (1999). Ecological Legacies: Impacts on Ecosystems of the McMurdo Dry Valleys. BioScience, 49(12), 1009. https://doi.org/10.2307/1313734

Mortimer, C. H. (1942). The Exchange of Dissolved Substances between Mud and Water in Lakes. Journal of Ecology, 30(1), 147–201. https://doi.org/10.2307/2256691

Müller, B., Bryant, L. D., Matzinger, A., & Wüest, A. (2012). Hypolimnetic Oxygen Depletion in Eutrophic Lakes. Environmental Science & Technology, 46(18), 9964–9971. https://doi.org/10.1021/es301422r

Münch, M. A., van Kaam, R., As, K., Peiffer, S., Heerdt, G. ter, Slomp, C. P., & Behrends, T. (2024). Impact of iron addition on phosphorus dynamics in sediments of a shallow peat lake 10 years after treatment. Water Research, 248, 120844. https://doi.org/10.1016/j.watres.2023.120844

Nürnberg, G. K. (1995). Quantifying anoxia in lakes. Limnology and Oceanography, 40(6), 1100–1111. https://doi.org/10.4319/lo.1995.40.6.1100

Nürnberg, G. K. (2019). Quantification of Anoxia and Hypoxia in Water Bodies. In Encyclopedia of Water (pp. 1–9). John Wiley & Sons, Ltd. https://doi.org/10.1002/9781119300762.wsts0081

Ogle, K., Barber, J. J., Barron-Gafford, G. A., Bentley, L. P., Young, J. M., Huxman, T. E., Loik, M. E., & Tissue, D. T. (2015). Quantifying ecological memory in plant and ecosystem processes. Ecology Letters, 18(3), 221–235. https://doi.org/10.1111/ele.12399

O'Reilly, C. M., Sharma, S., Gray, D. K., Hampton, S. E., Read, J. S., Rowley, R. J., Schneider, P., Lenters, J. D., McIntyre, P. B., Kraemer, B. M., Weyhenmeyer, G. A., Straile, D., Dong, B., Adrian, R., Allan, M. G., Anneville, O., Arvola, L., Austin, J., Bailey, J. L., Baron, J. S., Brookes, J. D., Eyto, E. de, Dokulil, M. T., Hamilton, D. P., Havens, K., Hetherington, A. L., Higgins, S. N., Hook, S., Izmest'eva, L. R., Joehnk, K. D., Kangur, K., Kasprzak, P., Kumagai, M., Kuusisto, E., Leshkevich, G., Livingstone, D. M., MacIntyre, S., May, L., Melack, J. M., Mueller-Navarra, D. C., Naumenko, M., Noges, P., Noges, T., North, R. P., Plisnier, P.-D., Rigosi, A., Rimmer, A., Rogora, M., Rudstam, L. G., Rusak, J. A., Salmaso, N., Samal, N. R., Schindler, D. E., Schladow, S. G., Schmid, M., Schmidt, S. R., Silow, E., Soylu, M. E., Teubner, K., Verburg, P., Voutilainen, A., Watkinson, A., Williamson, C. E., & Zhang, G. (2015). Rapid and highly variable warming of lake surface waters around the globe. Geophysical Research Letters, 42(24), 10,773-10,781. https://doi.org/10.1002/2015GL066235

Orihel, D. M., Baulch, H. M., Casson, N. J., North, R. L., Parsons, C. T., Seckar, D. C. M., & Venkiteswaran, J. J. (2017). Internal phosphorus loading in Canadian fresh waters: a critical review and data analysis. Canadian Journal of Fisheries and Aquatic Sciences, 74(12), 2005–2029. https://doi.org/10.1139/cjfas-2016-0500

Pace, M. L., & Prairie, Y. T. (2005). Respiration in lakes. In P. del Giorgio & P. Williams (Eds.), Respiration in Aquatic Ecosystems (pp. 103–121). Oxford University Press. https://doi.org/10.1093/acprof:oso/9780198527084.003.0007

Peter, S., & Sobek, S. (2018). High variability in iron-bound organic carbon among five boreal lake sediments. Biogeochemistry, 139(1), 19–29. https://doi.org/10.1007/s10533-018-0456-8

Peter, S., Agstam, O., & Sobek, S. (2017). Widespread release of dissolved organic carbon from anoxic boreal lake sediments. Inland Waters, 7(2), 151–163. https://doi.org/10.1080/20442041.2017.1300226

Pham, S. V., Leavitt, P. R., McGowan, S., & Peres-Neto, P. (2008). Spatial variability of climate and land-use effects on lakes of the northern Great Plains. Limnology and Oceanography, 53(2), 728–742. https://doi.org/10.4319/lo.2008.53.2.0728

Pilla, R. M., Williamson, C. E., Adamovich, B. V., Adrian, R., Anneville, O., Chandra, S., Colom-Montero, W., Devlin, S. P., Dix, M. A., Dokulil, M. T., Gaiser, E. E., Girdner, S. F., Hambright, K. D., Hamilton, D. P., Havens, K., Hessen, D. O., Higgins, S. N., Huttula, T. H., Huuskonen, H., Isles, P. D. F., Joehnk, K. D., Jones, I. D., Keller, W. B., Knoll, L. B., Korhonen, J., Kraemer, B. M., Leavitt, P. R., Lepori, F., Luger, M. S., Maberly, S. C., Melack, J. M., Melles, S. J., Müller-Navarra, D. C., Pierson, D. C., Pislegina, H. V., Plisnier, P.-D., Richardson, D. C., Rimmer, A., Rogora, M., Rusak, J. A., Sadro, S., Salmaso, N., Saros, J. E., Saulnier-Talbot, É., Schindler, D. E., Schmid, M., Shimaraeva, S. V., Silow, E.

A., Sitoki, L. M., Sommaruga, R., Straile, D., Strock, K. E., Thiery, W., Timofeyev, M. A., Verburg, P., Vinebrooke, R. D., Weyhenmeyer, G. A., & Zadereev, E. (2020). Deeper waters are changing less consistently than surface waters in a global analysis of 102 lakes. Scientific Reports, 10(1), 20514. https://doi.org/10.1038/s41598-020-76873-x

Pilla, R. M., Williamson, C. E., Overholt, E. P., Rose, K. C., Berger, S. A., Couture, R.-M., De Wit, H. A., Granados, I., Grossart, H.-P. F., Kirillin, G. B., Laas, A., Nejstgaard, J. C., Rusak, J. A., Swinton, M. W., Toro, M., & Yao, H. (2023). Deepwater dissolved oxygen shows little ecological memory between lake phenological seasons. Inland Waters, 1–12. https://doi.org/10.1080/20442041.2023.2265802

Reitzel, K., Ahlgren, J., DeBrabandere, H., Waldebäck, M., Gogoll, A., Tranvik, L., & Rydin, E. (2007). Degradation rates of organic phosphorus in lake sediment. Biogeochemistry, 82(1), 15–28. https://doi.org/10.1007/s10533-006-9049-z

Schindler, D. W. (1998). Whole-ecosystem experiments: replication versus realism: the need for ecosystem-scale experiments. Ecosystems, 1(4), 323–334. https://doi.org/10.1007/s100219900026

Sobek, S., Durisch-Kaiser, E., Zurbrügg, R., Wongfun, N., Wessels, M., Pasche, N., & Wehrli, B. (2009). Organic carbon burial efficiency in lake sediments controlled by oxygen exposure time and sediment source. Limnology and Oceanography, 54(6), 2243–2254. https://doi.org/10.4319/lo.2009.54.6.2243

Soued, C., & Prairie, Y. T. (2022). Patterns and Regulation of Hypolimnetic CO2 and CH4 in a Tropical Reservoir Using a Process-Based Modeling Approach. Journal of Geophysical Research: Biogeosciences, 127(8), e2022JG006897. https://doi.org/10.1029/2022JG006897

Topp, S. N., Pavelsky, T. M., Dugan, H. A., Yang, X., Gardner, J., & Ross, M. R. V. (2021). Shifting Patterns of Summer Lake Color Phenology in Over 26,000 US Lakes. Water Resources Research, 57(5), e2020WR029123. https://doi.org/10.1029/2020WR029123

Van Meter, K. J., Van Cappellen, P., & Basu, N. B. (2018). Legacy nitrogen may prevent achievement of water quality goals in the Gulf of Mexico. Science, 360(6387), 427–430. https://doi.org/10.1126/science.aar4462

Walker, R. R., & Snodgrass, W. J. (1986). Model for sediment oxygen demand in lakes. Journal of Environmental Engineering, 112(1), 25–43. https://doi.org/10.1061/(ASCE)0733-9372(1986)112:1(25)

Walter, J. A., Sheppard, L. W., Anderson, T. L., Kastens, J. H., Bjørnstad, O. N., Liebhold, A. M., & Reuman, D. C. (2017). The geography of spatial synchrony. Ecology Letters, 20(7), 801–814. https://doi.org/10.1111/ele.12782

Wen, S., Wang, H., Wu, T., Yang, J., Jiang, X., & Zhong, J. (2020). Vertical profiles of phosphorus fractions in the sediment in a chain of reservoirs in North China: Implications for pollution source, bioavailability, and eutrophication. Science of The Total Environment, 704, 135318. https://doi.org/10.1016/j.scitotenv.2019.135318

Weyhenmeyer, G. A., Prairie, Y. T., & Tranvik, L. J. (2014). Browning of boreal freshwaters coupled to carbon-iron interactions along the aquatic continuum. PloS One, 9(2), e88104. https://doi.org/10.1371/journal.pone.0088104

Woolway, R. I., Sharma, S., Weyhenmeyer, G. A., Debolskiy, A., Golub, M., Mercado-Bettín, D., Perroud, M., Stepanenko, V., Tan, Z., Grant, L., Ladwig, R., Mesman, J., Moore, T. N., Shatwell, T., Vanderkelen, I., Austin, J. A., DeGasperi, C. L., Dokulil, M., La Fuente, S., Mackay, E. B., Schladow, S. G., Watanabe, S., Marcé, R., Pierson, D. C., Thiery, W., & Jennings, E. (2021). Phenological shifts in lake stratification under climate change. Nature Communications, 12(1), 2318. https://doi.org/10.1038/s41467-021-22657-4

Yang, X., O'Reilly, C. M., Gardner, J. R., Ross, M. R. V., Topp, S. N., Wang, J., & Pavelsky, T. M. (2022). The Color of Earth's Lakes. Geophysical Research Letters, 49(18), e2022GL098925. https://doi.org/10.1029/2022GL098925

Yvon-Durocher, G., Caffrey, J. M., Cescatti, A., Dossena, M., Giorgio, P. del, Gasol, J. M., Montoya, J. M., Pumpanen, J., Staehr, P. A., Trimmer, M., Woodward, G., & Allen, A. P. (2012). Reconciling the temperature dependence of respiration across timescales and ecosystem types. Nature, 487(7408), 472–476. https://doi.org/10.1038/nature11205